UNIVERSIDADE FEDERAL DO CEARÁ
CENTRO DE TECNOLOGIA
DEPARTAMENTO DE ENGENHARIA HIDRÁULICA E AMBIENTAL
PROGRAMA DE PÓS-GRADUAÇÃO EM ENGENHARIA CIVIL

FRANCISCA KAMILA AMANCIO FRUTUOSO

ENGINEERING STRATEGIES TO ENHANCE RESOURCE RECOVERY IN AEROBIC GRANULAR SLUDGE SYSTEMS

FORTALEZA
2024

FRANCISCA KAMILA AMANCIO FRUTUOSO

ENGINEERING STRATEGIES TO ENHANCE RESOURCE RECOVERY IN AEROBIC GRANULAR SLUDGE SYSTEMS

Thesis presented to the Graduate Program in Civil Engineering at the Federal University of Ceará, as a partial requirement for obtaining the degree in Civil Engineering. Area of concentration: Environmental Sanitation.

Advisor: Prof. André Bezerra dos Santos (Ph.D.)
Co-advisor: Tânia Filomena Castro Valente Silva (Ph.D.)

FORTALEZA
2024

Dados Internacionais de Catalogação na Publicação
Universidade Federal do Ceará
Sistema de Bibliotecas
Gerada automaticamente pelo módulo Catalog, mediante os dados fornecidos pelo(a) autor(a)

F962e Frutuoso, Francisca Kamila Amancio.
Engineering strategies to enhance resource recovery in aerobic granular sludge systems / Francisca Kamila Amancio Frutuoso. – 2024.
187 f. : il. color.

Tese (doutorado) – Universidade Federal do Ceará, Centro de Tecnologia, Programa de Pós-Graduaçãoem Engenharia Civil: Saneamento Ambiental, Fortaleza, 2024.
Orientação: Prof. Dr. André Bezerra dos Santos.
Coorientação: Prof. Dra. Tânia Filomena Castro Valente Silva.

1. Aerobic Granular Sludge. 2. Resource Recovery. 3. Engineering Aspects. 4. Principal Component Analysis. 5. Molecular Microbiology. I. Título.

CDD 628

FRANCISCA KAMILA AMANCIO FRUTUOSO

ENGINEERING STRATEGIES TO ENHANCE RESOURCE RECOVERY IN AEROBIC GRANULAR SLUDGE SYSTEMS

Thesis presented to the Graduate Program in Civil Engineering at Federal University of Ceará, as a requirement to obtain a degree of Doctor in Civil Engineering. Concentration Area: Environmental Sanitation.

Approved on: __/__/____.

EXAMINATION BOARD

____

Prof. Dr. André Bezerra dos Santos (Advisor)
Universidade Federal do Ceará (UFC)

____

Dra. Tânia Filomena Castro Valente Silva (Co-advisor)
Faculdade de Engenharia da Universidade do Porto (FEUP)

____

Prof. Dr. Paulo Igor Milen Firmino (Internal member)
Universidade Federal do Ceará (UFC)

____

Prof. Dr. Vítor Jorge Pais Vilar (External member)
Faculdade de Engenharia da Universidade do Porto (FEUP)

____

Prof. Dr. Rejane Helena Ribeiro da Costa (External member)
Universidade Federal de Santa Catarina (UFSC)

____

Prof. Dr. João Paulo Bassin (External member)
Universidade Federal do Rio de Janeiro (UFRJ)

To my dear father, José Gomes
Frutuoso. You will forever remain in my
memory, with all my love and endless
longing.

ACKNOWLEDGEMENTS

First and foremost, I thank God, who has sustained me thus far, granting me the grace to endure the most challenging days. Undoubtedly, my faith has always been my foundation for overcoming obstacles and facing the future with hope.

To my husband, Luis, who has been with me from the beginning. His love, help, and support were essential for me to reach this point. I appreciate that every Saturday or Sunday, he assisted me in cleaning the reactors. He even helped me with the cycle analyses! This title is also yours!

To my family, who has always stood by my side, providing unwavering support and love. Especially to my mother, Evânia, who is a role model of strength, love, and generosity. With little formal education but extraordinary wisdom, this woman taught me the best of what I have and continues to guide me to be the best version of myself. Thank you, Mom!

To Dr. André Bezerra, my advisor, for the opportunity and trust placed in me. Thank you for every lesson; undoubtedly, you are a professional example whom I deeply admire. I cannot measure how much I have grown in these 4 years.

To Dr. Vítor Vilar and Dra. Tânia Silva, for the support and welcome during the sandwich doctorate period. I extend my gratitude to the entire LSRE-LCM team. Without naming names to avoid the risk of leaving someone out, thank you all for the help and support.

To all colleagues and friends from LABOSAN: Marcos, Clara, Plínio, Amanda, Naassom, Mauricio, Renan, Vicente, students of scientific initiation and PETs. The support of each one was undoubtedly essential to endure the arduous load of laboratory work. Finally, a special thanks to Ricardo for the support and guidance (AGS subject, HPLC use...) and for providing me with valuable advice.

To every friend who was present at some point during this journey and to those I made along the way. Thank you for the strength, support, and courage in difficult moments.

To every professor from the Department of Hydraulic and Environmental Engineering who, in some way, contributed to my education.

To the professors participating in the examining board for their valuable contributions and availability.

To the Brazilian National Council for Scientific and Technological Development (CNPq - grant 400324/2022-9), Ceará State Foundation for the Support of Scientific and Technological Development (Funcap - grant PS1-0186-00304.01.00/21), CAPES (Process 88887.603310/2021-00), FAPEMIG, INCT ETEs Sustentáveis (INCT Sustainable Sewage Treatment Plants), Microscopy Analytical Center, Bioinorganic Laboratory (LABIO), and CeGenBio of UFC.

“Not to us, Lord, not to us but to your
name be the glory, because of your
love and faithfulness.”
(Psalms 115:1)

RESUMO

O lodo granular aeróbio (LGA) é uma tecnologia emergente de tratamento de esgoto que combina a possibilidade de remoção simultânea de carbono, nitrogênio e fósforo com a elevada capacidade de recuperação de recursos, muitos de elevado interesse industrial. Associado à valorização da economia circular em estações de tratamento de águas residuárias (ETAR), a recuperação de subprodutos a partir da biomassa do LGA emergiu como uma estratégia eficiente e economicamente sustentável de gerenciamento de lodos, especialmente considerando que as substâncias poliméricas extracelulares (EPS, *extracellular polymeric substances*) podem compor até 40% da biomassa seca. Os exopolímeros semelhantes ao alginato (ALE, *Alginate-Like Exopolymers*) e triptofano (TRP), presentes na matriz extracelular do LGA, são subprodutos valiosos com aplicações promissoras na indústria. No entanto, a literatura ainda carece de uma compreensão abrangente dos impactos dos parâmetros operacionais na biossíntese desses recursos biológicos no lodo, bem como sua interconexão com a granulação e a estabilidade do sistema a longo prazo. Nesse contexto, a presente pesquisa investigou diversos aspectos operacionais e estímulos para a produção desses recursos, avaliando a eficiência de produção, a granulação e a estabilidade em cinco sistemas operacionais diferentes (OS I, OS II, OS III, OS IV e OS V). No OS I, a influência de diferentes fontes de carbono (acetato, propionato, glicerol, glicose e sacarose) na produção de ALE, EPS e TRP foi investigada. O acetato mostrou-se promissor, resultando na maior produção de biopolímeros e TRP, embora tenha sido observada uma desintegração parcial dos grânulos durante a operação. Por outro lado, o propionato foi o substrato que melhor proporcionou estabilidade ao LGA a longo prazo, além de apresentar uma produção considerável desses biorrecursos. No OS II, explorou-se o impacto da salinidade nas eficiências de remoção, estabilidade dos grânulos e produção de ALE, EPS e TRP. Baixas concentrações salinas (até 7,5 g/L) favoreceram a produção de ALE e o aumento da biomassa, mas concentrações mais elevadas (10 g/L) levaram ao colapso do sistema em determinado período. A análise detalhada revelou a identificação de aminoácidos, como tirosina e triptofano, em maiores quantidades nas substâncias poliméricas extracelulares de reatores operados com sal. No OS III, foi realizada uma comparação entre alimentação escalonada e convencional sob pressão osmótica. A alimentação escalonada mostrou benefícios significativos em termos de desnitrificação e estabilidade a longo prazo. O aumento gradual do sal (2,5 a 10 g/L) influenciou a produção de ALE, EPS e TRP, mas a alimentação escalonada não teve um impacto significativo na produção desses recursos. No OS IV, investigou-se os efeitos do estresse osmótico intermitente, comparando-o com o estresse constante e um sistema controle sem adição de sal, tanto como estratégia para diminuir o tempo de partida dos sistemas de granulação aeróbia quanto em avaliar se o estresse osmótico intermitente promove granulação rápida e produção estável de ALE. O reator sujeito a estresse salino intermitente revelou uma granulação rápida e completa em apenas 21 dias, contrastando com os 59 dias necessários para o reator com adição constante de sal. Além disso, a adição salina apresentou impactos positivos significativos na granulação em comparação com o reator controle, corroborando descobertas anteriores nos OS II e OS III. Essa constatação ressalta a importância crucial da variação nas condições salinas para promover a formação eficiente de grânulos. Diante disso, o destaque vai para o reator sob estresse salino intermitente, identificado como o mais eficiente em termos de granulação, estabilidade, produção de recursos e remoção de poluentes. No OS V, a pesquisa focou no co-tratamento de lixiviados com esgoto doméstico, com uma atenção especial ao controle do tempo de retenção celular ou idade de lodo (SRT, *sludge retention time*). Baixa proporção de lixiviado (5%) não prejudicou o desempenho e a estabilidade do LGA, enquanto o aumento da fração de lixiviado (10%) influenciou a remoção de matéria orgânica e a produção de ALE. A análise de componentes principais (PCA, *principal component analysis*) destacou o SRT como crucial para otimizar a síntese de biopolímeros, indicando uma produção ótima com SRT entre 10 e 20 dias. Em síntese, essa pesquisa proporciona uma compreensão detalhada dos fatores que influenciam a produção de biorrecursos em sistemas de granulação aeróbia. Acredita-se que os resultados alcançados fornecem contribuições significativas para a otimização do desempenho desses sistemas em termos de tempo de partida, estabilidade, produção de recursos e remoção de contaminantes em efluentes salinos e não salinos, abrindo novos caminhos para a evolução sustentável das práticas de tratamento de águas residuais.

Palavras-chave: Lodo Granular Aeróbio; Recuperação de Recursos; Aspectos de Engenharia; Análise do componente principal; Microbiologia Molecular.

ABSTRACT

Aerobic granular sludge (AGS) is an emerging sewage treatment technology that combines the possibility of simultaneous removal of carbon, nitrogen, and phosphorus, with the high capacity to recover resources, many of which are of high industrial interest. Associated with the valorization of the circular economy in wastewater treatment plants (WWTP), the recovery of byproducts from AGS biomass has emerged as an efficient and economically sustainable sludge management strategy, especially considering that extracellular polymeric substances (EPS) can make up to 40% of dry biomass. Alginate-Like Exopolymers (ALE) and tryptophan (TRP), present in the extracellular matrix of AGS, are valuable byproducts with promising applications in industry. However, the literature still needs a comprehensive understanding of the impacts of operational parameters on the biosynthesis of these bioresources in sludge, as well as their interconnection with granulation and the system's long-term stability. In this context, the present research addressed several operational aspects and stimuli for producing of these resources, evaluating the efficiency of production, granulation, and system stability in five operating systems (OS I, OS II, OS III, OS IV, and OS V). In OS I, the influence of different carbon sources (acetate, propionate, glycerol, glucose, and sucrose) on ALE, EPS and TRP production was investigated. Acetate showed promise, resulting in greater production of biopolymers and TRY, although partial disintegration of the granules was observed during operation. On the other hand, propionate was the substrate that best provided long-term stability to the AGS and stimulated a considerable production of bioresources. In OS II, the impact of salinity on removal efficiencies, granule stability, and ALE, EPS and TRP production was explored. Low saline concentrations (up to 7.5 g/L) favored ALE production and increased biomass, but higher concentrations (10 g/L) led to the system's collapse in a certain period. The detailed analysis revealed the identification of amino acids, such as tyrosine and tryptophan, in greater quantities in the extracellular polymeric substances of reactors operated with salt. In OS III, a comparison was made between staged and conventional feeding under osmotic pressure. Staggered feeding has shown significant benefits in terms of denitrification and long-term stability. The gradual increase in salt (2.5 to 10 g/L) influenced the production of ALE, EPS and TRP, but the staggered feeding did not significantly impact their production. In OS IV, the effects of intermittent osmotic stress were investigated, comparing it with constant stress and a control system without added salt, both as a strategy to reduce the start-up time of aerobic granulation systems and to evaluate whether intermittent osmotic stress has been shown to promote rapid granulation and maintain stable ALE production. The reactor subjected to intermittent salt stress revealed rapid and complete granulation in just 21 days, contrasting with the 59 days required for the reactor with constant salt addition. Furthermore, salt addition significantly positively impacts granulation compared to the control reactor, corroborating previous findings in OS II and OS III. This finding highlights the importance of variation in saline conditions to promote efficient granule formation. Given this, the highlight goes to the reactor under intermittent saline stress, which is identified as the most efficient in granulation, stability, production of resources, and removal of pollutants. In OS V, research focused on the co-treatment of leachate with domestic sewage, with special attention to controlling sludge retention time or sludge age (SRT). The low proportion of leachate (5%) did not harm the performance and stability of AGS, while increasing the leachate fraction (10%) influenced the removal of organic matter and ALE production. Principal component analysis (PCA) highlighted SRT as crucial for optimizing biopolymer synthesis, indicating optimal production in SRT between 10 and 20 days. In summary, this research provides a detailed understanding of the factors that influence the production of bioresources in aerobic granulation systems. The results achieved significantly contribute to optimizing the performance of these systems in terms of start-up time, stability, resource production, and contaminant removal in saline and non-saline effluents, opening new paths for the sustainable evolution of wastewater treatment practices.

Keywords: Aerobic Granular Sludge; Resource Recovery; Engineering Aspects; Principal Component Analysis; Molecular Microbiology.

LIST OF ABBREVIATIONS AND ACRONYMS

AGS	Aerobic Granular Sludge
ALE	Alginate-like exopolymers
ANAMMOX	Anaerobic Ammonium Oxidation
AOB	Ammonia-Oxidizing Bacteria
ASV	Amplicon Sequencing Variant
BOD	Biochemical Oxygen Demand
CAS	Conventional Activated Sludge
COD	Chemical Oxygen Demand
DNB	Denitrifying Bacteria
DGAOs	Denitrifying Glycogen-Accumulating Organisms
DO	Dissolved Oxygen
DOC	Dissolved Organic Carbon
DPAOs	Denitrifying Phosphorus-Accumulating Organisms
EPS	Extracellular Polymeric Substances
EPS-LB	Loosely Bound
EPS-TB	Tightly Bound
GAO	Glycogen Accumulating Organisms
GG	Polyguluronic acid
HA	Humic Acids
LD	Leachate Dilution
LTP	Leachate Treatment Plant
MLSS	Mixed Liquor Suspended Solids
MLVSS	Mixed Liquor Volatile Suspended Solids
MM	Polymannuronic acid
MG	Heteropolymeric acid
MSW	Municipal Solid Waste
NOB	Nitrite-Oxidizing Bacteria
NCBI	National Center for Biotechnology Information
NOB	Nitrite-Oxidizing Bacteria
OHO	Ordinary Heterotrophic Organisms
OLR	Organic Loading Rate
OS	Operating System
PAO	Phosphorus-Accumulating Organisms
PHAs	Polyhydroxyalkanoates
PHB	Polyhydroxybutyrate
PN	Protein
PS	Polysaccharide
RRF	Resource Recovery Factories
SBR	Sequencing Batch Reactors
SOR	Specific Oxidation Rate
SEM	Scanning Electron Microscopy
SND	Simultaneous Nitrification and Denitrification
SNDPR	Simultaneous Nitrification, Denitrification, and Phosphorus Removal
SRT	Sludge Retention Time

SVI	Sludge Volume Index
T_f	Feeding Time
TKN	Total Kjeldahl Nitrogen
TN	Total Nitrogen
TP	Total Phosphorous
TRP	Tryptophan
T_s	Settling Time
TSS	Total Suspended Solids
UASB	Upflow Anaerobic Sludge Blanket
VFA	Volatile Fatty Acids
VSS	Volatile Suspended Solids
WWTPs	Wastewater Treatment Plants

LIST OF VARIABLES

X_1	Biomass concentrations in the mixed liquor
X_2	Biomass concentrations in the effluent
V_r	Reactor working volume
Q_e	Daily discharge effluent flow
$q_{COD,\ NH4,\ NOx,\ TP}$	Biomass-specific rates of organic matter and nutrient removal
C_i	Initial COD or nutrient concentration
C_f	Final concentration of COD or nutrients
X_{VSS}	Concentration of volatile suspended solids in the reactor
Ve	Effluent volume of a reactor operating cycle
t_C	Time of one operating cycle of the reactor

LIST OF FIGURES

LIST OF TABLES

SUMMARY

1. INTRODUCTION

The cultivation of aerobic granules in sequential batch reactors (SBR) proved to be possible more than 25 years ago, marking the emergence of innovative aerobic granular sludge (AGS) technology, a pioneering variant of conventional activated sludge (CAS) (Beun *et al*., 1999; Morgenroth *et al*., 1997). Unlike CAS, which forms irregular microbial aggregates of 50-300 µm, AGS, under specific conditions, has the remarkable ability to generate spherical granules with minimum dimensions of 200 µm, as officially defined at the First Aerobic Granule Workshop in 2004 (Munich, Germany) (de Kreuk *et al*., 2007).

This granular structure not only enables the formation of compact and dense biomass, characterized by mature granules with a sludge volume index (SVI_{30}) below 80 mL/g, SVI_{30} close to SVI_5 ($SVI_{30}/SVI_5 \approx 1$), and settling velocity between 10 and 90 m/h but also generates gradients of dissolved oxygen (DO) and the substrate along the radial direction (de Kreuk *et al*., 2005; Nancharaiah and Raddy, 2018; Winkler *et al*., 2012). These gradients result in layers that foster the coexistence of diverse bacterial populations with specific functions in pollutant biodegradation (Liu *et al*., 2010; Winkler *et al*., 2013). This effect allows the simultaneous removal of nutrients (nitrogen and phosphorus) and organic matter in a single reactor, standing out compared to conventional activated sludge systems (CAS) (Nancharaiah and Sarvajith, 2019; Pronk *et al*., 2017a).

Additionally, the literature (Nancharaiah and Sarvajith, 2019; Pronk *et al*., 2017a) highlights other advantages compared to CAS systems, such as resistance to high organic loads, tolerance to high toxicity levels, and reduced environmental footprint and operational costs. This is due to the ability to achieve higher biomass concentrations in the bioreactor without the need for a support medium, and all phases (anaerobic, aerobic, and anoxic) can be operated in the same SBR, eliminating the need for sludge recirculation facilities.

In addition to their effective treatment properties, AGS systems have a high potential for material recovery from biomass, especially due to the high content of extracellular polymeric substances (EPS) in this type of sludge (Hamza *et al*., 2022). This feature gives the technology the ability to recover high-value products, such as alginate-like exopolymers (ALE) and tryptophan (TRP) (Rollemberg *et al*., 2020a; Schambeck *et al*., 2020). Therefore, these systems can be considered potential resource recovery factories (RRF), contributing significantly to the principles of the circular economy in the sanitation sector (Kehrein *et al*., 2020).

In this context, it is reasonable to accept that in recent years, research on AGS has evolved significantly, particularly by examining a range of applications from domestic to complex effluents like landfill leachates (Rollemberg *et al*., 2019; Rollemberg *et al*., 2020; da Silva *et al*., 2023). This includes granule formation and removing emerging contaminants, including parabens and antibiotics (Barros *et al*., 2020a; Barros *et al*., 2021; Argenta *et al*., 2021).

A principal focus of these studies is the optimization of cultivation parameters that are crucial for enhancing granule formation and stability. Research by Rollemberg *et al*. (2018) underscores the pivotal roles of hydrodynamic shear strength and feeding cycles in the robust formation and maintenance of granules. Furthermore, these studies suggest that the choice of carbon source profoundly influences the microbial biodiversity within the granules, thereby affecting the efficiency of carbon and nutrient removal (Rollemberg *et al*., 2019). However, a gap remains in understanding the influence of studied substrates on bioresources production.

Granule formation is recognized as a multifactorial phenomenon influenced by cations such as calcium, which, under specific conditions, can expedite granulation and affect granule stability (Barros *et al*., 2020b; Barros *et al*., 2021). Despite these findings, the nuanced impacts of calcium on granule characteristics, namely extracellular polymer production and microbial activity, require deeper investigation. Furthermore, it would be interesting to evaluate the influence of additives, such as calcium, sodium, and magnesium, in the production and recovery of bioresources, such as ALE.

The stability of the granules can also be significantly impacted by the type of operational cycle, with cycles that include short anoxic phases favoring the formation of more stable granules (Rollemberg *et al*., 2020c; 2020b). The same study highlights the potential for the recovery of valuable compounds such as ALE, suggesting a new perspective for waste valorization from AGS processes.

Additionally, the pilot-scale study by Rollemberg *et al*. (2020a) revealed that strategies such as fat separation and high exchange rates during rainy periods are essential to maintaining adequate organic load and preventing the disintegration of granules. This study also highlighted the importance of a selective sludge discharge methodology to maintaining reactor efficiency.

Regarding emerging contaminants, investigations by Barros *et al*. (2020a; 2020b; 2021) and Argenta *et al*. (2021) have examined the impacts of substances like parabens and antibiotics on the structural integrity of AGS granules. These studies reveal that while such contaminants do not significantly impair organic matter removal, they alter the granule structure and affect the production of EPS.

Further studies by Silva *et al*. (2021; 2023a; 2023b) have explored the application of AGS under challenging conditions, such as the treatment of landfill leachates. These studies show that adjustments in the feeding mode and understanding the interactions between different types of effluents can significantly improve the operation of AGS systems. However, they also highlight that the variability and complexity of the effluents can adversely affect granulation and the stability of granules, signaling the need for further investigations in this area.

The literature (Silva; Rollemberg; Santos, 2021; Chen *et al*., 2013) has also highlighted staggered feeding as a potential strategy in the operation of AGS systems, as it can favor the process of simultaneous nitrification and denitrification (SND) by allowing nitrification to occur with reduced organic load during the aerobic phase, thus accelerating the nitrification rate and ensuring greater availability of organic matter for denitrification throughout the cycle. Furthermore, this type of feeding can reduce toxic loads (Silva; Rollemberg; Santos, 2021), which can be advantageous in the case of saline effluents, reducing the osmotic shock due to dilution and increasing the adsorption capacity of the AGS system. This approach could be a new strategy for adapting AGS biomass by treating saline effluents and contributing to limitations such as nitrite accumulation, commonly reported in systems with high saline concentrations (Bassin *et al*., 2011; Pronk *et al*., 2012). In this context, such possibilities would be very important when considering that NaCl is present in high concentrations in several industrial effluents, especially in circular systems, where there is a tendency for a gradual increase in salt concentration.

However, despite AGS's numerous advantages for treating domestic and/or industrial wastewater, some limitations still hinder its widespread adoption in large-scale systems. Challenges such as prolonged granulation periods, low long-term biomass stability, and problems with granule disintegration represent recurring obstacles cited in the literature (Lin *et al*., 2020; Nancharaiah *et al*., 2018; Pronk *et al*., 2017a; Hamza *et al*., 2022).

Therefore, future research must focus on optimizing operational conditions, understanding the effects of effluent composition, stabilizing granules, and primarily on the production and recovery mechanisms of bioresources to leverage this innovative technology's advantages fully. In this sense, strategies involving the enrichment of slow-growing microorganisms, with adequate selection of inoculum sludge, addition of carrier particles, and the optimization of operational conditions, emerge as alternatives to overcome these challenges and enhance the stability and efficacy of AGS (Lin *et al.*, 2020).

In this context, the present research explores advances in the application of AGS under varied conditions, focusing on the production and recovery of bioresources such as ALE and TRP. It discusses how substrate selection can enhance both treatment efficiency and bioresource recovery. It also highlights the impact of staggered feeding and intermittent osmotic stress.

It has been demonstrated that these conditions not only facilitate rapid granulation and system stability but also promote the production of bioresources, especially in environments with salinity fluctuations. This is crucial for applying AGS systems in treatments involving industrial and domestic effluents, where such fluctuations are common. In the case of domestic effluents, these fluctuations are especially common in coastal regions. For instance, cities like Hong Kong and Qingdao in China utilize seawater for flushing toilets, thereby elevating the salinity levels of municipal waste (Li *et al.*, 2020).

The research also explored the impact of leachate with domestic sewage co-treatment, showing that dilutions of up to 10% are manageable without compromising nutrient removal. However, they influence the quality of the produced biopolymers, such as ALE.

Finally, solids retention time (SRT) adjustments emerge as a key strategy to optimize system stability and bioresource production. These advances offer a promising perspective for applying AGS systems in wastewater treatment, combining treatment efficacy with sustainability through the recovery of bioresources.

1.1. Extracellular Polymeric Substances (EPS)

Understanding the production of EPS is fundamental for cultivating dense and stable aerobic granular biomass (Corsino *et al*., 2016). EPS constitute a complex structure mainly composed of proteins (PN), polysaccharides (PS), nucleic acids, humic acids (HA), and lipids, with variations influenced by the microbial composition of the biofilm, environmental conditions and wastewater characteristics (Kehrein *et al*., 2020; Carvalho *et al*., 2021; Chen *et al*., 2022a, 2022b). The literature emphasizes the significant role of EPS in forming and preserving the biofilm, protecting bacterial cells against adverse conditions such as desiccation, antibiotics, and osmotic pressures. Furthermore, it is well-established that appropriately selected operational parameters play a crucial role in promoting bacterial aggregation (Cydzik-Kwiatkowska, 2021).

Numerous contributions have been dedicated to identifying new EPS contents, with a particular focus on PN, PS, and heteropolymers with specific functions (Boleij *et al*., 2019; Graaff *et al*., 2019; Lotti *et al*., 2019; Wong *et al*., 2019; Wong *et al*., 2020). For example, PN-like aromatic substances and PN-like tryptophan were identified as more abundant in the AGS matrix, contributing significantly to the granulation process and granule stability (Zhu *et al*., 2015). Regarding polysaccharides, ALE have been recognized as functional gel-forming constituents in the extracellular matrix of AGS (Lin *et al*., 2010; Schambeck *et al*., 2020). Recently, glycosaminoglycans and sulfated polysaccharides were discovered in EPS products in AGS (Felz *et al*., 2020).

In AGS technology, imposed selection pressures, including high aeration rates and alternating feast-famine conditions, contribute to increased EPS production (Feng *et al*., 2021). However, the underlying mechanisms of EPS production and its relationship with granulation are still unclear. Therefore, more in-depth research is needed to understand EPS production during the formation of aerobic granules and its correlation with the production of ALE and TRP.

1.2. Alginate-like exopolymers (ALE)

The ALE, despite not having its structure fully elucidated, is known to consist mainly of sugars, proteins, and humic substances due to the extraction process and is identified by its ability to form a gel upon contact with divalent cations (Ca^{2+} and Mg^{2+}) (Lin *et al*., 2008; Felz *et al*., 2019; Zahra *et al*., 2022; Schambeck *et al*., 2020). Currently, commercial alginates are derived only from algae (Gao *et al*., 2018), while earlier works suggest that alginates can be derived from algae and bacteria sources (Chen *et al*., 2022).

The literature has reported that ALE production is related to system stability, successful granulation, and controlled stress sources, indicating that its production is directly linked to the proper development of granules (Schambeck *et al*., 2020). On the other hand, Santos *et al*. (2022) reported that a stress source can stimulate bioresource production. However, they emphasize the need for controlled stress sources to maximize production without compromising long-term system stability.

The gel-forming capacity of alginate is determined by its chemical composition, specifically by the presence of polyguluronic acid (GG), polymannuronic acid (MM), and heteropolymeric (MG) blocks. Among these, AGS-derived ALE exhibited the highest proportion of GG blocks (78%) and the lowest proportion of MG blocks (14%). GG blocks have a stronger affinity for divalent cations such as Ca^{2+} than MG and MM blocks, contributing significantly to the mechanical stability and viscoelasticity of the biopolymer (Sarvajith *et al*., 2023). Studies indicate that variations in carbon sources and operational settings result in different concentrations of GG blocks, thus influencing the properties of the formed ALE (Li *et al*., 2022a). These properties make alginate a widely used material in the food, medical, pharmaceutical, biotechnological, horticultural, agricultural, construction, and paper industries (Pronk *et al*., 2017b; Chen *et al*., 2022d; Sethi *et al*., 2023; Zahra *et al*., 2022; Sethi *et al*., 2023; van Leeuwen *et al*., 2018). Notably, ALE-based materials stand out for their biodegradability and recyclability compared to conventional fossil-based materials (Zeng *et al*., 2023).

Given this potential, a collaborative initiative between Dutch public entities and private stakeholders led to the development of the "Nereda Technology" for large-scale AGS applications (Van Leeuwen *et al*., 2018). Currently, there are more than 100 Nereda® plants distributed across 22 countries, two of which, located in the Netherlands, have demonstration-scale facilities for extracting bio-ALE from Nereda® granules under the product name Kaumera (Royal HaskoningDHV, 2023; Bahgat *et al*., 2023). The recovery of this bio-ALE in these facilities, Zutphen and Epe, has demonstrated gains associated with operational costs (OPEX), with a 20-30% reduction in biomass produced, lower energy consumption, and reduced CO_2 emissions (Kaumera, 2023).

According to Van Leeuwen *et al*. (2018), in reports from Royal HaskoningDHV, 80 kg of Nereda granular sludge can generate 18 kg of bio-ALE, expecting the Zutphen facility to have an annual production capacity of approximately 400 tons of alginate. The total Dutch production is estimated at 85,000 tons, resulting in approximately 170 million euros in revenues. On the other hand, Rollemberg *et al*. (2020) concluded that the final yield, after extraction and refining costs, should be around 1,000-2,000 euros per ton of bio-ALE.

1.3. Tryptophan (TRP)

The amino acid L-tryptophan is considered essential for humans and is also vital for animals, plants, and some bacterial strains (Mustafa *et al*., 2018). In industrial contexts, tryptophan (TRP) plays a significant role, finding application in the food industry as a preservative and dietary supplement in animal feed. It also plays a crucial role in the pharmaceutical industry as an active component in medications for psychiatric disorders (Carvalho *et al*., 2021).

The production of TRP can occur in three distinct ways. Firstly, TRP is artificially manufactured through controlled chemical synthesis from organic compounds such as indole. The second approach involves biochemical synthesis, where the enzyme tryptophanase, produced by bacteria, is isolated and subsequently used to generate TRP from indole, pyruvate, and ammonia. Lastly, the third alternative is microbial fermentation, in which genetically modified bacteria, such as *Escherichia coli* and *Corynebacterium glutamicum*, produce TRP directly as part of their metabolism, utilizing precursors like glucose and xylose (Niu *et al*., 2019; Konosuke & Mitsugi, 1975; Watanabe & Snell, 1972).

Recently, fluorescence analyses revealed that the amino acid TRP can accumulate in the EPS matrix (Luo *et al*., 2014; Hamza *et al*., 2018). Guo *et al*. (2020) identified TRP as one of the dominant organic materials in the EPS matrix of aerobic granules among the compounds observed. Rollemberg *et al*. (2020a) achieved a TRP production of approximately 50 mg/g VSS (Volatile Suspended Solids) in a pilot-scale sanitary wastewater treatment system.

1.4. Operational parameters affecting granulation and resource production

The search for effective strategies aimed at improving granule stability, optimizing granular biomass formation, and gaining a deep understanding of mechanisms related to the production and recovery of bioresources has been emphasized in numerous studies (Lin *et al*., 2020; Nancharaiah and Reddy, 2018; Pronk *et al*., 2017). Various factors, such as cycle distribution, organic loading rate (OLR), sludge discharge, shear stress, temperature, and microbial diversity, have been identified as crucial in synthesizing these biological resources in AGS systems (Chen *et al*., 2022). Variations in OLR and organic loading shocks can trigger peaks in ALE, which are associated with increased formation of the second messenger cyclic guanosine monophosphate (c-di-GMP) (Yang *et al*., 2014). A C:N ratio close to 5 has been identified as ideal for TRP production, while higher C:N ratios favored ALE synthesis (Rollemberg *et al*., 2020b). Cultivating granules under saline stress and adding cations (Ca^{2+} and Mg^{2+}) were favorable for granulation and the production of these bioresources (Liu *et al*., 2010; Cui *et al*., 2021). Moreover, extended cellular retention times (>20 days) may reduce ALE and TRP content (Rollemberg *et al*., 2020b). This robustness and versatility have attracted significant interest, particularly in treating complex effluents such as landfill leachates.

Different substrates influence the microbial community's alteration due to various microbial metabolic processes. Consequently, feeding different substrates to reactors, considering the molecular size and category factors, influences the pattern of extracellular polymeric substances (EPS) secretion. Acetate and propionate favor phosphorus-accumulating organism (PAO) populations, which have been associated with increased ALE biosynthesis (Schambeck *et al*., 2020). Santos *et al*. (2022) observed higher ALE and TRP production associated with acetate and propionate; however, only propionate showed stable long-term biomass. In addition to being reported to support PAO-rich populations, glycerol is cited as one of the best substrates for alginate production. At the same time, glucose and sucrose negatively impact bacterial alginate production in pure cultures (Borgos *et al*., 2013). Furthermore, glycerol, glucose, and sucrose may stimulate tryptophan production since these substrates can generate PEP (phosphoenolpyruvate) as a metabolic intermediate consumed by microorganisms during tryptophan production (Niu *et al*., 2019).

Meng *et al*. (2019b) suggested that moderate salinity (around 1% NaCl, approximately 10 mg/L) triggered the expression of the AlgC gene in Pseudomonas, activating the enzyme phosphomannomutase, which is part of the alginate biosynthesis mechanism (Moradali *et al*., 2018). Moreover, Na^+ is involved in various transport processes and can be considered a promoter of enzymatic activity if maintained at appropriate concentrations, leading to increased EPS production at low salinity levels due to the stimulation of bacterial activity (Cui *et al*., 2015). However, excessive Na^+ presence can replace weakly bound divalent cation-EPS linkages, leading to the breakdown of the polymeric structure (Cui *et al*., 2015; Cui *et al*., 2021). Additionally, salinity is reported to positively affect the granulation process, as it reduces the electronegativity on the cell surface, promoting granulation and system stability (Campos *et al*., 2018; Cui *et al*., 2021).

Regarding operational configurations, the literature has reported that staged feeding, for example, is advantageous for aerobic granule stability, allowing system optimization by improving microbial community composition, granule size, and denitrification (Silva; Rollemberg; Santos, 2021; Chen *et al*., 2013). This is because, under these conditions, the influent is pumped into the system at different cycle times, in anoxic phases, increasing denitrification efficiency. It also allows nitrification with lower organic loadings in the aerobic phase, accelerating the nitrification rate and saving aeration consumption for organic matter (Chen *et al*., 2013). Silva, Rollemberg and Santos (2021) reported total nitrogen removal above 90% using staged feeding to treat synthetic effluents similar to leachate. It is essential to note that this type of feeding can reduce toxic loads, such as those from leachates (Silva; Rollemberg; Santos, 2021). In the case of saline effluents, for example, it can reduce osmotic shock, favoring dilution and the adsorption capacity of AGS.

On the other hand, Chen *et al*. (2015) reported that for denitrifying granule cultivation in an upflow anaerobic sludge blanket (UASB) reactor, intermittent Mg^{2+} supplementation is recommended. Niu *et al*. (2017) demonstrated that the semi-starvation fluctuation C/N ratio favored the denitrifying granule cultivation process, promoting improved nitrogen removal and increased microbial diversity compared to a constant C/N ratio. However, the effect of intermittent supplementation in AGS systems is not mentioned in the literature.

The solids retention time (SRT), in turn, has been highlighted as a parameter that plays a crucial role in granule stability, AGS efficiency during long operational periods, and bioresources production (Bassin *et al*., 2012; Zhu *et al*., 2013; Rollemberg *et al*., 2022; Rollemberg *et al*., 2020b). Rollemberg *et al*. (2022) reported that selectively discharging sludge by controlling the SRT between 10 and 20 days is an essential operational strategy for granule formation, maintenance, and AGS performance.

In this context, this study aimed to optimize SBR-AGS reactors concerning granulation and AGS system stability, as well as bioresources production and recovery. Different carbon sources were initially evaluated to determine the best-favored system stability and resource production. Once the carbon source was defined, the effects of salinity on resources production stability were assessed, as well as the effect of staged feeding and intermittent osmotic stress. Finally, the effects of SRT control through intentional biomass discharge in leachate co-treatment systems were investigated. Therefore, the research was divided into five periods, as presented in Figure 1.

To guide this investigation, we proposed the following general hypothesis: Variability in the feeding substrate (including acetate, propionate, glycerol, glucose, and sucrose), the feeding regime, and the controlled addition of salt in AGS systems significantly affect sludge characteristics, stability, and bioresource production. Certain substrates are expected to promote higher bioresource production. At the same time, different feeding regimes and salt addition may enhance granule stability under osmotic stress, thereby boosting AGS system resilience and overall performance.

This hypothesis led to some questions that guided the research, such as:

1) How do different substrates influence EPS, ALE, and TRP production in AGS systems?
2) How do various feeding regimes (conventional versus staged feeding) affect nutrient removal efficiency and stability of AGS under conditions of different saline concentrations?
3) What is the tolerance threshold for osmotic stress beyond which the treatment system's efficiency is compromised?
4) Does the controlled addition of salt improve bioresources production, contributing to the stability and formation of aerobic granules?
5) How does intermittent osmotic stress impact the stability and functionality of AGS systems, particularly regarding nutrient removal and resistance to toxic loads?
6) How do varying concentrations of leachate influence granule formation, system stability, and biopolymer production in AGS systems?
7) How does controlling SRT affect ALE production and nutrient removal efficiency in AGS systems?

Figure 1 – Thesis general structure.

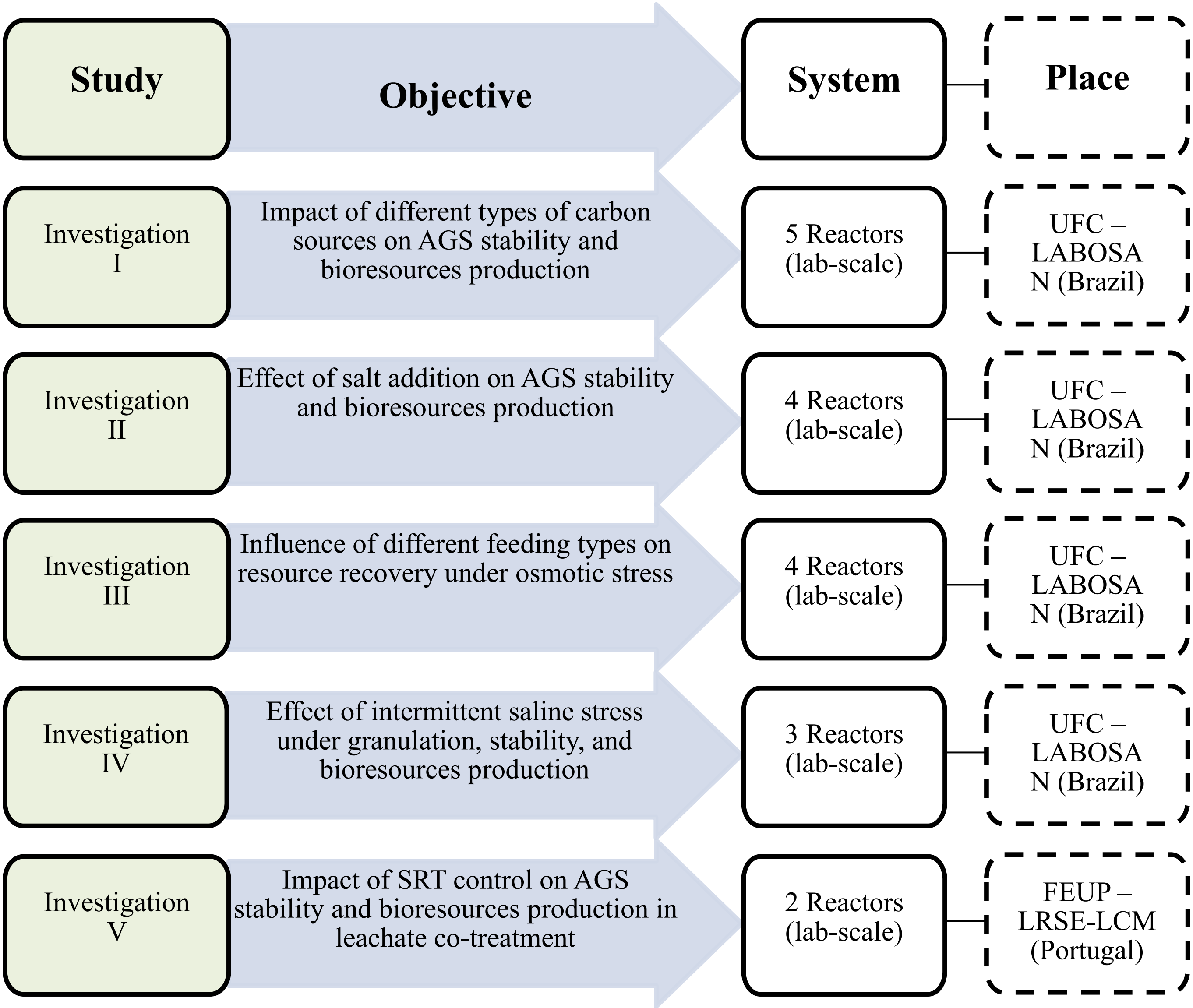

2. OBJECTIVE

2.1 General objective

To evaluate and optimize the granulation process, stability, and performance of aerobic granular sludge (AGS) in reactors focusing on the recovery of alginate-like exopolymers (ALE) and tryptophan (TRP).

2.2 Specific objectives

(i) To investigate the impact of different carbon sources on granulation, stability, and bioresource production in AGS systems (Chapter 4);

(ii) To evaluate how the gradual addition of salt influences the stability of aerobic granules in wastewater treatment systems (Chapter 5);

(iii) To investigate the impact of salt concentration on the production of bioresources, such as ALE and TRP, in AGS systems (Chapters 5 and 6);

(iv) To examine the effects of operating regime on bioresource recovery in AGS systems under osmotic stress, with an emphasis on the production of ALE, TRP, and EPS and long-term stability (Chapter 6);

(v) To investigate the impact of intermittent salt stress on the formation and stability of aerobic granules (Chapter 7);

(vi) To evaluate how intermittent salt stress affects the production and recovery of valuable bioresources, such as ALE and TRP, in AGS systems (Chapter 7);

(vii) To evaluate bioresource production in the co-treatment of leachate with domestic sewage in AGS systems (Chapter 8);

(viii) To analyze the effect of SRT control, through selective biomass removal, on stability and bioresource production in AGS systems (Chapter 8).

3. MATERIAL AND METHODS

The research was divided into five main stages, each outlining a subsequent chapter in the thesis structure. The first four phases were developed at the Environmental Sanitation Laboratory (LABOSAN), affiliated with the Department of Hydraulic and Environmental Engineering (DEHA) at the Federal University of Ceará (UFC). Meanwhile, the final stage was carried out at the Laboratory of Separation and Reaction Engineering - Laboratory of Catalysis and Materials (LSRE-LCM), located in the Department of Chemical Engineering (DEQ) at the Faculty of Engineering of the University of Porto (FEUP), Portugal.

Different operational conditions and stress sources were assessed in each experimental unit to optimize AGS systems in terms of stability and resource production. In Operational System I (OS I), during the initial phase, the influence of various carbon sources on granule formation, their stability, and the potential for resource production was investigated. Once the optimal carbon source was determined concerning stability and resource production, it was applied in subsequent stages. The impact of different stress sources and reactor configuration changes on granulation, stability, and resource production were evaluated in these phases. These included: saline stress in the second stage (Operational System II – OS II); staggered and conventional feeding under saline stress in the third stage (Operational System III – OS III); intermittent saline stress in the fourth stage (Operational System IV – OS IV); and finally, in the last stage (Operational System V – OS V), the influence of co-treatment of leachate with synthetic domestic sewage was assessed, along with the impact of controlling SRT.

3.1. Operating System I (OS I)

The experiment was conducted in five conventional configuration sequencing batch reactors (SBR) under similar operational conditions, varying only the influent carbon source, which was chosen as follows: acetate (R1), propionate (R2), glycerol (R3), glucose (R4), and sucrose (R5). Acetate and propionate were selected due to their ability to promote phosphorus-accumulating organisms (PAOs) growth, previously associated with increased ALE biosynthesis (Schambeck *et al.*, 2020). In addition to being reported as supportive of PAO-rich populations, glycerol is cited as one of the best substrates for alginate production. At the same time, glucose and sucrose negatively impact bacterial alginate production in pure cultures (Borgos *et al*., 2013). On the other hand, glycerol, glucose, and sucrose may stimulate tryptophan production since these substrates can generate PEP (phosphoenolpyruvate) as a metabolic intermediate consumed by microorganisms during tryptophan production (Niu *et al*., 2019).

The reactors were made of acrylic, with a working volume of 7.6 L and dimensions of 100 cm in height and 10 cm in internal diameter, resulting in a height/diameter ratio (H/D) of 10 (Figure 2). The experiment spanned 215 days, divided into three stages: Stage I (30 days), Stage II (35 days), and Stage III (150 days), as detailed in Table 1. The SBRs were operated at room temperature (28 ± 2 ◦C) and inoculated with biomass from a carousel-type activated sludge system designed to treat wastewater (Fortaleza, Ceará, Brazil). Approximately 3.8 L of biomass was introduced into each reactor, whose inoculum sludge had an initial concentration of VSS of 2.2 g/L and a sludge volume index in 30 minutes (SVI_{30}) of 218 mL/g.

Figure 2 – Schematic representation of the SBR-AGS system used in the experiment.

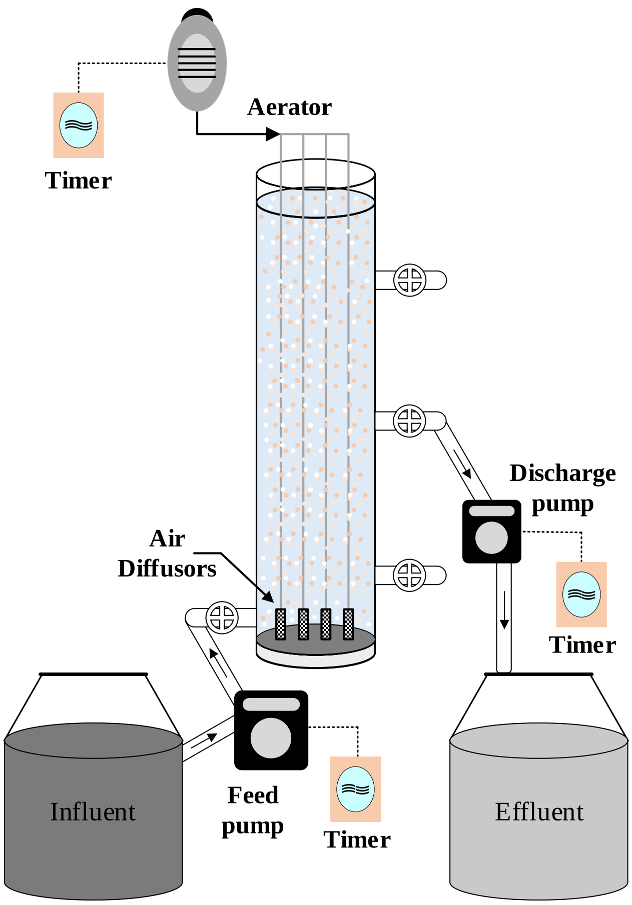

Initially, to gradually acclimate the biomass, the SBRs were operated for the first 10 days with 8-hour cycles, later reduced to 6 hours. Thus, the cycle was divided into anaerobic feeding (20 min), anaerobic reaction period (100 min), aerobic reaction period (210-330 min), anoxic period (0-10 min), settling (30-5 min), and withdrawal (< 1 min), with the settling period gradually reduced, and the surplus time added to the aerobic period (see Table 1). The literature recognizes this reduction as favorable for selecting slow-growing microorganisms (Rollemberg *et al*., 2018). The volumetric exchange ratio was also altered during operation, being 25% in Phase I (acclimatization) and 50% in subsequent phases (see Table 1). This increased the applied organic loading rate (ORL) over the phases, ranging from 0.5 to 2.0 g COD/L/day. Finally, the dissolved oxygen (DO) concentration remained around 3 to 6 mg/L throughout the entire experimental period.

During the anaerobic period, sludge mixing was carried out through 1-minute aeration pulses every hour. Aeration was provided by an air compressor (ACO003, Sunsun, China), injected by fine-bubble porous diffusers located at the reactor bottom, with an aeration rate of 10 L/min, resulting in a superficial air velocity of 2.1 cm/s. Notably, in this study, the sludge retention time (SRT) was not controlled by intentional sludge discharge. However, the average SRT was calculated based on the biomass washed out along with the final effluent, as per Equation 1.

$$SRT = \frac{X_1 V_r}{X_2 Q_e} [days] \tag{1}$$

Where X_1 and X_2 are the biomass concentrations (g VSS/L) in the reactor mixed liquor and effluent, respectively, Vr is the reactor working volume (L), Qe is the daily effluent flow withdrawn (L/day).

The feeding solution was prepared with potable water, a carbon source, a basal medium (macro and micronutrient solution), and a buffer. The composition of the synthetic wastewater was as follows: 1000 mgCOD/L, 50 mgNH_4^+-N/L (NH_4Cl), 10 mgPO_4^{3-}-P/L (KH_2PO_4), 2 mgCa^{2+}/L ($CaCl_2 \cdot 2H_2O$), 5 mgMg^{2+}/L ($MgSO_4 \cdot 7H_2O$) e 1mL/L of micronutrient solution (50mg/L of H_3BO_3; 2.7g/L of $FeCl_2 \cdot 4H_2O$; 50mg/L of $ZnCl_2$; 500mg/L of $MnCl_2 \cdot 4H_2O$; 38mg/L of $CuCl_2 \cdot 2H_2O$; 50 mg/L of $(NH_4)_6Mo_7O_{24} \cdot 4H_2O$; 90 mg/L of $AlCl_3 \cdot 6H_2O$; 2 g/L of $CoCl_2 \cdot 6H_2O$; 92 mg/L of $NiCl_2 \cdot 6H_2O$; 162 mg/L of $NaSeO_3 \cdot 5H_2O$; 1 g/L of EDTA). The feeding solution was buffered with 2.5 g/L of sodium bicarbonate ($NaHCO_3$) to maintain a neutral pH. In phases I and II, the COD concentration was 750 mg/L, maintaining the C:N ratio of 20, which was considered favorable for ALE production (Rollemberg *et al*., 2020b).

COD concentrations of 1000mg/L were adopted for similar effluents from decentralized units, in addition to being preferable concentrations to stimulate granulation.

Table 1 – Operating conditions applied in each phase of the experiment.

Phase	Duration (days)	Operational cycle						HRT (h)	Vol. Exc. (%)
		Anaer. feeding (min)	Anaer. (min)	Aerobic (min)	Anoxic (min)	Settl. (min)	Decanting (min)		
I	10	20	100	330	0	30	< 1	36	25%
	20	20	100	210	10	20	< 1	24	25%
II	35	20	100	220	10	10	< 1	12	50%
III	150	20	100	225	10	5	< 1	12	50%

3.2. Operating System II (OS II)

The experiments were carried out in four identical SBRs inoculated with the same biomass and operated under the same conditions, changing only by carbon source (acetate or propionate) and salt addition. Acetate was chosen for its higher resource production in AGS systems, while propionate was selected due to the greater stability in granulation and maturation in these systems, as observed in the results of the previous experiments (OS I). Additionally, salt stress has been evaluated because it can potentially increase resource production (Meng *et al*., 2019b).

Control systems R1 (acetate) and R2 (propionate) were fed without salt supplementation, with the operation divided into phases of granulation (32 days) and maturation (128 days). In comparison, the salt-supplemented systems R3 (acetate) and R4 (propionate) were operated with phases of granulation and increasing addition of NaCl (2.5, 5.0, 7.5, and 10.0 g/L), as can be seen in Figure 3.

Similar to OS I, the SBRs were made of acrylic material, with a working volume of 7.6 L, 1 m in height, and a height/diameter ratio of 10. The operational cycle consisted of anaerobic feeding (20 min), anaerobic period (100 min), aerobic period (220–225 min), anoxic period (0-10 min), settling (20-5 min), and withdrawal (<1 min), with a total duration of 6 h. The settling of AGSs was gradually reduced from 20 min to 5 min during the granulation stage, with the subtracted time being added to the aerobic period. During the aeration periods, the air was provided using an air compressor, with an aeration rate (10 L/min), surface gas velocity (2.1 cm/s), volumetric exchange ratio (50%), ORL (2.0 gCOD/L/d), operating temperature (28 ± 2 ◦C) and DO (around 3 to 6 mg/L) precisely the same of OS I. The SRT was not controlled by intentional sludge discharge but was calculated as described for the OS I (see topic 3.1). The systems were also inoculated with 3.8 L of biomass from a carousel-type activated sludge system (Fortaleza, Ceará, Brazil), such as OS I. The characteristics of the biomass were practically the same (MLVSS ~2.4 g/ L and SVI_{30}~215 mL/g).

Figure 3 – NaCl concentration in AGS systems over 160 operational days.

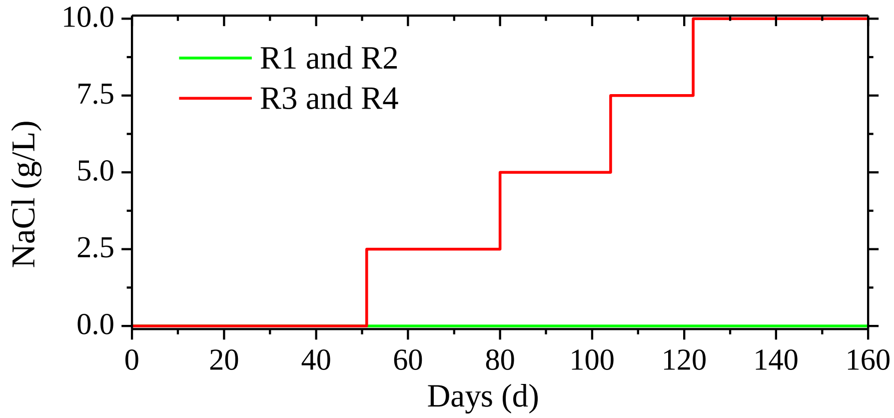

The feeding solution was also prepared according to OS I, using potable water, carbon source (1000 mg COD/L), macro and micronutrient solution, and buffer (see topic 3.2). Cooking NaCl was added, as already mentioned, at concentrations of 2.5, 5.0, 7.5, and 10 g/L and different research moments in R3 and R4, as indicated in Figure 3. Reagents were of analytical grade and were used without further purification.

Low saline concentrations were adopted, as the study aimed mainly to understand how saline stress can contribute to granulation, system stability and recovery of bioresources, after all, the idea would not be to lead the system to total collapse. Furthermore, these salt concentrations are typically found in a variety of systems, especially in circular systems, where there is a tendency for the salt concentration to gradually increase. This research aligns with broader findings, such as those reported by

Panagopoulos (2022), noting that saline concentrations in wastewater can range widely from 0.5 to 150 g/L. Concentration of around 5 g/L is particularly common in co-treatment systems or mixed effluents. For instance, cities like Hong Kong and Qingdao in China utilize seawater for flushing toilets, thereby elevating the salinity levels of municipal waste (Li *et al*., 2020b).

3.3. Operating System III (OS III)

Four identical AGS systems were operated for 157 days with increasing salt addition, changing only the carbon source (acetate or propionate) and feeding method, as represented in the scheme in Figure 4. Two reactors had conventional feed, using acetate (R1) and propionate (R2) as carbon sources. Another two reactors had staggered feed and operated with acetate (R3) and propionate (R4).

Acetate and propionate were chosen for the same reason as OS II, and previous research has demonstrated that staggered feeding (Silva; Rollemberg; Santos, 2021) improves simultaneous nitrification and denitrification (SND) conditions. The four systems were divided into six experimental stages, differentiated as follows:

- Stage 0 – granulation without salt addition;
- Stage 1 – beginning of maturation without salt addition;
- Stages 2, 3, 4, and 5 – salt addition in increasing concentrations of 2.5, 5.0, 7.5, and 10.0 g/L, respectively.

The reactors had the same configurations as previous systems. However, the staggered feeding systems had three anaerobic feedings during the cycle, the first of 10 min at the cycle beginning and the second and third of 5 min with 40% and 60% of the cycle time, respectively. In contrast, conventional systems had a single 20-min anaerobic feed at the cycle beginning, as in previous systems.

Similar to previous experiments, the operational cycle had, in addition to feeding, an anaerobic period (100 min), aerobic period (220–225 min), anoxic period (0-10 min), settling (20–5 min), and withdrawal (< 1 min), with a total duration of 6 h and the reduced of settling period was added to the aerobic period. Aeration during aerobic periods was carried out as described for the previous systems, with the same devices and parameters of aeration rate (10 L/min), surface gas velocity (2.1 cm/s), and DO (around 3 to 6 mg/L). The hydraulic retention time (HRT) was 12 hours with a volumetric exchange ratio of 50%. The applied organic load rate (ORL) was also 2.0 g/L/day, with operation at room temperature (28 ± 2 ◦C). Flocculent aerobic biomass was also used as inoculum, collected at the same wastewater treatment plant (WWTP) (Fortaleza, Ceará, Brazil). With similar characteristics (MLVSS ~2.6 g/ L and SVI_{30}~213 mL/g), approximately 3.8 L were introduced into each reactor during start-up. The SRT was not controlled by intentional sludge discharge but was calculated as described for the OS I (see topic 3.2).

The feeding solution was prepared according to the previous systems, using drinking water, carbon source (1000 mg COD/L), macro and micronutrient solution, and buffer (see topic 3.1), in addition to the increasing table salt addition at concentrations of 2.5, 5.0, 7.5, and 10 g/L, according to each stage of the experiment.

Figure 4 – Operational variations in the four AGS systems subjected to different carbon sources and feed types.

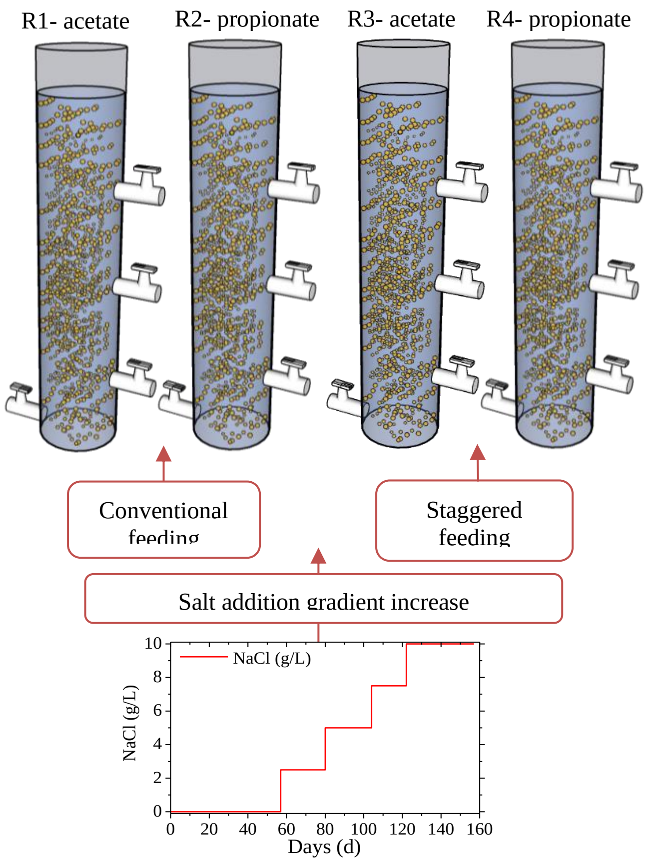

3.4. Operating System IV (OS IV)

Three sequential batch reactors (SBRs) with the exact dimensions as the previous systems (see topic 3.2) and manufactured in acrylic were operated under the following conditions:

- R1 – control system operated without saline addition;
- R2 – continuous stress of 5g/L NaCl; and
- R3 – system subjected to intermittent saline stress additions, that is, one cycle was fed with 5 g/L NaCl and the following cycle without salt addition. This intermittence in feeding continued throughout the operational period.

As already mentioned, salt stress can increase resource production and is cited as accelerating the granulation process (Meng *et al*., 2019a). A source of intermittent stress or semi-starvation, as cited by the literature on anaerobic granulation (Chen *et al*., 2015; Niu *et al*., 2017), is favorable to the growth process of denitrifying granules, promoting better nitrogen removal and increased microbial diversity. For these reasons, osmotic stress was used from the beginning of granulation under constant and intermittent conditions.

The AGS systems operated for 80 days with operating cycles equal to previous systems of conventional feeding: an anaerobic period lasting 120 minutes, of which 20 minutes was spent feeding, an aerobic phase spanning 220 to 225 minutes, an anoxic period of 0 to 10 minutes, settling for 20 to 5 minutes, and discharge in less than 1 minute, resulting in a cycle lasting 6 hours. The settling period was reduced from 20 min to 5 min in the first three operational weeks, with the subtracted time initially added to the anoxic period and later to the aerobic one.

In all reactors, namely OS I, II, III, and IV, the operation was automated through synchronized timers. During the aeration periods, the air was supplied using an air compressor (ACO-003, Sunsun, China) with an aeration rate of 10 L/min and a surface gas velocity of 2.1 cm/s. The reactors operated at room temperature (28 ± 2 °C), maintaining DO levels around 3 to 6 mg/L, volumetric exchange of 50% and OLR of 2.0 g/L/day. The SRT was not controlled through intentional sludge discharge but was calculated as described for OS I (see topic 3.2).

The inoculum sludge was collected from a secondary decanter of an aerated biofilter of a WWTP that was different from the other previous systems (Fortaleza, Ceará, Brazil). In the same way, around 3.8 L of sludge with a concentration of approximately 5.0 g/L and an SVI_{30} of 368 mL/g were used in each reactor during start-up.

The systems were fed using propionate as a carbon source (1000 mgCOD/L) since it was considered favorable for granule stability and resource production (Santos *et al*., 2022). Furthermore, the feeding solution was prepared with basal medium (macro and micronutrient solution) and buffer as described for OS I (see topic 3.1). Additionally, 5g/L of salt (NaCl) was introduced to the systems experiencing osmotic stress, while all reagents were used in their original state without further purification.

3.5. Operating System V (OS V)

Two cylindrical SBRs operated in parallel, maintaining identical operational conditions, except for the control of the SRT, were used. In R1, there was no intentional biomass wasting, while in R2, the SRT was controlled, as indicated in Table 2. The reactors, made of double-walled acrylic, had dimensions of 70 cm in height and 15 cm in internal diameter, resulting in a height/diameter (H/D) ratio of 4.6, however, the useful height was only 35 cm, leading to a working volume of 6.0 L and H/D ratio of 2.3, as represented in Figure 5. The temperature was kept around 25°C (±2°C) through a water recirculation thermostatic bath surrounding each reactor.

Each reactor was equipped with eight diffusers (porous stone, model AS-1) evenly distributed at the base and connected to the compressed air line. The airflow in the system was controlled using pressure-regulating valves, solenoid valves, and a rotameter. Additionally, an oxygen controller (HACH, model sc200) was used to maintain the DO between 2 and 4 mg/L during aerobic periods, a range considered optimal for achieving high simultaneous nitrification and denitrification (SND) efficiencies (Layer *et al*., 2020). During the anaerobic and anoxic feeding phases, the mixed liquor was stirred by a central mechanical agitator (VWR, model - VOS Power Control) in each reactor.

Over the 192 days of operation, seven distinct stages were conducted, involving variations in the percentage of landfill leachate used in co-treatment and the cycle time, as described in Table 2. In the granulation stages and stage 1, the cycle lasted 12 hours, and 5% leachate was used in co-treatment. In subsequent stages, the cycle time was reduced to 6 hours, maintaining the same leachate addition. In stage 5, there was an increase to 10% leachate with a subsequent decrease (5%) in stage 6 to assess whether the AGS system could readapt to initial conditions.

The low dilutions adopted are because the volume of leachate generated is usually less than 10% of the influent flow to the WWTPs (Silva *et al*., 2023a). At the same time, the reduction in treatment time was investigated to assess the impact of leachate in a 6-hour cycle, commonly adopted in domestic wastewater treatment.

Table 2 – Summary of investigation stages.

		Granulation	Stage 1	Stage 2	Stage 3	Stage 4	Stage 5	Stage 6
R1 and R2	Day	1 to 40	41 to 78	79 to 102	103 to 122	123 to 143	144 to 170	171 to 192
	COD	1045 mg/L (500 mg/L Acetate + 500 mg/L propionate + 45 mg/L Leachate)	1045 mg/L (500 mg/L Acetate + 500 mg/L propionate + 45 mg/L Leachate)	1045 mg/L (500 mg/L Acetate + 500 mg/L propionate + 45 mg/L Leachate)	1045 mg/L (500 mg/L Acetate + 500 mg/L propionate + 45 mg/L Leachate)	1045 mg/L (500 mg/L Acetate + 500 mg/L propionate + 45 mg/L Leachate)	1045 mg/L (500 mg/L Acetate + 500 mg/L propionate + 90 mg/L Leachate)	1045 mg/L (500 mg/L Acetate + 500 mg/L propionate + 45 mg/L Leachate)
	NH_4^+-N	70 mg/L (60 mg/L synthetic sewage + 10 mg/L leachate)	135 mg/L (125 mg/L synthetic sewage + 10 mg/L leachate)	135 mg/L (125 mg/L synthetic sewage + 10 mg/L leachate)	135 mg/L (125 mg/L synthetic sewage + 10 mg/L leachate)	135 mg/L (125 mg/L synthetic sewage + 10 mg/L leachate)	135 mg/L (125 mg/L synthetic sewage + 20 mg/L leachate)	135 mg/L (125 mg/L synthetic sewage + 10 mg/L leachate)
	PO_4^{3-}-P	18 mg/L (basically synthetic sewage)	18 mg/L (basically synthetic sewage)	18 mg/L (basically synthetic sewage)	18 mg/L (basically synthetic sewage)	18 mg/L (basically synthetic sewage)	18 mg/L (basically synthetic sewage)	18 mg/L (basically synthetic sewage)
	Cycle time (h)	12	12	6	6	6	6	6
	ORL(g/L/d)	1	1	2	2	2	2	2
	Leachate percentage	5%	5%	5%	5%	5%	10%	5%
R1	Sludge retention time (days)	Without control	Without control	Without control	Without control	Without control	Without control	Without control
R2		Without control	Without control	Without control	10 (±1)	23 (±3)	25 (±4)	Without control

Figure 5 – Schematic representation of the experimental SBR-AGS system used in this study.

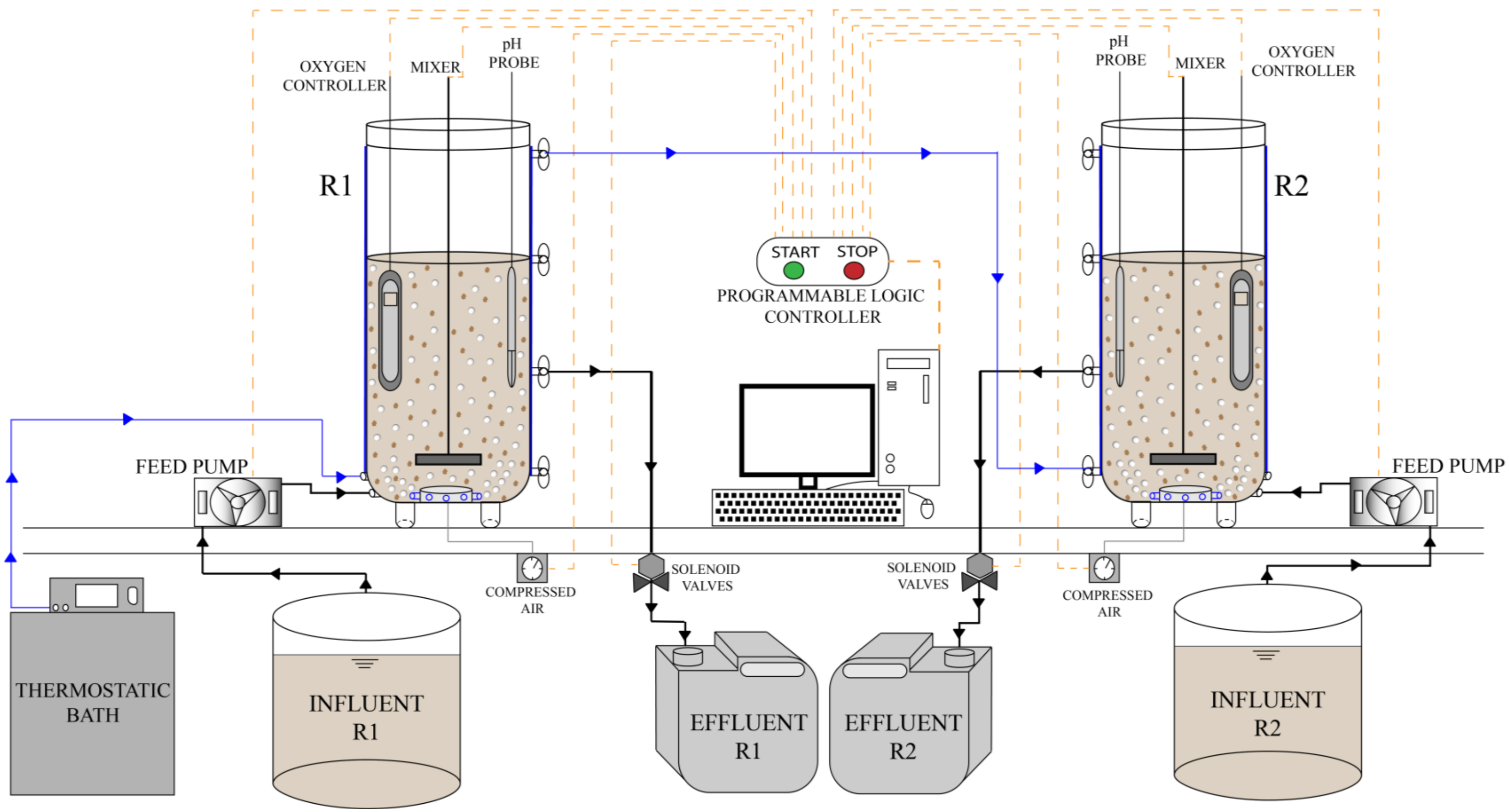

Fonte: da Silva *et al*. (2023a).

The operational cycle was managed through a programmable logic controller (PLC) (Delta model DVP-SS2) to automate the staggered feeding, anaerobic, anoxic, and aerobic periods, as well as settling and discharge at the end of the cycle, with a volumetric exchange ratio of 50%. Figure 6 provides detailed insights into the operational cycles of all the OS analyzed. Specifically, operational cycles of 12- and 6 hours were implemented for the OS V system. Previous research has demonstrated that staggered feeding (Silva; Rollemberg; Santos, 2021) improves simultaneous nitrification and denitrification (SND) conditions. Generally, this feeding practice involves introducing the influent into the SBR at three distinct moments: half of the influent at the beginning of feeding, followed by 1/4 and 1/4 with intervals of 40% and 60% from the start of the cycle, respectively (Figure 6c and d).

Figure 6 – Cycle distribution in operating systems I, II, III, IV, and V.

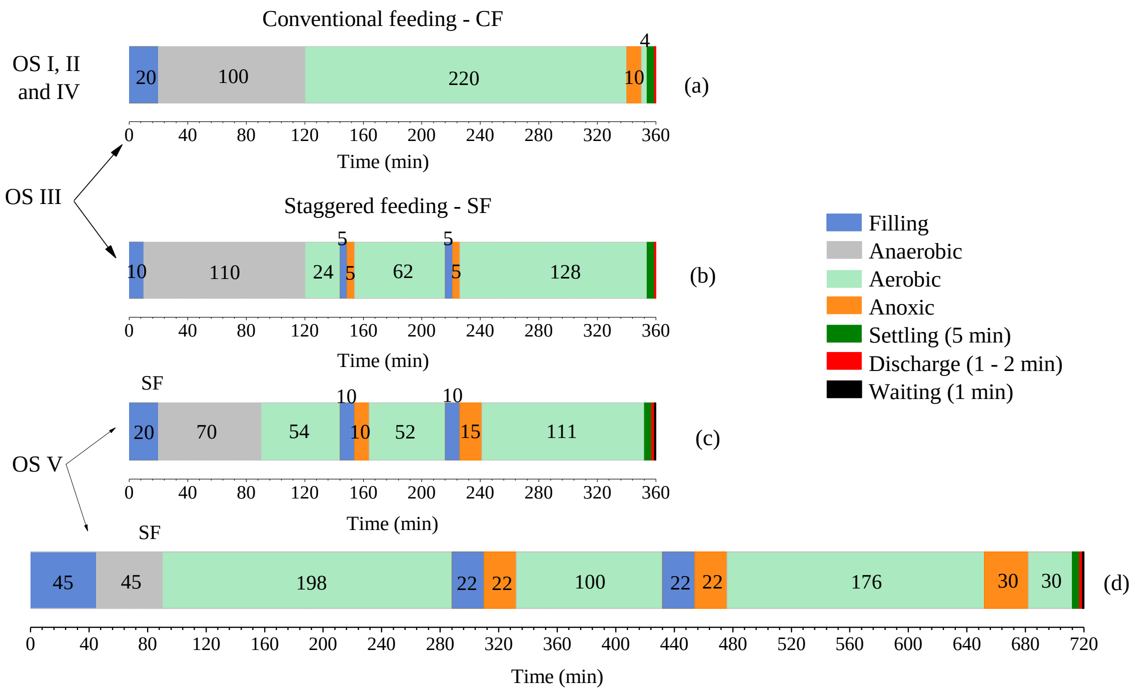

Daily, between days 103 and 170, a selective sludge discharge was performed in R2 to control the SRT. This discharge involved 30% of the granular sludge from the bottom and 70% of the more filamentous biomass from the top of the reactor, calculated based on the total mass, as described in protocol 1 by Rollemberg *et al*. (2022). The goal was to discharge the older P-rich/saturated granules at the bottom of the SBR and the filamentous/flocculent sludge at the top. In Table 2, the SRT in operational stages with selective sludge discharge can be observed. In other stages, even without intentional biomass discharge, the SRT was monitored based on the amount of biomass leaving with the final effluent, following the calculation presented for OS I.

Biomass from a leachate treatment plant (LTP) at an urban solid waste landfill in northern Portugal was used as the inoculum. The system comprised an aerobic stabilization pond, a biological process, and a coagulation-flocculation-flotation unit. Approximately 3.0 L (5.6 g/L) of biomass collected from the biological aeration tanks was inoculated into each reactor. The landfill leachate used in this study was collected in the aerobic stabilization pond, after the coagulation-flocculation-flotation unit at the same LTP. The characterization of the pre-treated leachate is shown in Table 3. This landfill has been operating since 1999 and receives 450,000 tons annually, generating between 100 and 150 m^3 of leachate daily.

The feed solution was prepared using potable water, a carbon source, a basal medium (macro and micronutrient solution), and a buffer as described for OS I (see topic 3.1), in addition to the leachate addition in the proportions described in Table 2.

Table 3 – Composition of pre-treated leachate collected from a sanitary landfill in Porto, Portugal, used in this research.

Parameter	Value
pH	8.5±0.7
Conductivity (µS/cm)	3896±325
COD total (mg/L)	896±97
NH_4^+-N (mg/L)	15±2
NO_2^--N (mg/L)	19±11
NO_3^--N (mg/L)	212±63
Chloride (mg/L)	3714±13
Sulfate (mg/L)	1289±44
Phosphate (mg/L)	9±2
Calcium (mg/L)	98±5
Magnesium (mg/L)	106±1
Potassium (mg/L)	1873±27

The composition and characteristics of leachate produced by landfills are directly influenced by a series of interrelated factors, including the age of the landfill, the nature and composition of the deposited waste, climatic conditions, and specific landfill characteristics such as topography, depth, and internal temperature (Bhalla *et al*., 2013; Gao *et al*., 2015; Renou *et al*., 2008). These elements determine the heterogeneity of the leachate, which goes through different degradation phases over time. From the beginning of its operation, the landfill undergoes aerobic, acetogenic, methanogenic, and stabilization stages, resulting in the formation of distinct types of leachates that can be classified as young (less than 5 years), intermediate (5 to 10 years), and mature or stabilized (more than 10 years), with properties varying according to the maturation of the landfill (Kjeldsen *et al*., 2002; Miao *et al*., 2019; Renou *et al*., 2008).

Given that the unit's operating time exceeds 10 years, it is assumed that the leachate originates from a landfill in the maturing or stabilized phase, characterized by low biodegradability and a chemical composition that reflects long-term transformation and accumulation processes.

Furthermore, the coagulation-flocculation-flotation unit through which the leachate was treated significantly contributed to reducing suspended solids and other contaminants, improving the final effluent quality through the aggregation and removal of colloidal particles. As a result, the characteristics presented in Table 3 are highlighted. It is worth noting that due to the low biodegradability of the leachate, after passing through the coagulation-flocculation-flotation system, organic matter in the aerobic stabilization lagoon is absent.

3.6. Analytical methods

The system performance was monitored through influent and effluent analyses and the physical-chemical characterization of biomass, conducted at intervals of 2 to 3 days.

In all the systems, the analyses of chemical oxygen demand (COD), ammonia (NH_4^+-N), nitrite (NO_2^--N), nitrate (NO_3^--N), phosphorus in the form of phosphate (PO_4^{3-}-P), mixed liquor suspended solids (MLSS), mixed liquor volatile suspended solids (MLVSS), and sludge volume index at 5 (SVI_5), 10 (SVI_{10}), and 30 (SVI_{30}), according to methodologies described in the Standard Methods (APHA, 2012). In the case of COD, the method was adapted using 2x sample dilutions at the determination time and mercury sulfate ($HgSO_4$) addition in the digester solution, in the proportion of 10:1 (10 g of $HgSO_4$ for each gram of NaCl (Kayaalp *et al*., 2010). The dissolved oxygen and pH were monitored using an analytical probe (YSI 5000, YSI Inc., USA). Total Nitrogen (TN) was determined by summing all nitrogen fractions (NH_4^+-N, NO_2^--N, and NO_3^--N), considering that the synthetic influent, supplemented only with ammonia, did not contain organic nitrogen fractions. However, in the case of OS V, total nitrogen was assessed using a colorimetric kit due to the addition of leachate to the influent, with readings taken from the spectrophotometer (Merck-Lange, Germany).

Ion chromatography in all experiments was conducted according to Mourão *et al*. (2021), except OS V. For this set-up, a Dionex™ ICS-2100 system equipped with an IonPac® AS11-HC column (4x250 mm) was used for the determination of anions, while a Dionex™ DX-120 system with an IonPac® CS12A column (4x250 mm) was employed for cation analysis. A sample volume of 5 μL, filtered through a 0.45 μm membrane, was injected into each system. Anions were eluted using an aqueous solution of 30 mM potassium hydroxide at a flow rate of 1.5 mL/min. In contrast, cations were eluted with a 20 mM methanesulfonic acid solution at a 1.00 mL/min flow rate. The column oven temperature was maintained at 30°C for anion analysis, with a current of 112 mA applied, and the total run time was set at 40 minutes. For cation analysis, the oven temperature was kept at ambient conditions, a current of 59 mA was applied, and the run time was approximately 12.5 minutes.

In OS V, the assessment extended to dissolved organic carbon (DOC), measured through NDIR spectrometry in a TC-TOC-TN analyzer equipped with an ASI-V autosampler (Shimadzu, model TOC-VCSN). Calibration was performed using standard solutions of potassium hydrogen phthalate (for total carbon) and a mixture of sodium hydrogen carbonate/sodium carbonate (for inorganic carbon). The DOC content was calculated as the difference between total dissolved carbon (TDC) and dissolved inorganic carbon (DIC) (DOC = TDC - DIC).

The granule size distribution was determined using the sieve methodology outlined by Bin *et al*. (2011), employing sieves with varying mesh opening diameters. The aerobic granulation stage in the reactor was considered achieved when more than 80% of the biomass exhibited a diameter greater than 0.2 mm.

Scanning electron microscopy (SEM) coupled with energy-dispersive X-rays (Inspect S50, FEI Company, USA) was employed to analyze the structure of mature granules. Granules underwent pretreatment involving fixing, washing, and lyophilization before the final procedure, following the methodology described by Motteran *et al*. (2014).

3.6.1. Extraction, quantification, and characterization of extracellular polymeric substances (EPS)

In OS I, II, and III, the extraction of extracellular polymeric substances (EPS) was carried out using a method that involves sodium hydroxide and heating, following the procedure by Hong *et al*. (2017) with modifications outlined in Santos *et al*. (2022). In OS IV, the EPS was fractionated into loosely bound EPS (LB-EPS) and tightly bound EPS (TB-EPS). The extraction of the LB-EPS fraction involved ultra-sonication. In contrast, the TB-EPS fraction was extracted using a combination of sodium hydroxide and heating, following the protocol by Hong *et al*. (2017). Similarly, in OS V, fractionation into TB-EPS and LB-EPS was performed; however, the extraction was solely carried out through heating, utilizing the method described by Li and Yang (2007).

The protein content (PN) was assessed using the modified Lowry method (Lowry *et al*., 1951), employing Pierce™ BCA Protein Assay Kits following the manufacturer's protocol, except for OS V. In OS V, protein contents in EPS were determined using the modified Lowry method with bovine serum albumin as a standard (Lowry *et al*., 1951). EPS's polysaccharide (PS) content was measured through the sulfuric acid-phenol method with glucose as a standard (Dubois *et al*., 1956).

Analysis of the fluorescent properties of EPS was performed as described by Li *et al*. (2021a), with adaptations. A fluorescence spectrophotometer (Shimadzu, RF-6000, Japan) located at the Bioinorganic Laboratory (LABIO) of the UFC Chemistry Department was used. The three-dimensional fluorescence spectrum of the excitation-emission matrix (3D-EEM) was obtained in excitation (Ex) wavelength ranges of 200–550 nm and emission (Em) wavelength ranges of 220–600 nm. The scanning increments of Ex and Em were 5 and 2 nm, respectively, with slits of 5 nm. Two aliquots of the EPS solution extracted with a 1:10 dilution at basic pH and neutral pH were prepared from the inoculum samples and granular sludge, collected at the end of the operation for equipment reading.

3.6.2. Extraction and quantification of alginate-like exopolymers (ALE)

The ALE extraction method from aerobic granular sludge was described by Lin *et al*. (2010) with modifications. 50 mL of an aliquot of mixed liquor was centrifuged at 3850 × g for 20 min, after which the supernatant was discarded. The sample was then freeze-dried (lyophilization) for about 24 hours (Freeze Dryer L101, Liotop, Brazil).

0.71 g of Na_2CO_3 and 100 mL of Mili-Q water were added to the dry biomass. This suspension was heated in a water bath at 80◦C, under stirring at 400 rpm, for 30 min to release ALE in the medium. Then, the sample was centrifuged at 3850 × g for 20 min, after which the supernatant was collected. The ALE was precipitated by adding 4 M HCl while adjusting the pH between 2.0 and 2.2. The solution was centrifuged, obtaining ALE in acidic form as a precipitate, then frozen, lyophilized, and weighed. The results were expressed following the recommendations of Felz *et al*. (2016).

Additionally, in OS V, in each phase, alginates were fractionated and characterized into polyguluronic acid blocks (GG), polymannuronic acid blocks (MM), and heteropolymeric blocks (MG). This fractionation of polymer blocks from the biopolymer samples was performed according to Leal *et al*. (2008) and Lin *et al*. (2010). To verify if the extracted ALE possessed properties for forming ionic hydrogel, sodium ALE was slowly dripped into calcium chloride (2.5%) in each phase to form Ca^{2+}-ALE spheres, as described in Felz *et al*. (2016). To monitor stability, the Ca^{2+}-ALE spheres were kept in CaCl for 30 minutes and then divided into two fractions and incubated in a 2% EDTA solution for 3 hours at 4 °C and a formaldehyde+NaOH solution for 3 hours at 4 °C (Felz *et al*., 2016).

3.6.3. Tryptophan (TRP) extraction and quantification

EPS aliquots were subjected to pH adjustment within the range of 6.5–7.5 using 4 M HCl, and the amount of acid added was meticulously accounted for in the dilution calculation. To maintain a minimum concentration of 25 ppm in each sample, a 2x dilution was implemented after doping the samples with a known tryptophan concentration of 50 ppm. Tryptophan content analysis was conducted through high-performance liquid chromatography (HPLC CTO20A, Shimadzu Corporation, Japan), considering previous work (Rollemberg *et al*., 2020b). The HPLC was equipped with a Hypersil BDSC-18 column (250 mm × 4.6 mm, 5 mm), UV 280 nm, and UV/VIS detector (injection volume 20 μL, 6 min run, isocratic elution). The mobile phase comprised methanol and water at a molar ratio of 3:10, with a 1 mL/min flow rate. Tryptophan concentration is calculated by the difference between the peak reading areas of the doped sample and Milli-Q doped water (blank).

3.7. Microbial community analysis

The molecular biology analyses for identifying microorganisms present in the sludge were conducted through the following steps: DNA extraction, amplicon sequencing of the 16S rRNA gene, and data processing. For each sample (0.5 g total wet weight) of the inoculum and mixed liquor collected during aeration, DNA was extracted using the PowerSoil® DNA Isolation Kit (MoBio Laboratories Inc., USA) following the manufacturer's instructions.

Amplicon sequencing, targeting the V4 region of the 16S rRNA gene, was prepared according to Illumina (2013) using specific primers (515F/806R). Following PCR, amplicons were purified using Agencourt AMPure XP-PCR purification beads (Beckman Coulter, Fisher Scientific, USA) as per the product manual and quantified using the dsDNA BR assay kit (Invitrogen, ThermoFisher Scientific, USA) on a Qubit 2.0 fluorometer (Invitrogen, ThermoFisher Scientific, USA). Sequencing was performed using the 300-cycle MiSeq chemistry reagent kit (Illumina, USA) on the MiSeq desktop sequencer (Illumina, USA) located at the Genomics and Bioinformatics Center (CeGenBio) of UFC.

Sequencing data were analyzed using bioinformatics tools. Sequencing reads were trimmed, assembled, and processed for noise removal using the DADA2 v1.20.0 package (Callahan *et al*., 2016). After noise removal, the resulting sequences were referred to as amplicon sequencing variants (ASVs). Taxonomic classification of ASVs was performed using the IDTAXA classifier (Murali; Bhargava and Wright, 2018), part of the DECIPHER v2.20.0 package, based on the Silva rRNA database version 138 (Quast *et al*., 2013).

A prevalence filter was applied to the entire dataset, excluding phyla found in only one of the samples. Absolute abundances of functions were predicted with PICRUSt2 (Douglas *et al*., 2020). KEGG orthology codes for the functions of interest were obtained by keyword search using the KEGGEST v1.32.0 tool (Keggrest, 2021), resulting in the following codes: K10944, K10945, K10946, K10535, K05601, and K15864 for ammonia-oxidizing bacteria (AOB); K00370 and K00371 for nitrite-oxidizing bacteria (NOB); K20932, K20933, K20934, and K20935 for anaerobic ammonia-oxidizing bacteria (ANAMMOX); K20812, K00975, K00688, and K02438 for glycogen-accumulating organisms (GAO); K00937 and K22468 for phosphorus-accumulating organisms (PAO); and K00372, K00360, K00367, K00370, K00371, K00373, K00374, and K10534 for denitrifying bacteria (DNB). The DADA2, DECIPHER, and KEGGREST packages from the Bioconductor project (Huber *et al.*, 2015) were executed in R, version 4.1.2.

The raw sequence data obtained in this study have been deposited in the National Center for Biotechnology Information (NCBI) BioProject database, ID PRJNA836880 (https://www.ncbi.nlm.nih.gov/bioproject/836880).

3.8. Statistical methods and kinetic parameters

Kruskal-Wallis and Mann-Whitney tests were applied to compare the reactors' performance. The test results were assessed based on the p-value. If $p \leq 0.05$, the null hypothesis is rejected, meaning the data groups are considered statistically different.

In OS IV and V, the Pearson test was used to evaluate the relationship between resource production, where a relationship was considered weak when $0.3 < r < 0.5$, moderate between $0.5 < r < 0.7$, and strong when $r > 0.7$.

A multivariate analysis was performed on the OS III and OS V datasets, using principal component analysis (PCA) to assess the correlation between the change in resource contents, EPS, and the main operating conditions. The data were all standardized to exclude interference from the different units, so the means were zero, and the standard deviations were the units. All analyses were performed using RStudio software, developed in R version 4.0.5. The variables chosen for analysis were: ALE, TRP, EPS, SRT, SVI_{30}, SVI_{30}/SVI_5, VSS, phosphorous, ammonia (NH_4^+-N), TN, and COD.

The values measured over the operating days were used, only connecting the cause-effect relationship between the data through the division of stages. The relationships were observed keeping the first three principal components (PC1, PC2, and PC3). In addition, the loads generated in PC3 were observed.

In a more specific PCA analysis, in OS V, considering only the period with controlled biomass discharge in R2 (days 103 to 170), the correlation between SRT, bioresources (ALE, EPS, PN, and PS), and phosphorus was examined. A multivariate analysis was performed on the dataset of each reactor,

Biomass specific rates of nutrient removal (q_{COD}, q_{NOx}, q_{NH4}, q_{TP}) were calculated based on Equation 2.

$$q_{COD,NOx,NH_4,TP} = \frac{(C_i - C_f)}{V_R \times X_{VSS}} \times \frac{V_e}{t_c} \qquad (2)$$

Where $q_{COD,\ NH4,\ NOx,\ TP}$ are the observed biomass specific rates of organic matter and nutrient removal (COD, NH_4^+-N, NO_x-N, or TP, in g/d/g VSS); C_i is the initial concentration (COD, NH_4^+-N, NO_x-N, or TP, in mg/L); C_f is the final concentration (COD, NH_4^+-N, NO_x-N, or TP, in mg/L); V_R is the useful volume of the reactor (L); X_{VSS} is the concentration of volatile suspended solids in the reactor (g VSS/L); *Ve* is the effluent volume of a reactor operating cycle (L); and t_C is the time of one operating cycle of the reactor (d).

The full version of this paper is published in Bioresource Technology (2022) under the same name as this subsection. DOI: https://doi.org/10.1016/j.biortech.2022.127355

Figure 7 – Graphical abstract: carbon source affects the resource recovery in AGS systems treating wastewater.

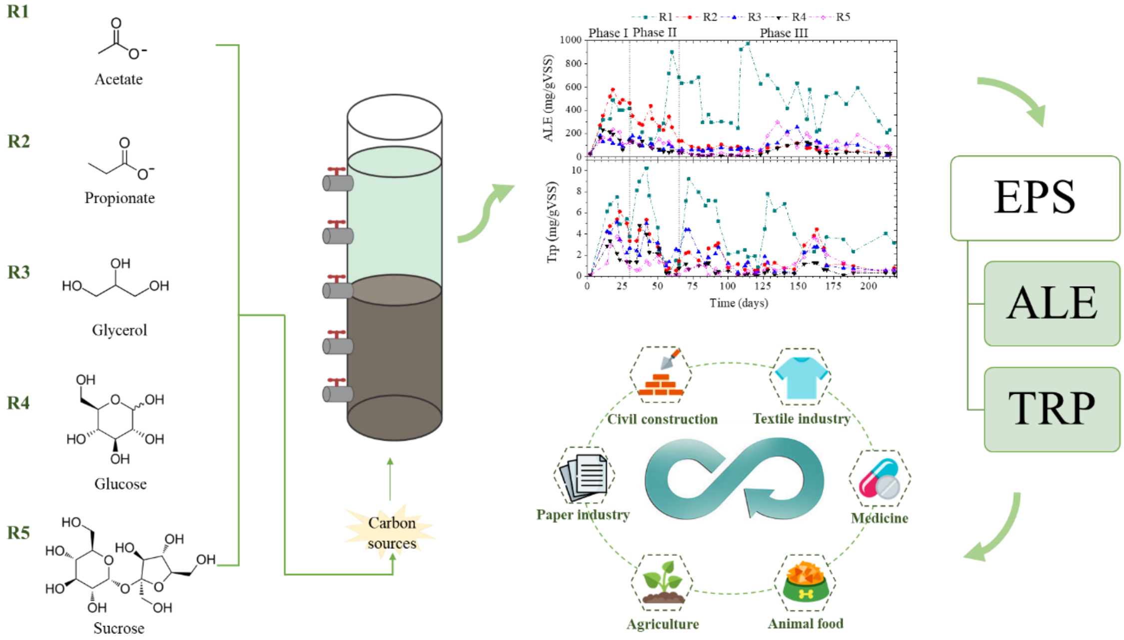

4. CARBON SOURCE AFFECTS THE RESOURCE RECOVERY IN AEROBIC GRANULAR SLUDGE SYSTEMS TREATING WASTEWATER

This study evaluated the influence of carbon sources on the biosynthesis of alginate-like exopolymers (ALE), extracellular polymeric substances (EPS), and tryptophan (TRP) in aerobic granular sludge (AGS). Using acetate, the highest levels of bioresources per gram of volatile suspended solids (VSS) were observed (418.7 mg ALE/g VSS and 4.1 mg TRP/g VSS), likely due to biomass loss throughout the operation, which resulted in lower sludge age (4–7 days) and shorter famine periods. During granulation, propionate showed promising results for ALE production (>250 mg ALE/g VSS), significantly higher than glycerol, glucose, and sucrose. For tryptophan production, propionate and glycerol proved to be suitable substrates, although their content was still lower than that with acetate (1.6 mg TRP/g VSS). Granules fed with glucose exhibited the poorest results compared to other substrates (38.5 mg ALE/g VSS and 0.6 mg TRP/g VSS) due to the abundance of filamentous microorganisms. This study provides insights into the value of producing compounds of industrial interest in AGS systems.

4.1. Formation and stability of aerobic granules

Figure 8 shows the results of MLVSS, SVI_{30}/SVI_5 ratio, and mean granule diameter throughout the operation. The five experimental systems were inoculated with activated sludge at an MLVSS concentration of 2.3 g/L and an SVI_{30}/SVI_5 ratio of 0.6. One week after start-up, a reduction in the initial MLVSS concentration was observed, as the flocculant biomass was washed out from the systems. In R4 and R5, a rapid recovery of the amount of biomass lost in this period is observed, indicating a better initial biomass retention capacity. With the application of operating conditions during stage I, all reactors kept the same or improved settleability (SVI_{30}/SVI_5 ratio).

Complete granulation is achieved when over 80% of the biomass within the system forms granules with a diameter exceeding 0.2 mm (de Kreuk *et al.*, 2007; Liu *et al.*, 2010). Furthermore, in systems with good settleability characteristics, SVI_5 closely resembles the SVI_{30}, resulting in an SVI_{30}/SVI_5 ratio near 1 (de Kreuk *et al.*, 2005; Nancharaiah and Raddy, 2018). Mature granules typically exhibit SVI_{30} values ranging from 30 to 80 mL/g (Derlon *et al.*, 2016). Based on this, it can be concluded that the systems reached complete granulation at different stages, as well as maturation.

In R1, R2, and R3, the formation of granules occurred between phases I and II, reaching complete granulation after 30 days of operation in phase II. On the other hand, in R4, granulation was reached only at the end of phase II, after about 60 days of operation. Late granulation in R4 can be explained because, when hydrolyzed, glucose has its products consumed preferentially by filamentous bacteria dispersed in the liquid medium, compromising sludge settling and hindering granule formation (Qiulai *et al.*, 2019). Thus, controlling filamentous microorganisms is essential to improve the operational performance of this type of substrate. For the R5 reactor fed with sucrose, the formation of granules was observed around 35 days of operation. At the end of phase II, >90% of aerobic granules above 0.2 mm in each system were observed.

Between the stage changes, there was a loss of solids in all systems due to a settling time reduction from 20 min to 10 min (phase II) and from 10 min to 5 min (phase

III), accompanied by an improvement in the sludge settleability, with gradual reductions in SVI_{30}, which is typical behavior of granular biomass.

Figure 8 – SVI_{30}/SVI_5 ratio, volatile suspended solids (VSS) and average granule diameter (Ø) in the five reactors during 215 days of operation.

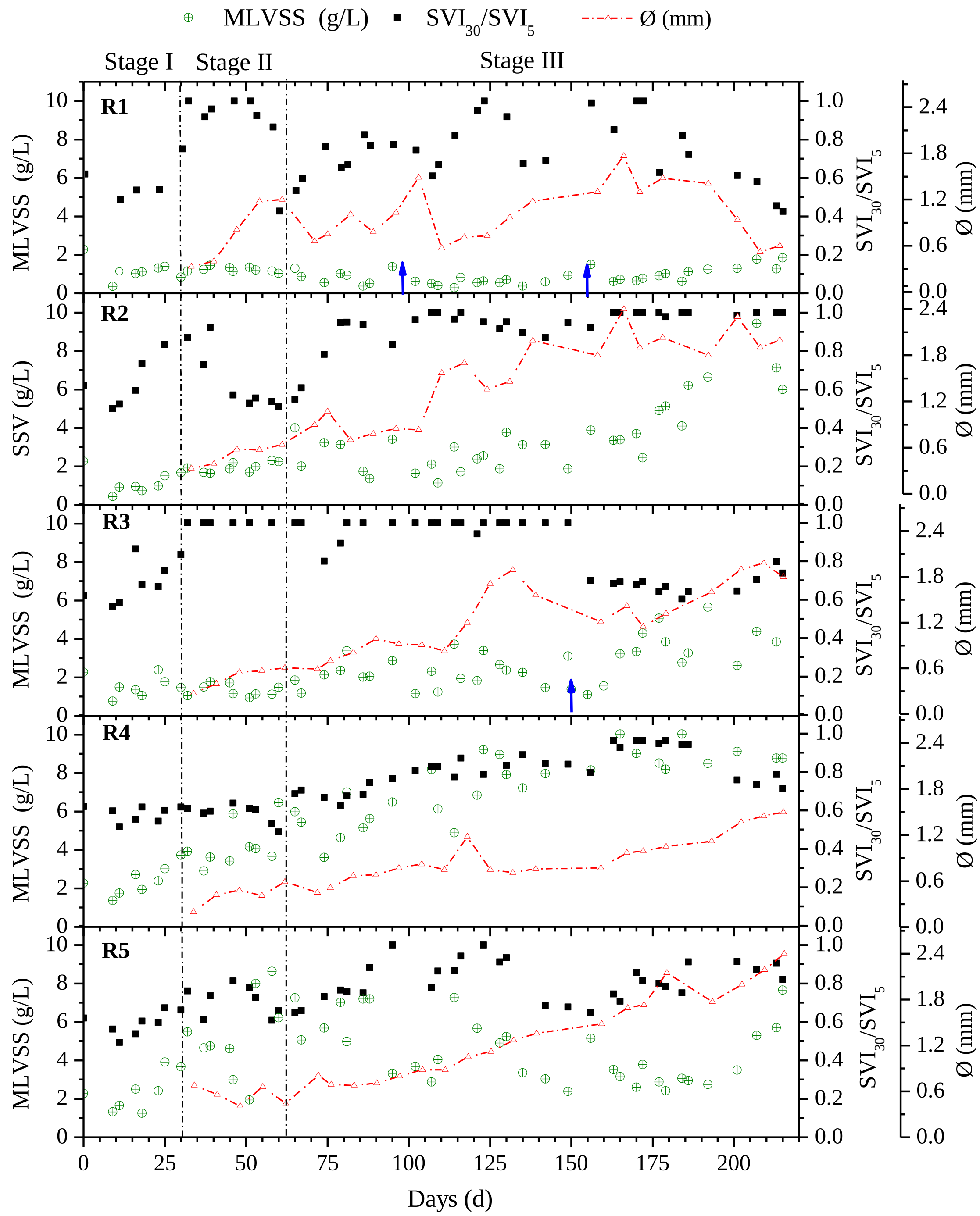

Note: R1 (acetate), R2 (propionate), R3 (glycerol), R4 (glucose) and R5 (sucrose). In R1 and R3, the blue arrows point to moments of instability.

During Phase II, an increase in biomass was observed in all reactors, especially in R4 and R5, while R1 and R3 exhibited an SVI_{30}/SVI_5 ratio close to 1.0. By the end of Phase II, all systems had already achieved an SVI_{30} below 80 mL/g, indicating that they had reached the maturation stage (Derlon *et al*., 2016). In Phase III, Reactor R1, operating with acetate, maintained the MLVSS concentration at an average of 1.8 g/L, but with an unstable SVI_{30}/SVI_5 ratio, averaging 0.7, and an SVI_{30} around 80 mL/g. During operation, this reactor experienced periods of instability, marked by biomass loss and a decrease in the SVI_{30}/SVI_5 ratio. The literature reports issues with granule disintegration when using acetate, especially during prolonged operations (Rollemberg *et al*., 2019; Long *et al*., 2015). The formation of fragile granules, which easily disintegrate, may explain the observed behavior in R1 due to the following mechanisms: (a) critical size of the granule formed with this substrate, up to 1.5 mm; (b) clogging of granule pores due to excessive EPS production; and (c) growth of filamentous microorganisms (Verawaty *et al*., 2013; Corsino *et al*., 2016b; Qiulai *et al*., 2019).Differently, R2, R3, R4, and R5 reached average concentrations of MLVSS between 3.0 and 7.0 g/L and SVI_{30}/SVI_5 higher than 0.8 and SVI_{30} between 27 and 51 mL/g, indicating high retention of biomass with good settleability. In R2 (propionate), MLVSS concentration increased during maturation, with an average of 3.6 g/L and the average diameter of its granules varying between 1.0 and 2.5 mm. In addition, it proved to be stable in terms of settleability, with an SVI_{30}/SVI_5 ratio close to 1.0 and SVI_{30} around 43 mL/g. The reactor fed with glycerol (R3) also showed increasing MLVSS concentration in the final phase (3.0 g/L). However, biomass settleability was affected around the 150th day by the aeration rate increase, which fragmented the granules, also causing biomass loss (He *et al*., 2018). In response to increasing MLVSS concentration in R2, R3, R4, and R5, a high sludge retention time (SRT) was achieved in phase III (28 –37 days). On the other hand, R1 maintained an SRT between 4 and 7 days throughout the experimental period, possibly due to system instabilities and subsequent biomass loss.

As also reported in the literature, glucose (R4) is a substrate that favors high biomass retention (MLVSS around 7.3 g /L) with good settleability (SVI_{30}/SVI_5 ~ 0.80 and SVI_{30} ~ 27 mL/g) compared to the other carbon sources, such as acetate (R1) (He *et al*., 2018). Sucrose (R5) promoted the development of compact granules capable of persisting in the reactor (MLVSS around 4.7 g/L). However, around day 130, settling efficiency was compromised due to the emergence of filamentous microorganisms visually identified in the system.

4.2. Reactor performance

The performance of the reactors was monitored for a period of 215 days (Table 4). A high COD removal efficiency was achieved in all reactors (>90%). No statistically significant difference was observed between the systems ($p = 0.25$), indicating that the type of substrate did not interfere with removing organic matter.

In all systems, improvement in total nitrogen (TN) removal efficiency was observed between the experimental phases. As the granules develop in size, a favorable environment is created, with aerobic and anoxic/ anaerobic conditions, within the granule itself that allows the coexistence of nitrifying and denitrifying bacteria (Liu *et al*., 2010; Winkler *et al*., 2013; Chen *et al*., 2011). The TN removal found ranged from 72% to 78% in the reactors in the final phase. Although a decrease in nitrification between phases was observed due to the synthesis of the biomass that consumes ammonia in its metabolism, the nitrification efficiency was high during the entire operation period (>80%), indicating that ammonia-oxidizing nitrifying bacteria (AOB) and nitrite oxidizers (NOB) remained stable in the reactors. By statistical analysis, TN removal was significantly different between systems ($p < 0.05$).

In R1 (acetate), during granule disintegration periods, there was a reduction in the ammonia removal efficiency, ranging from 15 to 30%, possibly due to the loss of nitrifying bacteria present in the disintegrated granules, even though, within a few days, the performance was restored. Acetate is reported to be a suitable electron donor, which justifies its good nitrogen conversion efficiency (~78%) (Adav *et al*., 2010). R2 (propionate) performance concerning TN removal was slightly inferior to the other reactors, reaching average values of 70% throughout the operation. In this reactor, a greater accumulation of nitrate (NO_3^-) was observed, around 13 mg NO_3^--N/L, when compared to the other systems, indicating a deficiency in denitrification.

Table 4 – Removal efficiency of organic matter and nutrients (N and P) in 215 days of reactors R1, R2, R3, R4, and R5 operation.

Reactor		**R1 (acetate)**			**R2 (propionate)**			**R3 (glycerol)**			**R4 (glucose)**			**R5 (sucrose)**		
Stage		**I**	**II**	**III**	**I**	**II**	**III**	**I**	**II**	**III**	**I**	**II**	**III**	**I**	**II**	**III**
Nº of samples		7	10	38	7	10	38	7	10	38	7	10	38	7	10	38
COD	Influent (mg/L)	606 (196)	856 (185)	838 (180)	695 (125)	1028 (222)	893 (203)	703 (138)	802 (152)	855 (142)	615 (97)	778 (114)	880 (171)	710 (92)	870 (136)	903 (178)
	Effluent (mg/L)	24 (8)	62 (44)	36 (25)	42 (16)	71 (41)	32 (29)	30 (15)	80 (46)	34 (25)	39 (27)	41 (37)	36 (34)	26 (14)	61 (44)	36 (27)
	Removal (%)	**95 (2)**	**92 (5)**	**96(3)**	**94 (3)**	**92 (6)**	**96 (3)**	**96 (2)**	**91 (5)**	**96 (3)**	**93 (4)**	**95 (4)**	**95 (3)**	**96 (2)**	**93 (5)**	**96 (3)**
Nitrogen fractions	NH_4^+ influent (mg NH_4^+-N/L)	49.8 (8.1)	49.8 (7.5)	51.7 (9.4)	54.9 (6.2)	51.6 (9.3)	52.1 (9.1)	44.7 (5.1)	50.5 (5.9)	51.7 (7.6)	46.7 (4.2)	45.7 (4.8)	47.4 (8.4)	53.6 (2.7)	51.3 (5.5)	48.4 (6.8)
	NH_4^+ effluent (mg NH_4^+-N/L)	1.4 (0.5)	4.2 (2.8)	3.2 (2.9)	6.3 (1.0)	3.7 (1.0)	1.1 (0.5)	1.6 (1.0)	2.7 (1.1)	3.0 (1.1)	0.7 (0.3)	3.9 (2.6)	3.4 (2.4)	0.9 (0.5)	6.0 (2.0)	7.3 (4.4)
	NO_2^- effluent (mg NO_2^--N/L)	1.3 (0.1)	3.2 (1.8)	2.1 (1.6)	1.5 (0.1)	0.9 (0.1)	0.5 (0.1)	1.5 (0.4)	1.1 (0.5)	0.5 (0.7)	1.5 (0.3)	0.8 (0.2)	0.8 (0.3)	1.9 (0.4)	1.3 (0.5)	0.8 (0.3)
	NO_3^- effluent (mg NO_3^--N/L)	17.5 (2.5)	7.2 (1.2)	7.0 (3.3)	18.2 (3.1)	14.4 (3.1)	11.5 (2.6)	10.8 (1.9)	10.9 (2.1)	11.2 (2.8)	10.9 (3.2)	9.4 (3.0)	8.6 (2.7)	13.6 (3.0)	8.7 (2.8)	4.4 (2.0)
	Removal (%)	**59 (4)**	**69 (7)**	**78 (10)**	**53 (6)**	**64 (12)**	**74 (9)**	**68 (11)**	**71 (10)**	**72 (9)**	**67 (5)**	**70 (10)**	**74 (10)**	**69 (10)**	**70 (11)**	**72 (11)**
Phosphorus	Influent (mg PO_4^{3-}-P/L)	11.4 (1.7)	9.8 (3.0)	11.2 (2.6)	11.6 (1.5)	10.8 (2.9)	11.2 (2.6)	11.2 (2.6)	9.7 (2.6)	10.1 (2.5)	9.1 (1.7)	7.4 (2.7)	11.0 (2.0)	9.7 (2.2)	7.4 (2.5)	10.3 (3.2)
	Effluent (mg PO_4^{3-}-P/L)	8.2 (1.5)	6.3 (1.8)	5.5 (1.0)	7.9 (1.9)	7.0 (1.9)	6.2 (1.8)	6.2 (1.8)	6.0 (1.8)	4.9 (1.5)	4.9 (1.9)	3.6 (1.5)	3.8 (1.4)	5.8 (1.9)	3.9 (1.3)	3.1 (1.0)
	Removal (%)	**27 (14)**	**34 (18)**	**49 (11)**	**31 (17)**	**35 (11)**	**45 (9)**	**38 (8)**	**49 (21)**	**51 (11)**	**47 (19)**	**49 (22)**	**65 (11)**	**40 (15)**	**41 (30)**	**72 (8)**

Note: data in parentheses refer to the standard deviation, read (± value).

Reactor R3 (glycerol) showed TN removal behavior similar to R2, with nitrate accumulation throughout the operation. It is suggested that, in addition to the rapid COD consumption during the anaerobic period, the high DO concentration in the aerobic phase (3–6 mg/L) may have favored nitrification over denitrification during the aerobic famine period, resulting in nitrate accumulation (Bella and Torregrossa, 2013). Reactors R4 (glucose) and R5 (sucrose) obtained TN removal efficiency of around 75% and, therefore, superior to R2 and R3 performances. These systems probably adapted better to the high DO concentration during the aerobic phase (3–6 mg/L) due to the complexity of these substrates, which demand a higher rate of oxygen to degrade them, interfering less with the denitrifying bacteria activity.

Regarding total phosphorus (TP) removal, efficiency also improved throughout the operation in all reactors, reaching averages of 49 to 72% in the last phase. Statistical tests showed significant differences in TP removals between systems ($p < 0.05$). A possible explanation for the low phosphorus removal is the high sludge retention time (SRT), between 28 and 37 days in the final phase. Without controlled sludge discharge, saturated phosphate-accumulating organisms (PAOs) remain in the system, interfering with phosphorus removal (Bassin *et al*., 2012a). On the other hand, although the sludge retention time of R1 was low (between 4 and 7 days) due to the continuous biomass loss, TP removal remained around 50%, probably due to competition between PAOs and GAOs (glycogen-accumulating organisms) (Carvalheira *et al*., 2014).

4.3. Bioresource production

The EPS, ALE, and TRP concentrations during granulation were markedly higher than those found in activated sludge flocs, corroborating findings in the current literature (Rollemberg *et al*., 2020a; Schambeck *et al*., 2020; Nancharaiah and Reddy, 2018). Figure 9 shows the ALE and TRP values over the 215 days of operation. In this sense, it is observed that granulation is a process that enriches the content of ALE, TRP, and EPS, confirming the importance of bioresources in the stability of the aerobic granular sludge structure in the granulation process (Zahra *et al*., 2022; Schambeck *et al*., 2020).

However, in mature granules, especially in phase III, there was a reduction in the formation of these compounds, with a significant difference between the granulation and maturation periods ($p < 0.05$), except in R1 in the production of EPS, ALE, and TRP, and R3 EPS production. The decrease in ALE production during granule maturation disagrees with the findings of Schambeck *et al*. (2020), in which the ALE content continued to increase with the granule maturation. However, it is worth noting that the authors worked with domestic wastewater, and the granulation phase took > 200 days, likely leading to different behaviors compared to the current study.

Figure 9 – ALE and Tryptophan production over the 215 days of operation.

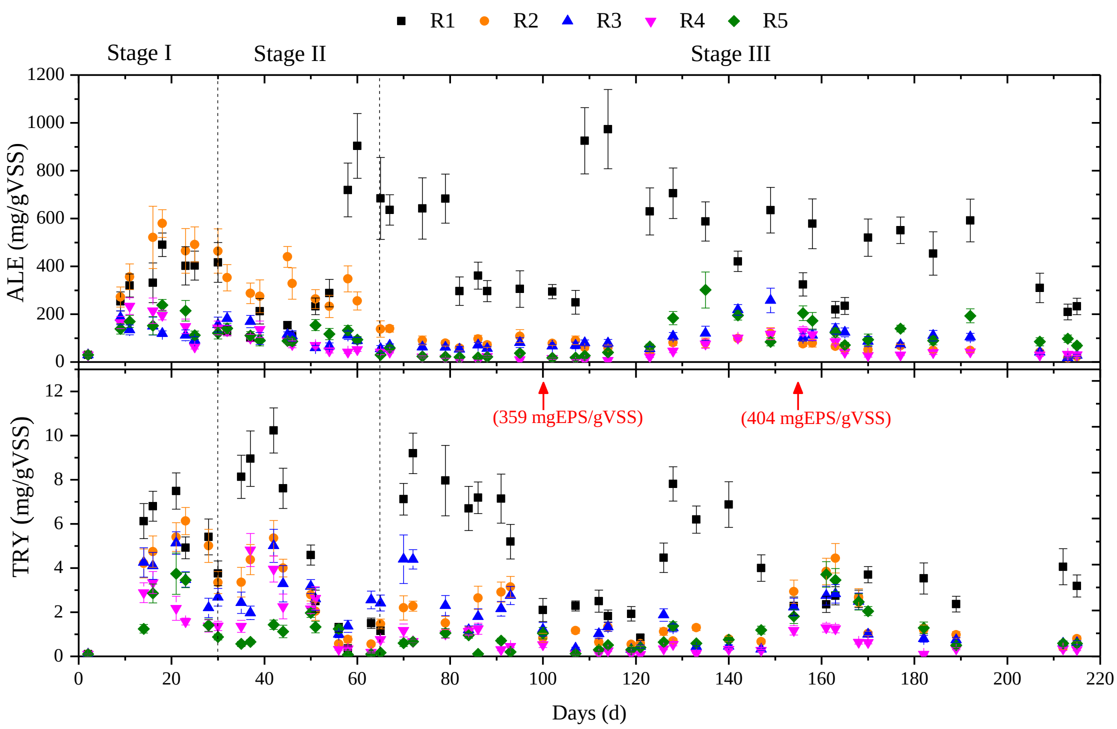

Note: R1 (acetate), R2 (propionate), R3 (glycerol), R4 (glucose) and R5 (sucrose). In R1, the arrows in red indicate moments of instability, and in parentheses, the production of observed EPS.

It is known in the literature that, under extreme conditions, EPS can serve as a carbon source for biological processes (He *et al*., 2018). Thus, the following phenomena may have occurred in R2, R4, and R5: (a) lower EPS production due to the increase in granule diameter caused by oxygen limitation and carbon diffusivity (Verawaty *et al*., 2013); (b) higher endogenous respiration rate due to increased SRT (Rollemberg *et al*., 2020b); and (c) very long starvation period, inducing microorganisms to use EPS as electron donors (Wu *et al*., 2012). Similarly, the reduction in ALE and TRP biosynthesis can also be explained by the increase in SRT and the long period of starvation. Cycle analysis reveals that most COD was consumed in the anaerobic period (Figure 11). This behavior agrees with the results reported by Rollemberg *et al*. (2020b), in which a high SRT caused a decrease in ALE content in aerobic biomass. In addition, the authors indicate the best ALE production with SRT between 10 and 15 days. In this study, R2, R3, R4, and R5 achieved SRT of 28–37 days in phase III and 4–7 days for R1.

EPS production showed no significant difference ($p > 0.05$) between the phases, only in R1 and R3. In the first case, there are strong indications that it is due to reactor instability events with subsequent biomass loss. Under stress conditions, microorganisms tend to secrete more EPS to maintain their shape (Nancharaiah and Reddy, 2018). In Figure 9, red arrows on days 100 and 155, which are precisely those in which R1 went through biomass loss, show that the highest values of EPS production were identified. In turn, R3 showed the highest productions between days 140 and 160. In this case, it is believed that they were in response to the change in aeration intensity, an event that caused the granules to break.

Recent studies in AGS systems have shown that the binding structures of proteins and carbohydrates, through hydrogen bonds, are involved in forming the EPS gel (Li *et al*., 2021b). These interactions are pivotal for the secondary structure of proteins, indicating robust interactions among the EPS components. However, system instabilities induced by factors such as organic load shocks, the addition of additives like calcium (Ca^{+}), magnesium (Mg^{+}), and sodium (Na^{+}), or operational issues can disrupt these EPS-EPS and EPS-surface interactions. Such disruptions often lead to granule disintegration and increased EPS production (Li *et al*., 2021a; Li *et al*., 2021b). Specifically, operational challenges observed in R1 likely impaired the protein-carbohydrate bonds, undermining the granular structure and triggering excessive EPS production.

It is interesting to note that, in these reactors featuring instabilities, especially in R1, after stress events with biomass loss, the increase in EPS was immediate. However, the response to the increase in ALE and TRP was days after the stress event, indicating that stress mechanisms in AGS to increase the production of resources possibly do not produce an immediate response. For this reason, intermittent stresses (pulse mechanisms) may be an interesting alternative to be studied. This different response in the production of ALE and EPS also indicates that although ALE is the main constituent of EPS (Zahra *et al*., 2022; Carvalho *et al*., 2021), different dynamics contribute to the production of these compounds (Schambeck *et al*., 2020). However, sludge age seems to be a very important parameter that also influences the biosynthesis of these bioresources.

Carvalho *et al*. (2021) demonstrated that lower sludge ages, approximately 6 days, enhance the production of TRP and protein-like substances, corroborating the observations in R1. This reactor, operated with acetate, exhibited the highest TRP production, with no significant differences observed across different phases ($p > 0.05$). Conversely, a significant reduction in TRP synthesis was noted in Phase III in the other reactors. This decline could be attributed to the larger granule diameters, exceeding 1.0 mm, which contrasts with the optimal TRP production observed in newly formed granules with diameters ranging from 0.5 to 1.0 mm (Rollemberg *et al*., 2020b).

R1 and R2 showed the highest production of TRP in phase I ($p < 0.05$). However, in phase II, R5 showed significantly lower production ($p = 0.01$), indicating that sucrose is not a suitable substrate for TRP biosynthesis. Glycerol is indicated as favorable to TRP production, as it can generate PEP (phosphoenolpyruvate) as a metabolic intermediate, which is consumed during TRP biosynthesis (Niu *et al*., 2019).

Comparing the current research data with the literature, it was found that the average ALE production in R1 (418 mg ALE/g VSS) exceeded the levels identified by Rollemberg *et al*. (2020b), which were 290 mg ALE/g VSS, both in the presence of acetate. Similarly, R2 exhibited higher ALE production levels (180 mg ALE/g VSS) compared to those reported by Yang *et al*. (2014), who observed 110 mg ALE/g VSS, with both instances utilizing propionate as the substrate.

There are few studies investigating the biosynthesis of TRP in AGS systems. Rollemberg *et al*. (2020a) achieved 48 mg TRP/g VSS, working with AGS fed by domestic sewage. However, when acetate was used as a carbon source with synthetic effluent, values around 54 mg TRP/g VSS were found (Rollemberg *et al*., 2020b), a result superior to what was found in this study, with TRP contents varying between 0.6 and 4.1 mg TRP/g VSS.

It is important to note that Pronk *et al*. (2017b), in studies carried out with AGS granules fed by a combination of acetate (85%) and methanol (15%), concluded that the ALE analyzed was not part of the EPS involved in the granule structure, because it remained intact after the ALE extraction procedure. In addition, the authors obtained ALE yield of only 1% of the granule organic fraction, while in this research, the average yields were 43% (R1), 7% (R2), 9% (R3), 4% (R4) and 9% (R5). However, the SRT used by Pronk *et al*. (2017b) was 51 to 24 days, similar to the SRTs in reactors R2, R3, R4, and R5. Possibly, this means that the endogenous consumption of biomass with the increase in SRT is predominantly ALE. Furthermore, no granule disintegration was observed after ALE extraction in reactors R2, R3, R4, and R5, corroborating the studies by Pronk *et al*. (2017b). It is worth noting that the methodology for extracting ALE in these works was the same.

Compared to tryptophan, the higher commercial values of ALE (US$ 80–140/kg) and its higher content are indicative that ALE recovery is much more viable. Actually, Kaumera Nereda® Gum is focusing on ALE recovery from the AGS biomass in full-scale WWTPs (Rollemberg *et al*., 2020b).

4.3.1. EPS composition: Analysis of 3D-EEM fluorescence spectra

According to previous studies, EPS is a complex composed mainly of polysaccharides, proteins, nucleic acids, humic acids, and lipids (Schambeck *et al*., 2020). Aromatic compounds that are part of this matrix have specific fluorescence characteristics. In this sense, the EPS composition of samples from the reactors and the inoculum was analyzed in the last phase by EEM fluorescence spectroscopy. The representative spectra are shown in Figure 10, and four regions for different EPS components can be observed.

In the first analysis, it is noted that a greater diversity and intensity of peaks of the compounds are found in all AGS reactors compared to the inoculum sludge. Regions I and IV were found only in AGS samples, forming intense peaks and compatible with the presence of the amino acid tyrosine (Ex/Em = 250–300/300–320) and fulvic acid-like substances (Ex/Em = 200–250/380–440), respectively (Luo *et al*., 2014). Differences in the EPS extraction methodology can explain the difficulty in visualizing certain substances (Hong *et al*., 2017). The choice of extraction method influences the total amount and the composition of the recovered polymers (Felz *et al*., 2016). For example, while modified heat extraction (with NaOH) was applied in this study, the formaldehyde-NaOH extraction method was applied in the studies by Luo *et al*. (2014).

Figure 10 – Fluorescence emission-excitation matrix (FEEM) plots of EPS extracted from inoculum and mature aerobic granules at basic and neutral pH. The X and Y axes represent the emission (Em) and excitation (Ex) spectra in nm, respectively, and the contour line.

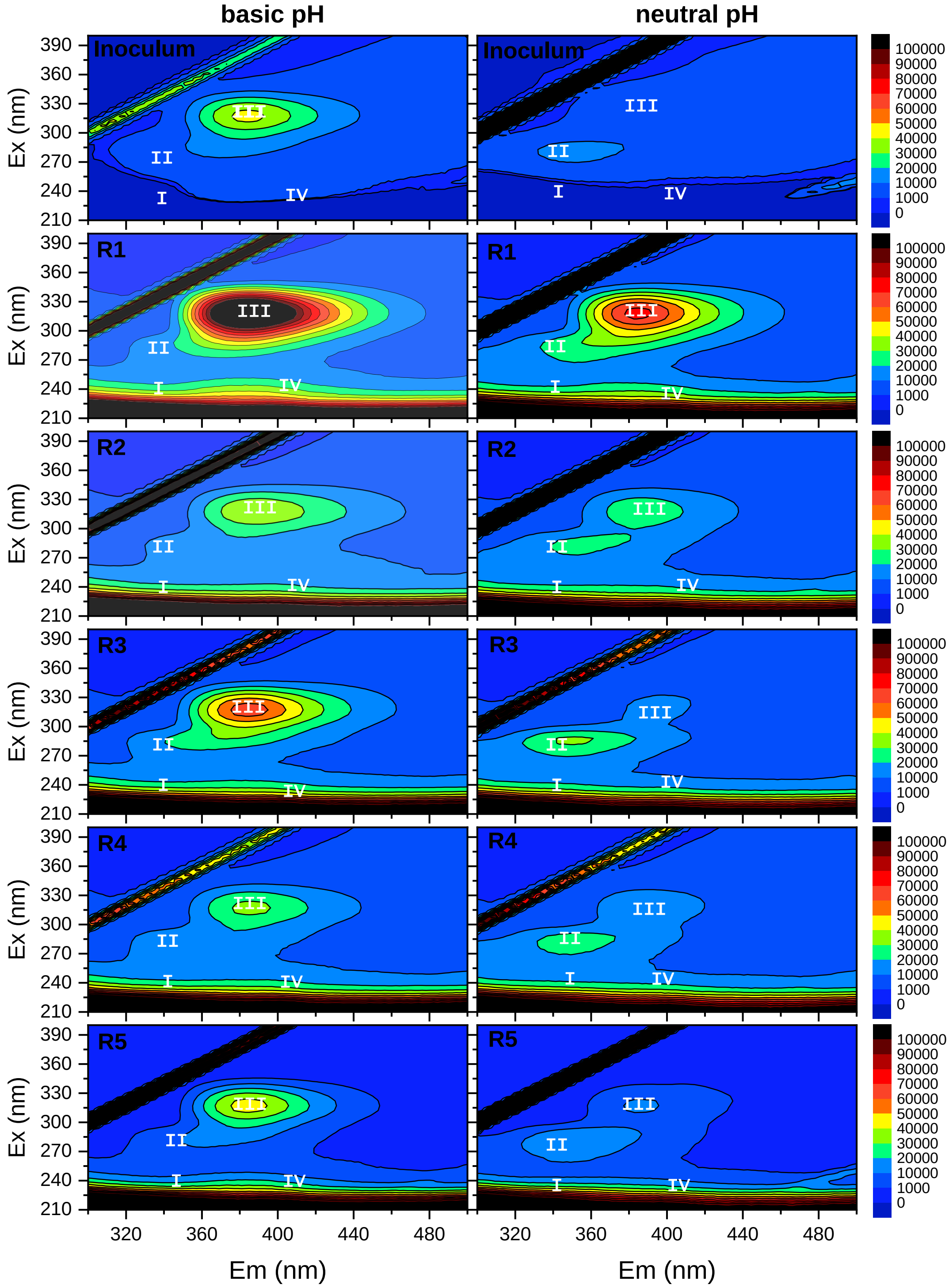

Note: R1 (acetate), R2 (propionate), R3 (glycerol), R4 (glucose) and R5 (sucrose). I (Tryptophan amino acid), II (tyrosine and Tryptophan proteins); III (microbial polysaccharides), IV (polyaromatic type humic acid).

Region II was identified between the excitation/emission (Ex/Em) wavelengths of 275 –285/350–360 nm, referring to tryptophan, and showed higher fluorescence intensity in neutral pH samples because probably at high pH, there is a change in the three-dimensional structure of the proteins, interfering with their identification by fluorometry. Studies have shown that the heat extraction (with NaOH) method used in this study can cause damage to the EPS structure by cell lysis or protein hydrolysis (Hong *et al*., 2017). Region III, characterized by polysaccharides (Ex/Em 300–360/330–390 nm), was well identified in all basic pH EPS extract systems. The neutralization of the solution possibly interferes with the structure of this group of compounds. In R1, due to the high concentration of polysaccharides in the sample at neutral pH, the region II peak converged to that of region III.

4.4. Production and consumption of bioresources throughout the reactor cycle

ALE and TRP productions varied throughout the reactor cycle (Figure 11). While, in R1, the granules showed higher ALE and TRP contents at the end of the cycle, after 3 h of aeration, the other reactors did not show a very clear trend, especially for ALE, possibly due to a higher endogenous respiration rate than would lead to EPS consumption.

At the end of the anaerobic period, there was around 35% of COD influent in R1. In contrast, it was around 20% in R2 and R3 and 13% in R4 and R5. This result shows that the rapid decay of the organic matter, especially in reactors with higher SRT, could have resulted in a prolonged starvation period, which led to increased exopolymers use as an organic matter source. This use is evident in the EPS data throughout the cycle. In R2, R3, R4, and R5, a drop in value can be observed after 3.5 h, strengthening the hypothesis that the part of the EPS consumed under these conditions is predominantly related to resources.

It is important to note that the highest levels of ALE and TRP may vary due to several factors, such as influent characteristics, biomass concentration, and dissolved oxygen, among others. Therefore, a monitoring plan must be carried out to combine AGS operational stability with efficiency to remove C, N, and P simultaneously and the productivity of the desired resources to be recovered (Rollemberg *et al*., 2020b).

Figure 11– Variation of compounds (ALE and TRP), COD and EPS throughout the operational cycle (6 hours).

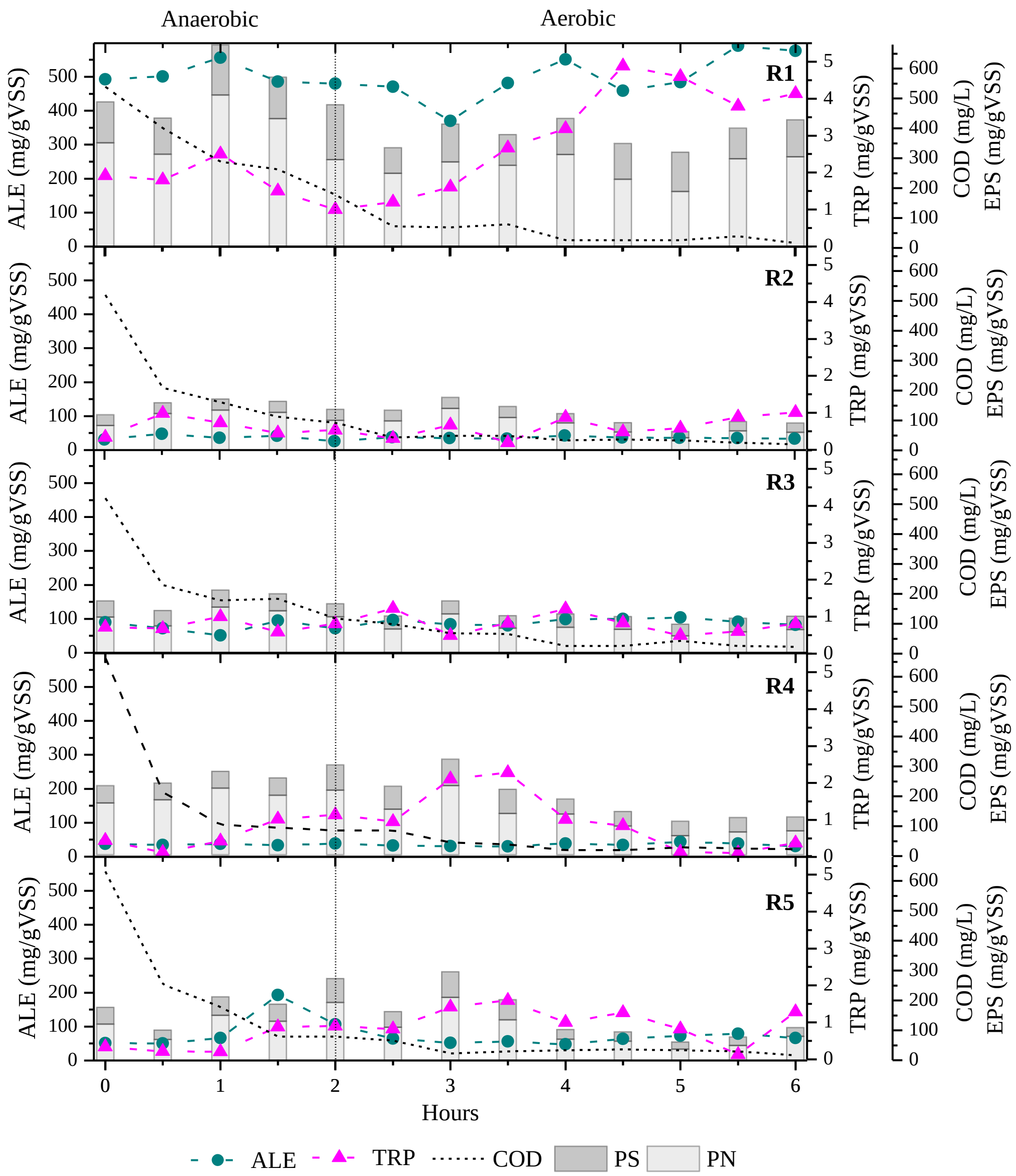

Note: R1 (acetate), R2 (propionate), R3 (glycerol), R4 (glucose) and R5 (sucrose).

4.5. Microbiological characterization: Potential microbial groups associated with the production of ALE and TRP

Microbiological analyses were performed at the end of the operation for all reactors biomass and inoculum sludge (I), in which microbial diversity by family and genus was evaluated. Each reactor presented a different microbial diversity, as expected.

Therefore, the carbon source seems to have influenced the population dynamics in AGS formation, thus impacting the physicochemical characteristics of the granules.

Figure 12 showcases the microbial families specifically engaged in the removal of carbon, nitrogen, and phosphorus. Families of Proteobacteria, such as *Flavobacteriaceae*, *Rhodobacteraceae*, and *Rhodocyclaceae*, appear to facilitate EPS release and granule development by encouraging the production of signaling molecules such as c-di-GMP (Yang *et al*., 2014; Meng *et al*., 2019b). The occurrence of these families in the reactors totaled the following relative abundances, with an emphasis on the *Rhodobacteraceae* family, which was primarily identified as PAOs and GAOs:40.8% in R1, 8.2% in R2, 10.5% in R3, 12.2% in R4 and 5.6% in R5. These groups, especially PAOs, are possibly associated with granule stability and also with ALE production (Schambeck *et al*., 2020).

Concerning nitrifying bacteria, there was a greater abundance of AOB, mainly in R1. On the other hand, NOB abundance was observed in R2, R3, R4, and R5, indicating better conversions from nitrite to nitrate. This may be related to the SRT since the values found for the reactors were completely different, that is, 4 days in R1 and above 30 days in R2, R3, R4, and R5. According to the literature, low SRT at a high temperature can inhibit NOB, leading to nitrite accumulation (Lemaire *et al*., 2008).

Denitrifying bacteria appeared in abundance in all reactors, mainly in R5. The lower abundance of denitrifiers in R2 and R3 may explain the high effluent nitrate concentration (> 10 $mgNO_3^-\text{-}N{\cdot}L^{-1}$), which was not observed in R1. Despite these differences between the microbial populations of nitrifiers and denitrifiers, the nitrogen removal efficiency was similar between the systems studied (between 72-78%). PAOs abundance was similar in all reactors. In addition, there was a predominance of GAOs over PAOs during substrate competition, justifying the low phosphorus removal (between 45-72%) compared to the literature (Bassin *et al*., 2012a).

Figure 12 – Functional groups identified by family in the inoculum and experimental systems (absolute abundance of functions ≥ 10).

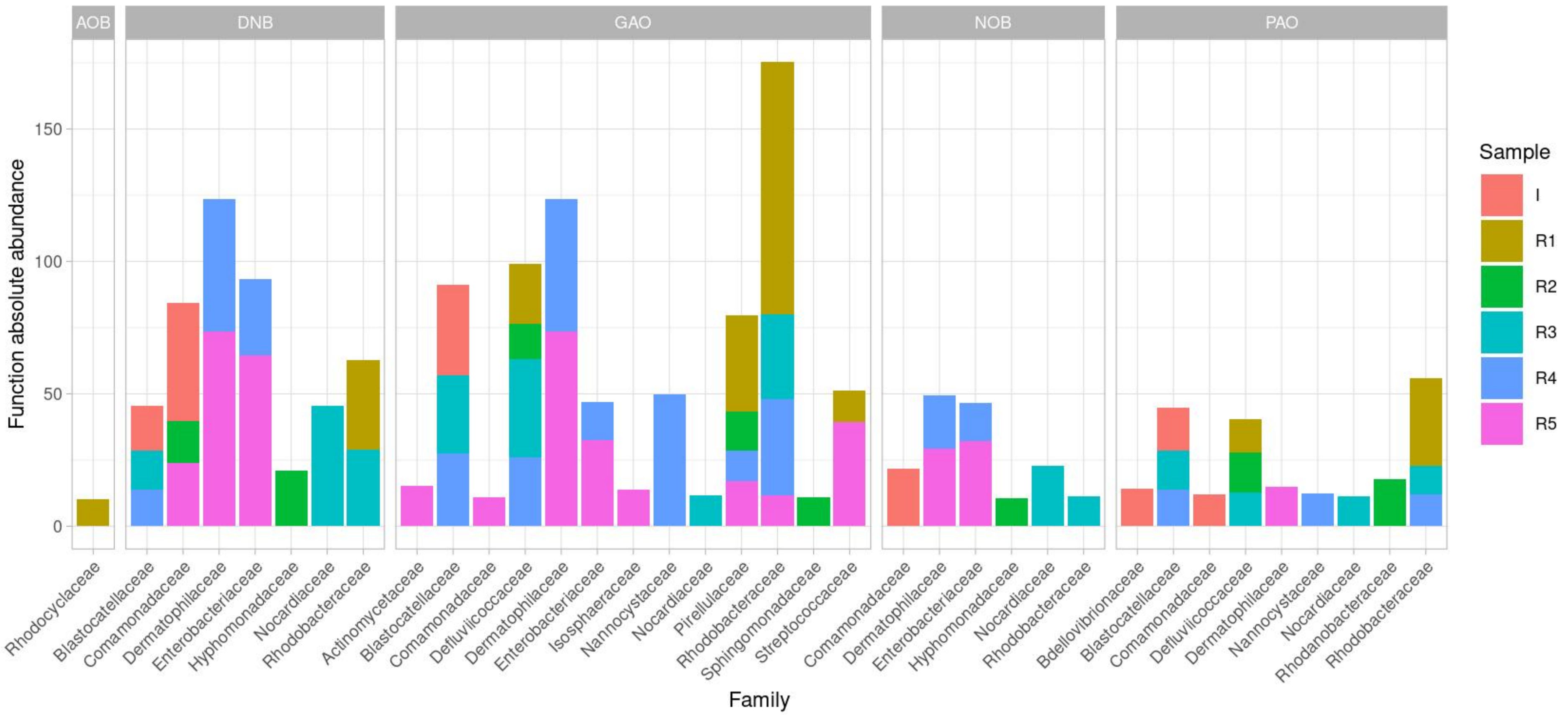

Note: ammonia-oxidizing bacteria (AOB), nitrite-oxidizing bacteria (NOB), glycogen accumulating organisms (GAO), polyphosphate accumulating organisms (PAOs), and denitrifying bacteria (DNB).

The microbial diversity at the genus level (Figure 13) of the inoculum and experimental systems is also presented. In all analyzed samples, the abundance of heterotrophic organisms was observed. In the inoculum, the dominant bacterial genera were *Bdellovibrio* (23.9%) and OLB17 (13.9%). *Bdellovibrio* species are highly active and mobile predators, which have a broad prey spectrum, which can significantly alter species composition (Feng *et al*., 2017). Moreover, OLB17, when found in abundance in filamentous form, can impair the granular structure (Qiulau *et al*., 2019). Therefore, it is considered that the operational conditions applied, such as the alternation between anaerobic and aerobic periods in the cycle, are unfavorable for the proliferation of these microorganisms in the AGS cultivation systems, as they were presented in low concentrations in the AGS biomasses.

The main genera identified in each reactor were: *Defluviicoccus* (12.2% in R1, 14.4% in R2, 11.9% in R3, and 9.5% in R4), *Pseudofulvimonas* (6.8% in R1 and 17.0% in R2), *Gordonia* (10.5%) in R3, *Nannocystis* (11.9%) in R4, in addition to *Lactococcus* (9.9%) and *Kineosphaera* (5.4%), both in R5. All these microorganisms can produce and secrete EPS (Pronk *et al*., 2017b; Chen *et al*., 2022a; Qiu *et al*., 2022; Li *et al*., 2020a).

Defluviicoccus was the main genus of glycogen-accumulating denitrifying organisms (DGAOs) found in R1, R2, R3, and R4 (Li *et al*., 2020a). The dominance of *Defluviicoccus* and *Pseudofulvimonas* in R1 and R2 indicates the preference of these microorganisms for easily biodegradable substrates, such as acetate and propionate. *Gordonia* are bacteria involved in removing ammonia via heterotrophic nitrification/aerobic denitrification, consuming complex substrates, including glycerol (Silva *et al*., 2019). *Nannocystis* are denitrifying bacteria (DNB) capable of secreting flocculating substances (Qiu *et al*., 2022). However, the bioflocculant excess in the medium, instead of contributing to the granular structure stability, can change the surface charge of microbial aggregates and hinder their adhesion and cohesion between them, impairing the granulation process, which possibly occurred in R4. Furthermore, genera of filamentous bacteria, such as *Actinomyces* and *Runella*, were found in this reactor. *Lactococcus*, known as facultative anaerobes, are highly competitive in substrate utilization (Zhang *et al*., 2019). In this case, the abundance of fermentative bacteria suggests the need to degrade the complex substrate (sucrose) into short-chain fatty acids for later use as a carbon source by other microorganisms.

Figure 13 – Relative microbial diversity at the genus level of the inoculum (I) and reactors. The heatmap presents the genera with more than 1% of total bacterial abundance in at least one of the samples.

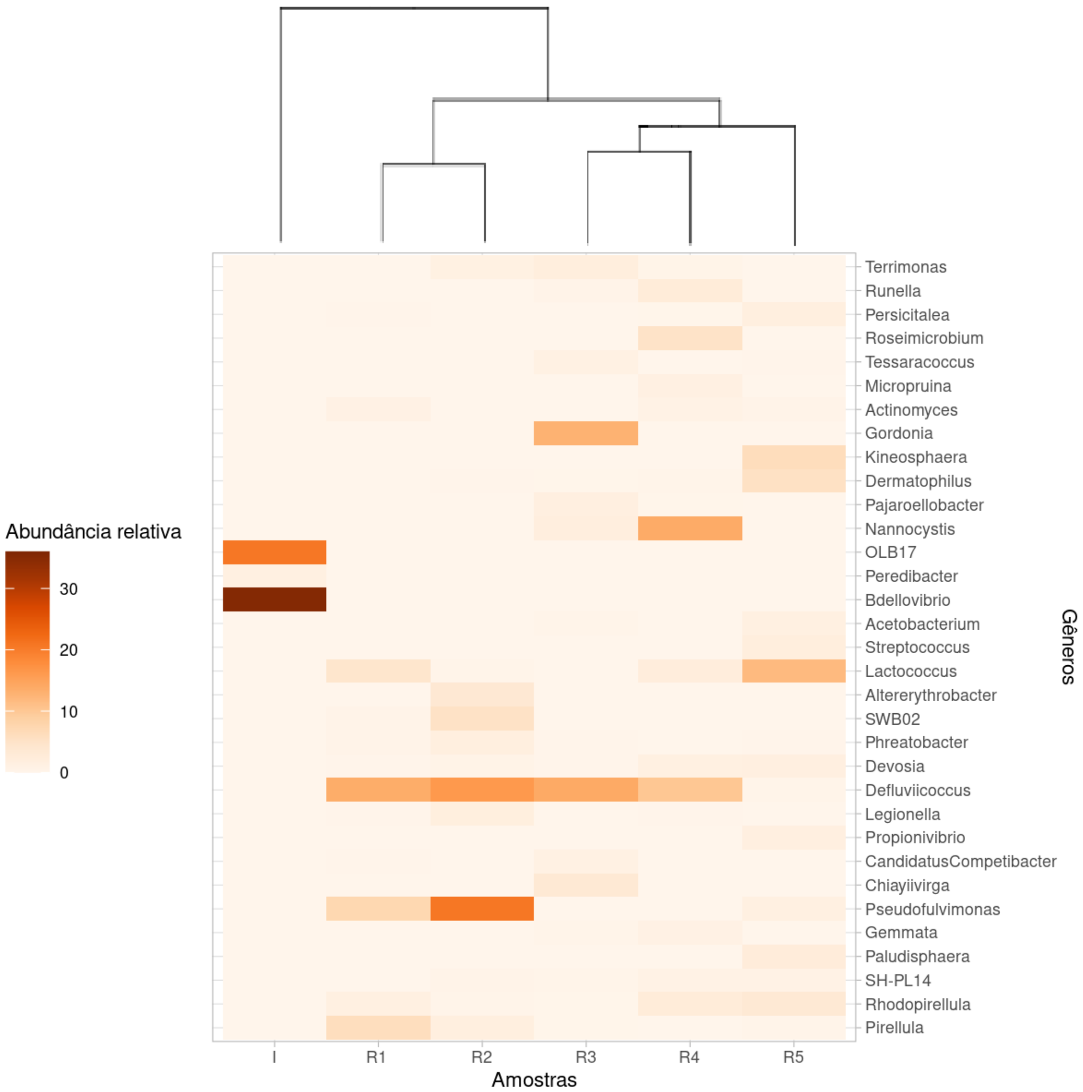

Regarding ALE production, Yang *et al*. (2014), when verifying the granulation under sudden variations in the OLR between 4.4 and 17.4 kg COD/m3/d, observed that such environmental changes stimulated the microorganisms to secrete the second messenger cyclic guanosine monophosphate (c-di-GMP). This molecular response is crucial as it signals the activation of genes specifically those encoding for the Psl and Alg polysaccharides. The resultant effect is the excessive production of exopolysaccharides, including ALE, which formed a large amount of viscous material, serving as a precursor of aerobic granules. Based on this, possible bacteria whose EPS production can be regulated by c-di-GMP were identified in abundance in each reactor: *Pirellula* (5.3% in

R1 and 3.0% in R2), *Pseudofulvimonas* (6.8 % in R1 and 17.0% in R2), *Gordonia* (2.3% in R3), and *Lactococcus* (3.7% in R1, 1.8% in R4 and 9.9% in R5) (Chou and Galperin, 2016; Chen *et al*., 2022a).

Few bacteria involved with tryptophan formation in AGS have been identified to date. It is reported that at low C:N ratios (around 5) in the influent, tryptophan accumulates in the system due to the favoring of bacteria of the *Thauera* and *Paracoccus* genera, therefore positively related to this amino acid biosynthesis (Zhang *et al*., 2018). These microorganisms are associated with the systems' denitrification capacity enhancement at the expense of nitrification efficiency. Thus, it is possible that operational strategies that promoted tryptophan production affected nitrogen removal from AGS systems (Carvalho *et al*., 2021).

Reinforcing the above conclusions, Wang *et al*. (2018) verified the existence of tryptophan in AGS dominated by aerobic AOB. Thus, this functional group may potentially be associated with tryptophan production. In agreement with the latter work, R1 had an abundance of AOB and even a higher tryptophan content (4.1 mg TRP/g VSS). Furthermore, tryptophan biosynthesis was apparently favorable in reactors with an anoxic environment, as in R2 and R3 (1.6 mg TRP/g VSS). Similarly, Rollemberg *et al*. (2020b) found that a short anoxic period in the operating cycle can stimulate tryptophan production. In general, the abundance of filamentous microorganisms in R4 was probably harmful to forming an extracellular matrix rich in high value-added resources (0.6 mg TRP/g VSS). As seen, sucrose as a carbon source (R5) enabled the development of fermenting bacteria, such as *Acetobacterium*, *Lactococcus*, *Propionivibrio*, and *Streptococcus*, in the medium, which may have increased tryptophan content in the granules (0.9 mg TRP/g VSS) compared to R4 (Rollemberg *et al*., 2020b).

4.6. Practical implications of this study

The biggest challenge identified in this study was the long-term operational stability of the systems. The literature consistently highlights issues with stability and granule disintegration in AGS systems (Nancharaiah *et al*., 2018; Pronk *et al*., 2017a; Hamza *et al*., 2022). While several factors contribute to these challenges, it is widely recognized (Lin *et al*., 2020; Lv *et al*., 2014) that the stability of granules during prolonged AGS operations is closely linked to microbial diversity and the maintenance of slow-growing microorganisms. Adverse conditions, such as environmental stresses, can significantly impact operational stability, leading to shifts in microbial community dynamics (Li *et al*., 2021a; Li *et al*., 2021b). In this sense, operational problems, observed mainly in R1, contributed to the observed instabilities. Additionally, periods of extended starvation (famine) are reported to promote the formation of dense, stable granules (Hou *et al*., 2021); however, they may also restrict denitrification due to a lack of available carbon sources (Silva; Rollemberg; Santos, 2021). It was noted that stress conditions stimulated bioresources production, suggesting that further research is required to explore how stress in AGS systems can enhance resource production without compromising system stability. Strategies to support the growth of slow-growing microorganisms are crucial. Therefore, experimenting with various stress types, such as osmotic stress, is recommended. Furthermore, studies focusing on controlled SRT with shorter durations (10 to 15 days), reducing the famine period during the aerobic stage, and using both complex and simple industrial wastewaters, are also suggested to optimize the operational efficacy and resource recovery.

4.7. Conclusions

The AGS fed with acetate showed higher production of ALE and tryptophan. However, this carbon monitoring is necessary to balance granule stability, operational performance, and resource production. Propionate showed encouraging results in ALE production during the granulation. Regarding tryptophan production, propionate and glycerol proved to be good substrates, although the content was lower than that of acetate. Due to filamentous microorganisms' overgrowth, complex substrates such as glucose and sucrose seem to limit resource production. In addition, the increase in SRT and a long famine period proved detrimental to resource production, indicating a higher endogenous respiration rate due to EPS consumption.

The full version of this paper is published in Chemosphere (2023) under the same name as this subsection. DOI: https://doi.org/10.1016/j.chemosphere.2022.137006

Figure 14 – Graphical abstract: influence of salt addition to stimulating bioresources production in AGS systems.

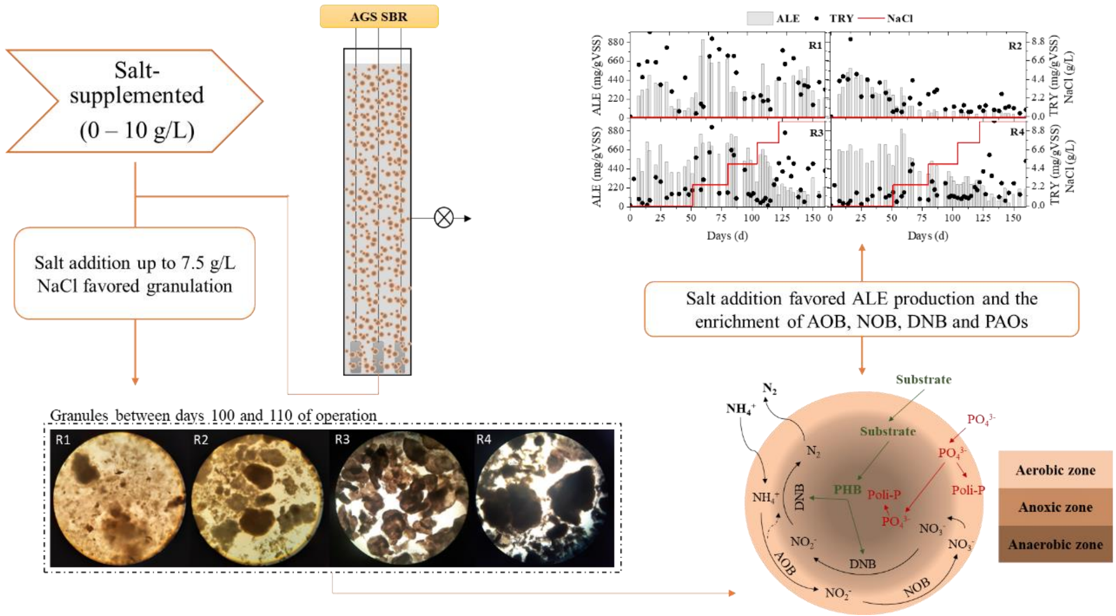

5. INFLUENCE OF SALT ADDITION TO STIMULATING BIORESOURCES PRODUCTION IN AEROBIC GRANULAR SLUDGE SYSTEMS

The influence of salt addition on stimulating bioresources production in aerobic granular sludge (AGS) systems was evaluated. The control systems (R1: acetate and R2: propionate) initially obtained less accumulation of mixed liquor volatile suspended solids (MLVSS), indicating that the osmotic pressure in the salt-supplemented systems (R3: acetate and R4: propionate) contributed to biomass growth. However, the salt-supplemented systems collapsed between days 110 and 130 of operation. R3 and R4 showed better performance regarding nutrient removal due to the greater abundance of nitrifying and denitrifying bacteria and phosphate-accumulating organisms. Salt also contributed to the higher production of biopolymers such as alginate-like exopolymers (ALE) per gram of volatile suspended solids (VSS) (R1: 397 mg ALE/g VSS, R2: 140 mg ALE /g VSS, R3: 483 mg ALE/g VSS, R4: 311 mg ALE/g VSS). Amino acids like tyrosine and tryptophan were better identified in extracellular polymeric substances extracted from salt-operated reactors. This study brings important results in the context of resource recovery by treating saline effluents.

5.1. Formation and stability of aerobic granules

Due to filamentous biomass washout, the initial MLVSS concentration (2.1 g/L) dropped shortly in all reactors after inoculation (Figure 15). Similar characteristics can be observed in the granulation phase, achieved shortly after 30 days of operation. The classical references consider aerobic biomass/systems the following aspects as indications: granulation beginning when the SVI_5 is closer to the SVI_{30} (de Kreuk *et al*., 2005; Nancharaiah and Raddy, 2018), mature granules present SVI_{30} between 30 and 80 mL/g (Derlon *et al*., 2016), aerobic granule when its diameter is greater than 0.2 mm, and complete granular system when more than 80% of the biomass is in the form of aerobic granules with an SVI_{30}/SVI_5 ratio greater than 80% (de Kreuk *et al*., 2007; Liu *et al*., 2010).

Comparing the control reactors R1 (acetate) and R2 (propionate) to the salt-supplemented reactors R3 (acetate) and R4 (propionate), it is noted that R3 and R4 obtained a greater solids accumulation up to a concentration of 7.5 g/L of NaCl, indicating that the osmotic pressure contributed to biomass growth and did not interfere with the settleability characteristics. NaCl possibly tends to destabilize the particles present in the water, facilitating particle agglomeration and microbial aggregation, then helping to maintain the granule without interfering with the removal performance of organic matter and nutrients.

In the control system R1 (acetate), a successful granulation was observed at the end of thirty days of operation, with an SVI_{30}/SVI_5 ratio of approximately 0.95 and an SVI_{30} of 57 mL/g. However, these values were stable for only 20 days. During maturation, the system went through instabilities that led to biomass loss. Despite the presence of granules, there was a filamentous biomass formation, indicated by the poor settleability, and presenting an SVI_{30}/SVI_5 ratio of around 0.74 and SVI_{30} of 161 mL/g. The solids remained approximately constant, reaching 1.49 g/L at the end of the operation.

Santos *et al*. (2022) observed that AGS granules developed when propionate was the carbon source were more stable than those from acetate. In another study with AGS systems, Rollemberg *et al*. (2019) observed that the granules were unstable when acetate was the carbon source. This behavior may be associated with some possible reasons: (a) a readily biodegradable COD source may favor the growth of fast-growing heterotrophic microorganisms, especially filamentous microorganisms (Hamza *et al*., 2022), (b) the formation of large granules, making it difficult to oxygen and carbon penetration and favoring subsequent breakage of granules (Rollemberg *et al*., 2019), and (c) obstruction of granule pores by excessive EPS production (Corsino *et al*., 2016b).

Figure 15 – SVI_{30}/SVI_5, SVI_{30}, and mixed liquor volatile suspended solids (MLVSS) ratio in the control reactors R1 (acetate) and R2 (propionate), and the salt-supplemented reactors R3 (acetate) and R4 (propionate) over the 160 days of operation.

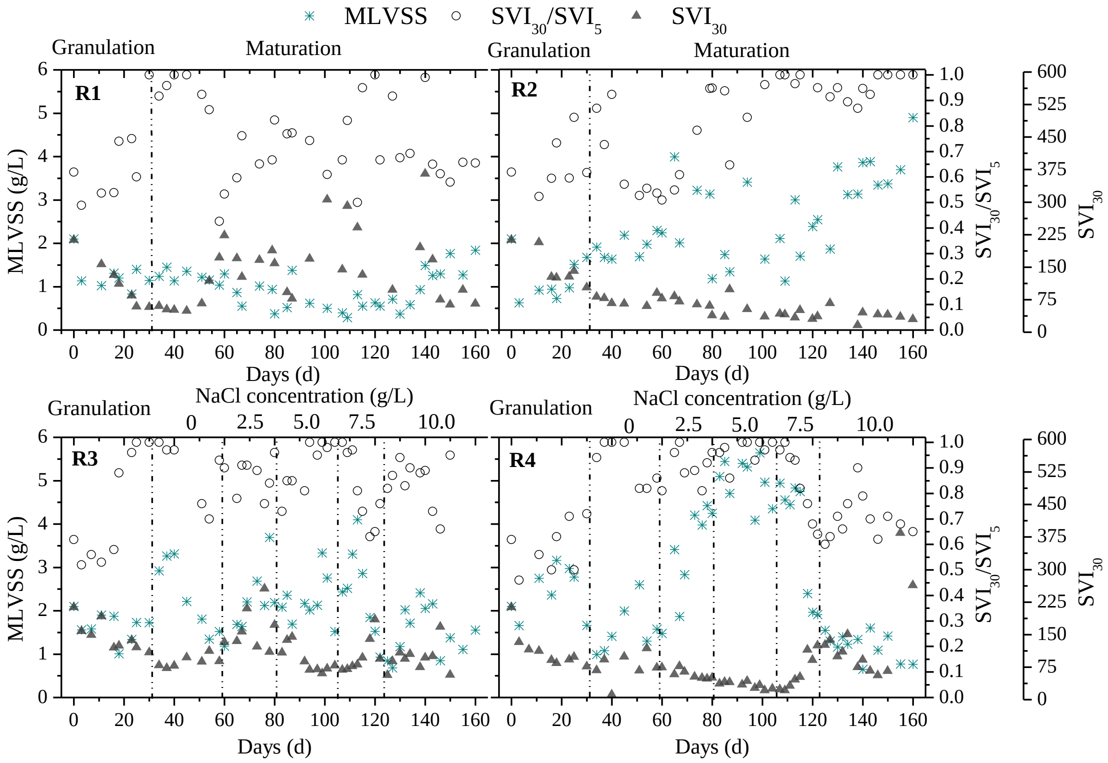

In the control reactor R2 (propionate), the MLVSS concentration increased during the granule maturation period, with an average of 2.72 g/L, and reaching an average of 3.84 g/L at the experiment completion. Its aerobic granules were stable in terms of settleability, with SVI_{30}/SVI_5 ratio close to 1.0 and SVI_{30} around 44 mL/g.

In the salt-supplemented reactor R3 (acetate), unstable values could also be observed, similar to R1. It is important to mention that, for 2.5 and 7.5 g/L NaCl concentrations, the system improved the SVI_{30}/SVI_5 ratio and SVI_{30}, especially at the end of the 5.0 g/L NaCl phase, in which the values were, respectively, close to 1.0 and 72 mL/g. It is believed that the biomass tends to develop denser granules and present better settleability results in the presence of low NaCl concentrations.

The other salt-supplemented reactor, R4 (propionate), also presented similar results to R2, i.e., increasing MLVSS, reaching 4.97 g/L on average for 5.0 g/L of NaCl, SVI_{30}/SVI_5 close to 1.0 and SVI_{30} around 31 mL/g. At the NaCl concentrations of 7.5 and 10 g/L, the R3 and R4 systems collapsed, leading to granule disintegration and sludge settleability deterioration, which resulted in effluent biomass washout and MLVSS concentration drop.

R1 and R3 presented a low SRT (between 4 and 8 days) throughout the experimental period, possibly due to recurrent biomass loss. R2 reached an SRT of around 25–35 days at the end of the maturation phase. R4 also reached an SRT of around 25 and 35 days between days 80 and 105 of operation. However, at the end of the operation, the SRT dropped to around 1 and 4 days in R4.

5.2. Reactors' performance

During the operation period, all systems showed COD removal efficiency greater than 90% (Table 5). They were considered statistically equal ($p = 0.69$), indicating that R3 and R4 maintained the efficiency in removing organic matter even under osmotic pressures up to a limit. In 10 g/L NaCl, the removal efficiency dropped slightly, showing to be statistically different from the other operating conditions ($p < 0.05$). These results are in agreement with those found in the literature, in which satisfactory COD removals are observed, especially at low concentrations. However, it also shows adverse effects at salt concentrations above 10 g/L (Han *et al*., 2022; Wu *et al*., 2020; Wang *et al*., 2017).

In all systems, an improvement in total nitrogen (TN) removal was noticed between granulation and granule maturation, even in reactors supplemented with salt, as shown in Table 5. As a result of the granule development, a stratified structure was developed with aerobic and anoxic/anaerobic zones, allowing the coexistence of nitrifying and denitrifying microorganisms (Liu *et al*., 2010; Winkler *et al*., 2013; Corsino *et al*., 2016a).

In R1, total nitrogen removal was significantly higher in the maturation phase ($p = 0.03$). However, in R2, there was no significant difference ($p = 0.58$). The ammonium (NH4+) removal was high during the entire operation period (>90%), considered statistically equal between the granulation and maturation phases ($p = 0.20$), indicating that nitrifying bacteria (ammonia-oxidizing bacteria, AOB, and nitrite-oxidizing bacteria, NOB) remained stable (Lashkarizadeh *et al*., 2015).

The denitrification capacity of the systems is also shown in Table 5. It can be verified that the reactors fed with acetate as a carbon source (R1 and R3) showed slightly higher values than those operated with propionate (R2 and R4) ($p = 0.05$ comparing R1 and R2, and $p = 0.03$ comparing R3 and R4) since acetate is reported as a suitable electron donor (Rollemberg *et al*., 2019). The denitrification observed in R3 was higher than R1 ($p \leq 0.05$) and R4 higher than R2 ($p \leq 0.05$), possibly due to the better formation of granules. It is believed that low saline concentrations (2.5 and 5.0 g/L) had a strong influence on the better initial granule formation, favoring denitrification. This aspect was confirmed by the molecular microbiology analysis, which showed a better development of these microorganisms in saline systems (R3 and R4). However, in R3 and R4, a significant drop in TN removal was observed ($p < 0.05$) from the salt concentration of 7.5 g/L, especially in R4, due to granule disintegration and biomass washout, mainly affecting nitrifying microorganisms. In this case, there was a drop in NH_4^+ removal, with no accumulation of nitrite or nitrate, indicating that denitrification was maintained. Wang *et al*. (2017) showed in aerobic tests that the specific oxidation of ammonium was significantly reduced after adding 10 g/L of NaCl. However, salt addition did not significantly affect nitrate oxidation, corroborating the current study findings. Wang *et al*. (2017) and Bassin *et al*. (2012b) showed that the gradual adaptation of AGS to saline conditions allowed the total and stable removal of nitrogen, which also agrees with our results. However, high concentrations (>20 g/L) and saline shocks (20, 40, and 60 g/L) caused adverse and irreversible effects on AGS systems (Han *et al*., 2022; Wu *et al*., 2020; Wang *et al*., 2017; Wan *et al*., 2014).

The average phosphorus removal efficiency in R1 and R2 was around 46 and 42%, respectively, with no significant difference between the data ($p = 0.23$). In the case of R2, this low performance can be associated with the high system SRT (between 25 and 35 days). Bassin *et al*. (2012a) demonstrated that microbiomes without controlled biomass discharge could lead to phosphorus-accumulating organisms (PAOs) saturation, negatively interfering with the system’s performance. On the other hand, although the R1 SRT was low (between 4 and 8 days), the phosphorus removal efficiency remained low, probably due to the competition between glycogen-accumulating organisms (GAOs) and PAOs (Carvalheira *et al*., 2014; Santos *et al*., 2022).

Table 5 – Performance of the control reactors, R1 (acetate) and R2 (propionate), and the salt-supplemented reactors, R3 (acetate) and R4 (propionate), over the 160 days of operation.

Reactor		**R1**		**R2**		**R3**						**R4**					
Stage		Granulation	Maturation	Granulation	Maturation	Granulation	NaCl (g/L)					Granulation	NaCl (g/L)				
							0	2.5	5.0	7.5	10.0		0	2.5	5.0	7.5	10.0
COD	Influent (mg/L)	806 (196)	838 (180)	895 (125)	893 (175)	968 (92)	987 (104)	938 (92)	865 (85)	872 (72)	938 (77)	1078 (165)	974 (138)	966 (52)	908 (80)	910 (82)	1001 (99)
	Effluent (mg/L)	54 (8)	38 (23)	72 (16)	34 (27)	64 (20)	40 (18)	29 (13)	28 (11)	43 (17)	78 (48)	58 (14)	45 (31)	37 (24)	24 (9)	40 (14)	90 (37)
	Removal (%)	**95 (2)**	**95 (3)**	**94 (3)**	**96 (3)**	**94 (2)**	**96 (2)**	**96 (2)**	**96 (2)**	**95 (2)**	**92 (5)**	**94 (2)**	**95 (3)**	**96 (2)**	**96 (2)**	**96 (2)**	**91 (3)**
Nitrogen fractions	NH_4^+ influent (mg NH_4^+-N/L)	46.5 (11.8)	51.6 (12.4)	52.3 (10.1)	54.1 (13.3)	55.9 (3.5)	57.3 (4.4)	58.1 (4.0)	53.8 (5.1)	56.8 (1.1)	48.9 (8.1)	61.7 (5.0)	59.2 (5.5)	61.3 (4.0)	59.8 (3.3)	59.8 (2.9)	51.5 (7.9)
	NH_4^+ effluent (mg NH_4^+-N/L)	1.1 (0.7)	3.7 (3.5)	1.1 (1.0)	3.9 (4.2)	10 (15)	2.7 (5.0)	0.9 (0.5)	0.6 (0.7)	6.9 (10.1)	8.5 (6.9)	3.3 (4.5)	3.3 (4.3)	1.2 (1.2)	0.6 (0.9)	14.7 (5.7)	14.9 (7.0)
	NO_2^- effluent (mg NO_2^--N/L)	1.0 (0.7)	2.0 (1.9)	1.9 (0.7)	0.7 (0.6)	4.9 (4.3)	3.0 (2.9)	0.6 (0.2)	0.3 (0.5)	1.3 (0.2)	1.3 (0.1)	4.7 (3.1)	2.8 (1.5)	0.7 (0.2)	0.3 (0.5)	1.3 (0.3)	1.1 (0.5)
	NO_3^- effluent (mg NO_3^-–N/L)	15.7 (4.0)	6.7 (4.6)	12.4 (3.4)	13.5 (4.9)	1.0 (0.6)	2.7 (3.2)	6.2 (3.2)	4.4 (1.4)	1.4 (0.9)	1.4 (0.6)	4.8 (3.2)	2.4 (2.4)	7.8 (2.9)	6.3 (2.6)	1.7 (1.1)	1.4 (0.9)
	NH_4^+ removal (%)	**98 (2)**	**92 (9)**	**98 (2)**	**92 (8)**	**94 (8)**	**95 (9)**	**98 (1)**	**99 (1)**	**88 (18)**	**84 (12)**	**95 (7)**	**94 (8)**	**98 (2)**	**99 (1)**	**75 (10)**	**73 (11)**
	TN removal (%)	**59 (16)**	**76 (12)**	**68 (7)**	**71 (11)**	**78 (11)**	**85 (9)**	**87 (5)**	**90 (3)**	**83 (18)**	**78 (12)**	**79 (12)**	**86 (9)**	**84 (5)**	**88 (5)**	**70 (10)**	**67 (10)**
Phosphorous	Influent (mg PO_4^{3-}–P/L)	11.4 (1.7)	9.5 (3.7)	11.6 (1.5)	9.6 (3.6)	9.0 (1.6)	10.0 (1.8)	10.3 (1.8)	9.1 (2.8)	10.3 (2.5)	9.1 (0.9)	10.0 (1.3)	9.6 (3.0)	10.5 (1.7)	11.3 (3.6)	9.1 (2.5)	9.3 (1.0)
	Effluent (mg PO_4^{3-}–P/L)	8.2 (1.5)	6.1 (1.9)	7.9 (1.9)	6.7 (1.6)	5.4 (2.5)	4.4 (1.5)	2.8 (0.7)	4.0 (2.6)	3.9 (2.0)	2.9 (2.4)	6.1 (2.2)	4.4 (1.5)	3.0 (1.3)	5.3 (3.9)	2.1 (2.6)	0.3 (0.3)
	Removal (%)	**27 (14)**	**46 (15)**	**31 (17)**	**42 (9)**	**40.1 (24)**	**53 (16)**	**72 (9)**	**61 (11)**	**65 (18)**	**68 (23)**	**40 (16)**	**53 (19)**	**71 (10)**	**60 (16)**	**84 (15)**	**96 (3)**

Note: Standard deviations are shown in parentheses.

In turn, salt supplementation in reactors R3 and R4 justified significant improvements in phosphorus removal ($p \leq 0.05$). In contrast, Wang *et al*. (2017) observed a deterioration in phosphate removal in AGS systems, even with 5 g/L of NaCl, possibly due to the predominance of GAOs in systems under osmotic pressure. In R3 fed with acetate, the best phosphorus removal efficiency was achieved at 2.5 g/L NaCl (72%), although the values did not show significant differences between the periods of salt addition. On the other hand, the reactor R4 fed with propionate achieved 96% removal efficiency in the last stage of salt addition (10.0 g/L NaCl), significantly equal to the 7.5 g/L NaCl period.

Propionate is reported as a preferred substrate for growing PAO-rich biomass (Shen and Zhou, 2016). In R4, these microorganisms were probably enriched in the granulation, explaining the continuous improvement in phosphorus removal until the salt addition began. However, with increasing solids concentration and high SRT, at a concentration of 5.0 g/L of NaCl, a decline in phosphorus removal is observed, similar to R2, likely due to saturation of PAOs. Subsequently, due to biomass loss and SRT decrease, phosphorus removal was reestablished and improved, reaching almost its total removal.

5.3. Bioresource production

5.3.1. EPS production

Concerning EPS production, an increase in PS and PN contents was observed during the granulation process in all reactors studied, as shown in Figure 16. This is consistent since aerobic granular biomass has a higher EPS amount than activated sludge flocs used as inoculum (Nancharaiah and Reddy, 2018). Furthermore, there is no significant difference ($p = 0.41$) between the EPS data in the different reactors in the granulation period. In the following phases, the control reactor R1 (acetate) shows a significantly higher production ($p < 0.05$).

It is observed in all systems a maximum production of EPS soon after start-up, with a PN/PS ratio of 12 and 6, for acetate and propionate, respectively, creating favorable hydrophobic conditions for biomass aggregation and subsequent stability of the granular structure (Nancharaiah and Reddy, 2018; Hong *et al*., 2017). Over the remaining operation days, the reactors showed a ratio of around 2.0–3.0, indicating a hydrophobic surface of the granules. Similarly, in studies with acetate and propionate, Wan *et al*. (2015) found a PN/PS ratio of around 2.0. However, they observed better EPS production and hydrophobicity characteristics in propionate-fed reactors.

The higher EPS production in the control reactor R1 (acetate) is probably due to eventual instabilities found, which occurred especially between days 80 and 130. Granule structure instability boosted EPS production since, under adverse conditions, microorganisms usually secrete more of this matrix to maintain its shape (Nancharaiah and Reddy, 2018). On the other hand, it is believed that EPS excess can cause the clogging of granule pores, leading to fragmentation (Corsino *et al.*, 2016b). As can be seen, between days 70 and 85, there is a greater EPS production, with subsequent biomass loss between days 80 and 130 (Figure 16).

Figure 16 – EPS production of the control reactors, R1 (acetate) and R2 (propionate), and the salt-supplemented reactors, R3 (acetate) and R4 (propionate), over the 160 days of operation.

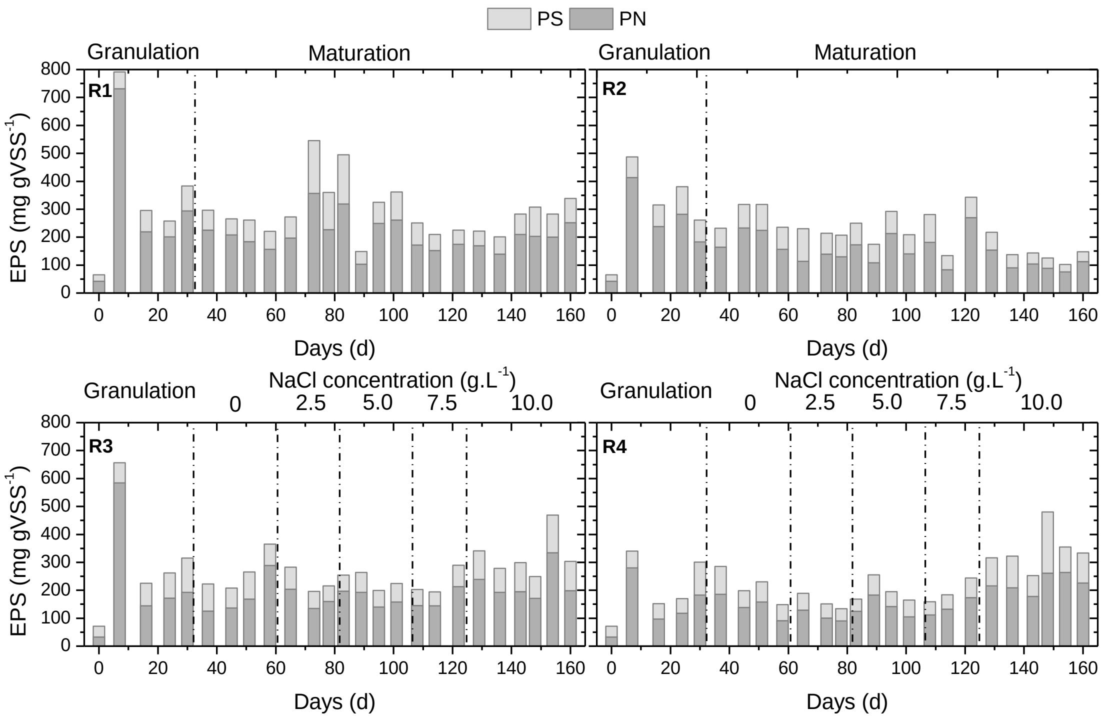

On the other hand, at the end of the operation for the salt-supplemented reactors R3 and R4 (10 g/L NaCl), there is an increase in EPS production, possibly in response to granules’ disintegration that started at a concentration of 7.5 g/L NaCl. Similar to R1 granule break times, more EPS are produced to maintain the granules' shape (Nancharaiah and Reddy, 2018).

It is known that EPS are formed mainly of proteins, polysaccharides, humic acids, nucleic acids, and lipids (Kehrein *et al*., 2020; Carvalho *et al*., 2021). Some of these substances are aromatic and have specific fluorescence characteristics, with specific excitation and emission wavelength ranges. Some commonly found compounds and the Ex/Em range reported in the literature are shown in Table 6 (Wang *et al*., 2014; Liu and Cinquepalmi, 2021).

Table 6 – Excitation/emission bands detected in 3D-EEM for EPS analysis.

Region	Ex/Em	Compounds
A	220-235/295-310	Tyrosine amino acid
B	220-235/330-350	Tryptophan amino acid
C	280-290/330-360	Tyrosine/Tryptophan-containing proteins
D	220-240/400-450	Fulvic acid-like substances
E	300-330/355-375	Microbial polysaccharides
F	260-290/420-460	Polyaromatic type humic acid
G	330-370/420-460	Humic acid type polycarboxylate

Fonte: (Wang *et al*., 2014; Liu & Cinquepalmi, 2021).

The sludge composition analyzed by EEM fluorescence spectroscopy and spectra is shown in Figure 17. Five regions for different EPS components were found. All reactors showed a greater diversity of compounds than the inoculum and greater fluorescence intensity. In salt-supplemented reactors, R3 and R4, greater fluorescence intensity is observed in regions A, B, C, and D. Tyrosine (A) and tryptophan (B) amino acids, tyrosine and tryptophan-containing proteins (C), and fulvic acid-like substances (D) had a higher production with salt addition. Microbial polysaccharides (E) were well identified in the non-neutralized EPS extract. The neutralization in the solution possibly interferes with the compound's three-dimensional structure, thus interfering with the reading. Likewise, proteins are not well identified in the non-neutralized sample since high pH can favor their denaturation process.

Figure 17 – Fluorescence emission-excitation matrix (EEM) graphs of EPS extracted from granules between days 90 and 100 of operation. On the left are the readings in the extract without neutralization, and on the right are those with neutralization. The contour lines represent the intensity of fluorescence.

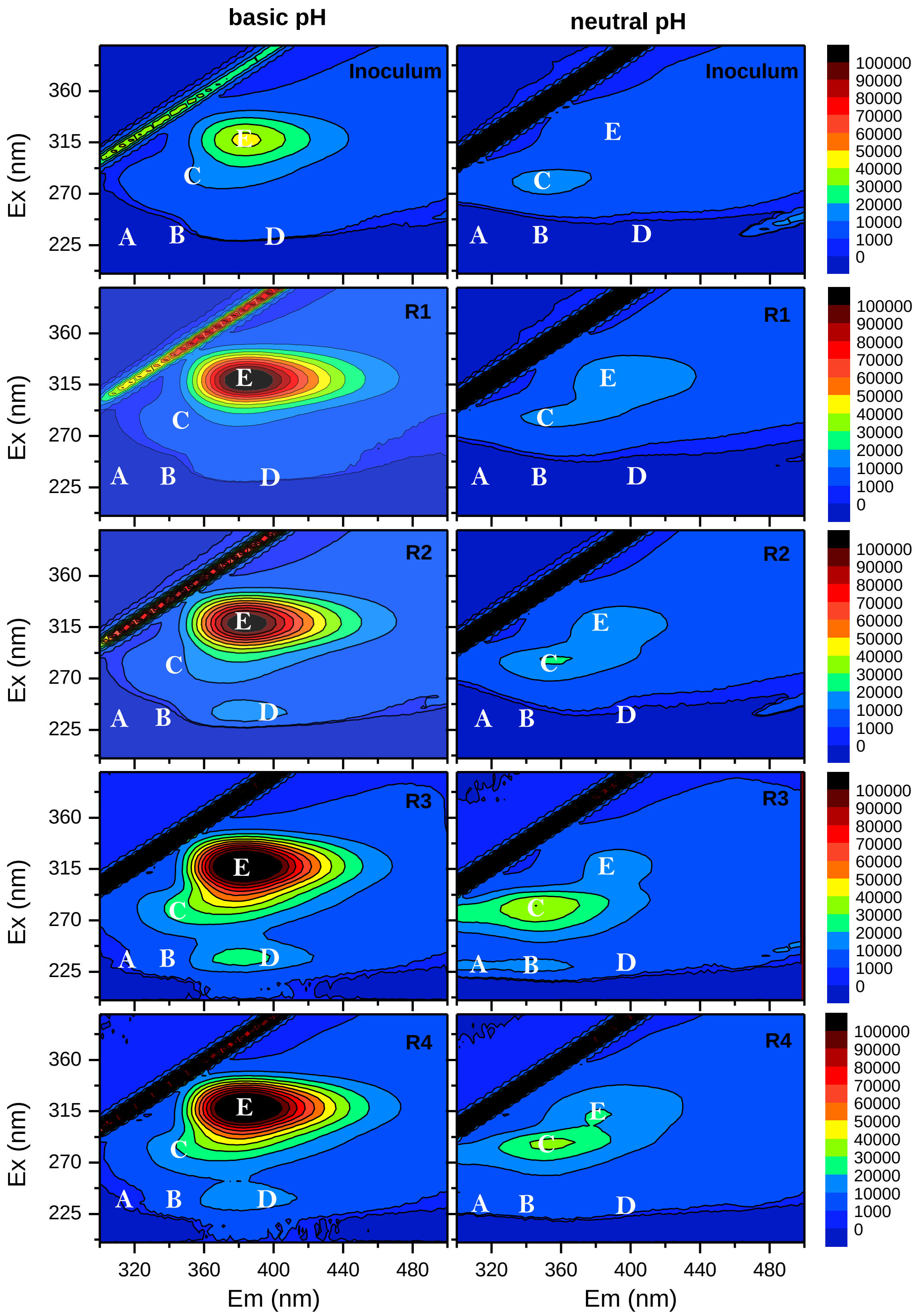

Note: A (tyrosine amino acid), B (Tryptophan amino acid); C (Tyrosine/Tryptophan-containing proteins), D (Fluvic Acid-Like Substances), E (Microbial Polysaccharides).

The difficulty in visualizing certain substances may be due to the EPS extraction method, as reported in the literature (Hong *et al*., 2017; Felz *et al*., 2019). For instance, hot and alkaline extraction methods affect EPS structure, especially proteins, sometimes leading to different results (Chen *et al*., 2022b, 2022c; Felz *et al*., 2016).

5.3.2. ALE and TRP production

In the granulation phase in all reactors, a high concentration of ALE and TRP was found soon after activated sludge inoculation (Figure 18), similar to EPS formation behavior. Therefore, the AGS system, as expected, has favorable conditions for producing resources (Schambeck *et al*., 2020; Rollemberg *et al*., 2020a).

No significant difference ($p = 0.07$) between the reactors was found in ALE production in the granulation phase. However, in the following phases, it can be seen that R3 and R4 presented significantly higher values than the control reactors R1 and R2 ($p < 0$ 0.05). Thus, the addition of salt up to a limit (7.5 g/L) favors ALE production. On the other hand, R1 showed significantly higher TRP production ($p < 0.05$) than the other reactors. Concerning TRP production in the granulation phase, the control reactors R1 and R2 showed significantly higher values ($p > 0.05$) than the salt-supplemented reactors R3 and R4.

Regarding the granule maturation phase, the ALE content in the control reactor R1 (acetate) increased on average from 331 to 396 mg ALE/g VSS, although there was no significant difference in its production ($p = 0.77$). However, in the other control reactor, R2 (propionate), there was a significant drop ($p = 0.002$) in ALE production in the maturation phase, from 397 to 140 mg ALE/g VSS. In contrast, Schambeck *et al*. (2020) observed ALE production increase with granules' maturation. It is observed that, between days 80 and 120 of operation, there is a drop in ALE and TRP productions in R1, possibly due to operational instabilities with biomass loss. On the other hand, it is believed that these instabilities that the R1 system went through during its maturation phase also stimulated ALE production. That is, at the same time that the instabilities and biomass loss affected the sludge settleability characteristics, its microbiota could bring a second response with the structural EPS production (Chen *et al*., 2022a, 2022b) as a response mechanism to the stress suffered. For this reason, such oscillating data are observed in R1.

In the salt-supplemented reactor R3 (acetate), the highest ALE productions were observed at the salt addition beginning, with mean values of 695 and 632 mg ALE/g VSS, corresponding to 2.5 and 5.0 g/L NaCl, respectively. Similarly, there is an increase in the average TRP production (3.5 mg TRP /g VSS) in R3 at 2.5 g/L NaCl, despite being significantly different only from the granulation. Such ALE data can be considered very high. However, two things must be considered: (i) ALE quantification was equivalent to EPS structural, which its composition is complex and composed not only of polysaccharides, but also of proteins, humic acids, and lipids (Bassin *et al*., 2012b); and (ii) extraction method influenced its quantification and composition, similar to EPS (Felz *et al*., 2016; Chen *et al*., 2022b, 2022c).

Figure 18 – Production of ALE and TRP in the control reactors, R1 (acetate) and R2 (propionate), and the salt-supplemented reactors, R3 (acetate) and R4 (propionate), over the 160 days of operation.

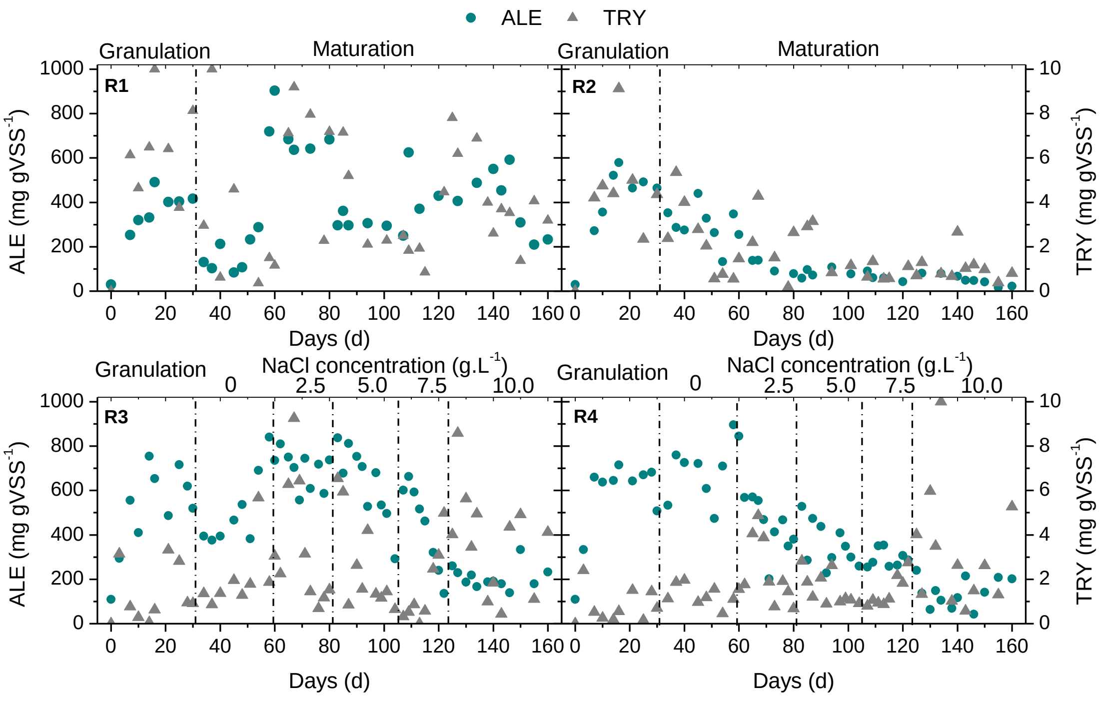

According to Chen *et al*. (2022b, 2022c), gravimetric methods can quantify higher values than alginate-like substances themselves, as it is intended to determine the content of all components. Based on this, the data from this study indicate that salt addition was an important source of stress to boost ALE production, as the instabilities observed in R1. However, other complex hydrogel fractions may have been quantified, overestimating the actual value of ALE.

Contrary to R3, the highest ALE production in salt-supplemented reactor R4 (propionate) was observed in the initial stage of granule formation when salt was absent (679 mg ALE/g VSS). However, significantly lower productions ($p < 0.05$) in both reactors were observed in the last phase (10.0 g/L NaCl), with mean values of 209 and 141 mg ALE/g VSS, respectively, for R3 and R4. This drop may result from granules' fragmentation and collapse.

It is important to note that, in R3 and R4, there are some TRP concentration peaks between each salt addition phase, similar to the EPS data trend, which may result from the imposed osmotic pressure. However, for 10.0 g/L NaCl, despite the ALE concentration having dropped, the TRP concentration increased to 3.7 (R3) and 3.3 mg TRP/g VSS (R4), similar to EPS behavior. Perhaps the higher TRP production in R3 and R4 in the last phases and throughout the operation of R1 is due to the low SRT since the literature has indicated that higher productions of TRP and protein-like substances were favored in lower sludge ages (close to 6 days) (Carvalho *et al*., 2021). Furthermore, Rollemberg *et al*. (2020b) indicate that higher TRP production is mainly associated with newly formed granules.

The increase in SRT can also explain the decrease in ALE and TRP production in the control reactor R2 (propionate) in the same way as in R4 (propionate) between the salt addition phases of 5.0 and 7.5 g/L NaCl. This behavior follows the results of Rollemberg *et al*. (2020b), who indicate that AGS operation with lower STR (between 10 and 15 days) may favor ALE production.

On the other hand, in the last phase of R3 and R4, despite the low SRT, there was no ALE recovery, perhaps because the microbial groups responsible for its production were the most affected in this osmotic condition. Although studies indicate that PAOs may be responsible for ALE production (Schambeck *et al*., 2020), they were probably unaffected since phosphorus removal was improved. The disintegrated biomass in this last condition, especially in R4, produced a gelatinous material. However, it was impossible to identify through the ALE methodology used.

Therefore, the present study highlights the production of biopolymers as a governance mechanism for EPS production, in which the ALE produced is essentially part of the structural EPS, characterized by its ability to form hydrogels. However, other mechanisms, such as increased interactions between biopolymers or bacteria at high salt concentrations, cannot be ruled out. Nonetheless, part of the complexity and specificity of the structures and functions of extracellular biopolymers remain unclear (Chen *et al*., 2022a, 2022b).

5.4. Microbiological characterization

Microbiological analyses were performed on inoculum sludge (I) and biomasses from all reactors. Regarding the control reactors R1 and R2, samples after the experiment completion were analyzed. For the salt-supplemented reactors R3 and R4, the different phases of increasing salt addition (2.5, 5.0, 7.5, and 10 g/L NaCl) were evaluated. Microbial population indicators of AGS samples and inoculum were estimated using alpha diversity indexes such as Chao1 (richness) and Gini-Simpson (diversity).

The Chao1 index presented values of 290 and 200 for R1 (acetate) and R2 (propionate), respectively. Values of 210, 285, 175, and 170 were observed for 2.5, 5.0, 7.5, and 10.0 g/L NaCl in R3 (acetate), respectively, and 280, 320, 210, and 80, respectively, for R4 (propionate). On the other hand, the values observed in the Gini-Simpson index were 0.93 in R1 and 0.95 in R2. For R3, 0.92, 0.94, 0.89, and 0.90 were found in salt concentrations of 2.5, 5.0, 7.5, and 10.0 g/L, respectively, in that exact order values of 0.93, 0.94, 0.84 and 0.65 were found in R4. These results indicate that R1 and R2 showed similar microbial community diversity. In R3 and R4, an evident influence of salt gradient on microbial diversity was observed, with an increase followed by a decrease in microbial diversity and richness, which agrees with the observed system stability data.

Figure 19 shows the relative distribution of the microbial diversity by phylum in each sample. In the inoculum sludge, the following groups were observed: *Bdellovibrionota* (24.3%), *Acidobacteriota* (23.0%), *Gammaproteobacteria* (17.9%), *Alphaproteobacteria* (11.9), *Chloroflexi* (4.6%) and *Planctomycetota* (4.1%). With the granulation process, the dominance of the *Bdellovibrionota* and *Acidobacteriota* phyla present in the inoculum sludge was drastically reduced in all AGS reactors. On the other hand, an increase in *Proteobacteria* and *Bacteroidota* abundance was observed. Salt addition in reactors R3 (acetate) and R4 (propionate) favored, especially at higher salt concentrations, the abundance of *Gammaproteobacteria* and the appearance of *Patescibacteria* and *Myxococcota*.

Gammaproteobacteria and *Alphaproteobacteria* are classes of gram-negative bacteria of the phylum *Proteobacteria*, commonly predominant in aerobic granular sludge with the function of secreting EPS to form aerobic granules (Liu *et al*., 2017). These exopolymers are mostly polysaccharides and proteins, so the *Proteobacteria* fraction seems to have been important for producing ALE and tryptophan in the experimental systems (Meng *et al*., 2019b).

Figure 19 – Relative distribution of microbial diversity of activated sludge inoculum (I) and aerobic granular sludge cultured in the control reactors, R1 (acetate) and R2 (propionate), and the salt-supplemented reactors, R3 (acetate) and R4 (propionate). The bar graph represents only phyla with more than 1% total bacterial abundance in samples.

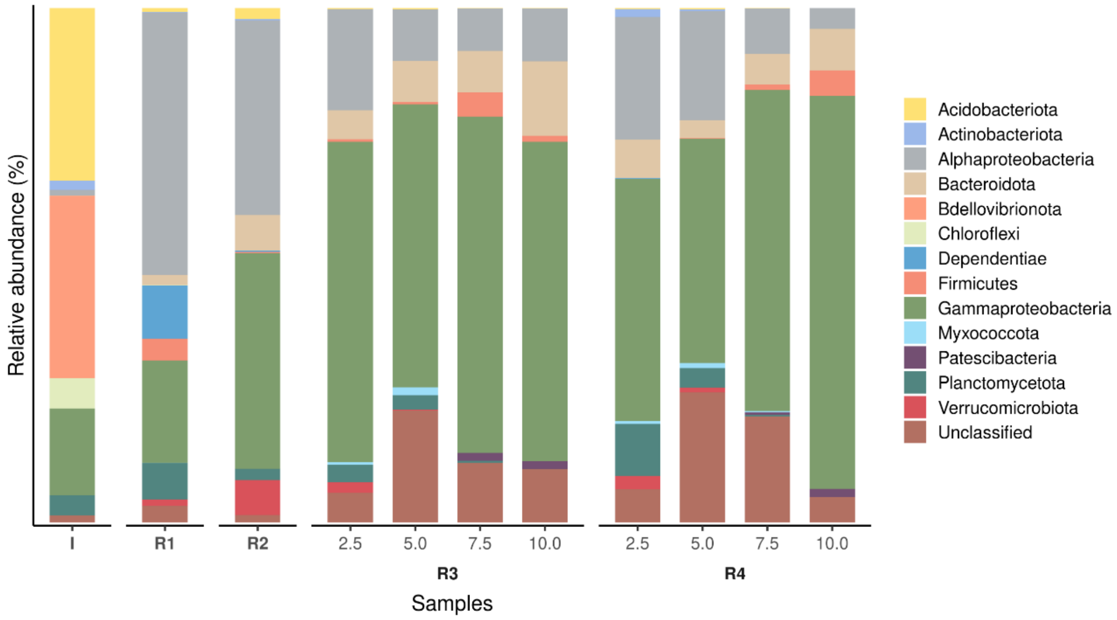

Note: 2.5, 5.0, 7.5, and 10.0 are increasing concentrations of NaCl (g/L) added to reactors R3 and R4.

At the family level, in the inoculum sludge, the highest abundances of the following groups were observed: *Bdellovibrionaceae* (22.4%), *Blastocatellaaceace* (13.8%), and *Comamonadacea* (9.6%). In the control reactor R1 (acetate), higher abundances of *Rhodobacteraceae* (29.4%), *Defluviicoccaceae* (11.6%), and *Rhodocyclaceae* (9.1%) were observed. In turn, in R2 (propionate), the groups *Rhodanobacteraceae* (16.2%), *Defluviicoccaceae* (13.7%), and *Xanthomonadaceae* (8.0%) were verified. *Rhodobacteraceae* and *Rhodocyclaceae* were also enriched in the salt-supplemented reactors, reaching relative abundances of 38.2% and 54.8% (*Rhodobacteraceae*) and 8.8% and 29.9% (*Rhodocyclaceae*) for R3 (acetate) and R4 (propionate), respectively.

Bacteria of the *Flavobacteriaceae* family were enriched in the halophilic systems, in which values ranging from 1.4% to 10.7% were observed in R3 (acetate) and 2.3%–

4.0% in R4 (propionate). Research has shown that microorganisms from the *Flavobacteriaceae* family secrete large amounts of EPS in marine environments, especially PN-rich EPS, and favor ALE production (Cui *et al.*, 2021). In addition, *Flavobacteriaceae* bacteria are reported to have the ability to degrade organic and nitrogenous compounds in wastewater and, under anaerobic conditions, can provide readily available carbon sources for heterotrophic denitrification, demonstrating their ability to efficiently remove pollutants (Zhang *et al*., 2020; Cui *et al*., 2021). The greater abundance of this microbial group may have contributed to the better performance in removing nutrients in R3 and R4.

Literature has reported that families of Proteobacteria, such as *Rhodobacteraceae*, *Rhodocyclaceae*, and *Flavobacteriaceae,* seem to facilitate the EPS release and granules' development, encouraging the production of signaling molecules, such as cyclic di-guanosine monophosphate (c-di-GMP) (Han *et al*., 2022; Jiang *et al*., 2021).

Figure 20 shows the microbial diversity at the genus level in the activated sludge inoculum and AGS biomasses. The diversity was drastically changed after applying operating conditions for aerobic granular sludge cultivation, such as the imposition of a high aeration rate and alternation between feast and famine periods in the operating cycle. Bacteria genera *Bdellovibrio* (23.9%) and *OLB17* (13.9%) dominant in the inoculum did not exist in the AGS samples. *Bdellovibrio* are predatory species that can impair the operational performance of wastewater treatment systems, while *OLB17* in the filamentous form, when present in abundance, can affect the granular structure (Feng *et al*., 2017).

Important proteobacteria capable of producing and secreting EPS were identified in abundance in the control reactors R1 (acetate) and R2 (propionate): *Defluviicoccus* (12.2% in R1 and 14.4% in R2) and *Pseudofulvimonas* (6.9% in R1 and 17.1% in R2) (Pronk *et al*., 2017b; Yan *et al*., 2022). Both *Defluviicoccus* and *Pseudofulvimonas*, in addition to denitrifying, are characterized by their resistance to low saline concentrations (He *et al*., 2020; Wang *et al*., 2022). Together, these bacteria were found in greater abundance in R3 (2.82%) and R4 (10.87%) in the concentration phase of 5.0 g/L NaCl.

In addition to them, other bacteria that adapted to the saline environment with an abundance greater than 5% were: *Aquicella*, *Acinetobacter*, and *Planktosalinus* in R3 (acetate) and *Thauera, Rhodopirellula, Alishewanella, Stappia*, and *Vicingus* in R4 (propionate).

Figure 20 – Relative distribution of microbial diversity of activated sludge inoculum (I) and aerobic granular sludge cultured in the control reactors, R1 (acetate) and R2 (propionate), and the salt-supplemented reactors, R3 (acetate) and R4 (propionate). The bar graph represents only genera (B) with more than 1% total bacterial abundance in samples.

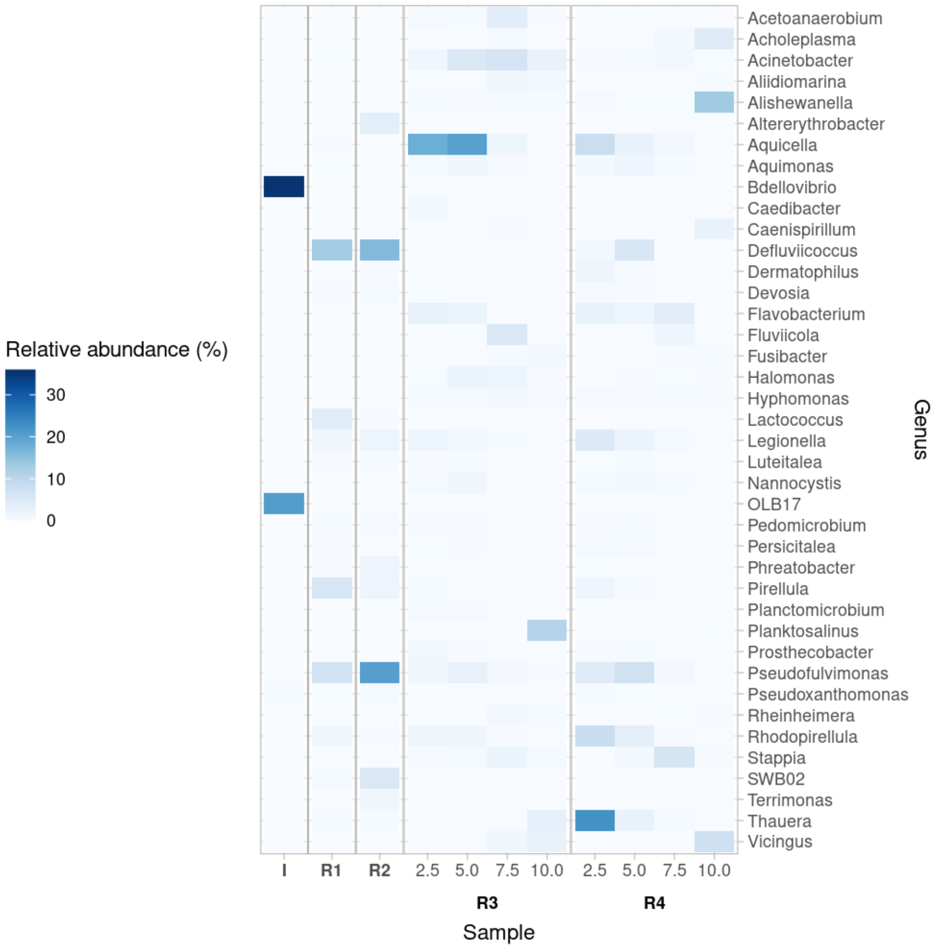

Note: 2.5, 5.0, 7.5, and 10.0 are increasing concentrations of NaCl (g/L) added to reactors R3 and R4.

Recent studies have reported a direct correlation between the secretion of second messenger cyclic di-guanosine monophosphate (c-di-GMP) and excess ALE production (Yang *et al*., 2014). The stimulation of quorum sensing may also occur due to osmotic stress caused by salt supplementation (Meng *et al*., 2020). Among the genera hypothetically related to this mechanism are: *Acholeplasma*, *Acinetobacter*, *Flavobacterium*, *Fuviicola*, *Halomonas*, *Hyphomonas*, *Lactococcus*, *Legionella*, *Pirellula*, *Pseudofulvimonas*, *Pseudoxanthomonas*, *Rhodopirellula*, and *Thauera* (Chou and Galperin, 2016; Chen *et al*., 2022a, 2022d). These species were particularly found with an abundance above 10% in the control reactors R1 and R2, and in the salt-supplemented reactor R3 (acetate) in all phases except 10.0 g/L and in R4 (propionate) for 2.5 and 5.0 g/L NaCl, which possibly justifies a higher ALE production under these operating conditions.

Little is known about the bacteria associated with tryptophan production in AGS. Reports indicate a positive correlation between tryptophan accumulation in a low influent C:N ratio (around 5) and the favoring of *Thauera* genera bacteria (Yu *et al*., 2020; Zhang *et al*., 2018). This study identified these bacteria in abundance only in R4 (propionate) at 2.5 g/L (20.7%) and 5.0 g/L (2.2%). Protein-secreting bacteria, such as *Flavobacterium*, may be related to the increase in tryptophan production, mainly in the phases of 2.5 and 5.0 g/L NaCl, with relative abundance between 2.0 and 4.0% (Rollemberg *et al*., 2020b).

Figure 21 presents the functional groups involved in carbon, nitrogen, and phosphorus removal at the family level. In general, a greater abundance of AOB, NOB, and DNB is observed in salt-supplemented reactors R3 (acetate) and R4 (propionate), indicating better conversions from nitrite to nitrate and denitrification and better system performance in removing TN. This condition must be due to better granule development in these systems. These results also show that the salt addition did not negatively affect the groups involved in nitrogen conversion.

The abundance of PAOs was similar between the control reactors R1 (acetate) and R2 (propionate). However, there was a predominance of GAOs over PAOs concerning substrate competition, especially in R1, justifying the low phosphorus removal achieved. In the salt-supplemented reactors R3 (acetate) and R4 (propionate), an increase in PAOs is observed. At the same time, there is an increase in GAOs in R3 and a decrease in R4, thus justifying the high phosphorus removal efficiency achieved in R4 due to competition for substrate between GAOs and PAOs.

Figure 21 – Functional groups identified by family in the inoculum, control reactors R1 (acetate) and R2 (propionate), and the salt-supplemented reactors R3 (acetate) and R4 (propionate) (absolute abundance of functions ≥ 10).

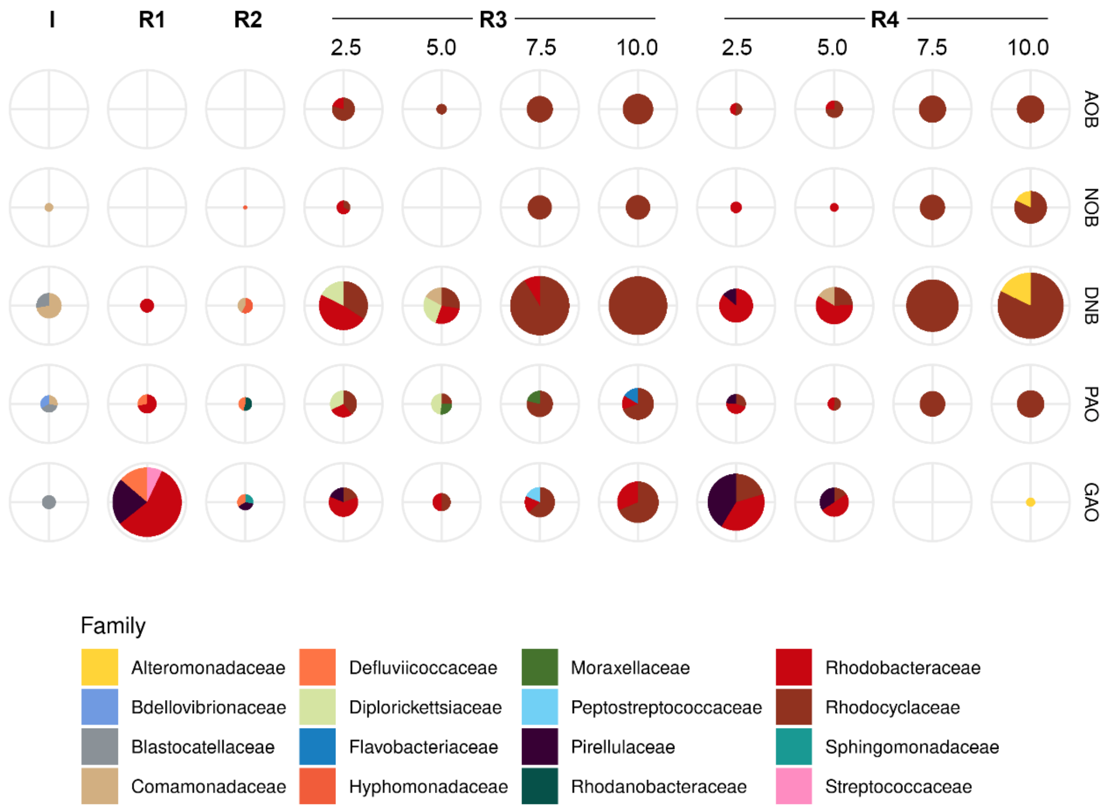

Legend: ammonia-oxidizing bacteria (AOB), nitrite-oxidizing bacteria (NOB), glycogen accumulating organisms (GAOs), polyphosphate accumulating organisms (PAOs), and denitrifying bacteria (DNB). Note: 2.5, 5.0, 7.5, and 10.0 are increasing concentrations of NaCl (g/L) added to reactors R3 and R4.

5.5. Conclusions

Saline wastewater concentrations up to 7.5 g/L NaCl did not compromise the physical characteristics or stability of the granules. Systems that are appropriately acclimated to such salt concentrations demonstrated optimal removal efficiencies for nitrogen and phosphorus. The addition of salt enhanced the production of ALE and fostered the enrichment of AOB, NOB, DNB, PAOs, and other bacteria associated with bioresource production. In contrast, the production of TRP did not follow the same pattern. Although TRP concentrations showed fluctuations in response to osmotic pressure, similar to EPS, the variability in its production appeared to be more significantly influenced by the SRT rather than the salt concentration alone.

The full version of this paper is published in Bioresource Technology (2023) under the same name as this subsection. DOI: https://doi.org/10.1016/j.biortech.2023.128850

Figure 22 – Graphical abstract: influence of operating regime on resource recovery in aerobic granulation systems under osmotic stress.

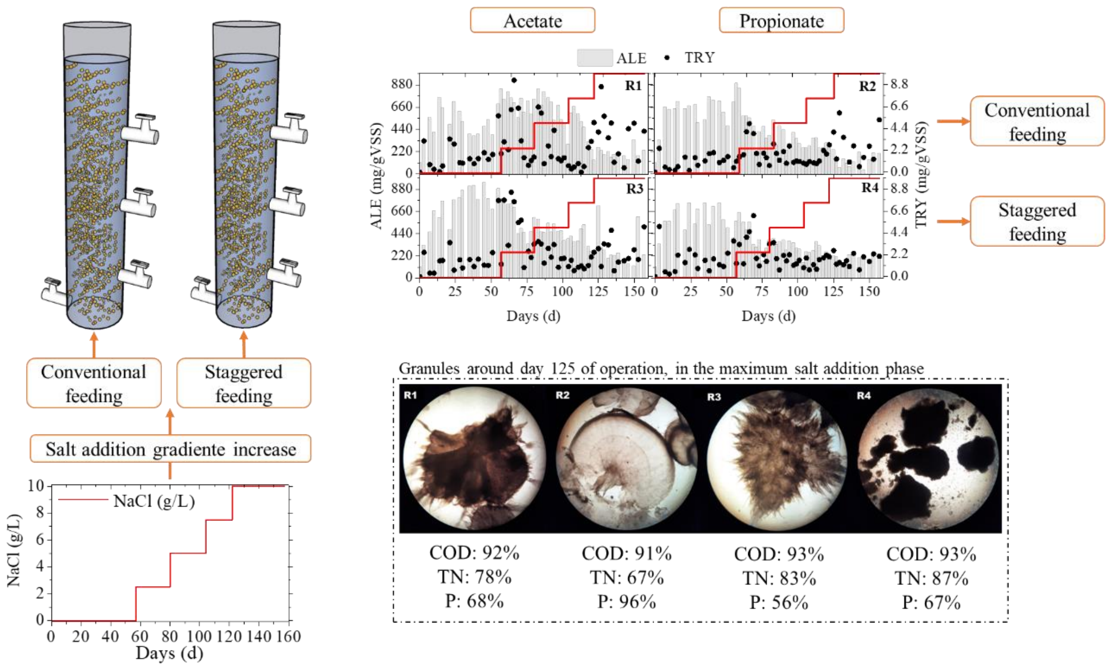

6. INFLUENCE OF OPERATING REGIME ON RESOURCE RECOVERY IN AEROBIC GRANULATION SYSTEMS UNDER OSMOTIC STRESS

This study evaluated the production of alginate-like exopolymers (ALE), extracellular polymeric substances (EPS), and tryptophan (TRP) under osmotic pressure in conventional and staggered feeding regimes. The results revealed that systems operated with conventional feed accelerated the granulation, although less resistant to saline pressures. The staggered feeding systems favored better denitrification conditions and long-term stability. The increase in salt addition gradient influenced bioresources' production. However, staggered feeding did not influence the production of ALE, EPS and TRP despite decreasing the famine period. Sludge retention time (SRT), which was not controlled, proved to be an important operational parameter with a negative influence on bioresources' production for values greater than 20 days. Thus, the principal component analysis confirmed that the production of ALE at low SRT is related to better-formed granules with good settling characteristics and good AGS performances.

6.1. Granule formation and stability

The reactors started with activated sludge biomass, whose MLVSS concentration and SVI_{30} were 2.9 g/L and 213 mL/g, respectively. Right after the initial operation cycles, MLVSS concentration dropped due to the low settling velocity biomass washout (Figure 23). In the four reactors, sludge granulation was reached after 30 days of operation, characterized by the SVI_{30}/SVI_5 ratio above 0.8 and SVI_{30} with a decreasing trend, in addition to 80% of the aerobic granules with a higher average diameter of 0.2 mm. It was also noted that there was a rapid increase in biomass in the four systems soon after salt addition, to the detriment of the greater accumulation of inorganic materials in the biomass under osmotic pressure (Meng *et al*., 2019b).

The classical references consider aerobic biomass/systems the following aspects as indications: granulation beginning when the SVI_5 is closer to the SVI_{30} (de Kreuk *et al*., 2005; Nancharaiah and Raddy, 2018), mature granules present SVI_{30} between 30 and 80 mL/g (Derlon *et al*., 2016), aerobic granule when its diameter is larger than 0.2 mm, and complete granular system when more than 80% of the biomass is in the form of aerobic granules with an SVI_{30}/SVI_5 ratio greater than 0.8 (de Kreuk *et al*., 2007; Liu *et al*., 2010).

Figure 24 shows the morphology of the granules around day 125 of stage 4, and at that time, only R4 maintained well-formed granules, indicating that the staggered feeding and propionate as a carbon source favored the system's stability.

R1 presented MLVSS oscillations over the operational period, with mean values of around 2.0 g/L (±0.7). However, it showed better results for the SVI_{30}/SVI_5 ratio (close to 1) and SVI_{30} (69 mL/g) at the end of stage 3 (Figure 23). R2, R3, and R4 showed continuous improvement in the MLVSS (5.0, 3.2, and 6.0 g/L), SVI_{30}/SVI_5 ratio (close to 1.0), and SVI_{30} (34, 63, 20 mL/g) data, respectively, but in different stages; R2 in stage 3, R3 between stages 3 and 4, and R4 between stages 4 and 5.

Figure 23 – Mixed liquor volatile suspended solids (MLVSS), SVI_{30}/SVI_5 ratio, and SVI_{30} in the four reactors throughout the 157 days of operation. Stages of granulation (0), no salt addition (1), and salt gradient increase of 2.5 (2), 5.0 (3), 7.5 (4), and 10.0 (5).

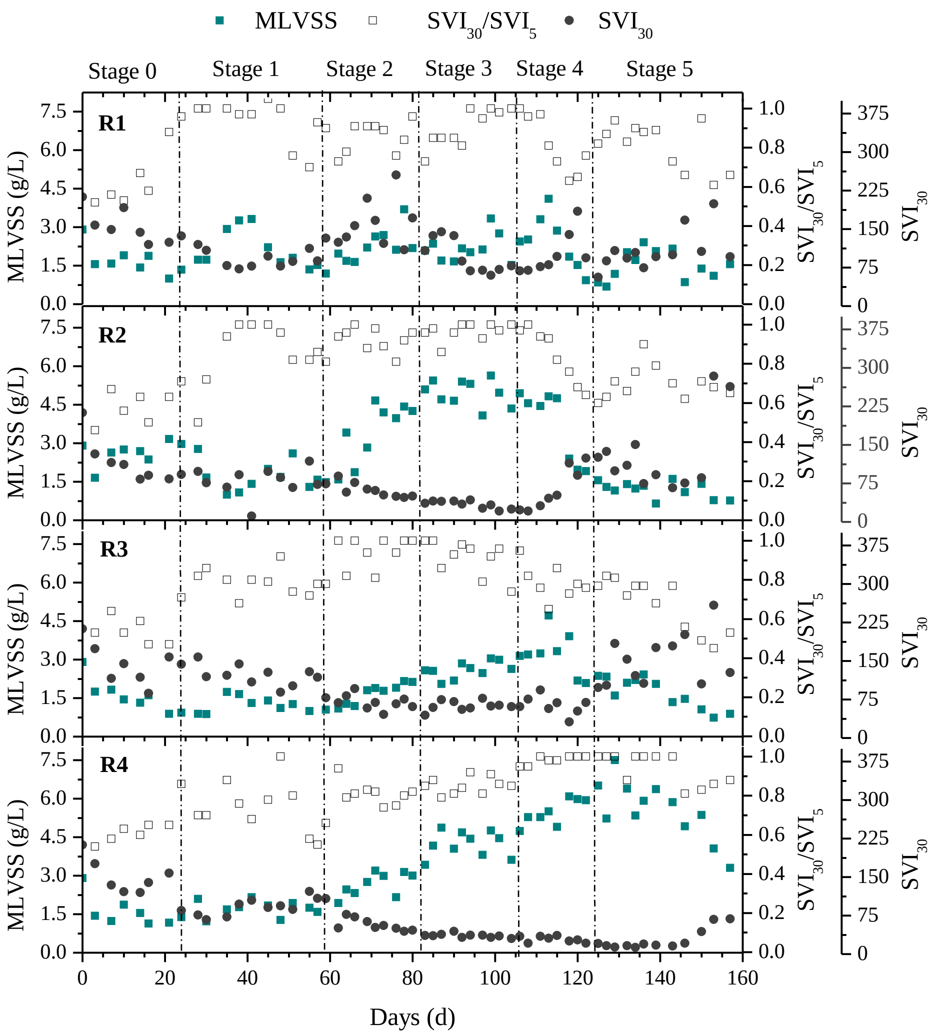

Overall, it can be observed that R1 and R2, operated under conventional feeding, achieved faster operational stability since, even in stage 1, these systems showed better results, maintaining the best performances until stage 3. This behavior indicated that systems with conventional feeding favor granulation since the selection pressure by the feast/famine regime, i.e., rapid rate of carbon source consumption and long famine period, is possibly established faster (Rollemberg *et al.*, 2018). Therefore, a more extended famine period after the start-up is likely a critical selection pressure for granulation to reach stability. However, as the system stabilizes, the granules have greater support capacity for shorter famine periods, as those established in staggered feeding. Thus, optimal distinct feast/famine periods must be adopted in the granulation and maturation of an AGS system.

Figure 24 – Microscope and scanning microscopy images (100µm) of each reactor from the end of Stage 4 (~125 days) (A) R1, (B) R2, (C) R3, and (D) R4.

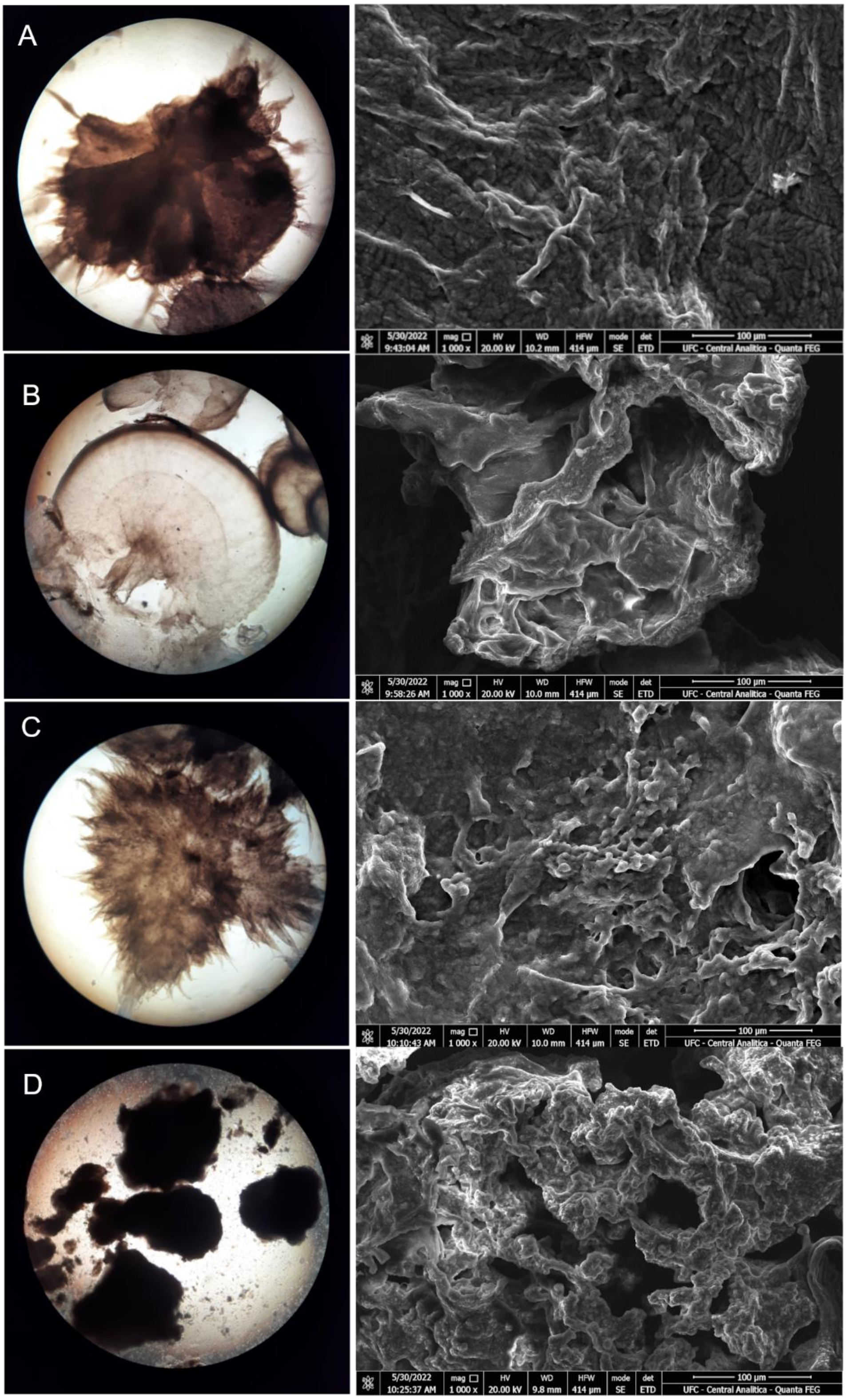

However, systems R1 and R2 collapsed in stage 4, while reactors R3 and R4, operated under staggered feeding, showed destabilization only in stage 5 (Figure 23), indicating that this form of SBR operation helped to maintain granule stability, possibly in dampening the osmotic shock, since the load is diluted throughout the cycle (Silva; Rollemberg; Santos, 2021). As previously found, salt addition affected granule settling velocity (Wang *et al*., 2017), possibly due to water density increase, which affects this physical property (Winkler *et al*., 2012).

The EDS analysis of the different systems indicated that the acetate fed to the reactors had a greater salt accumulation on the granule surface, especially sodium, reaching stage 4 with 12.5% and 9.8% sodium in R1 and R3, respectively. However, R2 and R4 only showed salt accumulation on the granule surface from stage 3 (5 g/L), presenting only 8.7% and 6.0% sodium in stage 4 for R2 and R4, respectively. R2 showed about 30% sodium on the granule surface in stage 5. Therefore, the greater or lesser salt presence in the biomass can explain the trends observed regarding system stability.

Peng *et al*. (2022) indicated that granules with higher PN production have higher hydrophobicity and zeta potential. In this study, systems operated with acetate showed higher PN production, implying a higher zeta potential. The greater the zeta potential, the greater the negative charge on the granules' surface, and the greater the attraction by cations in the search for the isoelectric potential (neutrality), justifying a higher sodium accumulation. On the other hand, this more significant accumulation of cations on granules' surface can lead to higher biomass stress and PN production. The literature has reported that acetate is a favorable substrate for granulation, despite having long-term instabilities (Rollemberg *et al*., 2019). As seen in the present research, although the systems that operated with this substrate reached stability first, they suffered subsequent recurrent instabilities. Such a behavior follows the trends observed in studies by Rollemberg *et al*. (2019) and Santos *et al*. (2022).

Between stages 4 and 5, especially reactors R1, R2, and R3, showed a biomass washout, MLVSS concentration drop, and poor settleability characteristics, possibly explained by the increase in osmotic pressure that caused plasmolysis and cell disintegration (Quartaroli *et al*., 2019), as the gradual increase in salt causes a change in granule morphology. Systems with salt concentrations around 7.5 g/L (Stage 4) started to show fluffy and irregularly shaped granular biomass, except R4, which at that moment was maintained with dense and good settleability granules, showing a change in their characteristics only at the end of stage 5 (addition of 10 g/L of salt) (Figure 24). Such behavior concerning the effect of salt addition on granule morphology corroborates previous studies (Wang *et al*., 2017; Quartaroli *et al*., 2019).

Sludge retention time (SRT) remained stable between 6 and 10 days in R1, between operation stages 1 and 4. However, R2 maintained an increasing SRT until stage 3, reaching values around 20 to 25 days. At the end of the operation, the SRT dropped to 1–4 days in both reactors, possibly due to osmotic pressure, which led to the system's collapse. R3 and R4 showed a gradual increase in SRT. In R3, 16 to 20 days values were found in stage 3, falling to 3 to 5 days in the following stages. On the other hand, R4 reached an SRT of 25 to 30 days in stage 3, which was maintained until the end of the operation.

6.2. Reactors' performance

The COD removal in the systems was greater than 90% during the entire experimental period, indicating that organic matter removal remained high even with salt addition (Table 7). However, stage 5 presented significantly lower mean values (91 ± 1%) ($p < 0.05$) than the other stages, especially in R1 and R2.

An improvement in total nitrogen (TN) removal was observed in all systems (90 ± 2%), indicating good granule development. Possibly the existence of an aerobic outer layer and anoxic and anaerobic inner layers favored the coexistence of AOB; NOB, and DNB (Liu *et al*., 2010; Winkler *et al*., 2013; Corsino *et al*., 2016a;). However, TN removal dropped between stages 4 and 5, especially in R1 (78 ± 12), R2 (67 ± 10%), and R3 (83 ± 16).

The NOB had a higher salinity tolerance since the reactors did not show significant nitrite accumulation, as shown in the cycle analysis item. This result corroborates with Wang *et al*. (2017), who observed that nitrite's specific oxidation rate (SOR) was not affected by salt addition up to 30 g/L NaCl, while the AOB showed an ammonia SOR decrease with increasing salinity. Using pure cultures, Hunik *et al*. (1993) and Moussa *et al*. (2006) also reported that NOB were less affected by salt stress than AOB. However, other studies have reported nitrite accumulation in highly saline systems, showing that NOB are more affected by salinity (Meng *et al*., 2022b).

Although nitrification dropped in R1, R2, and R3, only R2 showed significantly lower NH_4^+-N removal values ($p < 0.05$) between stages 4 and 5, indicating that possibly simultaneous nitrification and denitrification (SND) continued via aerobic nitrification and heterotrophic denitrification. However, the granule structure changed throughout the experiment, similar to the findings of Quartaroli *et al*. (2019). Ammonium removal decrease in R2 can be explained by biomass washout since nitrifying microorganisms have a lower SRT than other microorganisms in AGS biomass, as they colonize the outer (aerobic) layer of the granules, which is more rapidly fragmented and subsequently washed out of the reactor compared to the inner layer (anoxic/anaerobic) (Winkler *et al*., 2012).

Reactors R3 and R4 showed higher resistance to salt addition in the denitrification since the removal values were significantly ($p < 0.05$) higher than R1 and R2 (Table 7). In this way, the organic load distributed throughout the cycle, in addition to providing a reduction in toxicity, can favor the SND process. Similarly, Silva, Rollemberg and Santos (2021) observed low nitrite and nitrate concentrations and TN removals of around 92% in a staggered-feed system in their studies evaluating the feeding impact on AGS systems' performance and operational stability.

Furthermore, maintenance and balance of these microorganisms, nitrifies and denitrifies, may be one factor that favored the reactors' greater stability with staggered feeding. Granule long-term stability in AGS systems is strongly linked to microbiological diversity and the maintenance of slow-growing microorganisms since faster-growing heterotrophic bacteria suppress them in the competition for resources (Lin *et al*., 2020; Lv *et al*., 2014). However, microbiology showed that these microorganisms were enriched in all reactors. Therefore, this improvement in TN removal is attributed to staggered feeding, which allows for nitrification with a reduced organic load during the aerobic phase, thereby accelerating the nitrification rate (Chen *et al*., 2013), and ensures greater availability of organic matter for denitrification throughout the cycle (Silva; Rollemberg; Santos, 2021).

Significant phosphorus removals were achieved even with salt addition (Table 7). The highest efficiency (69 ~ 72%) observed in the systems was in stage 2, indicating phosphorus-accumulating bacteria (PAOs) enrichment. As confirmed by molecular biology analysis, acetate-fed reactors (R1 and R3) showed a decrease in phosphorus removal in the following stages, probably due to competition between GAOs (glycogen-accumulating organisms) and PAOs.

Table 7 – Reactors' performance throughout the different experimental stages.

Reactor	R1 (conventional, acetate)						R2 (conventional, propionate)						R3 (staggered, acetate)						R4 (staggered, propionate)					
	Stage						Stage						Stage						Stage					
Parameters	**0**	**1**	**2**	**3**	**4**	**5**	**0**	**1**	**2**	**3**	**4**	**5**	**0**	**1**	**2**	**3**	**4**	**5**	**0**	**1**	**2**	**3**	**4**	**5**
COD_i mg L^{-1}	968 (92)	987 (104)	938 (92)	865 (85)	872 (72)	938 (77)	1078 (165)	974 (138)	966 (52)	908 (80)	910 (82)	1001 (99)	962 (91)	987 (104)	939 (93)	854 (85)	867 (92)	938 (77)	1117 (217)	967 (132)	955 (60)	924 (67)	909 (76)	986 (68)
COD_e mg L^{-1}	64 (20)	40 (18)	29 (13)	28 (11)	43 (17)	78 (48)	58 (14)	45 (31)	37 (24)	24 (9)	40 (14)	90 (37)	51 (9)	49 (32)	40 (35)	56 (30)	30 (8)	61 (31)	59 (17)	41 (24)	28 (16)	30 (8)	40 (37)	71 (40)
E (%)	93 (2)	96 (2)	97 (1)	97 (1)	95 (2)	92 (5)	94 (2)	95 (3)	96 (2)	97 (1)	96 (2)	91 (3)	95 (1)	95 (4)	96 (3)	93 (4)	97 (1)	93 (4)	95 (2)	96 (3)	97 (2)	97 (1)	96 (4)	93 (4)
NH_4^+-N_i mg L^{-1}	55.9 (3.5)	57.3 (4.4)	58.1 (4.0)	53.8 (5.1)	56.8 (1.1)	48.9 (8.1)	61.7 (5.0)	59.2 (5.5)	61.3 (4.0)	59.8 (3.3)	59.8 (2.9)	51.5 (7.9)	55.9 (3.5)	57.3 (4.4)	58.1 (4.0)	53.8 (5.1)	56.8 (1.1)	48.6 (7.7)	61.7 (5.0)	59.2 (5.5)	61.3 (4.0)	59.8 (3.3)	59.8 (2.9)	51.4 (7.9)
NH_4^+-N_e mg L^{-1}	10 (15)	2.7 (5)	0.9 (0.5)	0.6 (0.7)	6.9 (10.1)	8.5 (6.9)	3.3 (4.5)	3.3 (4.3)	1.2 (1.2)	0.6 (0.9)	14.7 (5.7)	14.9 (7.0)	2.4 (3.3)	0.9 (1.1)	1 (0.8)	0.9 (1.1)	3.2 (2.8)	5.5 (6.7)	2.3 (3.3)	0.7 (1.0)	0.7 (0.9)	0.6 (1.2)	1 (0.6)	3.6 (4.6)
NO_2^--N_e mg L^{-1}	4.9 (4.3)	3 (2.9)	0.6 (0.2)	0.3 (0.5)	1.3 (0.2)	1.3 (0.1)	4.7 (3.1)	2.8 (1.5)	0.7 (0)	0.3 (0.5)	1.3 (0.3)	1.1 (0.5)	1.9 (1.0)	2.1 (1.4)	0.6 (0.2)	0.3 (0.5)	1.3 (0.2)	1.1 (0.5)	2.7 (2.4)	1.7 (1.3)	0.7 (0.1)	0.3 (0.3)	1.2 (0.2)	1.1 (0.5)
NO_3^--N_e mg L^{-1}	1 (0.6)	2.7 (3.2)	6.2 (3.2)	4.4 (1.4)	1.4 (0.9)	1.4 (0.6)	4.8 (3.2)	2.4 (2.4)	7.8 (2.9)	6.3 (2.6)	1.7 (1.1)	1.4 (0.9)	1.9 (1.3)	2 (1.7)	6.1 (1.8)	3.5 (1.4)	1.3 (0.7)	1.4 (0.7)	1.8 (1.3)	2.8 (2.0)	6.9 (3.6)	5.7 (2.1)	4.2 (1.9)	1.9 (1.2)
E_{nit} (%)	83 (25)	95 (9)	98 (1)	99 (1)	88 (18)	84 (12)	95 (7)	94 (8)	98 (2)	99 (1)	75 (10)	73 (11)	96 (6)	98 (2)	98 (1)	98 (2)	94 (5)	88 (15)	96 (6)	99 (2)	99 (2)	99 (2)	98 (1)	93 (9)
E_{den} (%)	72 (22)	85 (9)	87 (5)	90 (3)	83 (18)	78 (12)	79 (12)	86 (9)	84 (5)	88 (5)	70 (10)	67 (10)	89 (6)	91 (3)	87 (3)	91 (3)	90 (5)	83 (16)	89 (9)	91 (3)	86 (6)	89 (4)	89 (4)	87 (9)
PO_4^{3-}-P_i mg L^{-1}	9 (1.6)	10 (1.8)	10.3 (1.8)	9.1 (2.8)	10.3 (2.5)	9.1 (0.9)	10 (1.3)	9.6 (3.0)	10.5 (1.7)	11.3 (3.6)	9.1 (2.5)	9.3 (1.0)	8.9 (1.4)	10 (3.1)	10.3 (1.8)	9 (2.8)	10.1 (2.7)	9.1 (1.3)	10.2 (1.8)	9.6 (2.9)	10.5 (1.7)	10.8 (3.6)	9.1 (2.5)	9.2 (1.1)
PO_4^{3-}-P_e mg L^{-1}	5.4 (2.5)	4.4 (1.5)	2.8 (0.7)	4 (2.6)	3.9 (2.0)	2.9 (2.4)	6.1 (2.2)	4.4 (1.5)	3 (1.3)	5.3 (3.9)	2.1 (2.6)	0.3 (0.3)	5.3 (2.1)	3.6 (1.1)	3.3 (0.8)	3 (0.9)	4.4 (2.9)	3.8 (2.4)	5.2 (2.6)	4.2 (1.3)	2.9 (0.5)	3.7 (1.8)	4.8 (2.5)	2.8 (2.4)
E (%)	40.1 (24)	58 (15)	72 (9)	61 (11)	65 (18)	68 (23)	40 (16)	58 (19)	71 (10)	65 (10)	84 (15)	96 (3)	40 (19)	67 (20)	69 (6)	66 (8)	62 (17)	56 (25)	50 (15)	59 (20)	72 (6)	67 (7)	53 (15)	67 (27)

*i – Influent; e – Effluent; E – Efficiency; nit – Nitrification; den – Denitrification. Stages of granulation (0), no salt addition (1), and salt gradient increase of 2.5 (2), 5.0 (3), 7.5 (4), and 10.0 (5).

In R2, the reactor fed with propionate, average phosphorus removals of 84 and 96% were achieved in stages 4 and 5, respectively. In this period, molecular biology indicated a greater presence of PAOs (59 and 63% abundance in stages 4 and 5, respectively) compared to GAOs (< 10% abundance). This condition, associated with the lower SRT, contributed to the complete phosphorus removal. In turn, R4, a propionate-fed reactor, also showed a higher presence of PAOs (59% abundance) to GAOs (14% abundance) in the last stage. However, a complete removal is not achieved in this case, probably due to PAOs saturation in the biomass by the high SRT (Bassin *et al*., 2012a). In addition, their granules reached 17.2% sodium accumulation. According to Corsino *et al*. (2019), a relatively long SRT (~27 days) leads to salt accumulation in the granules, thus affecting the granular sludge's biological activity and performance.

These results reaffirm that: a) propionate is a preferred carbon source for PAOs since they favor phosphorus removal, and b) SRT is a key parameter to achieving complete phosphorus removal. Furthermore, the results indicated that salt addition does not affect phosphorus removal, as PAOs can compete with GAOs at saline concentrations up to 22 g/L NaCl (Pronk *et al*., 2014). However, while the study by Pronk *et al*. (2014) showed no improvement in phosphorus removal by salt addition, Meng *et al*. (2019a) showed improvement at moderate NaCl levels (10 g/L).

6.3. Cycle analysis

The profile of organic matter and nutrients consumption during an operational cycle was investigated (Figure 25). From the oxygen analysis during the cycle, DO was kept between 3 and 5 mg/L during the first hour of aeration of R1 and R2. On the other hand, in R3 and R4, this value remained between 1 and 5 mg/L during the first two hours of aeration. This difference is due to the second and third feeding of R3 and R4, which leads to a greater DO demand for consuming carbonaceous organic matter. Furthermore, the lower DO established in R3 and R4 during the first hours of aeration were possibly fundamental to establish the best TN removals in these reactors, since better anoxic conditions were established under low DO.

After this period, the DO was higher than 5 mg/L in all reactors. These times coincided with the famine period, i.e., when no more soluble COD was available. This is because they enter the endogenous phase and require lower oxygen concentrations for their metabolism. Thus, the COD was practically all consumed after 1 h of the aerobic period beginning in R1 and R2. On the other hand, in R3 and R4, more than two hours were needed due to the second and third feedings in the aerobic period. Similar behavior is observed for ammonium consumption. After 1 h and 2 h of the aerobic period beginning, all ammonium was consumed in the conventional (R1 and R2) and staggered (R3 and R4) feeding systems, respectively. However, it is worth noting that this profile was performed on day 100 and that at the operation completion, a drop in nitrification was observed, with ammonium accumulation.

Figure 25 – Cycle analysis of the reactors R1 (conventional, acetate), R2 (conventional, propionate), R3 (staggered, acetate), and R4 (staggered, propionate) performed at the end of Stage 3 (100 days of operation) at 5.0 g/L of salt concentration.

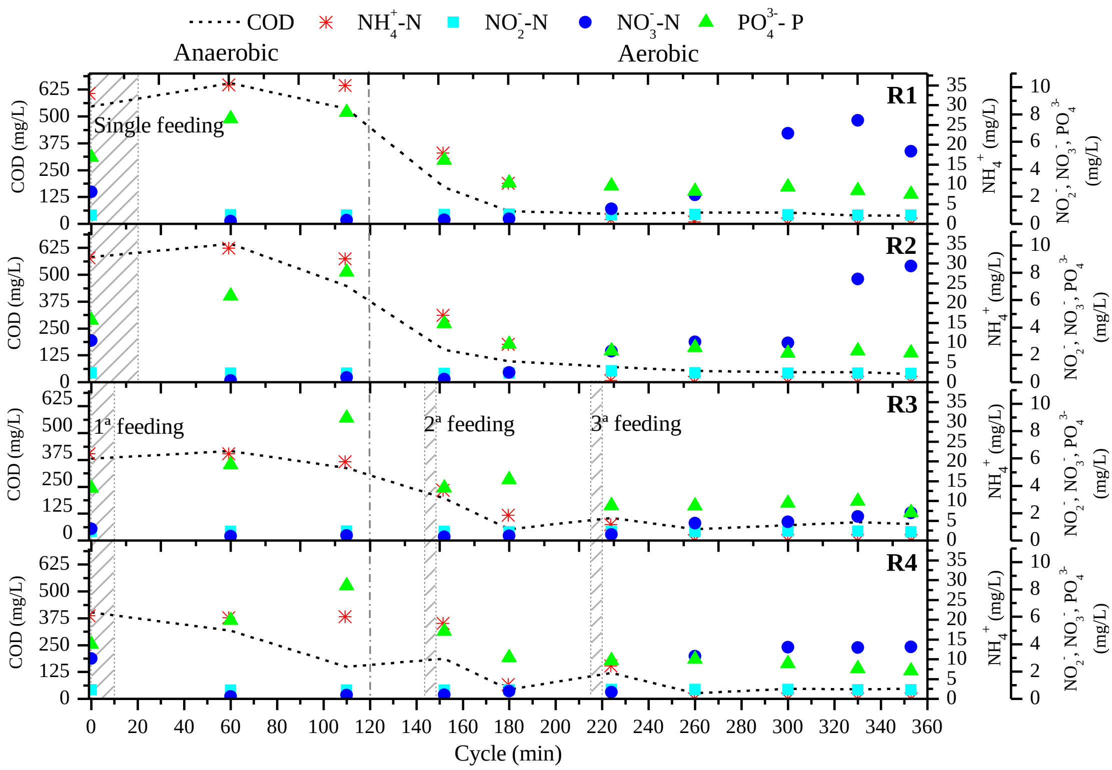

In R1 and R2, no significant nitrite (NO_2^-) accumulation is observed, although nitrate (NO_3^-) slightly increased after all ammonia and COD were consumed. Therefore, especially in the last hour of the oxic period, no carbon source was available to reduce this remaining nitrate, possibly caused by the long famine period associated with the rapid rate of carbon source consumption. However, it is believed that total nitrogen removal occurred preferentially via SND. In R3 and R4, no significant accumulations of NO_2^- and

NO_3^- are observed throughout the profile. Therefore, SND during the oxic period was also the primary mechanism for removing nitrogenous fractions. After complete nitrification, there was sufficient time in the oxic phase for the remaining nitrite to be converted to nitrate by the NOBs since, in this reactor configuration, free ammonia did not cause toxicity to the NOBs.

It is possible to verify in staggered feeding systems that TN removal can occur through different processes: (1) the nitrogen fractions were immediately converted using the influent organic matter as an electron donor during the feeding period through exogenous respiration; (2) in the oxic periods, the SND process prevailed; and (3) other nitrogenous fractions may have been removed using intracellular organic constituents as electron donors, through endogenous processes. These results agree with other investigations that observed that staggered feeding positively influenced the main microbial functional groups distribution, including the ones responsible for the denitrification process (Silva; Rollemberg; Santos, 2021; Rollemberg *et al*., 2016a; Chen *et al*., 2013).

Phosphorus removal in all systems was done through phosphorus-accumulating microorganisms (PAOs). As can be seen, there is an increase in phosphorus in the first anaerobic stage through its release and subsequent assimilation in the aerobic stage for polyhydroxyalkanoates (PHA) production.

6.4. Production and recovery of bioresource

Figure 26 shows the behavior of bioresources' production (EPS, ALE, and TRP) in the four reactors studied during the 157 days of operation. There is a similar trend in the oscillations of these data, especially between EPS and TRP, possibly due to the higher fraction of proteins (PN) present in EPS.

The PN/PS ratio found was around 2 in all reactors, demonstrating the hydrophobic character of the granules throughout the experiment (Peng *et al*., 2022). It is possible to observe a higher PN/PS ratio (3 ~ 4) soon after the beginning of each stage, indicating a PN production stimulation when the salt concentration was increased. Studies have shown a positive relationship between salt use and EPS production, especially PN, in which microorganisms secrete more EPS as a protective mechanism against osmotic pressure (Cui *et al*., 2015; Corsino *et al*., 2017; Meng *et al*., 2019b).

Figure 26 – Production of EPS, ALE, and TRP in the reactors R1 (conventional, acetate), R2 (conventional, propionate), R3 (staggered, acetate), and R4 (staggered, propionate) over the 157 days of operation. Stages of granulation (0), no salt addition (1), and salt gradient increase of 2.5 (2), 5.0 (3), 7.5 (4), and 10.0 (5).

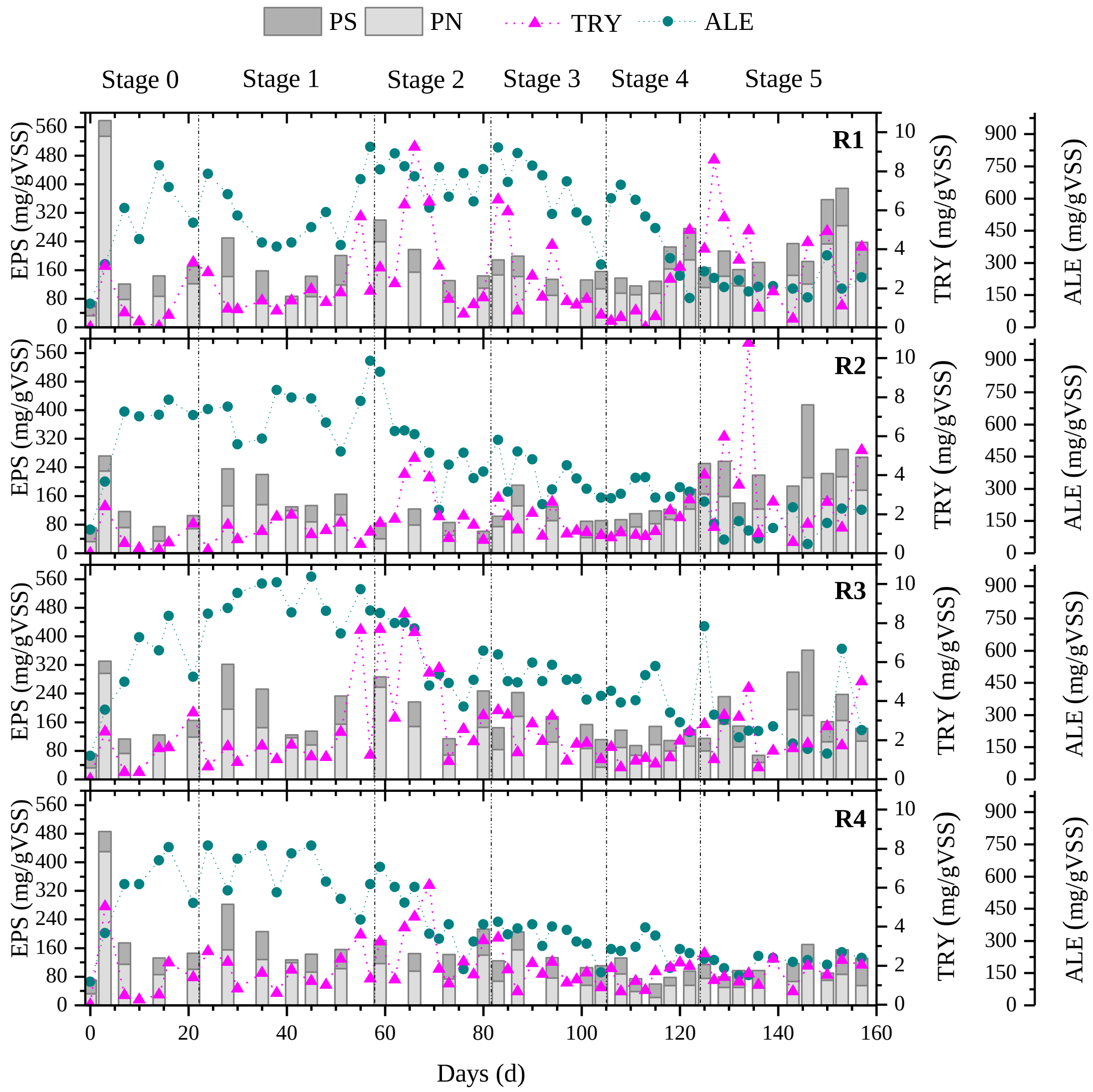

However, there was a polysaccharides concentration increase (PS) in stage 5, especially in R1, R2, and R3, possibly due to the higher osmotic pressure, influencing granules' hydrophobicity and contributing to their disintegration. Furthermore, literature reports that Na^+ excess can replace the bonds between divalent cation and EPS, causing the polymeric structure breakdown and subsequent granules breakage (Cui *et al*., 2015). Interestingly, at this stage, the reactors presented a visibly gelatinous material, probably the consequence of bonds between EPS and sodium, resulting in gelation and the formation of some polysaccharides. The literature reports that the formation of ALE-type hydrogels can occur by binding several divalent cations at different pH and that the presence of salt can favor the production of these biopolymers (Zahra *et al*., 2022). EPS production had no significant difference between the reactors ($p = 0.37$) in the granulation and granules development phases without salt addition (Stage 1). However, in the following stages, with salt addition, PN production in R4 was significantly lower than R1 and R3 ($p < 0.05$) but similar to R2 ($p = 0.416$). It is observed, therefore, that a longer feast period in R3 and R4 did not influence EPS production. However, the SRT seems to have a greater influence on the EPS endogenous consumption. In the case of R2, this trend is best observed between stages 3 and 4, where there were the highest MLVSS concentrations, highest SRT, and lowest EPS production. With granule destabilization, still in stage 4 and extending to stage 5, there is a solids' concentration drop and SRT, with an EPS production increase, driven by microorganisms in an attempt to maintain granule structure (Santos *et al*., 2022). The same trend is observed in R4, but only at the end of stage 5.

ALE production average in the systems were (mg ALE/g MLVSS): 491.5 (R1), 404.5 (R2), 506.0 (R3), and 379.4 (R4), equivalent to 49, 40, 51 and 38%, respectively. Similar results were found in AGS investigations with synthetic effluent with acetate as a carbon source (42%) (Santos *et al*., 2022) and real wastewater (44%) (Sarvajith & Nancharaiah, 2023). Based on these data, it was found that there was no significant difference ($p > 0.05$) between the productions of conventional (R1 and R2) and staggered (R3 and R4) feeding systems, indicating that the highest famine period in R1 and R2 (evidenced in the analysis cycle) did not lead to an ALE consumption by endogenous activity. Therefore, similar to the EPS data, endogenous consumption is more related to higher SRT than a longer famine period.

On the other hand, the data showed significantly higher yields ($p < 0.05$) of systems fed with acetate, in agreement with previous findings that observed better ALE yields in systems fed with acetate (Santos *et al*., 2022). On the other hand, ALE production has been associated as a prerequisite for forming mature granules. However, a higher ALE content alone does not necessarily result in granulation (Yang *et al*., 2014; Schambeck *et al*., 2020). Sarvajith and Nancharaiah (2023) observed ALE recovery of 32% even in conventional activated sludge systems.

In R1, the highest ALE production is observed between stages 3 and 4, in which salt addition possibly contributed to the maintenance of this resource. However, with the granules' fragmentation, this production decreased significantly. In the other systems, a decrease in ALE production is also observed with biomass fragmentation. However, in these reactors, the highest production is presented in stage 1, with constant decay in the following stages.

It is worth noting that, in general, ALE is a fraction of EPS, characterized by its ability to form hydrogels. Similar to EPS, it is a complex compound formed not only by polysaccharides but also by proteins, humic acids, and lipids (Schambeck *et al*., 2020; Chen *et al*., 2022b). However, in this study, ALE values were higher than EPS, possibly due to the applied extraction and quantification method. Felz *et al*. (2016) demonstrated different EPS concentrations for different extraction methods, while Chen *et al*. (2022b) alerted to differences found in the ALE quantification through colorimetric and gravimetric methods.

Similar to the observations made for ALE, TRP production (mg TRP/g MLVSS) showed no significant difference ($p = 0.30$) between the conventional and staggered feeding systems. However, R2 (2.7) was slightly higher than R1 (2.0), and R4 (1.9) was slightly lower than R3 (2.6).

In general, it was observed that the salt addition to the systems contributed to the granulation and resource production. It is assumed that NaCl in low concentrations (up to 7.5 g/L) helps reduce electronegativity on the cell surface (Li *et al*., 2017), favoring system granulation and stability and being a stress source that favors production of ALE, EPS and TRP.

However, reducing the famine period in staggered feeding systems did not stimulate higher bioresources production, as indicated by other authors (Santos *et al*., 2022; Rollemberg *et al*., 2021). The consumption of ALE, EPS, and TRP can be associated with endogenous consumption due to both high SRT and extended famine periods. Therefore, to better observe the influence of the feast/famine period on bioresources production, it is essential to control the SRT uniformly across all systems.

6.5. Principal component analysis (PCA)

The multivariate analysis reduced PCA into three significant principal components (PC), representing 50 and 60% of the total variance (Table 8). Different behaviors can generally be observed between the four systems since biomass with specific characteristics is formed in each reactor, depending on the different feeding methods and carbon sources. However, systems fed with acetate, R1 and R3, had more dispersed scores, indicating more unstable biomass, as shown in Figure 27. On the other hand, R4 seems to be the reactor with the best pattern throughout the five operational stages, showing some dispersed scores only at the beginning (Stage 0, granulation) and at operation completion (Stage 5), in which there are more significant system instabilities.

It is also observed in Figure 27 that the arrows indicate the directions of loads of each variable in the data set. From this analysis, the systems R2 and R4 presented opposite correlations between SRT and EPS based on CP1, which explains 42.6 and 41.1% of the total variation, respectively. However, this correlation is not observed in R1 and R3, thus indicating that SRT greater than 20 days influenced EPS production, as is the case of R2 and R4.

Still, in PC1, the variables ALE and EPS showed opposite correlations in R1 and R2. However, in R4, this correlation was directly proportional. This fact is probably due to the EPS content increase in the last experimental phase (Stage 5) due to instabilities caused by granule fragmentation in Stage 4. However, there was no ALE recovery. In R4, this fragmentation occurred at the end of stage 5. In the case of R3, the low ALE load (-0.053) and EPS (0.320) values showed no correlation with PC1. However, they present a direct correlation in CP2 (Table 8).

Table 8 – Correlation between the variables and the first three principal components. In bold, loads greater than the absolute value of 0.5 were used to assess the variables' correlation.

Variables	**R1**			**R2**			**R3**			**R4**		
	PC1	**PC2**	**PC3**	**PC1**	**PC2**	**PC3**	**PC1**	**PC2**	**PC3**	**PC1**	**PC2**	**PC3**
ALE	**-0.5309**	-0.2666	-0.3465	**-0.568**	**-0.630**	0.316	-0.053	**0.687**	-0.471	**0.818**	-0.204	0.362
TRP	0.2512	**-0.7035**	-0.4424	0.316	**0.509**	**0.690**	-0.095	**0.625**	0.355	0.217	-0.276	**-0.698**
EPS	**0.7298**	-0.1961	-0.3006	**0.718**	-0.072	0.127	0.320	**0.501**	**0.719**	**0.696**	0.199	**-0.490**
SRT	-0.3306	-0.0719	**-0.7863**	**-0.633**	0.457	0.358	**-0.611**	-0.308	0.378	**-0.614**	0.076	-0.474
VSS	**-0.7147**	0.3945	0.0832	**-0.761**	0.327	-0.333	**-0.696**	**-0.611**	0.052	**-0.926**	0.144	-0.147
SVI_{30}	**0.6106**	-0.406	0.2661	**0.869**	0.126	0.164	**0.809**	-0.143	0.368	**0.902**	0.187	-0.101
SVI_{30}/SVI_5	**-0.6277**	-0.0255	-0.1754	**-0.541**	**0.523**	-0.074	**-0.773**	0.276	0.107	**-0.838**	-0.144	-0.013
Phosp	0.1379	**0.7008**	-0.4568	**-0.569**	-0.486	0.446	0.007	-0.351	0.321	0.409	-0.009	-0.367
COD	**0.6325**	**0.5361**	-0.0836	**0.705**	-0.385	-0.107	**0.717**	-0.104	-0.127	0.020	**0.852**	0.03
Amm	**0.7665**	0.3035	-0.2748	**0.690**	0.349	-0.014	**0.636**	-0.400	-0.126	-0.045	**0.773**	0.03
Variance	32.71	18.01	14.24	42.62	17.46	8.171	31.45	19.21	12.915	41.10	15.74	12.52
Cumulative variance	32.71	50.73	64.97	42.62	60.08	70.81	31.45	50.66	63.57	41.22	56.84	69.37

Note - R1 (conventional, acetate), R2 (conventional, propionate), R3 (staggered, acetate), and R4 (staggered, propionate).

Figure 27 – Biplot model for principal components analysis, representing in colored circles the scores of each stage and in arrows the loads of each variable. Stages of granulation (0), no salt addition (1), and salt gradient increase of 2.5 (2), 5.0 (3), 7.5 (4), and 10.0 (5).

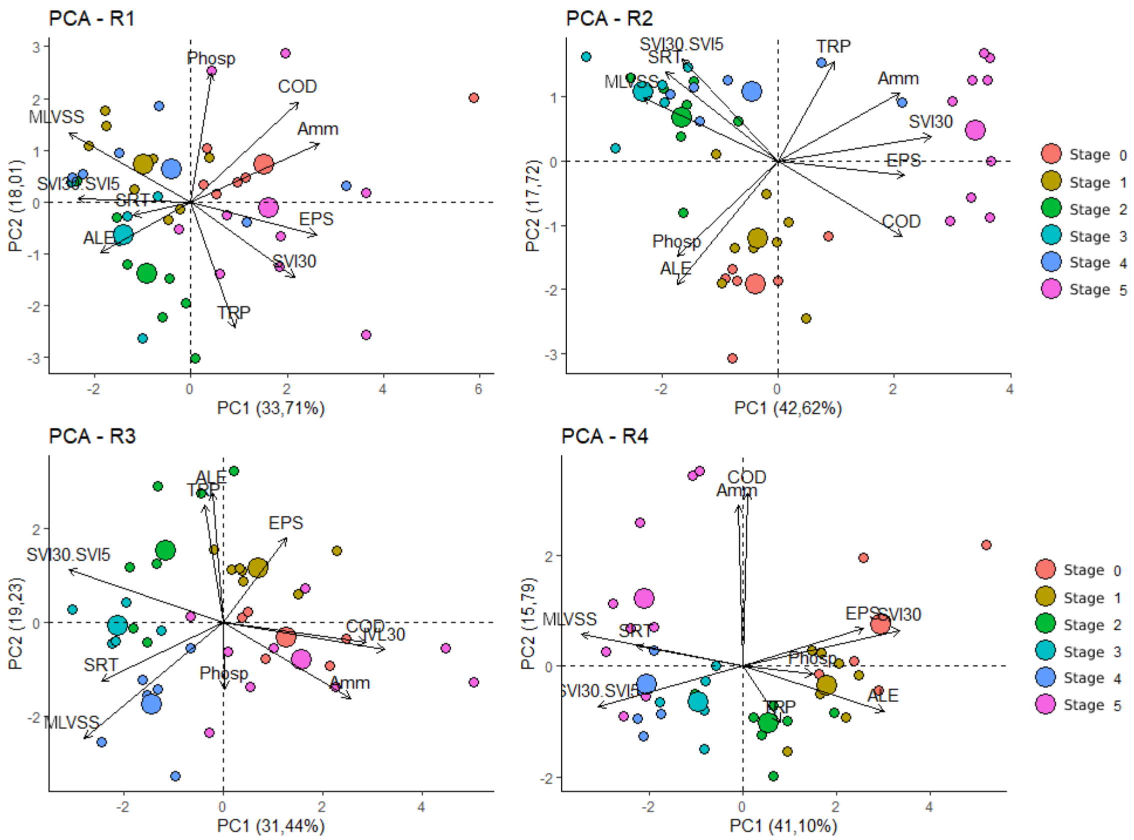

Note - Highlighted variables are: ALE - alginate-like exopolymers; TRP- tryptophan; EPS - extracellular polymeric substances; MLVSS – Mixed liquor volatile suspended solids; SVI_{30} - sludge volume index in 30 min; SVI_{30}/SVI_5 – Relationship between sludge volume index in 30 min and 5 min; SRT - Sludge retention time; COD - chemical oxygen demand; Amm - Ammonia; Phosp – Phosphorous.

Still, concerning ALE production, it is observed that the SRT had an influence only on R4, similar to what was observed between SRT and EPS, probably because this was the only reactor that remained stable throughout the 157 days of operation, maintaining a high SRT, which must have influenced not only the lower EPS production but also ALE production, unlike the other reactors that did not show a relationship between ALE production and SRT. This difference between the systems resulted in different behaviors in the relationship between the data from MLVSS, SVI_{30}, and ALE, since there is a direct relationship between ALE and MLVSS, and an opposite relationship between ALE and SVI_{30}. That is, the higher the MLVSS content, the lower the SVI_{30} and the higher the ALE production in reactors R1 and R2. However, in long periods of operation with high MLVSS and very low SVI_{30}, the ALE content also tends to decrease due to endogenous consumption, as in R4.

There is no strong correlation between phosphorus removal and ALE production, in contrast to some previous studies (Meng *et al*., 2019a; Schambeck *et al*., 2020), indicating that higher ALE yields are associated with significant increases in phosphorus removal efficiency. PC1 in R2 showed a direct and positive relationship between phosphorus and ALE content. However, this indicates exactly the opposite; higher ALE levels are proportional to higher phosphorus levels. This trend is possibly because it was the only reactor that reached very low phosphorus concentrations and low ALE values at the end of the operation.

COD and ammonia (Amm) showed an opposite correlation to ALE production in PC1 in R1 and R2, similar to Schambeck *et al*. (2020), suggesting that the ALE content in the maturation stage may be associated with the removal of organic matter and ammonia. ALE and TRP showed an inverse and direct correlation in PC2, respectively, in R2 and R3. However, PC2 explains only 17.5 and 19.2% of the total variation. In PC3, a direct correlation between EPS and TRP for R4 is observed. However, it explains only 8 and 12% of the total variation.

6.6. Microbiological communities

The sequencing of the 16S rRNA gene of AGSs in the four stages and inoculum sludge was classified into 31 bacterial phyla, 62 classes, 129 orders, 180 families, 180 genera, and 242 species identified. In the inoculum sludge, the most abundant phyla were *Chloroflexi* (27.3%), *Planctomycetota* (10.1%), *Proteobacteria* (5.2%), and *Bacteroidota* (1.9%) (Figure 28a). In the granulation, there was a drastic reduction of the phylum *Chloroflexi* since this group comprises filamentous microorganisms disadvantaged during this process. On the other hand, there is an enrichment of the *Proteobacteria*, *Bacteroidota*, and *Firmicutes* phyla (Figure 28a).

It is very common to report the phyla *Proteobacteria*, *Bacteroidetes*, *Actinobacteria*, and *Firmicutes* in wastewater treatment systems involved in nutrient removal, especially with increased salinity. In addition, these groups, particularly Proteobacteria, are recognized in the AGS system with the function of secreting EPS, one of the main components of granule formation (Corsino *et al*., 2019; Quartaroli *et al*., 2019; Zahra *et al*., 2022).

Figure 28 – Relative distribution of microbial diversity of inoculum sludge and cultured aerobic granular sludge in R1 (conventional, acetate), R2 (conventional, propionate), R3 (staggered, acetate), and R4 (staggered, propionate), distributed at phyla level (a) and families (b) with relative abundance ≥ 1 and (c) distribution by functional groups at the family level, with absolute abundance ≥ 10. Stages of granulation (0), no salt addition.

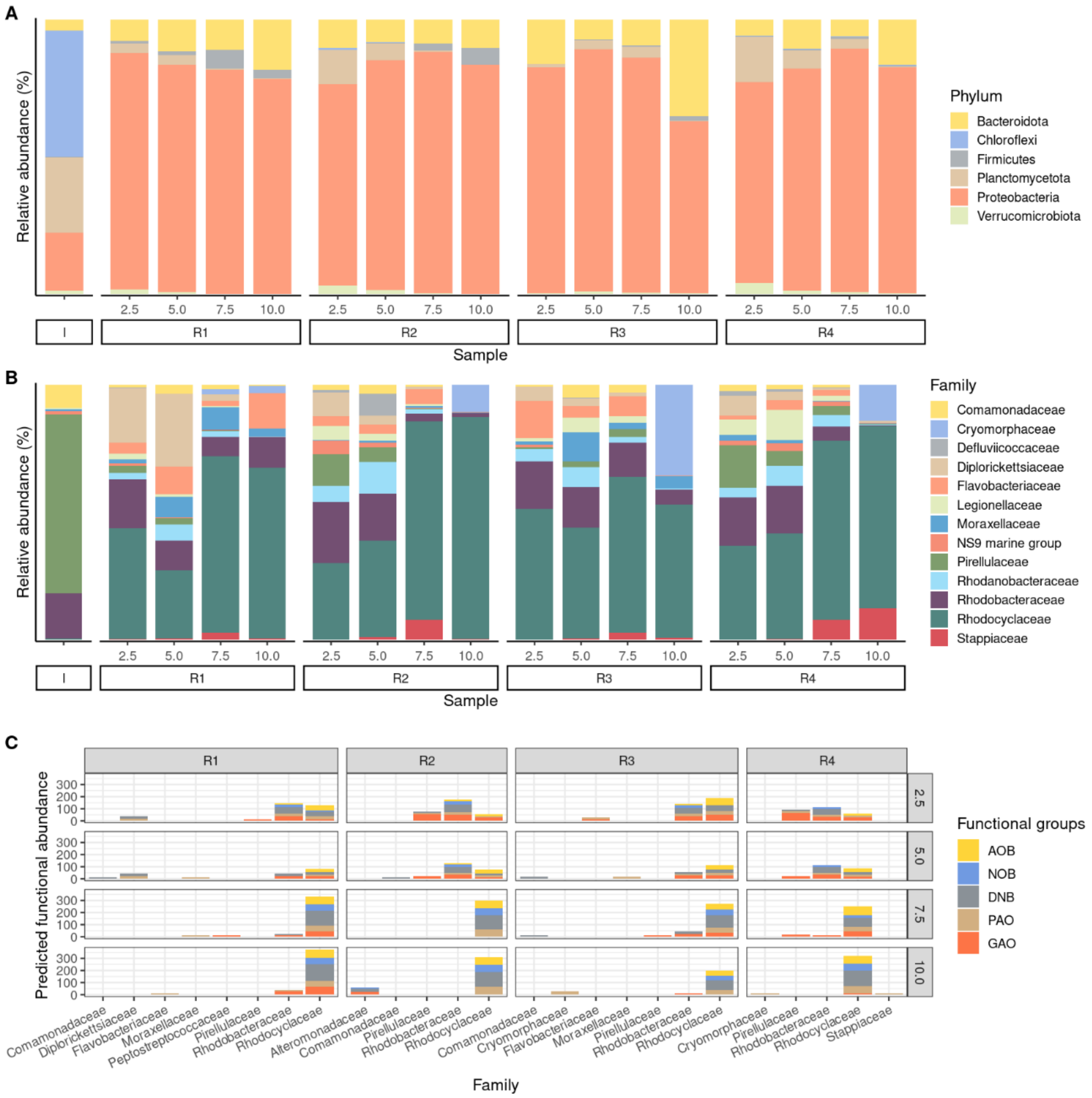

Recent research has reported that microbiological communities of the phylum Proteobacteria are related to biopolymers production, specifically ALE (Pronk *et al.*, 2017b; Han *et al.*, 2022; Zahra *et al.*, 2022). Families such as *Flavobacteriaceae*, *Rhodobacteraceae*, and *Rhodocyclaceae*, found in abundance in this study (Figure 28b), were reported to be present in high production of aerobic ALE granules (Pronk *et al.*, 2017b; Han *et al.*, 2022; Zahra *et al.*, 2022). In addition to these groups of microorganisms facilitating EPS secretion and granule development, they appear to encourage the production of signaling molecules, such as cyclic diguanosine monophosphate (c-di-GMP) (Han *et al*., 2022).

There is no extensive knowledge about the communities associated with TRP production, but studies indicate that the greater the presence of the fermentative microorganism group Bacteroidetes, the greater the biomass of TRP production. In the present research, the genus *Flavobacterium* (*Flavobacteriaceae* family) presented a relative abundance between 2 and 10% in stages 2 and 3 in all systems (Rollemberg *et al*., 2020b; Roager & Licht, 2018). Studies also indicate that there is a direct correlation between TRP accumulation in a low influent C:N ratio (around 5) and the favoring of bacteria of the genus *Thauera* (Yu *et al*., 2020). In this study, these bacteria were abundant in all reactors, especially in R2 (19.2%) and R4 (18.3%), both in stage 2.

The genus *Pseudofulvimonas* of the *Rhodanobacteraceae* family was in greater abundance in stage 3 (addition of 5 g/L of salt), with relative abundances of 2.8% (R1), 6.6% (R2), 3.7% (R3) and 9.2% (R4). According to the literature, *Pseudofulvimonas* are characterized by their excellent ability to resist salt and denitrifying (He *et al*., 2020; Wang *et al*., 2022). The *Defluviicoccus* genus, from the *Defluviicoccaceae* family, is also cited as a group resistant to low saline concentrations (Wang *et al*., 2022). An abundance between 1 and 4% was observed at 2.5 and 5 g/L concentrations, especially in R2.

Regarding the specific microbiological groups in the removal of carbon and nutrients, it was observed, in general, that there was an enrichment of AOB, NOB, DNB, and PAOs with the granulation, justifying the total nitrogen and phosphorus removals improvement (Figure 28c). The reactors operated with acetate, R1 and R3, despite having enrichment of PAOs reaching an abundance of around 50% in the last stage, also had enrichment of GAOs. The competition between these two groups disfavors phosphorus removal. For this reason, its complete removal was not achieved.

On the other hand, in R2 and R4, there is a predominance of PAOs over GAOs, especially in R2, which presented an increased relative abundance of PAOs, reaching 59 and 63%, respectively, in the last two stages. In comparison, the abundance of GAOs was lower by 10% in the same period, leading to the complete phosphorus removal. In addition, the literature (Bassin *et al*., 2012a) has already shown that lower SRT favors phosphorus removal, as they allow the removal of saturated biomass by PAOs. This fact is in line with the present research results since, during this period, the R2 reactor operated with the lowest SRT, around 4 days. However, in R4, a complete phosphorus removal was not achieved, although, in the last stage, relative abundances of PAOs and GAOs were reached, respectively, 59 and 14%. Unlike R2, this reactor maintained a high SRT until the experiment completion, and its biomass was saturated with PAOs, likely negatively interfering with the system's efficiency.

6.7. Conclusion

Despite decreasing the famine period, staggered feeding did not influence bioresources production. However, SRT can be considered an important operational parameter, as values greater than 20 days negatively impact the production of these resources.

PCA also showed that ALE production is related to better-formed granules at low SRT, with better settling characteristics and higher MLVSS concentration, as well as better COD and ammonia removals.

In addition, staggered feeding systems favored denitrification and presented better conditions to support osmotic pressures, with better long-term stability, presenting itself as a potential system in treating saline effluents.

The full version of this paper is published in Journal of Environmental Chemical Engineering (2024) under the same name as this subsection. DOI: https://doi.org/10.1016/j.jece.2024.112948

Figure 29 – Graphical abstract: Aerobic granulation and bioresource production under intermittent saline stress.

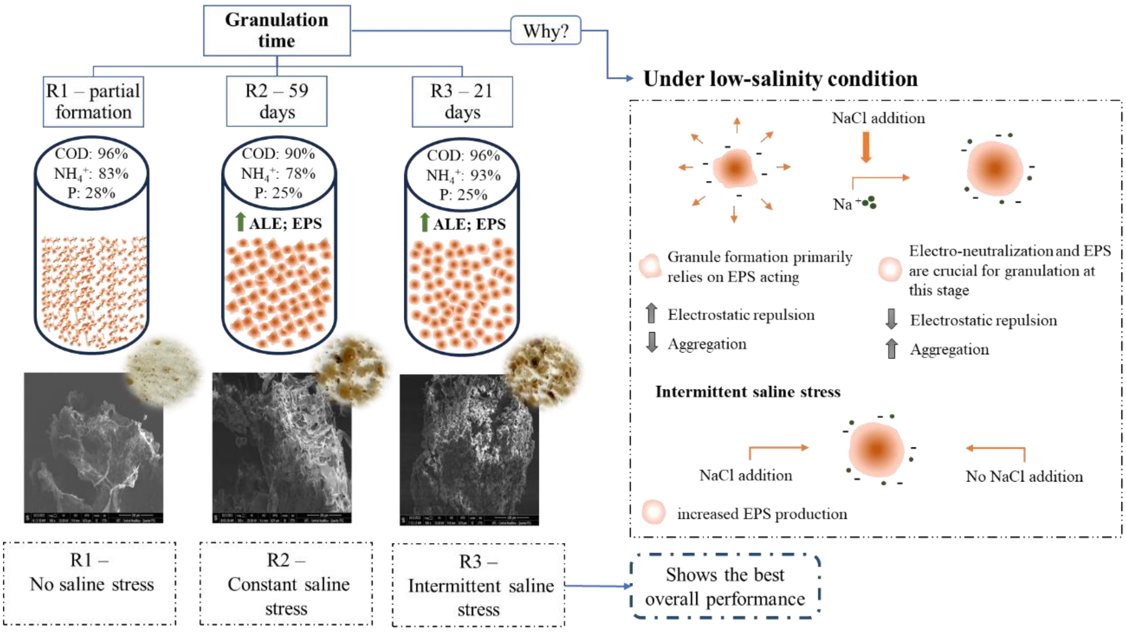

7. AEROBIC GRANULATION AND BIORESOURCE PRODUCTION UNDER INTERMITTENT SALINE STRESS

Aerobic Granular Sludge (AGS) systems have gained prominence for liquid waste treatment and bioresource recovery. In this regard, various strategies are employed to accelerate granulation processes in sequencing batch reactors (SBRs) and maximize stability and bioresource production. Intermittent stress supplementation can facilitate granule development, promoting slow-growth microorganisms. At the same time, osmotic stress may enhance bioresource production. In this study, an AGS reactor control with no saline stress (R1) was compared to two AGS systems operated under constant (R2) and intermittent (R3) saline stress in terms of efficiency, stability and bioresource productions. Granulation occurred around day 59 and 21 in R2 and R3, respectively, while complete granulation was not achieved in R1 within the 80-day operational period. However, the reactor performed well after 45 days, with 70% of the biomass being granular. The production of the biopolymer ALE remained more stable in reactors with osmotic stress compared to R1. The microbiological analysis revealed specific responses and adaptations to environmental factors, with genera such as *Thauera* and *Pseudofulvimonas* showing higher abundance in reactors with complete granulation, indicating a positive correlation with saline conditions (5 g/L). These insights are crucial for optimizing the performance of AGS systems in future applications, emphasizing the benefits of intermittent saline stress in promoting rapid granulation, stability in bioresource production, contaminant removal, and robust granule formation.

7.1. Formation and stability of aerobic granules

The SBRs were inoculated with biomass removed from a secondary settling tank of a submerged aerated biofilter system, which had an SVI_{30} of 368 mL/g. In each reactor, 50% of the useful volume of MLVSS biomass was inoculated at a concentration of 5.0 g/L. In all systems, most of this biomass was washed out shortly after the start due to poor biomass settleability, as shown in Figure 30. Similar observations have been made in other studies (Silva *et al*., 2022; Rollemberg *et al*., 2020b; Cui *et al*., 2021). Chen *et al*. (2024) also found that the addition of NaCl acted as a selective pressure, which eliminated poorer quality sludge, resulting in an initial reduction in MLSS with a subsequent increase until adaptation.

The criteria used for successful granulation are when over 80% of the biomass is larger than 0.2 mm, the SVI_{30}/SVI_5 ratio is greater than 80%, and SVI_{30} is less than 80 mL/g, values well-documented in the literature (de Kreuk *et al*., 2005; Nancharaiah and Raddy, 2018; Derlon *et al*., 2016; de Kreuk *et al*., 2007; Liu *et al*., 2010; Silva; Rollemberg; Santos, 2021). In this regard, in R1, a system operated without salt addition, complete granulation was not observed within the 80-day operation. However, after 45 days, stability in the concentrations of MLVSS of approximately 2.6 g/L (±0.13), MLTSS of 2.9 g/L (±0.14), and a decreasing trend in SVI_{30}, reaching approximate values of 70 mL/g (±9), was observed. However, only 70% of the granules measured more than 0.2 mm, and the SVI_{30}/SVI_5 ratio was also around 70%, although the SVI_{30}/SVI_{10} ratio showed values higher than 80%.

The delayed granulation in R1 is possibly a consequence of the inoculum used. The literature reports that the granulation time in AGS systems will depend on the quality of the inoculum sludge floc and the selection pressures imposed in the new environment

(Penagos *et al*., 2022). Additionally, other similar operations achieved complete granulation around 30 days using activated sludge inoculum (Santos *et al*., 2022), which has been the most commonly utilized inoculum in aerobic granulation due to its ease of obtainment, high density, and microbiological diversity (Penagos *et al*., 2022).

On the other hand, in R2, the system with constant saline addition, complete granulation was achieved around day 59, with 83% of granules larger than 0.2 mm, SVI_{30} of 55 mL/g (±13), and an SVI_{30}/SVI_5 ratio close to 100%. The concentration of solids reached values around 5.3 g/L of MLVSS and 6.7 g/L of MTLSS at the end of the operation. The rapid increase in biomass, especially in inorganic materials, is possibly due to the saline addition, similar to what was observed by Meng *et al*. (2019a). In contrast to R1, observations in R2 suggest osmotic pressure contributed to granulation, as the system achieved complete granulation, albeit delayed (59 days). This observation aligns with the findings of Li *et al*. (2017), who noted that the presence of saline in AGS systems can decrease the electronegativity on the cell surface, thereby promoting faster granulation and enhancing system stability.

Also similar to that indicated by the anaerobic granulation literature, the following mechanism has been proposed (Lu *et al*., 2023): at low levels of salinity, the negatively charged sludge granules show electrostatic repulsion, making it difficult to aggregate, and in this phase, the granule formation primarily relies on EPS acting as a bridge between granules. However, with increasing salinity, the biggest concentration of Na^+ ions compress the colloid electric bilayer, neutralizing the electrical charge of the granular sludge. When electrostatic repulsion becomes weaker than the van der Waals attraction, the repulsion barrier disappears, allowing aggregation. The process heavily relies on electro-neutralization and EPS bonding, playing pivotal roles in facilitating granulation.

The best results in terms of granulation were observed in R3, i.e., the system operated under alternating saline stress, reaching the stage of complete granulation around day 21. At this point, the system already had 91% of granules larger than 0.2 mm, an SVI_{30}/SVI_5 ratio of 91%, and an SVI_{30} of 58 mL/g (±6), reaching even lower SVI_{30} values (< 40 mL/g). The accumulation of solids remained stable between days 25 and 55, with 5.0 (±0.4) g/L of MLVSS and 5.8 (±0.5) g/L of MTLSS. Around day 55, the system experienced an operational issue that caused the washout of most of the biomass, resulting in granule breakage and compromising the system's good settleability, as can be observed and indicated by a red arrow in Figure 30. However, shortly after, the system experienced a rapid recovery.

Figure 30 – Mixed liquor volatile suspended solids (MLVSS) and total suspended solids (MLTSS), SVI_{30}/SVI_5 ratio, and SVI_{30} in the three reactors over 80 days of operation.

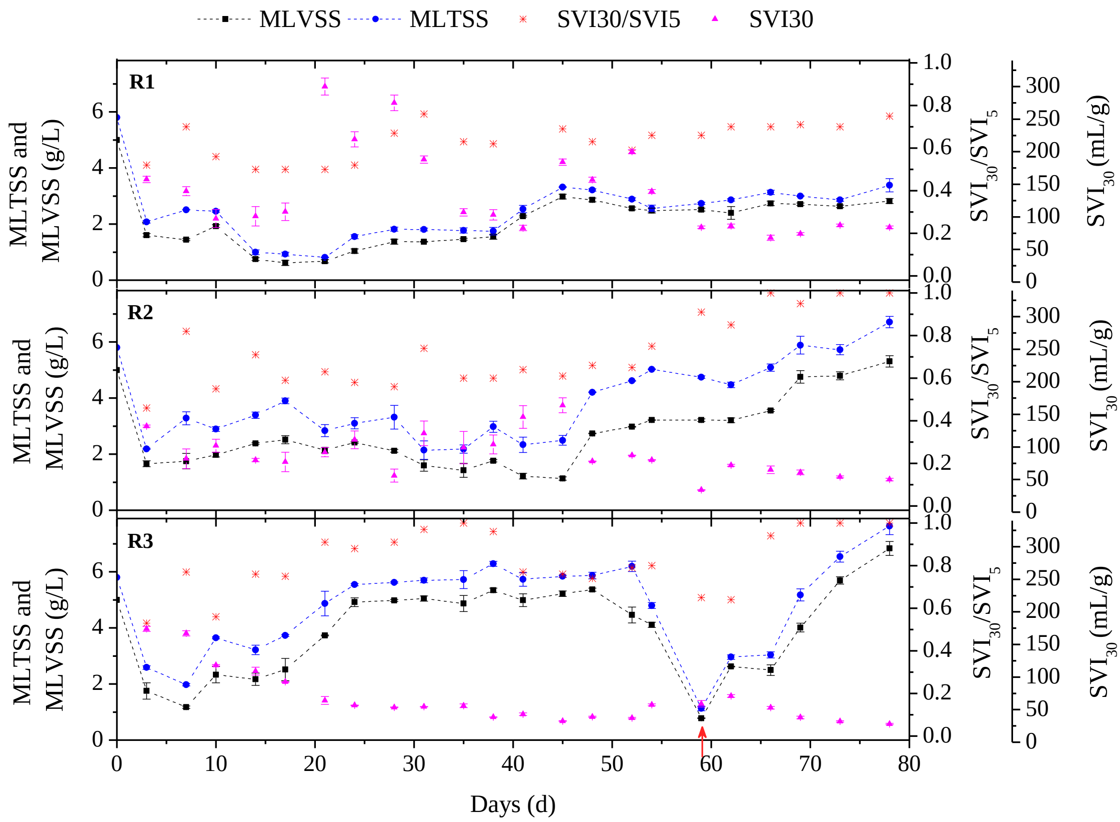

It is believed that alternating cycles of saline stress favored granulation by providing the microbiota with different conditions alternately. Under saline stress, the microbiota initially produces adaptation mechanisms, such as increased EPS production. In the subsequent cycle without saline stress, the stability of the granules may be favored. Moreover, alternating conditions allow for dilution of the saline load, as evidenced by the lower accumulation of inorganic materials in R3. Figure 30 shows a noticeable difference between MLTSS and MLVSS in R2, followed by R3 and R1. Similarly, Chen *et al.* (2015) and Niu *et al.* (2017) observed improved performance in UASB system granules when subjected to alternating stimuli. The former authors worked on granule cultivation with intermittent Mg^{2+} supplementation, and the latter studied semi-starvation fluctuating C/N ratios.

It is interesting to note that in all three reactors, a solid positive Pearson correlation was observed between SVI_{30} data and the F/M ratio in R2 (r = 0.81), and a positive and moderate correlation in R1 (r = 0.69) and R3 (r = 0.56), indicating that F/M is an essential parameter for granulation control and maintaining good stability of AGS systems. Wang *et al*. (2023) demonstrated that AGS systems can achieve good treatment efficiency and good settling when operated under F/M conditions of < 1.38 kg COD/(kg MLVSS·d). In this study, R1 exhibited values higher than this range, around 35 to 40 initial days, due to the high biomass loss.

Regarding the SRT, R1 maintained low values throughout the operational period, around 9 (±2) days. In contrast, R2 reached 18 (±2) days during the maturation phase, and R3 reached 19 (±5) days after 30 days of operation, although with a decline after day 55 (4 ±2 days).

It was observed in the morphology of the granules that around day 47 of operation, only R3 presented well-formed granules with well-defined spherical structures. R2 exhibited transparent spheres resembling a gelatinous material, while R1 displayed biomass with irregular morphology, as can be seen in Figure 31. At the end of the operation (day 73), in R1, well-formed granules were visible, albeit still with filamentous biomass. In R2, a more brownish biomass was formed, with large and dense granules, although still irregular in shape. On the other hand, R3 still showed many well-rounded granules, but larger ones and some irregularly shaped granules were also observed.

Figure 31 – Granule morphology in the middle and end of the 80-day operation.

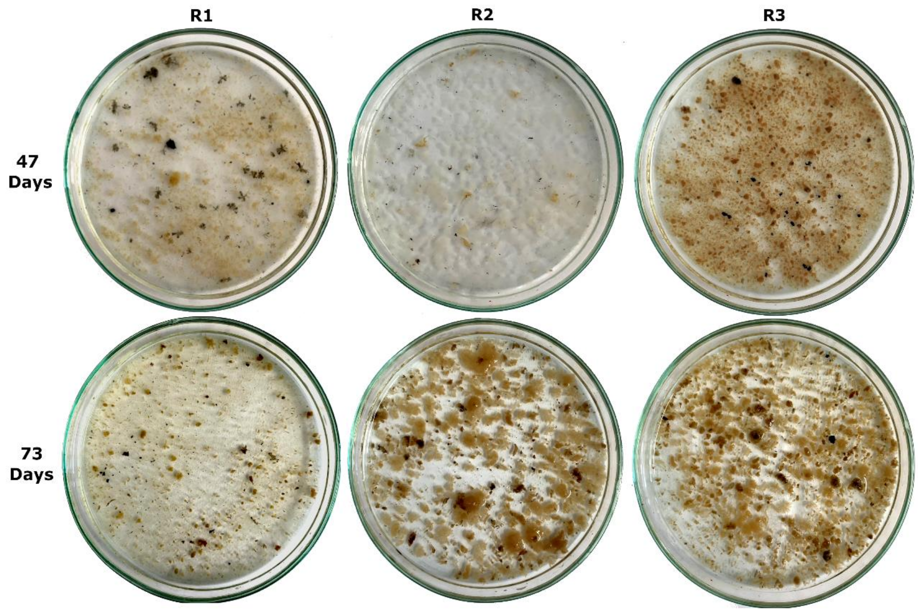

7.2. Reactors' performance

In Figure 32, the performance of the systems over the 80-day operation period can be observed in detail. In terms of COD removal, it is observed that in the first 30 days of operation, no significant difference was observed ($p > 0.05$) between the systems, with average efficiencies around 90% (±7%). The greater fluctuation in the data during this period is justifiable due to biomass adaptation. R1 only showed stable removal after 45 days of operation (~96% ± 3). In R2, there was no significant difference compared to R1 ($p > 0.05$). Although there is no clear stability, it maintained an average removal of 90% (±6%) throughout the experimental period. Conversely, R3 showed stability with maturation; around day 20 of operation, it had an average efficiency of 96% (±3). These results from saline systems align with findings by Wang *et al*. (2017) and Han *et al*. (2022), where satisfactory COD removals were observed, particularly at lower concentrations. Similarly, the performance in R1 was comparable to that observed by dos Santos *et al*. (2022), who reported COD removals exceeding 90% even in a system with late granulation (60 days).

Figure 32 – Performance of the reactors over the 80 days of operation.

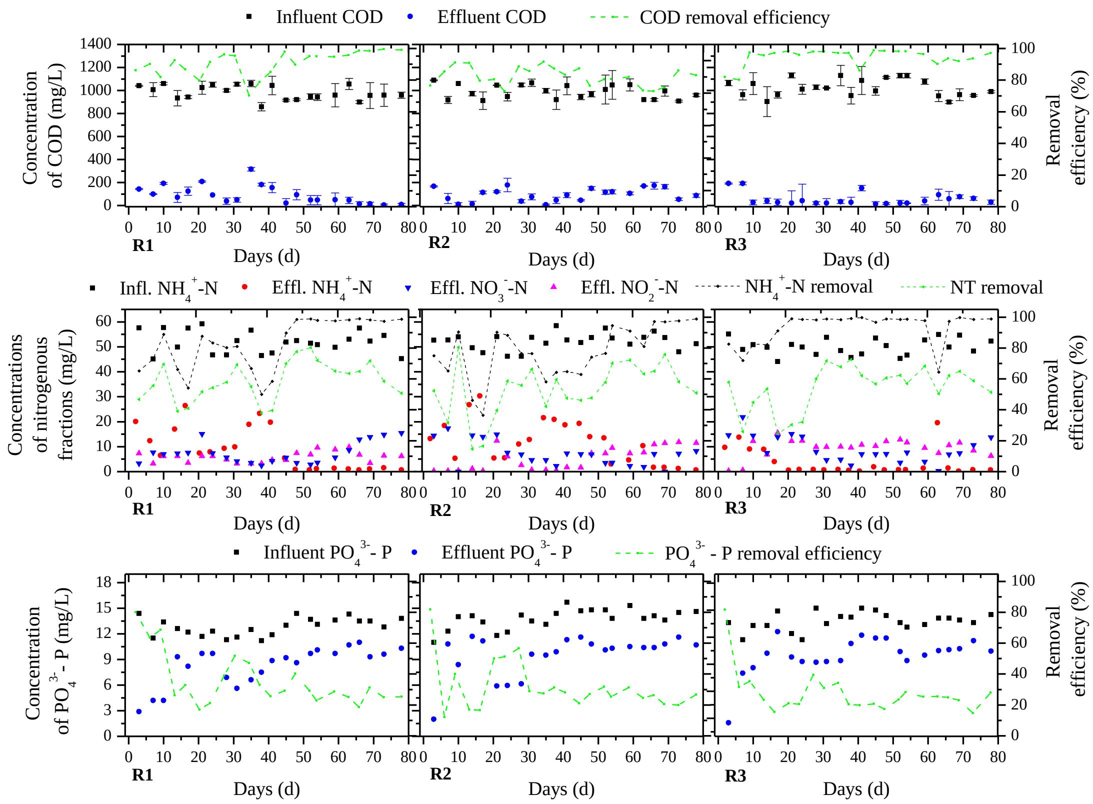

Nitrification efficiency is improved with granulation, stabilizing values after 45 days of operation in R1 and with maturation in R2 (59 days) and R3 (21 days). It can be observed that R3 (93 ± 10%) showed a significantly higher average removal compared to R1 ($p = 0.007$) (83 ± 16%) and R2 ($p = 0.0002$) (78 ± 17%). This likely occurred because the system exhibited better granulation and faster development, allowing it to maintain good efficiency from day 20 of operation, supporting the hypothesis that intermittent stimuli favor better granule development (Chen *et al*., 2015; Niu *et al*., 2017). However, considering only the values after stabilization, no significant differences between the reactors were found, with values around 97% (±3), 95% (±3), and 99% (±1) in R1, R2, and R3, respectively.

Denitrification, on the other hand, failed to demonstrate a significant difference ($p > 0.05$) among the systems, with average removals of 67% (±8), 67% (±8), and 62% (±6) for R1, R2, and R3, respectively. Higher removals were not achieved due to the accumulation of nitrogen fractions (NOx). The accumulation of nitrite and nitrate (Figure 32) is likely related to: (1) the rapid consumption rate of the carbon source, (2) the lack of biodegradable organic matter necessary for complete denitrification, (3) the lack of anoxic conditions, and (4) insufficient accumulation of polyhydroxyalkanoates (PHA) (Silva; Rollemberg; Santos, 2021).

This study is consistent with the findings of Wang *et al*. (2017), which demonstrated that the progressive adaptation of AGS to saline conditions or low saline concentrations allowed for the stable and complete removal of carbon and nitrogen. Although the present study did not achieve complete nitrogen removal, the deficiency was not caused by osmotic pressure. In addition, studies have demonstrated that salinity higher than 1% could cause a severe negative effect on the activity of NOB, compromising complete nitrification (Zhang *et al*., 2023).

Interestingly, in R1, despite incomplete granulation, COD and nitrogen removal stability are evident after day 45, coinciding with stability in the system’s solids concentration. This suggests that even without achieving complete granulation, 70% of the granules present in the system were sufficient to maintain good performance. In R3, a drop in COD, nitrification, and denitrification performance can be observed around day 59, which can be attributed to a biomass reduction during this period. However, a swift re-adaptation followed.

The phosphate removal throughout the experimental period was relatively low in all systems, with statistically equal efficiency ($p > 0.05$). Removal rates of 28% (±6), 25% (±4), and 25% (±6) were achieved in R1, R2, and R3, respectively. This limited removal could be attributed to various reasons (Carvalheira *et al*., 2014; Rollemberg *et al*., 2022; Bassin *et al*., 2012a; Liu *et al*., 2023): (1) the inoculum sludge did not favor the growth of phosphorus-accumulating organisms (PAOs); (2) glycogen-accumulating organisms (GAOs) were predominant, and in the substrate competition, PAOs were at a disadvantage; and (3) uncontrolled biomass discharge may have maintained PAOs-saturated granules in the system. Furthermore, it is possible that the accumulation of nitrite and nitrate may have interfered with the phosphate release mechanism during the anaerobic period by PAOs, as denitrifying bacteria may have a stronger competitive advantage.

7.3. Cycle analysis

The consumption profile of organic matter and nutrients throughout an operational cycle has been examined and is depicted in Figure 33. Analysis of dissolved oxygen (DO) concentration during the cycle revealed that DO remained between 3.0 and 4.5 mg/L during the first 30 minutes of aeration in R1, while in R2, this value persisted for approximately two hours, and in R3, for about one hour. The higher DO demand in R2 and R3 could be associated with two possible reasons: (1) a higher amount of biomass in these systems, leading to higher endogenous activity and consequently a greater DO demand; (2) the presence of salt influenced the microbiota’s metabolism, indicating that the degradation of organic matter was slower, thus maintaining the DO demand for degradation over a more extended period.

After this period, DO levels above 5 mg/L were observed in all reactors, reaching values close to 7 mg/L, these times coincided with the famine period, signifying the absence of soluble COD. During this phase, microorganisms transition to an endogenous state, necessitating lower oxygen concentrations for their metabolic processes.

Not considering the volumetric exchange of 50%, which would immediately lead to 50% efficiency in COD removal in all systems, a very slow decay of organic matter in R2 during the anaerobic period was found, with an approximate removal of 22%, while in R1 and R3, this removal was around 62%. After one hour of aeration, 90% of COD had already been removed in R1; however, only 55% in R2 and 75% in R3. These data agree with the oxygen demand in each system and indicate that the addition of salt possibly influenced the degradation rate of heterotrophic microorganisms; however, there was no detrimental effect on the overall efficiency of the systems.

Figure 33 – Cycle analysis of the reactors R1 (no saline stress), R2 (constant stress), and R3 (intermittent saline stress) at the end of the operational period.

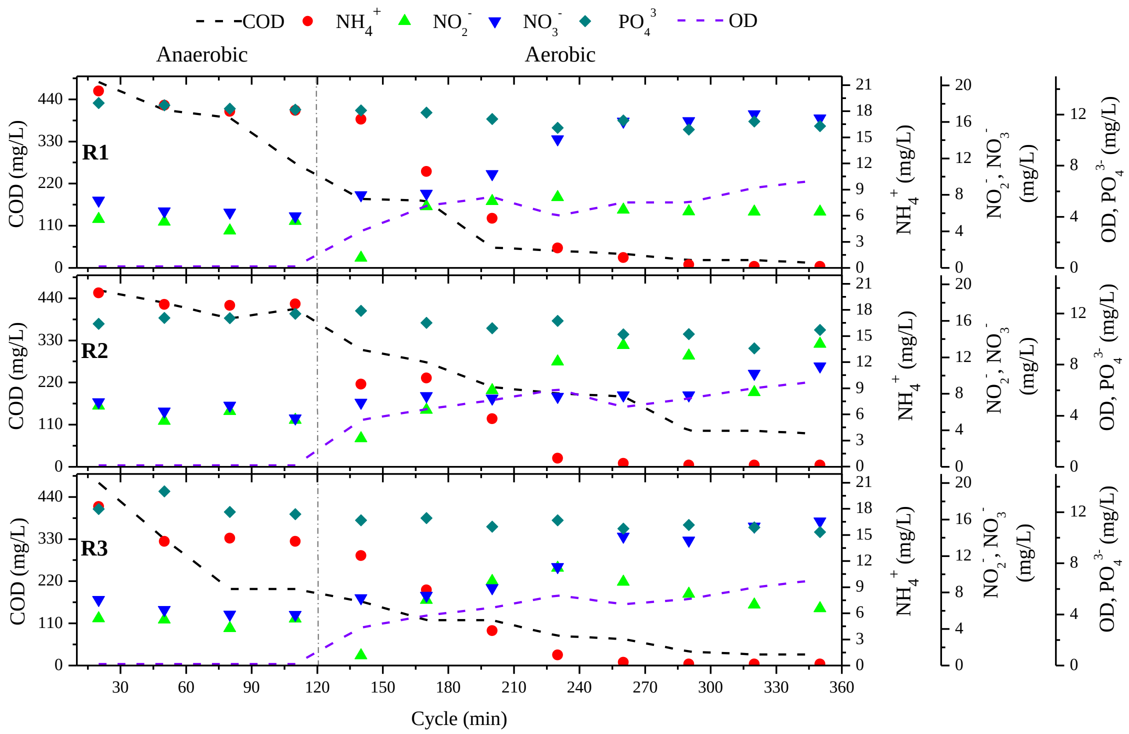

Regarding ammonia removal, after 2 hours of the aerobic period, all ammonia had already been consumed in all systems. A similar behavior among the systems is also achieved regarding the accumulation of nitrite (NO_2^-) and nitrate (NO_3^-). It is noted that reactors R1 and R3, at the end of the cycle, reached an accumulation of NO_3^- and NO_2^- of 15 (±2) mg-N/L and 6 (±1) mg-N/L, respectively. On the other hand, R2 presented a slightly higher accumulation of NO_2^- (14 ±1 mg-N/L) than NO_3^- (11 ±1 mg-N/L). This same pattern is observed in the systems' performance data in the last weeks of operation, with accumulation of nitrite and nitrate concentrations. Despite the high COD/TN ratio, there was carbon consumption during the anaerobic phase, probably to reduce the accumulation of NOx from the previous cycle, since the concentration of these nitrogenous fractions were inconsistent in this phase. Thus, the remaining carbon was quickly consumed at the beginning of the aerobic period, becoming unavailable for complete denitrification to occur in the remainder of the cycle. During this short period of COD depletion in the aerobic phase, the accumulation of polyhydroxyalkanoates (PHA) is not sufficient to sustain the denitrification process (the phosphorus data allows us to infer this). Additionally, the available carbon is used for both microbial growth and development and denitrification. And thus, it becomes insufficient to sustain these processes and results in partial and incomplete removal of nitrogen.

No significant phosphorus removal was achieved in either system. This is probably due to two reasons: (1) During the anaerobic phase, the presence of NOx impaired the metabolism of PAOs, since denitrifying bacteria compete with PAOs and win (Liu *et al.*, 2023). This fact is clearly visible in R2 where the presence of DNB is greater than PAOs. In the other reactors, despite PAOs being more dominant than DNBs, the results converge to believe that the DPAOs route was the preferred one. (2) According to microbiological analysis (see section 7.5), the GAOs group was predominant in relation to the PAOs group in all reactors, discouraging the removal of phosphorus by PAOs.

Cheng *et al.* (2023) observed that influent concentrations exceeding 60 mg/L led to the accumulation of NOx, inhibiting PAOs' activity, in their investigation of various influent ammonia loads in an AGS system. This led to a reduction in the phosphorus removal rate to approximately 49.7%. Barros *et al.* (2020b) reported a similar behavior, relating the kinetic advantage of heterotrophic denitrifying microorganisms compared to PAOs. Silva, Rollemberg and Santos (2021) also observed a comparable trend, although they did not explicitly discuss this behavior in their study. Notably, as noted in their work, the systems with higher NOx accumulation did not exhibit a significant phosphate buildup.

Furthermore, the literature (Rollemberg *et al.*, 2022; Bassin *et al.*, 2012a) has suggested that controlled sludge removal (bed or bottom) is crucial for removing PAO-saturated granules and improving phosphorus removal. However, controlled and selective biomass removal was not adopted for this study.

7.4. Production and recovery of bioresource

The bioresource production (EPS, ALE, and TRP) over the 80 days of operation is shown in Figure 34. A Pearson correlation showed that EPS and ALE data have a moderate correlation, with correlation coefficients of 0.4, 0.4, and 0.6, respectively, in

R1, R2, and R3. However, no correlations were observed between EPS and TRP. R3 showed a higher correlation, possibly due to its greater stability in producing these resources over time, which may be associated with intermittent osmotic stress.

When considering the initial granulation days (~45 days), a significantly lower PS production ($p=0.019$) was observed in R1. Literature has related (Lu *et al.*, 2023) that certain bacteria tend to elevate their cellular and extracellular polysaccharide content in anaerobic granules under salt shock. This phenomenon is believed to serve as a defense mechanism, protecting bacteria against phagocytosis, predation, and stress. As expected, a significantly higher production ($p << 0.05$) of TB fractions compared to LB was noted, similar to Liu & Cinquepalmi (2021). Interestingly, the LB fraction in R2 was higher than in R3 (Table 9), possibly due to higher osmotic pressure. The literature (Lu *et al.*, 2023) has reported that the LB-EPS fraction tends to increase with increasing salinity while the TB-EPS fraction decreases.

Although higher PN-TB production was observed in R3, followed by R2 and R1 (Table 9), the differences among the samples did not reach statistical significance. Similarly, no significant disparity was observed in overall EPS production among the reactors ($p = 0.43$). In general, fluctuations in osmotic pressure induced by elevated salinity levels may stimulate microbial cells to release EPS, enabling them to counteract these alterations (Cui *et al.*, 2015; Corsino *et al.*, 2017; Meng *et al.*, 2019a; Lu *et al.*, 2023).

However, several factors can influence its production, such as SRT, F/M ratio, inoculum sludge, and substrate used (Rollemberg *et al.*, 2020b; Lu *et al.*, 2023). According to the literature (Rollemberg *et al.*, 2020b), higher SRT stimulates endogenous consumption of bioresources, especially at SRTs exceeding 20 days. Although this study did not reach SRT values exceeding 20 days, SRT in R1 was significantly lower than in R2 and R3. Additionally, Wang *et al*. (2023) demonstrated that EPS production is directly related to the F/M ratio. It was evident that in R1 (1.2 ± 0.7) and R2 (0.9 ± 0.4), the F/M ratio was significantly ($p < 0.05$) higher than in R3 (0.7 ± 0.6). Therefore, it is inferred that EPS production in R2 and R3 is lower due to the lower F/M ratio and higher SRT; however, osmotic pressure likely favored EPS production, compensating for endogenous consumption.

Figure 34 – EPS, ALE, and TRP production over the 80-day operational period.

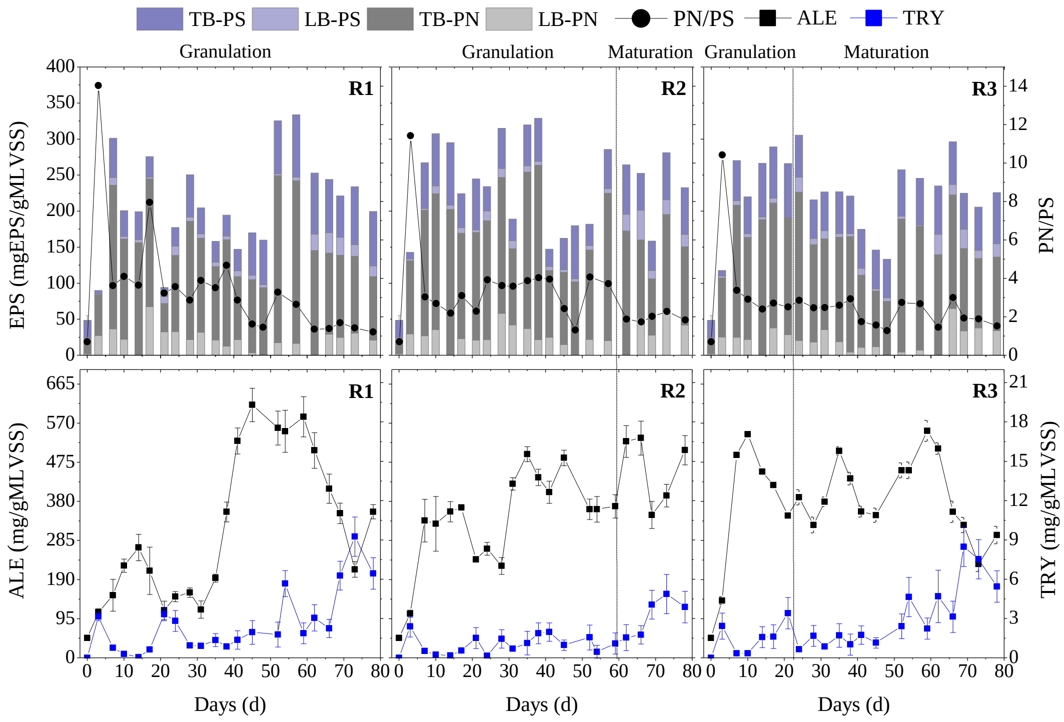

Table 9 – Average EPS production in the inoculum, R1, R2, and R3 during the granulation and maturation phases.

		PN (mg/g MLVSS)		PS (mg/g MLVSS)		PN/PS
		LB	TB	LB	TB	
Inoculum		2 (1)	18 (6)	3 (1)	25 (7)	0.7 (0.2)
Granulation	R1	28 (13)	129 (47)	6 (3)	34 (16)	4 (3)
	R2	24 (11)	157 (49)	6 (4)	55 (21)	3 (2)
	R3	25 (4)	168 (39)	5 (2)	63 (26)	3 (3)
Maturation	R1					
	R2	46 (14)	120 (35)	23 (11)	58 (12)	2 (1)
	R3	24 (7)	133 (36)	11 (9)	58 (7)	2 (1)

Note: Standard deviations are shown in parentheses.

Figure 35 shows the three-dimensional fluorescence spectrum of the emission-excitation matrix (3D-EEM) for samples from each reactor at different operational times. The literature (Liu & Cinquepalmi, 2021) has described each spectrum region as a specific substance commonly found in the EPS matrix (Table 10).

Table 10 – Excitation/emission bands detected in 3D-EEM for EPS analysis.

Region	Ex/Em	Compounds
A	220-235/290-320	Tyrosine amino acid
B	220-235/330-360	Tryptophan amino acid
C	260-290/290-320	Tyrosine-containing proteins
D	280-290/330-360	Tryptophan-containing proteins
E	300-330/360-390	Polysaccharides
F	220-240/380-440	Fulvic acid-like substances
G	260-290/420-460	Polyaromatic type humic acid
H	330-370/420-460	Humic acid type polycarboxylate

Fonte: (Liu & Cinquepalmi, 2021).

Observations around day 7 of operation indicate that all three reactors exhibited similar characteristics with the production of tyrosine amino acid (A), tryptophan amino acid (B), tyrosine-containing proteins (C), tryptophan-containing proteins (D), polysaccharides (E) and fulvic acid-like substances (F). Predominantly, during this initial phase, the selective stressors were the major contributors, leading to an increase in these key substances crucial for granulation. Similar results were found by Santos *et al*. (2022). However, effective and rapid granulation was only achieved in R3. As seen around day 35 of operation, it was the only system to maintain an intense production of all these substances.

At the end of the operation, around the 78th day, there is a recovery of diversity and intensity of substances in R1 and R2. In R3, an increase in intensity is observed, showing a particularly higher production of tyrosine and tryptophan amino acid in R2 and R3. This aligns with the findings of Cui *et al*. (2015), and with the results found in SO II and III, highlighting that systems under osmotic stress positively influence the production of EPS, particularly proteins.

Concerning ALE production (Figure 34), significantly lower production is observed in R1 ($p = 0.013$) when considering the initial granulation days, similar to what was found in the EPS data. Furthermore, R2 and R3 showed greater stability over time compared to R1, suggesting that the imposed osmotic pressure possibly induced this behavior. ALE production was also stable in the experiments by Sui *et al*. (2024) with salt stress, averaging 50.8 ± 1.7 mg/gVSS. These values were much lower than those found in this research under similar salinity conditions, possibly due to the quantification methodology that was different from the present study.

Figure 35 – Three-dimensional fluorescence excitation-emission matrix spectrum (3D-EEM) of EPS extracted from aerobic granules of each reactor on days 7, 35, and 70 of operation.

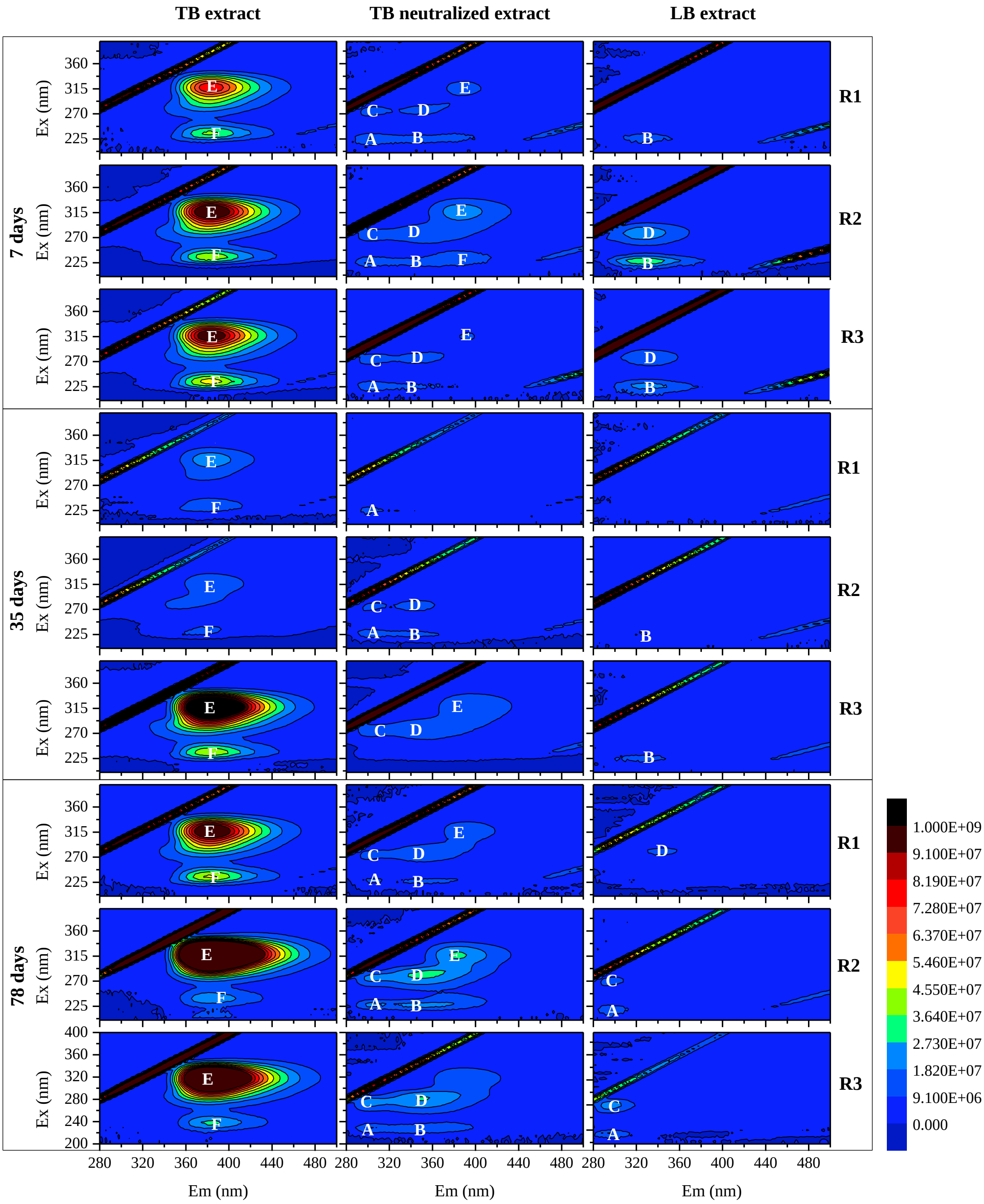

Note: Tyrosine amino acid (A), Tryptophan amino acid (B), Tyrosine-containing proteins (C), Tryptophan-containing proteins (D), Polysaccharides (E) e Fulvic acid-like substances (F). R1 (no saline stress), R2 (constant stress), R3 (intermittent saline stress).

In R1, a higher production of ALE was found, which was proportional to the improvement in biomass quality and settleability characteristics. Statistically, a moderate Pearson correlation is observed (r = -0.47) between ALE data and SVI_{30} in R1. In R2 and R3, an inverse correlation (r = -0.38) is also verified, but it is weak. In general, ALE production is directly correlated with the good development of granules; however, other factors may interfere with its lower production, such as the F/M ratio and SRT. Similar findings were reported by Schambeck *et al*. (2020).

Furthermore, according to Meng *et al*. (2019a), moderate levels of salinity induce the activation of the algC gene in *Pseudomonas*, resulting in the activation of the enzyme phosphomannomutase, which plays a crucial role in the alginate biosynthesis process. This group of microorganisms was found in the composition of the granules in this work and is reported to facilitate the production of EPS. This justifies the interrelationship between EPS and ALE in reactors.

Like the production of EPS and ALE, the production of TRP did not show a significant difference among the reactors, considering the total dataset. However, all three reactors exhibited a similar pattern, with an initial increase in TRP production attributed to the selection stress responsible for the initial granulation, followed by subsequent oscillations and a final increase. In this regard, a weak positive Pearson correlation was found between TRP production and PN in R1 (r = 0.25) and R2 (r = 0.34) and a moderate positive correlation in R3 (r = 0.52). Additionally, akin to what was observed in EPS, the F/M ratio in R1 likely contributed to a higher production of this biopolymer.

7.5. Microbiological communities

At the end of the operation, microbial diversity was evaluated by phylum, family, and genus on samples collected from both the inoculum sludge (I) and biomass samples extracted from reactors R1, R2, and R3 (Figure 36).

The dominant phyla observed in the inoculum sludge comprised *Proteobacteria* (39.8%), *Firmicutes* (19.3%), *Euryarchaeota* (8.7%), *Actinobacteriota* (6.88%), and *Bacteroidota* (1.43%) (Figure 36a). The *Proteobacteria* and *Bacteroidota* phyla were enriched with granulation, while the other phyla were inhibited. For instance, the

Euryarchaeota and *Firmicutes* phyla were significantly reduced, where the former is highly sensitive to oxygen and the latter are typically found in anaerobic fermentation, both commonly present in extreme environments (Quartaroli *et al*., 2019; Wang *et al*., 2022).

The literature has indicated that groups within the *Proteobacteria* phylum play a crucial role in sludge granulation and structural stability, commonly associated with EPS secretion for aerobic granule formation (Li *et al*., 2020b). These microorganisms exhibited a relative abundance of 77.0%, 78.5%, and 83.6% in R1, R2, and R3, respectively, indicating the granulation level and reactor stability. Notably, R1, with 30% filamentous biomass, exhibited the lowest relative abundance of this group, contrasting with R3, which showed faster granulation and better stability throughout the operation.

The *Bacteroidetes* phylum, known for its halotolerant nature and prevalence in marine environments, is dominant in high-salinity activated sludge systems (Quartaroli *et al*., 2019). It exhibited a relative abundance of 14.8% in R2, likely due to the system's higher osmotic pressure.

The *Planctomycetota* phylum showed an abundance of 8.2% in R1, 0.13 in R2, and 3.9% in R3. These microorganisms are associated with organic matter oxidation, typically found in activated sludge biomass, but are also commonly cited in AGS systems (Quartaroli *et al*., 2019). The higher abundance of this group in R1 is likely justified by the greater presence of filamentous biomass in that system.

At the family level (Figure 36b), in the inoculum sludge, groups with abundances greater than 5% were *Moraxellaceae* (23.4%), *Methanobacteriaceae* (8.7%), and *Rhodobacteraceae* (5,8%). While *Moraxellaceae* (<0.04%) and *Methanobacteriaceae* (<0.05%) were significantly reduced during the granulation process, the abundance of *Rhodobacteraceae* increased. This increase seems to have been influenced by osmotic stress, as they exhibited values proportional to the imposed stress (8.2%, 53.2%, and 21.8%, respectively, in R1, R2, and R3).

Other predominant family groups with varying relative abundances include *Defluviicoccaceae* (20.4%, 0.1% and 33.7%), *Legionellaceae* (7.8%, 0.05% and 1.6%), *Rhodocyclaceae* (3.8%, 18.8% and 6.9%), *Flavobacteriaceae* (0.6%, 10.8% and 0.3%), *Rhodanobacteraceae* (1.8%, 2.6% and 9.0%), *Isosphaeraceae* (4.1%, 0.05% and 0.61%), and *Pirellulaceae* (3.6%, 0.04% and 2.9%) in R1, R2, and R3, respectively.

Han *et al*. (2022) indicated that families, such as *Rhodocyclaceae*, *Rhodobacteraceae*, and *Flavobacteriaceae*, play essential roles in EPS production and the development of granules, stimulating the release of signaling molecules like cyclic guanosine monophosphate (c-di-GMP). *Flavobacteriaceae* members are known for their notable ability to secrete EPS, particularly PN-rich EPS, in marine environments. They are associated with ALE production, explaining the high PN and ALE production in R2 despite late granulation (Cui *et al*., 2021).

Among the most abundant genera (Figure 36d) that were possible to be successfully classified were: *Acinetobacter* (19.5%) and *Methanobacterium* (6.7%) in the inoculum; *Defluviicoccus* (20.5%), *Legionella* (7.8%), and *Phreatobacter* (5.8%) in R1; *Planktosalinus* (9.2%) and *Thauera* (9.4%) in R2; and *Defluviicoccus* (33.7%), *Pseudofulvimonas* (8.5%), and *Thauera* (6.5%) in R3. *Legionella* (Luo *et al*., 2014) and *Phreatobacter* (Wu *et al*., 2021) are associated with nitrogen removal in granular systems like activated sludge and moving bed biofilm reactors.

Defluviicoccus microbes from the *Defluviicoccaceae* family are linked to denitrification and glycogen accumulation (DGAOs). He *et al*. (2020) observed a reduction in these microbes at 0.5% saline concentrations, similar to what was seen in R2, indicating increased competitiveness and adaptive capabilities of PAOs/DPAOs. However, despite this group's inhibition at 5g/L saline concentrations (R2), other GAOS/DGAOs from the *Rhodobacteraceae* family were enriched in R2. On the other hand, this group was enriched in R3, indicating that these microorganisms may be resistant to low saline concentrations (Wang *et al*., 2022).

Thauera, Pseudofulvimonas belonging to the *Proteobacteria* phylum, are known for their strong salt resistance, justifying their higher abundance in R2 and R3 (Wang *et al*., 2022). *Planktosalinus* from the *Flavobacteriaceae*, present in greater abundance in R2, are halotolerant microorganisms.

Thauera genus is also associated with EPS production, granule formation, and stability, as it can promote c-di-GMP production, which is crucial for the maturation of granules and the enduring stability of the system (Li *et al*., 2020b; Wan *et al*., 2013). High correlations between c-di-GMP, EPS, and *Pseudofulvimonas* relative abundance were observed by Chen *et al*. (2022a), consistent with this study showing higher abundance of these groups in R2 and R3, where complete granulation was achieved. Other authors (Yang *et al*., 2014) suggested that quorum sensing stimulation (c-di-GMP) may lead to excessive ALE production. Therefore, it is possible to infer that low saline concentrations

(0.5%) may contribute to enriching these groups and subsequently improve granulation and bioresource production.

Figure 36 – Relative abundance of microbial clusters in inoculum sludge and SBRs: (a) relative abundances at the phylum level; (b) relative abundances at the family level; (c) distribution of functional groups in each AGS; and (d) relative abundances at the genus level.

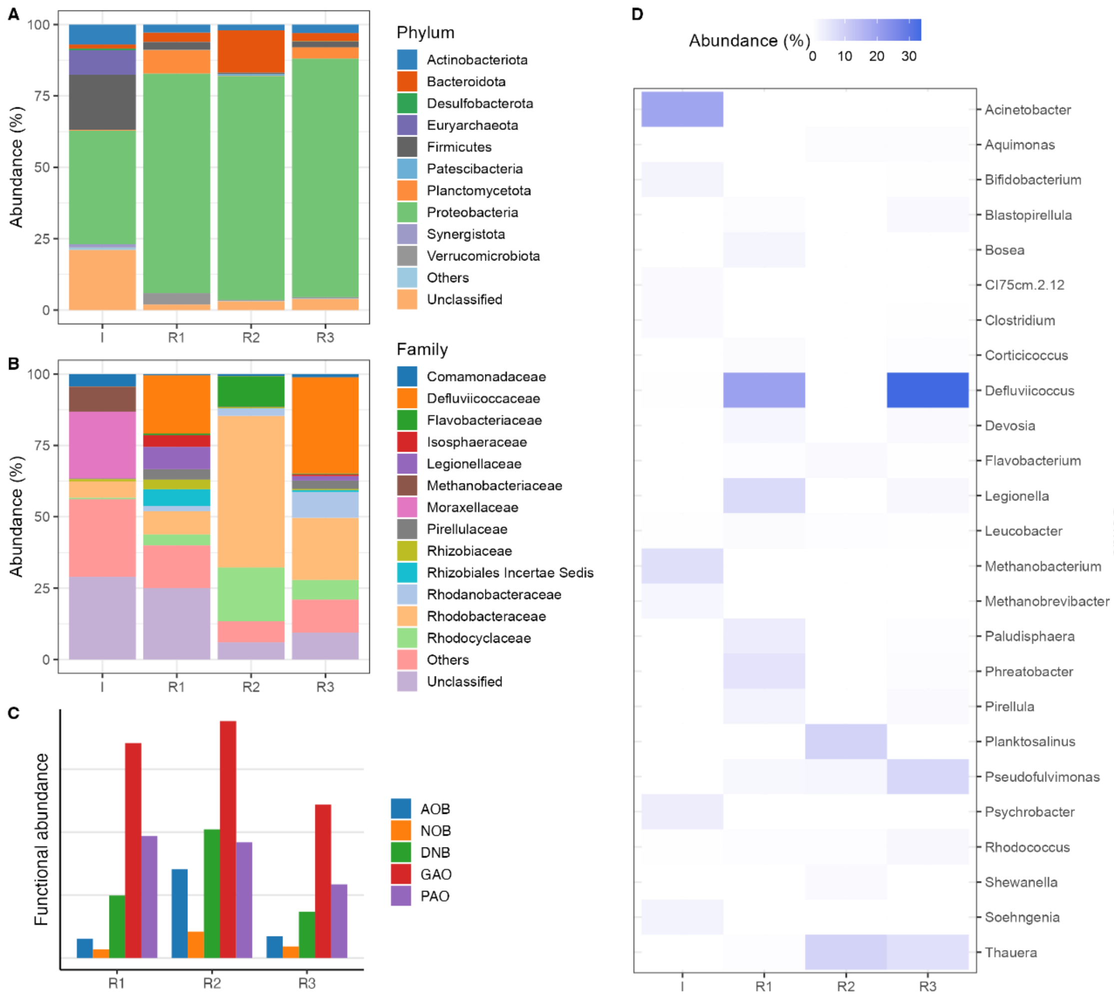

Regarding specific microbial groups involved in carbon and nutrient removal (Figure 36c), a higher abundance of AOB and NOB was observed in R2, possibly due to SRT, which showed values around 18 (±2) days in R2 and 4 (±2) in R1 and R3, at the end of the operation period. This difference may be attributed to a low SRT at high temperatures inhibiting NOB, leading to nitrite accumulation, which is consistent with earlier findings (Santos *et al.*, 2022). While a higher abundance of DNB relative to AOB and NOB was observed in all three systems, complete denitrification was not achieved

(~65%), possibly due to a lack of biodegradable organic matter required for complete denitrification. The dominance of GAOs over PAOs in all three reactors indicates GAOs' advantage in substrate competition, justifying low phosphorus removal (~25%).

7.6. Conclusion

The production of biopolymers, especially ALE, remained more stable in reactors with osmotic stress, particularly in R3, with intermittent stress. The production of ALE was proportional to the improvement in biomass quality and settling characteristics. Feeding subjected to intermittent saline stress proved to be a potential alternative for aerobic granule cultivation, showing fast granulation, stability in resource production, good contaminant removal, and well-formed granules with good settleability characteristics.

The microbiological analysis revealed significant changes in microbial diversity, showing specific responses in each reactor and indicating adaptations to environmental factors. Genera such as *Thauera* and *Pseudofulvimonas*, associated with EPS production and granule maturation, exhibited higher abundance in reactors with complete granulation, suggesting a positive correlation between saline conditions (0.5%) and enhanced granulation and bioresource production.

These findings provide important insights for optimizing the performance of AGS systems in future applications regarding the treatment of sewage, landfill leachate and saline wastewater.

A modified version is under preparation for submission.

Figure 37 – Graphical abstract: evaluation of leachate impact on domestic sewage co-treatment in AGS systems.

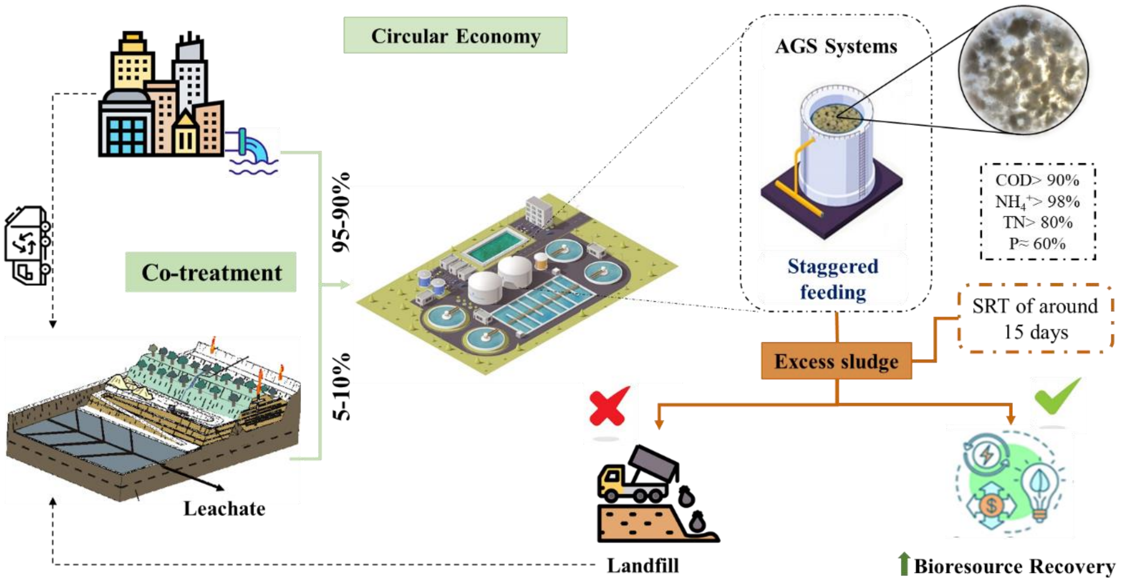

8. EVALUATION OF LEACHATE IMPACT ON DOMESTIC SEWAGE CO-TREATMENT IN AEROBIC GRANULAR SLUDGE SYSTEMS

The aerobic granular sludge (AGS) system has attracted interest in treating various effluents, including leachates from sanitary landfills. However, its direct utilization for such effluents is hindered by their highly intricate composition. The co-treatment of leachate with domestic sewage in municipal wastewater treatment plants (WWTPs) using AGS systems is a promising but still early-stage approach. This study assessed the influence of this co-treatment on granule formation, system stability, and resource production in two AGS units (R1 and R2) under a staggered feeding regime. In R2, control of the SRT was employed to evaluate its effect on system stability. The results indicate that successful granulation with leachate and domestic sewage is achievable, and low dilutions (5%) did not negatively affect system performance and stability. However, an increase to 10% co-treatment, while not affecting nitrogen and phosphorus removal, influenced organic matter removal and decreased alginate-like extracellular polymeric substances (ALE) quantity and quality. Principal component analysis (PCA) revealed that, although the production of biopolymers, especially ALE, is related to various factors, SRT emerged as a key operational parameter to optimize the synthesis of these compounds. Furthermore, SRT control significantly improved total nitrogen (TN) removal in R2. Thus, the importance of selective biomass disposal in granule formation and stability is highlighted, directly influencing treatment system efficiency and resource production.

8.1. Effect of SRT and leachate co-treatment in AGS system

8.1.1. Formation of aerobic granules

During the granulation phase, the settling time was gradually reduced from 20 to 5 minutes to avoid excessive biomass removal at the operation beginning. At this stage, a gradual decrease in solids' concentration in the mixed liquor was observed due to biomass washout, carried away by the final effluent, as shown in Figure 38a. As expected, this behavior occurred in both reactors as they had the same operating conditions at this point. Similar results were presented by da Silva *et al*. (2023a), who also worked with leachate co-treatment.

An initial biomass washout could also be observed in studies where leachate co-treatment was not employed (Xavier *et al*., 2023; Santos *et al*., 2022) due to the hydraulic shock imposed as a selection pressure. However, biomass adaptation is usually fast. For example, Xavier *et al*. (2023) observed a decrease in MLVSS concentration in the first 5 days, followed by growth, while Santos *et al*. (2022) observed a decrease between the first 10 to 15 days of operation, followed by an increase.

Complete granulation was achieved in both reactors after 40 days of operation, at which point the biomass had 80% granules with a diameter greater than 0.2 mm (de Kreuk *et al*., 2007; Liu *et al*., 2010), as illustrated in Figure 38b. On the other hand, Silva *et al*. (2023a) achieved complete granulation after 120 days in a step-feeding system, similar to the conditions in this study; however, during the initial 30 days, the authors operated the reactors with an organic load of 0.3 g/L/d to acclimate the biomass, and only started co-treatment after 62 days. It is possible that this low organic load initially contributed to delaying granulation. Additionally, the authors utilized activated sludge biomass from a WWTP, which may have required a more extended period for adaptation to leachate conditions.

Figure 38 – Physical stability of the biomass granulometry over the 192 days of operation in terms of (a) MLVSS, effluent VSS, SVI_{30}, and (b) SVI_{30}/SVI_{10} ratio.

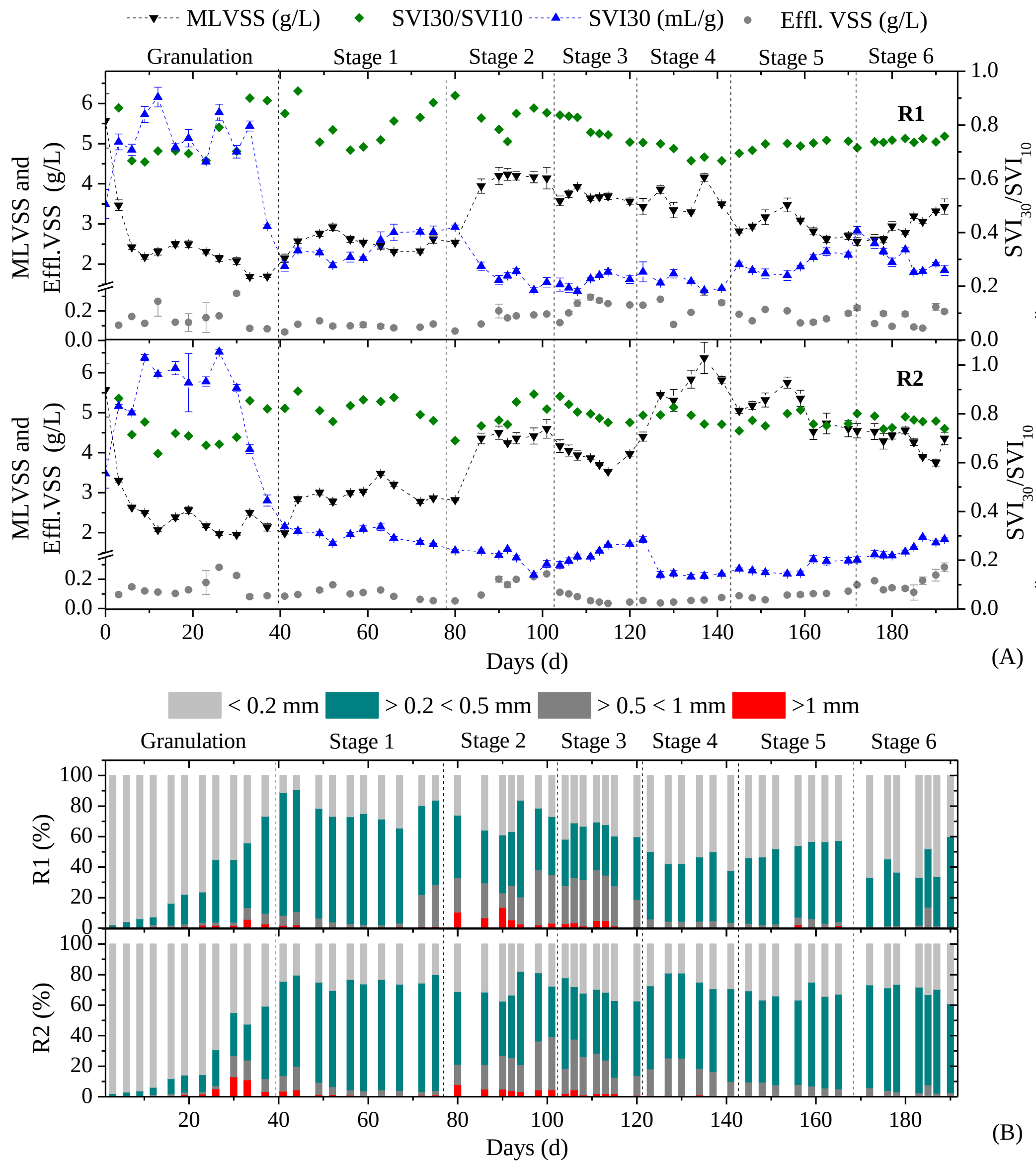

In contrast, in the present study, a biomass previously adapted to leachate was used, and the reactors were initiated with a 5% leachate co-treatment. These conditions may have facilitated more rapid granulation. Research on granule formation (Penagos *et al.*, 2022) indicates that using an inoculum not acclimatized to the new environment can lead to extended start-up periods before granule maturation is achieved. Furthermore, there is evidence suggesting that the addition of NaCl can expedite the granulation process

(Li *et al*., 2017). Given that leachates typically contain a high concentration of inorganic materials, and assuming that all the chlorides identified in the leachate analysis mainly originated from NaCl, the saline concentration would be around 6 g/L. When diluted at a 5% rate, this would result in an effective saline addition of approximately 300 mg/L.

In comparison with studies that did not use co-treatment, it is evident that complete granulation can be achieved in about 30 days (Santos *et al*., 2022). However, previous work by Xavier *et al*. (2023) in a similar SBR system to this study reported that 80% of the biomass acquired granule form after 40 days. It is important to note that these authors used a COD of only 0.6 g/L/day, possibly delaying the granulation process. Therefore, it can be inferred that, in addition to the influence of COD on granulation, the presence of leachate in co-treatment may also delay the achievement of complete granulation and favor a higher proportion of filamentous biomass and the predominant formation of small-sized granules (Figure 38b).

8.1.2. Stability of aerobic granules

After granulation, in stage 1, the stabilization of the granules begins, during which an increase in MLVSS concentration is observed, with average values around 2.5 g/L (±0.2) for R1 and 2.9 g/L (±0.3) for R2. The SVI_{30}/SVI_{10} ratio remained at an average of 0.82 (±0.04) in both systems, while the SVI_{30}/SVI_{5} ratio had an average of 0.65 (±0.05). The SVI_{30} values were on average 89 mL/g (±11) in R1 and 76 mL/g (±5) in R2. The formed granules were predominantly small, ranging between 0.2 mm and 0.5 mm. Similar findings were reported by Silva *et al*. (2023a).

In stage 2, the cycle time was reduced from 12 to 6 hours. At this point, biomass rapidly increased in both R1 (3.9 ±0.6 g/L) and R2 (4.2 ±0.6 g/L). The OLR increased from 1 to 2 g/L/day, favoring biomass growth in both reactors, similar to what was observed in Silva *et al*. (2023a) when organic supplementation was adopted. Furthermore, there was evidence of an increase in granule size (0.5 and 1.0 mm), as seen in Figure 39b and granulometry data (Figure 38b). However, an increase in filamentous biomass was also found, leading to an increase in unintentional sludge disposal with the final effluent (Figure 38a), causing a decrease in SRT, as shown in Figure 39a.

In R1, during stages 2, 3, and 4, no significant difference in the data was observed, as there was no change in operating conditions. Thus, the solid concentration remained around 3.6 mL/g (±0.2), and SVI_{30} reached its lowest value (63±5 mL/g). However, there was a considerable increase in the filamentous fraction, evidenced by both the drop in the granulometric profile (Figure 38b) and the MLVSS concentration in the final effluent (216±61 mg/L) (Figure 38a). The SVI_{30}/SVI_{10} ratio, although better than in stage 1, showed a slight decline (0.77 ±0.6), and a significant decrease in SRT (9 ±3 days) was observed (Figure 39a), probably due to the increase in filamentous biomass intensified by the co-treatment of synthetic effluent with leachate. Silva *et al.* (2023a) reported instability issues related to very small granules.

Figure 39 – Variation of the sludge retention time over the 192 days of operation (a) and Microscopy images of aerobic granules in each stage (b).

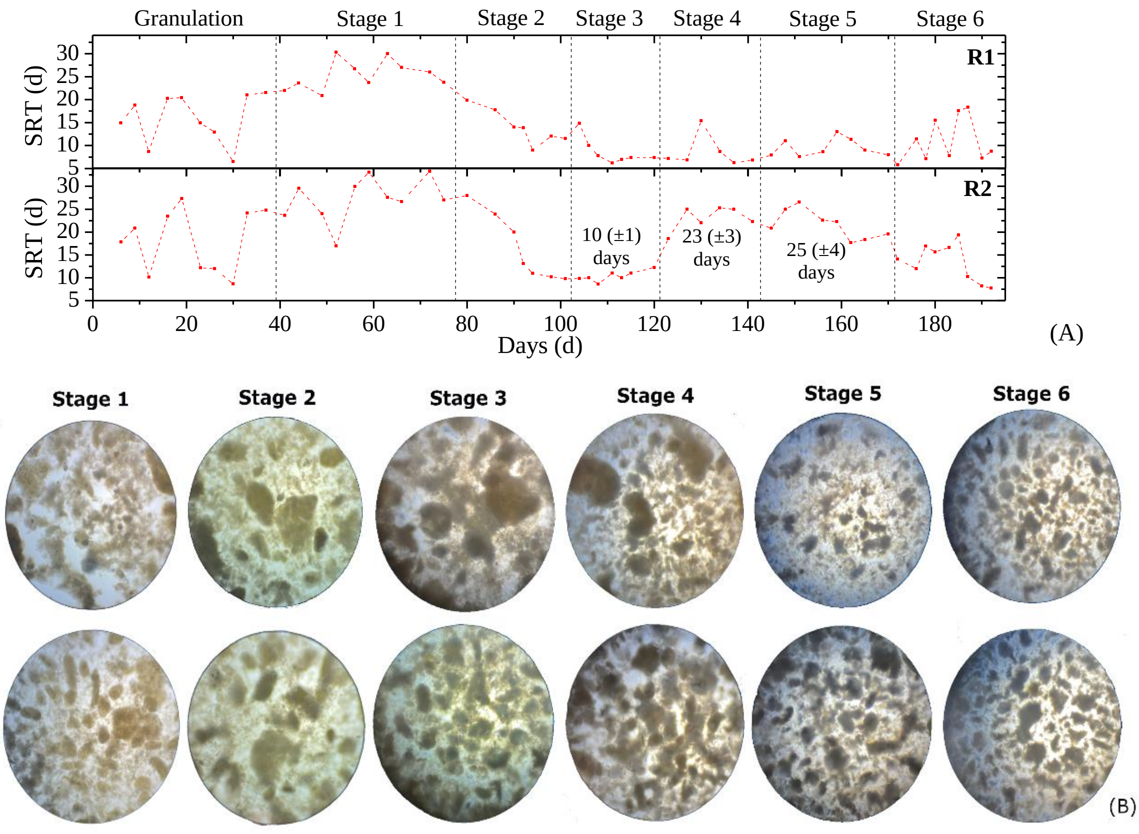

On the other hand, in R2, the analysis of each stage is necessary due to the implementation of intentional and selective biomass discharge. In stage 3, with an SRT of 10 days (±1), the concentration of volatile suspended solids in the final effluent decreased, reaching values around 44 mg/L (±8). The selective discharge of 70% of the biomass from the top, essentially composed of the filamentous fraction, prevented this biomass from being eliminated during the volumetric exchange. However, a slight reduction in the concentration of solids in the mixed liquor was observed (3.9±0.2 g/L). The SVI_{30}/SVI_{10} ratio remained around 0.8 (0.04) during stages 2, 3, and 4, while the SVI_{30} remained around 59 mL/g (±7) in stages 2 and 3. On the other hand, in stage 4, with an SRT of 22 days (±3), a significant increase in the concentration of MLVSS (5.5 ±0.6 g/L) was observed, along with a decrease in SVI_{30} (44 ±12 mL/g), while solids in the final effluent remained low (49 ±8 mg/L).

In general, the controlled and selective biomass discharge in R2 positively contributed to the operational stability of the system as it allowed the removal of most of the filamentous fraction, which, as in R1, contributes to the drag of granules in the volumetric exchange, causing a decrease in the granulometric profile and contributing to system instability.

In stage 5, co-treatment occurred with 10% leachate. At this point, in both reactors, a decrease in MLVSS concentration was observed, and a worsening of systems settling characteristics, possibly due to the higher leachate load, corroborating the findings of da Silva *et al*. (2023a).

In R2, despite the selective biomass discharge, solids concentrations in the final effluent gradually increased. This compromised the SRT control, as the intention was to operate with an SRT of 30 days. The result was an initial increase, with a subsequent decline in the SRT throughout stage 5 (26 ± 4 days) (Figure 39a).

In stage 6, the operation returned to using 5% leachate; however, the biomass was not stabilized. In R1, although the MLVSS concentration increased and the sludge settleability improved, the granule fraction remained low, around 42% (±11). On the other hand, in R2, the MLVSS concentration continued to decrease, sludge settleability worsened, and the VSS concentration in the final effluent increased. This led to the interruption of intentional sludge discharge, and the SRT was around 13 days (±4).

In summary, adding leachate can be conditionally beneficial, depending on specific operating conditions. SRT control, for example, is a strategy that positively favored the operational stability of the system, and ultimately, the reduction of leachate after an increase was not beneficial.

8.1.3. Production and stability of bioresources

Figure 40 presents the production of ALE and EPS over the 192 operational days.

Based on the collected data, there is an increase in EPS production during the granulation process in both systems. However, significantly lower EPS production ($p < 0.05$) is evident in R1 and R2 during the granulation phase, mainly due to the low PS production. Naturally, the granulation process contributes to increased EPS. Additionally, with the increase in organic load in stage 2, there is an increase in the TB-PS fraction.

When comparing only the period without SRT control between R1 and R2 (granulation, stage 1 and 2), there is no significant difference in EPS production ($p = 0.189$). However, with sludge age control in R2, distinct conditions are established in each system, making a direct comparison between them inappropriate. In this scenario, EPS production in R1 was significantly higher than in R2 ($p = 0.001$), attributable to the low SRT maintained by R1 during this period (10±3 days) and the higher food-to-microorganism ratio (F/M). R1 presented significantly higher values (0.7±0.14 kg COD/kg MLVSS.d) compared to R2 (0.4±0.07 kg COD/kg MLVSS.d) ($p = 0.007$). The literature has already shown that different factors influence EPS production; higher SRT, for example, stimulates endogenous consumption of biopolymers, especially in SRT exceeding 20 days (Rollemberg *et al*., 2020b), and the F/M ratio has been directly correlated with EPS production (Wang *et al*., 2023).

No significant difference ($p < 0.05$) in EPS production is observed in R1 from stage 3 onwards, although some production peaks are noticeable in stages 3 and 6, especially with significantly higher PS production. Conversely, in R2, Phase 3 revealed significantly higher ($p < 0.05$) EPS production compared to other stages. This may be attributed to the lower SRT adopted in this stage, as opposed to stages 4 and 5, where the SRT was more than 20 days, possibly leading to endogenous consumption of biopolymers as a source of ATP. Regarding co-treatment with leachate, in both systems, no significant influence is observed since there were no relevant changes in stage 5, even with the increase in co-treatment to 10%. Based on the complete dataset, a weak and moderate Pearson correlation between EPS and SRT was identified in R1 (-0.35) and R2 (-0.50), respectively. In both systems, a moderate and inverse correlation (-0.58 and -0.56) was observed between PS production and SRT, suggesting that PS was the predominantly consumed fraction at higher SRT. Interestingly, when considering only the SRT control period in R2, there is a strong and inverse correlation between EPS production and SRT (-0.90) and PS and SRT (-0.72). However, for this same period, no correlations were identified in R1. Based on this, the direct influence of SRT on these biopolymer fractions is evident, highlighting the importance of SRT control to optimize bioresources production in AGS systems.

Figure 40 – Biopolymer production over the 192 operational days in terms of (a) EPS, (b) ALE, and (c) ALE composition among GG, MG, and MM fractions.

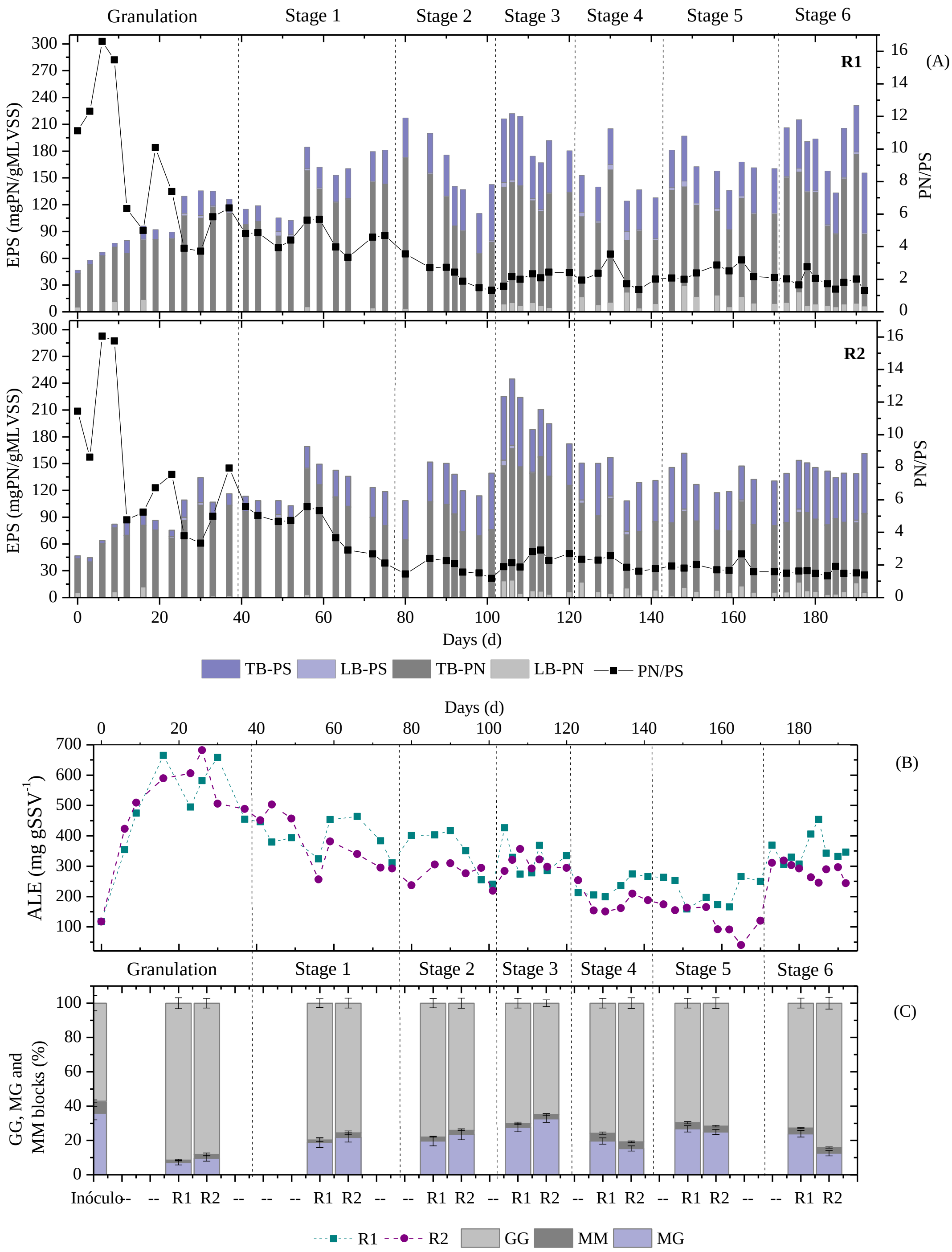

Regarding ALE production, a significantly higher ($p < 0.05$) production is observed during the granulation period, followed by a gradual decrease upon granule maturation. A study published by Santos *et al*. (2022) reported that peaks in ALE production may be associated with moments of instability and increased selection pressure, as is the case during the granulation period in AGS systems.

Additionally, experiments with salt stress, for instance, show that can maintain high ALE production for extended periods, although the production tends to decrease over long-duration operations, possibly related to longer SRT. In contrast, Schambeck *et al*. (2020) observed increased ALE concentration with granule maturation. Based on this, it is evident that a series of operational and environmental factors profoundly influence the dynamics of AGS systems.

In stage 5, a significant reduction ($p < 0.05$) in ALE production is observed in both systems. The increased co-treatment of leachate to 10% negatively affected this production, as in stage 6, upon returning to co-treatment at 5%, there was a recovery in ALE production. In R2, stage 4, a significantly lower production ($p < 0.05$) is also observed, attributed to the increased SRT adopted (23±3 days), and possibly in stage 5, SRT also influenced (25±4 days). This hypothesis is confirmed by the Pearson test, showing a strong inverse correlation (-0.80) between ALE production and SRT when considering only the SRT control period. Conversely, in R1, no such correlation is observed for the same period.

These findings align with the literature. For instance, Santos *et al*. (2022) conducted a study with varying SRTs and substrate sources and found that the ALE yield was higher in the reactor with a shorter SRT, suggesting that increasing SRT leads to ALE endogenous consumption. Similarly, Pronk *et al*. (2017b) observed a yield of only 1% of ALE in systems with SRTs ranging from 51 to 24 days. Rollemberg *et al*. (2020b) indicated that SRTs greater than 20 days lead to endogenous consumption of bioresources as an energy source.

It was observed that in all stages, the extracted ALE, corresponding to the structural EPS, revealed ionic hydrogel-forming properties, generating drop-shaped spheres when adding sodium ALE in calcium chloride (2.5%) (Figure 41) (Ca^{2+}-ALE spheres) (Felz *et al*., 2016). However, there was a greater dispersion of these spheres in both reactors in stages 3 and 5. In the first situation, the low SRT (Figure 39), 10 days (±1) in R2 and 9 days (±3) in R1, indicates that, although the low SRT favors the formation of biopolymers, their stability may be compromised.

In stage 5, the greater dispersion of Ca^{2+}-ALE spheres is probably due to the increase in co-treatment to 10% leachate. Furthermore, there was greater disintegration when the stability of these spheres was tested by adding EDTA (2%) and formaldehyde + NaOH for 3 hours at 4ºC. This suggests that the 10% co-treatment, although it did not influence the total amount of EPS formed, affected its properties, decreasing its structural stability, consistent with the reduction in ALE recovery in stage 5 (Figure 40b). In R1, in stage 6, stability was not fully reestablished as disintegration continued. In general, it was also observed that the Ca^{2+}-ALE spheres were more stable in EDTA than those soaked in formaldehyde + NaOH, which formed small brownish flocs on the surface, similar to what was observed by Felz *et al*. (2016).

The gel-forming capacity of alginate is intrinsically linked to its chemical composition, particularly the presence of the GG, MG, and MM blocks. Figure 40c shows the fractionation of these blocks in each stage. The content of GG blocks in the inoculum sludge increased from 57.1% to 91.4% in R1 and 88.1% in R2 with the granulation process, indicating a rapid change in biomass properties with the high selection pressure imposed for AGS cultivation. In AGS systems, gelling capacity is associated with a higher proportion of GG blocks (> 69%), as indicated by previous studies (Sarvajith *et al*., 2023; Lin *et al*., 2010; Leal *et al*., 2008). GG blocks have a stronger affinity for divalent cations such as Ca^{2+} than MG and MM blocks, attributing significant mechanical stability and viscoelasticity to the biopolymer (Sarvajith *et al*., 2023). On the other hand, the MM and MG blocks provide flexibility to the polymer chains (Lin *et al*., 2010).

Studies indicate that variations in carbon resources and operational configurations result in different concentrations of GG blocks, thus influencing the properties of the ALE formed (Li *et al*., 2022). Therefore, the different operational conditions of this study must have influenced the different concentrations of GG blocks in each stage (Figure 40c). Stages 3 and 5 had the lowest concentrations of GG block, with 70.1% and 69.6% in R1 and 64.7% and 71.7% in R2, respectively. Similar to what was observed in the ionic hydrogel formation and stability test, the low SRT and increasing the leachate co-treatment to 10% may have contributed to this result.

Figure 41 – Formation and stability of structural EPS (Ca^{2+}-ALE spheres). On the left, beads were stored in demineralized water for 4 hours at 4 °C; in the center, spheres were stored in 2% EDTA for 3 hours at 4 °C; and on the right, spheres were stored in formaldehyde + NaOH for 4 hours at 4 °C.

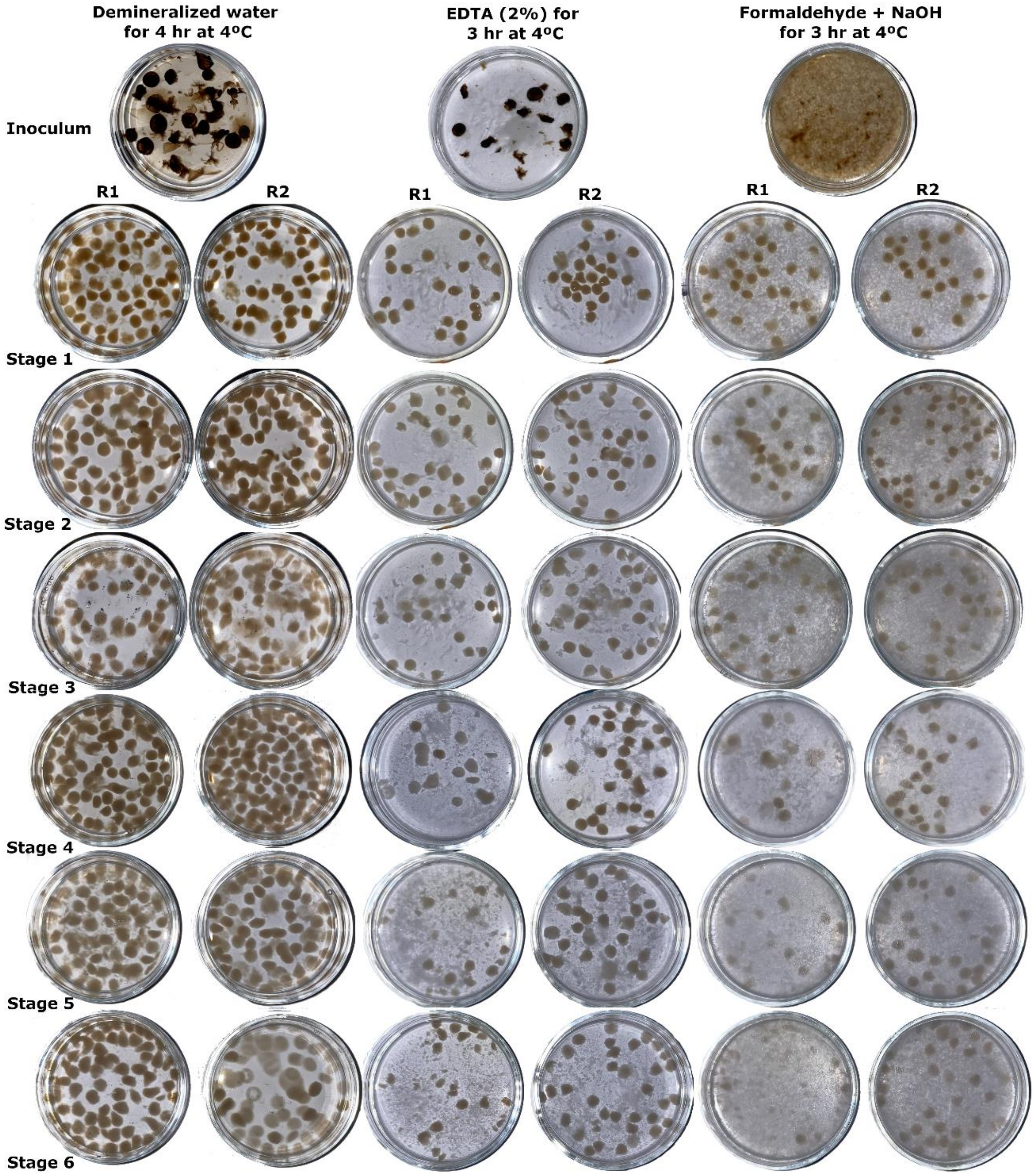

8.2. Reactors' performance

During the 192-day operational period, reactors R1 and R2 demonstrated remarkable efficiency in removing organic matter, as shown in Figures 42a and 42b. The average efficiency was around 96% (±1) for COD and 95% (±2) for DOC. However, in stage 5, during co-treatment with 10% leachate, both systems exhibited a significant reduction in COD and DOC removal efficiency ($p < 0.05$), a trend similarly observed by da Silva *et al*. (2023a). A significantly lower DOC removal in the granulation phase was also observed, followed by a continuous improvement in this data. This behavior can be expected since the granulation phase is the biomass adaptation to new operational conditions.

The decrease in organic matter removal efficiency in stage 5 suggests that adding leachate, with its complexity of organic substrates, may challenge the AGS system stability (da Silva *et al*., 2023a). However, this behavior is likely linked to an increase in the load of recalcitrant COD that occurs when the proportion of leachate is raised.

On the other hand, ammonia removal was consistent and complete throughout the experiment, with no nitrite accumulation and no significant difference between reactors R1 and R2, converting 99% (±1) of the influent ammonia nitrogen (Figure 42c). However, nitrate accumulation was observed in the initial stages of both reactors, reaching values of 10 mg/L (±5) in R1 and 11 mg/L (±4) in R2. This nitrate accumulation began to decrease in stage 4 in R1 (4 ±3 mg/L) and stage 3 in R2 (5 ±3 mg/L), indicating system adaptation over time, and the higher organic load applied from stage 2 may have contributed to a higher denitrification rate. Da Silva *et al*. (2023a) also observed nitrate accumulation in a similar system with a 12-hour cycle. The authors observed higher accumulation levels, possibly due to a higher ammonia load and the smaller size of the granules formed.

In the granulation phase, total nitrogen (TN) removal was significantly lower ($p < 0.05$) in both reactors, with an average of 65% (±8). This can be attributed to the initial granule adaptation and the lower organic load applied. However, in stages where the SRT was controlled in R2, TN removals were significantly higher ($p \approx 0.03$) when compared to R1. The decrease in TN removal in R1 in stages 3, 4, and 5 may be attributed to excess sludge washed along with the final effluent, as NOx accumulation was low, and ammonia removal was complete. In R2, although there was no significant difference between stages

($p > 0.05$) post-granulation, in stages 5 and 6, TN removal showed a slight decrease to 83% (±2) and 80% (±4), respectively. This likely reflects the increase in filamentous biomass washout in the final effluent.

These results suggest that the increase in organic load applied from stage 2 improved the denitrification rate. Furthermore, controlling the SRT in R2 proved effective in improving performance compared to R1, emphasizing the importance of this parameter in system operation.

Regarding phosphorus removal, results revealed that the highest removal efficiencies in R1 were observed in stages 4 (66±12%) and 5 (44±12%), exhibiting significantly ($p \approx 0.004$) higher values compared to other stages. On the other hand, in R2, stages 3 (57±4%) and 4 (46±5%) presented the highest efficiencies, with stage 4 statistically ($p=0.11$) equal to stage 5. These findings suggest that the SRT control in stages 3 and 4 may have improved phosphorus removal in R2. However, in R1, the mechanisms contributing to this result are unclear since there is no selective SRT control. Indeed, there was possibly an enrichment of phosphorus-accumulating organisms (PAOs) in this stage, especially in R1, demonstrated by the cycle analysis, in which a release of polyphosphate is observed in the anaerobic period, with subsequent assimilation (session 3.3).

However, it is paramount to highlight that complete phosphorus removal was not achieved in any stages evaluated in reactors R1 and R2. Similar results were also observed in a municipal wastewater treatment system (Santos *et al*., 2022; Xavier *et al*., 2023), indicating that low dilutions in leachate co-treatment (5 and 10%) do not interfere with phosphorus removal, different from what was observed by Silva *et al*. (2023a). This limitation may be related to the predominance of glycogen-accumulating organisms in the systems, which may have impaired phosphorus removal efficiency even under selective SRT control (Carvalheira *et al*., 2014). These results demonstrate the complexity of phosphorus removal in aerobic granular sludge systems and highlight the need for additional strategies to optimize this process.

Figure 42 – Performance of reactors R1 (left) and R2 (right) in terms of (a) COD, (b) DOC, (c) nitrogen fractions, and (d) phosphorus over 192 days.

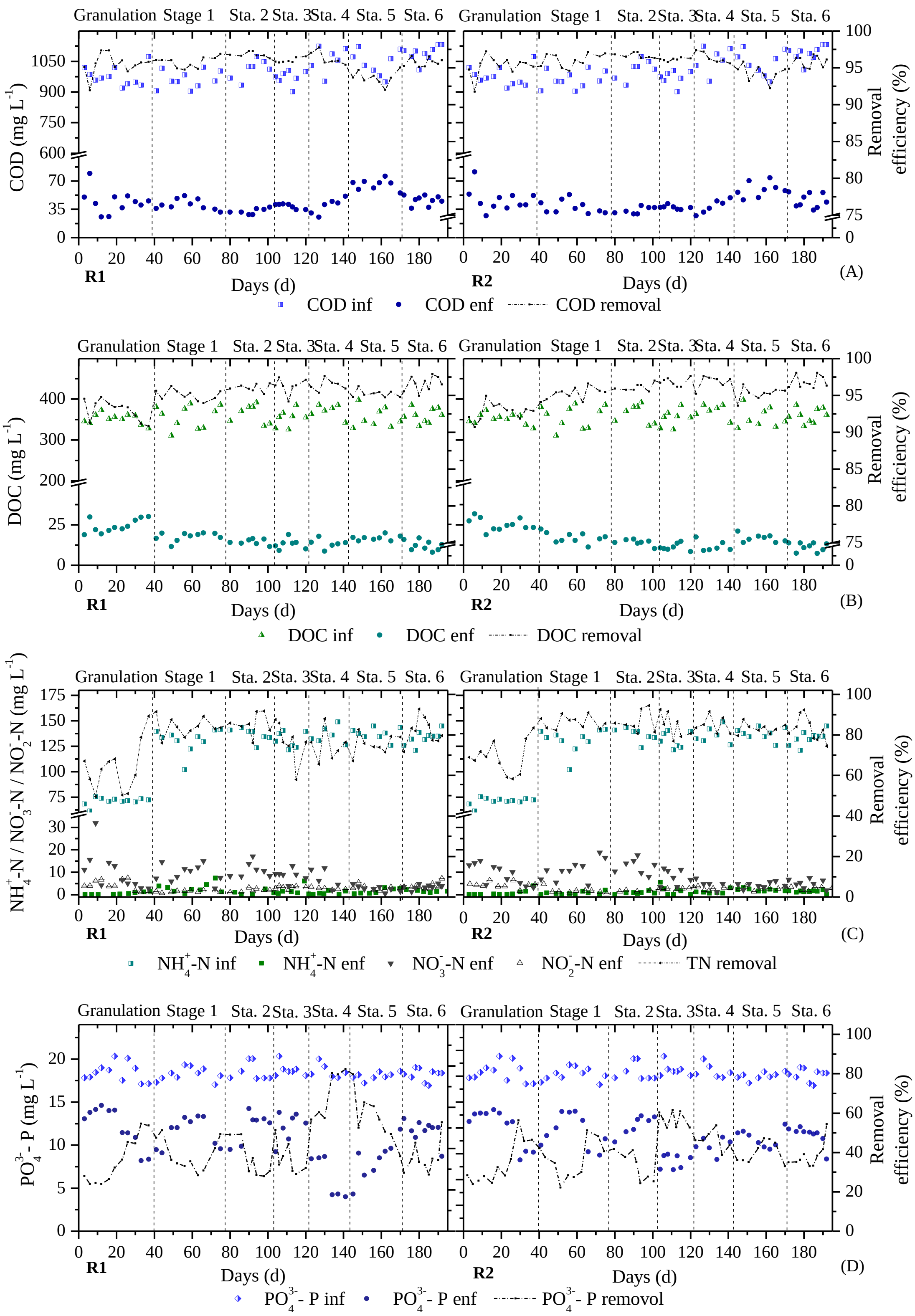

The co-treatment of 5% to 10% leachate, while influencing the removal of organic matter, appears not to have affected nitrification or the accumulation of NOx fractions and phosphorus removal. Therefore, although co-treatment of leachate with domestic sewage may impair the performance of AGS systems in simultaneous C:N:P removal, as reported in other studies (Silva *et al*., 2023a; Bella & Torregrossa, 2014), this outcome may vary depending on the feeding strategy, reactor configuration adopted, and carbon supplementation (Silva *et al*., 2023a).

8.3. Cycle analysis and kinetic parameters

The cycle analysis was conducted around day 134 of operation, corresponding to stage 4. During this period, the systems exhibited stability in terms of physicochemical and biological aspects. The cycle analysis was, therefore, carried out to understand the behavior of granules under stable conditions. Figure 43 illustrates the profile of organic matter and nutrient consumption, and Table 11 presents the consumption and production rates of organic compounds, ammonia, nitrite, nitrate, and phosphate.

During the operational cycle, both systems significantly decreased COD during the anaerobic period. The removal rate during the anaerobic period (0.079~0.049 gCOD/d/g VSS) was significantly higher than during the aerobic period (0.013~0.016 gCOD/d/g VSS), respectively, in R1 and R2. The two subsequent feedings in R2 minimally delayed the decrease in COD and contributed to the denitrification process. These data underscore the importance of COD availability in the denitrification process.

The ammonia concentration profile during the anaerobic and aerobic periods proved to be predictable, with a relatively stable concentration during the anaerobic period and more pronounced consumption during the aerobic period (Table 11). Nitrite and nitrate fractions remained low throughout the experiment, with a slight accumulation during the aerobic periods. For example, the nitrate production rate was 0.004 and 0.003 g NO_3^--N/d/g VSS in the first aeration in R1 and R2, respectively. These values were significantly lower than those found by da Silva *et al*. (2023a) and Xavier *et al*. (2023). However, the present study did not exhibit the limitations observed by the authors in the former case, predominantly small granules (0.2 mm) and, in the latter, elevated levels of dissolved oxygen (DO). According to Layer *et al*. (2020), SND can only be achieved when DO saturation varies between 14% and 39% in AGS systems, with biomass presenting a diameter of 0.5 mm. It can be inferred, therefore, that the SND process was developed in both reactors.

Figure 43 – Cycle analysis of R1 and R2 carried out around day 134 of operation, in stage 4.

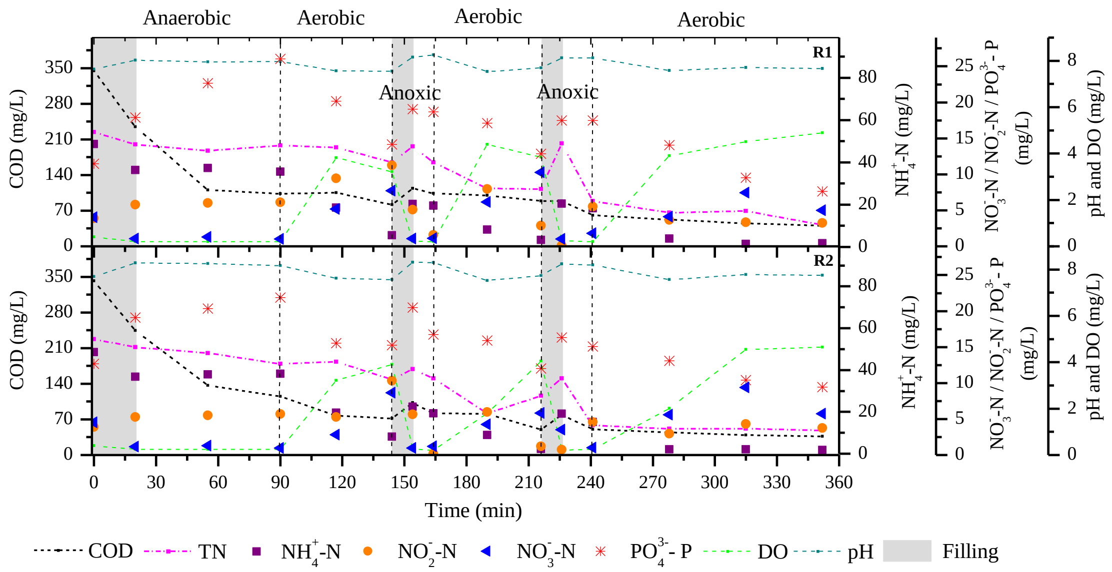

*The initial concentrations indicated at t=0 are the theoretical mixing concentrations if the influent wastewater were fed at once and not in buffer flow mode for 20 min. They were calculated based on measured concentrations of influents and effluents.

The pH showed a slight variation (7.5~8.2), with a trend influenced by nitrification and denitrification. As expected, there was a slight increase during denitrification reactions throughout the feeding and anoxic periods and a decrease during nitrification throughout the aerobic periods (Rollemberg *et al*., 2019; Xavier *et al*., 2023). The use of readily available organic matter by denitrifiers during feeding suggests possible substrate competition among denitrifiers, PAOs, and GAOs (glycogen-accumulating organisms) (Carvalheira *et al*., 2014; Liu *et al*., 2023).

Table 11 – Kinetic parameters of biomass activity (q) in terms of consumption and production rates of organic (COD), nitrogen (NH_4^+-N, NO_3^--N), and phosphorus (PO_4^{3-}-P) compounds in reactor R1 and R2 during leachate co-treatment.

Parameter (g/d/g VSS)	R1	R2
qCOD **– Initial Feeding**	0.066	0.037
qCOD **– Anaerobic**	0.079	0.049
qCOD **– Aeration 1**	0.013	0.016
qCOD **– Feeding 2 (Addition)**	0.019	0.011
qCOD **– Anoxic**	0.006	0.008
qCOD **– Aeration 2**	0.009	0.012
qCOD **– Final feeding (Addition)**	<0.001	0.011
qCOD **– Anoxic 2**	0.017	0.011
qCOD **– Final aeration**	0.012	0.005
qNH_4^+ **– Initial Feeding**	0.007	0.004
$q\ NH_4^+$ **– Anaerobic**	<0.001	<0.001
$q\ NH_4^+$ **– Aeration 1**	0.018	0.011
$q\ NH_4^+$ **– Feeding 2 (Addition)**	0.009	0.005
$q\ NH_4^+$ **– Anoxic**	0.0004	0.001
$q\ NH_4^+$**– Aeration 2**	0.010	0.006
$q\ NH_4^+$ **– Final feeding (Addition)**	0.010	0.006
$q\ NH_4^+$ **– Anoxic 2**	0.001	0.001
$q\ NH_4^+$ **– Final aeration**	0.010	0.005
qNO_3^--N **– Initial Feeding (Consumption)**	0.002	0.001
qNO_3^--N **– Anaerobic**	<<0.001	<<0.001
qNO_3^--N **– Aeration 1 (Production)**	0.004	0.003
qNO_3^--N **– Feeding 2 (Consumption)**	0.004	0.003
qNO_3^--N **– Anoxic**	<<0.001	<<0.001
qNO_3^--N **– Aeration 2 (Production)**	0.005	0.002
qNO_3^--N **– Final feeding (Consumption)**	0.006	0.001
qNO_3^--N **– Anoxic 2 (Consumption)**	<0.001	0.001
qNO_3^--N **– Final aeration (Production)**	0.002	0.002
qPO_4^{3-}-P **– Initial Feeding (Release)**	0.004	0.002
qPO_4^{3-}-P **– Anaerobic (Release)**	0.005	0.001
qPO_4^{3-}-P **– Aeration 1 (Capture)**	0.007	0.002
qPO_4^{3-}-P **– Feeding 2 (Addition+ Release)**	0.003	0.002
qPO_4^{3-}-P **– Anoxic (Capture)**	<0.001	0.001
qPO_4^{3-}-P **– Aeration 2 (Capture)**	0.003	0.002
qPO_4^{3-}-P **– Final feeding (Addition+ Release)**	0.003	0.002
qPO_4^{3-}-P **– Anoxic 2 (Capture)**	<0.001	<0.001
qPO_4^{3-}-P **– Final aeration (Capture)**	0.006	0.003

*The initial concentrations indicated at t=0 are the theoretical mixing concentrations if the influent wastewater were fed at once and not in buffer flow mode for 20 min. They were calculated based on measured concentrations of influents and effluents.

Phosphorus removal was carried out mainly through bioaccumulation by PAOs in both systems. Phosphate release can be observed during feeding and anaerobic periods, being more pronounced in the latter, possibly due to the greater availability of readily biodegradable organic material. However, the phosphorus release rate in R1 was double that of R2, which may justify the higher COD consumption rate in R1. Conversely, substrate scarcity during aerobic periods favored phosphate capture, indicated by an increase in dissolved oxygen (DO). Although DO levels were controlled between 2 and 4 mg/L, a trend toward lower values was observed at the beginning of the aerobic period, while values around 4 mg/L were observed from the middle to the end.

Nevertheless, complete phosphorus removal was not achieved, possibly due to substrate competition among PAOs, denitrifiers, and GAOs during feast periods (Carvalheira *et al*., 2014; Liu *et al*., 2023). In the anoxic phases of R2, denitrification via denitrifying phosphorus-accumulating organisms (DPAOs) was also observed, indicated by the reduction in phosphate and NO_3^- fractions.

8.4. Correlation between biopolymer production, granule stability and reactor performance

A PCA was applied to reactors R1 and R2, and the results are presented in Figure 43. A higher dispersion of scores is noticeable over the 192 operational days in R1, indicating a wider variation of data. In contrast, distinct groups covering each stage are visualized in R2 (Figures 44b and 44d). The PCA analysis of R2, considering all the data (Figure 44b), reveals similarities between stages 4 and 5, suggesting that the increase in co-treatment in this system during stage 5 may not have significantly influenced treatment performance. On the other hand, in R1, the similarity between these stages is not apparent due to the greater dispersion of scores (Figure 44a). It is important to note that, when considering PC3, the total variation of the data in R1 and R2 reaches 72% and 74%, respectively (Table 12), while PC1 and PC2 together represent only 59% and 58% of the total variation, in R1 and R2, in that order.

When analyzing the data set correlations, which encompasses all stages except the granulation phase due to its tendency to have a more significant dispersion due to the initial biomass adaptation, it is possible to observe a direct correlation between ALE and SVI_{30}/SVI_5 in R1. This suggests a positive relationship between ALE production and improved granule settleability. On the other hand, in R2, this relationship is not evident, as SVI_{30}/SVI_5 presents a low correlation (0.541) in PC1. However, there is a direct correlation with SVI_{30}, possibly due to the gradual increase in MLVSS concentrations over longer periods of operation. In these cases, it is common to verify an increase in MLVSS concentrations, a reduction in SVI_{30}, and a tendency towards a decrease in ALE content due to endogenous consumption, especially when SRT is greater than 20 days, as found in some stages in R2. This dynamic also justifies the inverse relationship between MLVSS and ALE and between MLVSS and SVI_{30} in PC1.

Similar to previous studies (Schambeck *et al*., 2020), ALE production also demonstrated an inverse correlation with nitrogen and COD concentrations. This suggests that ALE content at the ripening stage may be linked to the removal of organic matter and nitrogen, indicating a positive association between ALE production and effective granule formation. These results also confirm previous findings in the literature (Hengge, 2009 and Yang *et al*., 2014), which associate the production of ALE with denitrifying microorganisms, such as *Pseudomonas*.

In the PCA carried out with a specific set of data, covering only the control period of the SRT through the controlled discharge of biomass in R2, the first two PCs explain approximately 75% and 89% of the total variation in the data in R1 and R2, respectively (Table 12). In R1, there is a direct correlation between the production of ALE and EPS, both in the PN and PS fractions. However, no correlation was identified with SRT, which appears as an independent set correlated with PC2 (Figure 44c). Furthermore, it is observed that the highest values of biopolymers are associated with stage 3, while stages 4 and 5 present similar data. In contrast, in R2 (Figure 44d), all variables show a high correlation with PC1, with biopolymers (ALE, EPS, PN and PS) directly and inversely correlated with SRT. These results confirm that selective biomass discharge is a key parameter in the optimization of AGS systems, especially concerning the production of biological resources.

The literature has indicated a correlation between phosphorus content and ALE production (Schambeck *et al*., 2020). However, this relationship still needs to be clarified. Schambeck *et al*. (2020) observed a direct and positive correlation between the phosphorus content at the end of the anaerobic phase and ALE in their PCA, indicating that PAOs may be associated with the synthesis of ALE. However, they did not achieve high phosphate removal due to the low concentrations used. On the other hand, this study has verified a direct and positive correlation between the phosphorus content at the end of the cycle and ALE, as shown in Figure 44a and similar to results obtained in the OS III experiment. The literature has also associated the formation of ALE with the presence of GAOs (Zahra *et al*., 2022; Schambeck *et al*., 2020). Therefore, no relationship between ALE and P may be found since systems rich in GAOs disadvantage PAOs, consequently compromising their efficiency.

Figure 44 – Principal Component Analysis (PCA) considering data from all experimental stages in R1 (a) and R2 (b), and only data from stages with SRT control from intentional sludge disposal in R2 (d), and considering the same period in R1 (c).

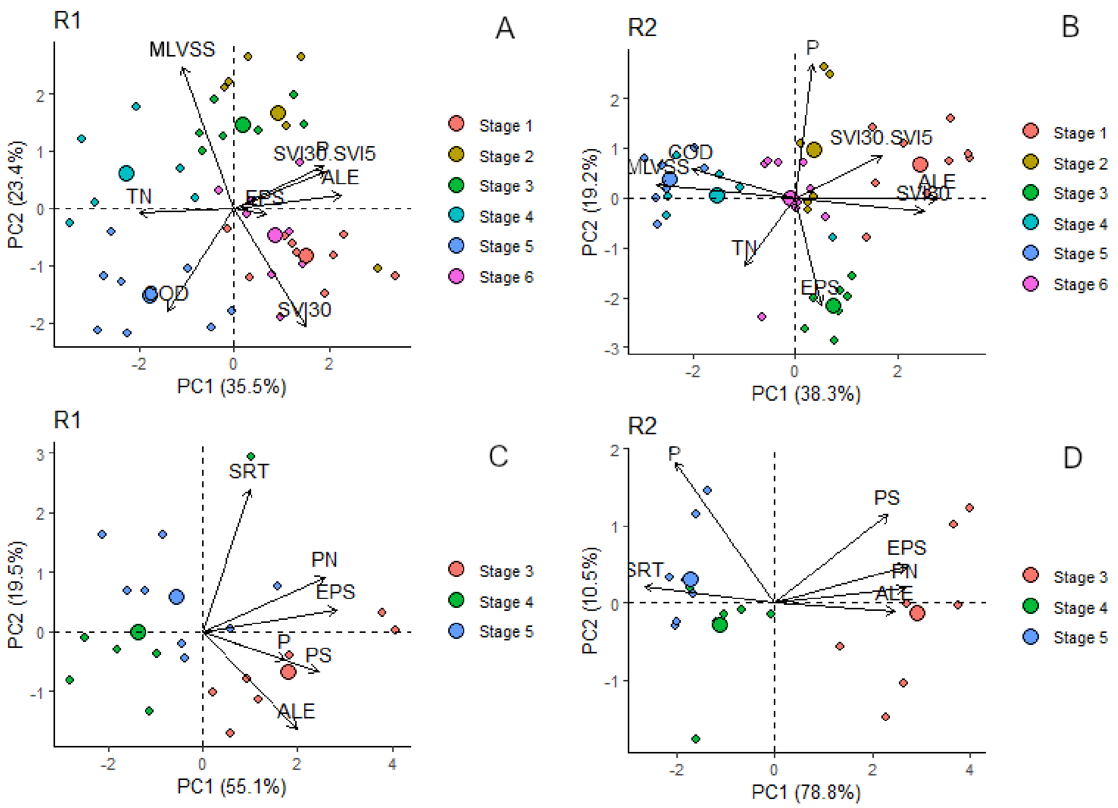

The influence of SRT on phosphorus removal is well established (Bassin *et al*., 2012a), and high SRTs can saturate PAOs, reducing their efficiency. This relationship was confirmed by PCA performed in R2 during the period of selective biomass discharge (Figure 44d). A pattern can be seen in the scores, with the highest P and SRT values in stage 5, median values in stage 4, and the lowest values in stage 3. This same trend, however inverse, is observed for biopolymers. Therefore, lower P concentrations indicate higher ALE contents for this data set, suggesting that the enrichment of PAOs may have contributed to the higher ALE production.

Considering the observations relating the predominance of GAOs and PAOs (*Rhodobacteraceae* and *Competibacteraceae*) (Rollemberg *et al*., 2020b), as well as denitrifiers (*Pseudomonas*) to ALE production, it is plausible that the synthesis of this biopolymer is the result of a complex interaction between these microorganisms. Despite different observations in the literature, we believe that SRT is a critical operational parameter to optimize the production of this biopolymer.

Table 12 – Correlation between the values of the standardized variables and the scores of the first three main components. Absolute load values greater than 0.6 (highlighted in bold) were adopted to consider the existence of a correlation between the variables.

All stage[1]	**R1**			**R2**		
	PC1	**PC2**	**PC3**	**PC1**	**PC2**	**PC3**
ALE	**0.808**	0.085	-0.104	**0.898**	-0.006	0.056
EPS	0.239	-0.041	**0.940**	0.16	**-0.691**	-0.477
P	**0.675**	0.261	0.177	0.108	**0.863**	0.182
TN	**-0.714**	-0.033	0.253	-0.318	-0.438	**0.688**
COD	-0.519	**-0.644**	0.159	**-0.647**	0.185	0.126
MLVSS	-0.386	**0.882**	0.119	**-0.867**	0.088	-0.254
SVI_{30}	0.543	**-0.739**	0.009	**0.808**	-0.083	0.471
$SVI_{30}.SVI_5$	**0.703**	0.231	0.061	0.541	0.271	-0.542
Variance	35.46	23.38	12.92	38.27	19.21	16.66
Cumulative variance	35.46	58.84	71.76	38.27	57.48	74.14
SRT control stage[2]	**R1**			**R2**		
	PC1	**PC2**	**PC3**	**PC1**	**PC2**	**PC3**
ALE	**0.675**	-0.557	-0.240	**0.876**	-0.038	0.400
SRT	0.337	**0.816**	-0.219	**-0.945**	0.075	-0.013
EPS	**0.964**	0.124	-0.024	**0.973**	0.175	-0.023
PS	**0.832**	-0.233	-0.439	**0.828**	0.408	-0.324
PN	**0.876**	0.311	0.214	**0.957**	0.067	0.094
P	0.592	-0.164	**0.737**	**-0.719**	**0.650**	0.224
Variance	55.11	19.48	14.82	78.81	10.51	5.41
Cumulative variance	55.11	74.59	89.41	78.81	89.32	94.73

*[1]PCA variables considering data from all experimental stages, except the granulation phase, in R1 and R2, and [2]variables considering data from R1 and R2 only from the period of the stages in which SRT control from the intentional disposal of sludge in R2 was employed.

8.5. Microbiological communities

Microbial diversity was evaluated at each operational phase of the biomass extracted from reactors R1 and R2, as well as from the inoculum sludge (I), at the phylum, family, and genus levels, as presented in Figure 45.

The dominant phyla in the inoculum sludge (Figure 45a) were *Actinobacteriota* (11.3%), *Chloroflexi* (16.7%), *Patescibacteria* (21.9%), and *Proteobacteria* (28.7%). With the granulation process, a significant reduction in the phyla *Actinobacteriota* (2.7% in R1 and 0.7% in R2) and *Patescibacteria* (0.2% in R1 and 0.3% in R2) was observed, probably due to the biomass washout caused by the short settling time.

The *Actinobacteriota* phylum is predominantly heterotrophic and has the ability to degrade organic compounds, as reported in other studies on leachate treatment (Silva *et al*., 2023a). This group was associated with the filamentous sludge volume (Hou *et al*., 2020; Geng *et al*., 2020), which justifies its higher abundance in the inoculum sludge and the final operational phase (~10%), in line with granulometry data that indicated an increase in filamentous biomass. On the other hand, *Patescibacteria* possess small genomes and limited metabolic capabilities, often found in activated sludge and involved in symbiotic interactions with other microorganisms (Fujii *et al*., 2022). Similar to *Actinobacteriota*, *Patescibacteria* showed an increase in relative abundance in period VI, reaching 13.6% in R1 and 7.5% in R2. During the sludge age control phases, this group was more abundant in R1 (~5.0%) compared to R2 (~1.6%), possibly reflecting the higher filamentous fraction in R1 biomass and indicating that sludge age control in R2 was an effective strategy for controlling microorganisms associated with filamentous biomass.

The *Chloroflexi* phylum includes both autotrophic and heterotrophic microorganisms, essential for the formation of flocs and biofilms, frequently cited in activated sludge and AGS systems (Silva *et al*., 2023a; Saxena *et al*., 2022; Liu *et al*., 2017). This group showed a slight decrease in relative abundance (<10%) with granulation, although it is indicated as more sensitive and less tolerant to leachate toxicity, it was present in the inoculum sludge adapted to treat leachates.

On the other hand, the granulation process favored the *Proteobacteria* phylum, which was dominant throughout the experiment. The literature has indicated that groups within the *Proteobacteria* phylum play a crucial role in sludge granulation and structural stability, commonly associated with EPS secretion for aerobic granule formation (Pronk *et al*., 2017b; Zahra *et al*., 2022; Quartaroli *et al*., 2019). These microorganisms, characterized by heterotrophic gram-negative bacteria, play important roles in COD and nitrogen removal (Liu *et al*., 2017; Geng *et al*., 2020). Granulation also favored groups such as *Bacteroidota* and *Firmicutes*, cited in activated sludge and AGS systems, also associated with carbon and nutrient removal (Saxena *et al*., 2022; Li *et al*., 2020b; Barros *et al*., 2021; Liu *et al*., 2017).

Finally, the *Planctomycetota* phylum presented a higher relative abundance during period I, with 18.0% in R1 and 8.4% in R2, indicating that longer operational cycles, such as 12 hours, may favor this group. These microorganisms, associated with the oxidation of organic matter, are typical of activated sludge biomass and are commonly cited in AGS systems (Saxena *et al*., 2022; Liu *et al*., 2017; Quartaroli *et al*., 2019).

At the family level (Figure 45b), in the inoculum sludge, the groups with abundances greater than 5% were *Comamonadaceae* (7.3%) and *midas_f_34838* (11.2%). While *midas_f_34838* was significantly reduced (<0.5%) with granulation and subsequent phases, *Comamonadaceae* showed enrichment (16.9%) in R2 during period V. This family is composed of fast-growing denitrifying microorganisms without the ability to accumulate polyphosphate (Guimarães, 2017; Nielsen *et al*., 2010; Rollemberg *et al*., 2018). The enrichment of this group was likely related to the emergence of filamentous biomass at the end of this period, caused by the increase in co-treatment to 10% leachate, which compromised SRT control. In the following phase, the reduction of this group is likely due to biomass washout along with the final effluent.

The families *Rhodobacteraceae* (18.1% in R1 and 6.55% in R2), *Rhodocyclaceae* (10.2% in R1 and 37.8% in R2), *Fimbriimonadaceae* (8.1% in R1 and 24.2% in R2), and *Schlesneriaceae* (16.4% in R1 and 6.61% in R2) showed a considerable increase in abundance with granulation. In the following periods, a reduction was observed, but they still presented abundances greater than 6% for *Rhodobacteraceae*, 12% for *Rhodocyclaceae*, 5% for *Fimbriimonadaceae*, and 2% for *Schlesneriaceae*. In R1, during period V, there was an even greater reduction in the abundance of all these groups, indicating lower resistance to leachate toxicity due to the increased load. In period VI, only *Rhodobacteraceae* showed recovery. In R2, the reduction of these groups occurred with the increase in SRT, and only *Rhodobacteraceae* showed an increase still in period V. The reduction of these groups between periods IV and V may be associated with a decrease in EPS and ALE production, especially related to *Rhodobacteraceae* and *Rhodocyclaceae*, as the literature has associated these families with EPS release and granule development, encouraging the production of signaling molecules such as cyclic di-guanosine monophosphate (c-di-GMP), also associated with increased ALE production (Yang *et al*., 2014; Zahra *et al*., 2022; dos Santos *et al*., 2022).

The *Schlesneriaceae* family, belonging to the *Planctomycetota* phylum, is composed of moderately acidophilic and mesophilic bacteria, exhibiting unique characteristics compared to other *Planctomyces* groups. They are known to participate in important nutrient cycling processes, although the specific metabolic capacities and ecologies of many of their members are still being investigated (Kulichevskaya *et al*., 2007). Although the *Planctomycetota* phylum is typically found in activated sludge and AGS systems (Saxena *et al*., 2022; Liu *et al*., 2017; Quartaroli *et al*., 2019), there were no specific mentions of the *Schlesneriaceae* family in the literature.

The taxonomic analysis at the genus level (Figure 45c) showed an inoculum with an abundance of *Neochlamydia*, which decreased significantly in both reactors over all periods. According to Macêdo *et al*. (2019), this genus is reported as common in activated sludge biomass and is quite sensitive to the shear force promoted by AGS systems.

In period I, with a higher concentration of influent nitrogen, almost the same genera can be found in both reactors, differing in terms of abundance. In R1, *Planctopirus* and *midas_g_8924* were the most abundant genera, followed by *Thauera*, *midas_g_5022*, and *midas_g_169*. *Planctopirus* is considered a rare genus, positively correlated with ammonia and organic matter, found in AGS reactors aimed at resource recovery, with a high PN/PS ratio (Zhang *et al*., 2019; Li, Li, and Fan, 2022). In R2, *Thauera* was the most abundant genus (33.01%), followed by *midas_g_5022* and *Ca Berkiella*. *Thauera* is found in various AGS reactors and is associated with EPS production, granule formation, and stability, promoting the production of c-di-GMP which can lead to excessive ALE production (Wan *et al*., 2013; Zhang *et al*., 2019; Li *et al*., 2020c; Yang *et al*., 2014). *midas_g_8924* and *Planctopirus* also showed significant abundance in R2. *midas_g_8924* has been associated with the *Rhodobacteraceae* family and can accumulate phosphorus and promote denitrification (Hamza *et al*., 2018; Dueholm *et al*., 2023).

Figure 45 – Relative abundance of microbial clusters in inoculum sludge and AGS biomass at the (a) phylum; (b) family; and (c) genus levels.

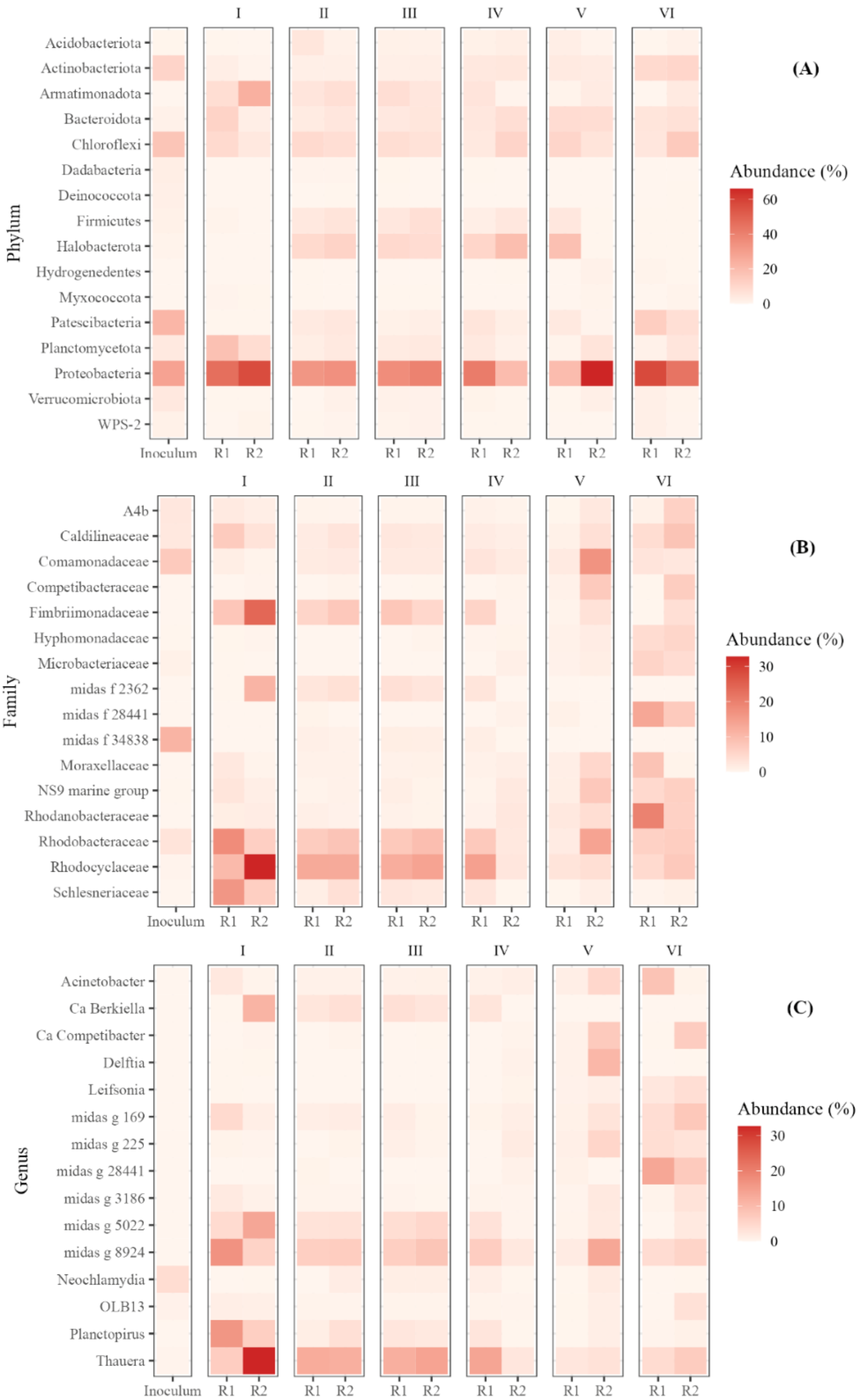

In period II, with the reduction in cycle time, the same profile was observed in both reactors, with *Thauera* being the most significant genus. However, in R1, there was a growth of *Thauera* while in R2 there was a reduction of this genus. In both reactors, *midas_g_8924* and *midas_g_5022* were also significant. At the beginning of sludge age control in period III, there were no differences in composition in both reactors, reflecting that initially, this strategy does not drastically alter the microbiological characteristics of the biomass. However, with the increase in SRT, greater heterogeneity of genera is observed. In period IV, R1 maintained its taxonomic composition, while in R2, by practically doubling the SRT, a more uniform distribution among all evaluated genera occurred, with a small prevalence of *Thauera* and *midas_g_8924*.

In period V, the situation reversed, and the reactor without sludge age control showed a uniform distribution, with a prevalence of *Thauera* and *midas_g_8924*. Despite no changes occurring in this reactor, the maturation of the biomass may act as a selection pressure for microorganisms. In R2, the SRT of approximately 25 days was crucial for the significant development of other genera such as *Acinetobacter*, *Ca Competibacter*, and *Delftia*, along with midas_g_8924. These functional groups have been reported to belong to microorganisms that favor SND, and thus, TN removal efficiencies above 80% were found during this period.

In the last phase of the experiment, with the interruption of sludge age control, there was a diversification of groups in both reactors. In R1, *midas_g_28441* and *Acinetobacter* stood out. In R2, besides *midas_g_28441*, *midas_g_169*, and *Ca Competibacter* were prominent. According to Dueholm *et al*. (2023), *midas_g_169* has filamentous characteristics, which can easily be found in this reactor due to the interruption of sludge control.

In Figure 46, the main functional groups related to the removal of C, N, and P are presented, subdivided into AOB (ammonia-oxidizing bacteria), NOB (nitrite-oxidizing bacteria), DNB (denitrifying bacteria), GAOs (glycogen-accumulating organisms), and PAOs (polyphosphate-accumulating organisms).

In periods I and II, both reactors exhibited similar microbial compositions, as the same operational parameters were maintained. The reduction in cycle time from period I to period II did not significantly influence the microbial composition in this study. With the beginning of sludge age control in R2, in periods III, a slight increase in the abundance and diversity of AOB, NOB and DNB were observed, suggesting a greater efficiency in the SND process. Despite a decrease in the *Rhodobacteraceae* family among the DNB in period IV, the SND process remained efficient, with TN removal above 80%. In R1, there was a higher abundance of DNB during period IV compared to R2, indicating that the deficiency in TN removal in R1 was caused by the loss of filamentous biomass along with the final effluent, a problem R2 avoided thanks to SRT control, which allowed for the removal of filamentous biomass before volumetric exchange.

Figure 46 – Functional distribution of the taxonomic classification of the R1 and R2 systems at the family level.

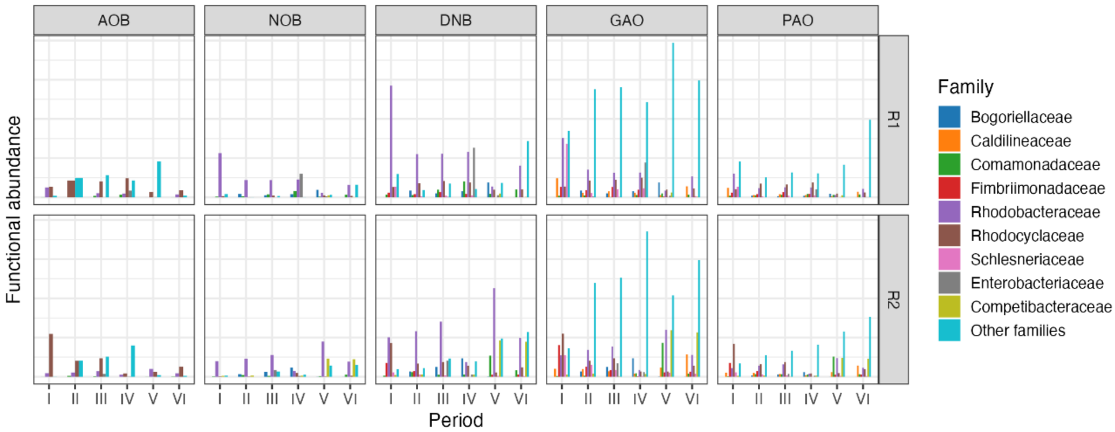

During period V, a reduction in the abundance of AOB was observed in both R1 and R2, along with a decrease in diversity in R1. There was also a reduction in NOB in R1. These changes can be attributed to the increase in leachate; however, in R2, the higher SRT was crucial for maintaining these groups. Silva *et al*. (2023a), working with similar configurations, reported AOB inhibition due to increased leachate load. During this same period, R1 also showed a reduction in the abundance of DNB, GAO, and PAO, which partially recovered during period VI, while R2 showed a reduction in GAO and PAO as early as period IV, with a subsequent increase in the *Comamonadaceae*, *Competibacteraceae*, and *Rhodobacteraceae* families. This behavior may be related to the production of bioresources in these systems, which decreased between periods IV and V, indicating that different microorganisms may be associated with EPS and ALE biosynthesis.

In both reactors, the competition among PAOs, GAOs, and DNBs is notable. Clearly, the DNB and GAO groups had a competitive advantage, reflecting the low phosphorus removal found in both reactors. Although R2 showed a positive relationship between phosphorus removal and SRT, this indicates that, at high SRT, phosphorus removal, already compromised by the greater abundance of GAOs, was further hampered by the saturation of existing PAOs.

8.6. Conclusions

The granulation process employing leachate with domestic sewage was successfully observed. However, it is believed that the biomass adapted to the leachate favored faster granulation. In general, the presence of leachate, operational changes, and selective disposal of biomass played crucial roles in the formation and stability of granules, directly influencing the efficiency of the treatment system.

On the other hand, increasing leachate co-treatment to 10%, although it did not affect nitrification or the accumulation of NOx fractions and phosphorus removal, influenced the removal of organic matter and decreased the quantity and quality of the hydrogel formed.

The PCA highlighted the complexity of the influencing factors in producing biopolymers, especially ALE, in AGS treatment systems. Although several correlations have been identified, SRT has emerged as a key operational parameter to optimize the synthesis of these biopolymers. While it has been observed that high SRT (> 20 days) can lead to endogenous consumption of biopolymers, low SRT (≤ 10 days) can compromise the stability of the hydrogel formed. Furthermore, SRT control demonstrated significant improvements in TN removal.

Therefore, controlling SRT through selective biomass disposal proved an effective strategy for maintaining granule stability and optimizing bioresources production in AGS systems.

9. FINAL CONSIDERATIONS

Several final considerations can be outlined considering the results obtained in this research on the formation and stability of aerobic granules in wastewater treatment systems. The studies analyzed different substrates and operational conditions, revealing that the choice of substrate, such as glucose, acetate, and propionate, can directly impact the granule formation patterns, as observed in Chapter 4. Additionally, the control of filamentous microorganisms and the optimization of operational parameters, such as feeding type, stress source, and SRT control, were identified as crucial factors to ensure the stability of the AGS system.

Observations regarding the influence of feeding type (conventional or staggered) in Chapter 6 highlight its importance in system stability. Reactors operated with conventional feeding showed a faster initial operational stability, suggesting that the prolonged famine period after start-up is crucial for granulation establishment. However, it is important to note that, even with the initial stability observed in conventional feeding reactors, these systems eventually faced operational collapses in subsequent stages, indicating that initial granulation may not guarantee long-term stability. Conversely, reactors operated with staggered feeding maintained superior stability until the advanced stages of the experiment, suggesting that this strategy may be more effective in promoting granule resistance to disturbances. In this scenario, the indication that a reduction in the famine period might be beneficial clearly indicates that the optimal feast/famine ratio during the granulation period differs from that in the maturation period. Staggered feeding not only contributed to granule stability but also created conducive conditions for denitrification, leading to a reduction in the accumulation of NOx fractions. This effect is particularly evident and serves as an effective strategy for treating complex effluents, as demonstrated in the co-treatment of leachate with domestic sewage, highlighted in Chapter 8, and for saline effluents, as noted in Chapter 6.

Reactors operated under saline concentration demonstrated that adding NaCl to a specific concentration positively impacted solids accumulation, indicating that osmotic pressure may contribute to biomass growth without affecting settling characteristics (Chapters 5 and 6). NaCl can promote particle agglomeration in water, facilitating the formation and maintenance of aerobic granules. Furthermore, the analysis of the impact of saline stress evaluated in Chapter 7 revealed intriguing results. The reactor operating with intermittent saline stress demonstrated rapid and complete granulation (21 days) compared to the reactor with constant salt addition (59 days). This finding suggests that the addition of NaCl, as well as variations in saline conditions, play a crucial role in promoting efficient granule formation, as well as decreasing granulation time.

However, using salt to optimize granulation in wastewater treatment systems can significantly increase the final effluent conductivity, requiring a temporary and well-planned approach. In this context, two configurations are possible for using saline pulse strategies: the first involves AGS systems designed to receive saline pulses during system start-up, as illustrated in Figure 47. This approach aims to promote rapid granulation and favor microorganisms related to granulation and bioresource production, and it can be reused in operational problems, such as system degranulation, to form new granules quickly. The second configuration uses a secondary system for accelerated granule production, where the generated sludge is transferred to the main line, as detailed in Figure 48. This strategy may be more efficient for resource production and recovery in the long term because the constant renewal of biomass under saline stress enhances system efficiency. In the first case, the temporary process avoids issues with increased salinity in the final effluent, while in the second, there is dilution of the saline load since only the produced sludge is used.

In terms of performance, all systems showed remarkable efficiency in removing organic matter, nitrogen, and phosphorus, even those with salt addition, demonstrating performance proportional to granule formation, indicating a stratified structure conducive to the coexistence of nitrifying and denitrifying microorganisms. However, variations in nitrification efficiency were observed, particularly during operational transitions, with decreases in total nitrogen removal at higher NaCl concentrations (10 g/L), especially in conventionally fed systems. Variations in phosphorus removal were also observed, presenting greater or lesser efficiency related to a greater abundance of PAOs and SRT control.

Moreover, it is crucial to recognize that the best outcomes obtained closely align with recent literature and international standards for effluent discharge and reuse, as evidenced by the review of Semaha *et al*. (2023), which highlights the effectiveness of AGS systems in contaminant removal and resource recovery in wastewater treatment. The present study confirmed that systems with staggered feeding not only achieved the best efficiencies in removing carbon, nitrogen, and phosphorus but also produced final effluents with concentrations of COD, nitrites, nitrates, and phosphorus within the limits recommended by international guidelines, such as the EU Urban Wastewater Treatment Directive and the Brazilian CONAMA Resolution nº. 430 of 2011.

However, it should be noted that under certain conditions, particularly in systems with co-treatment, a specific deficiency in phosphorus removal was observed, and in systems subjected to intermittent saline stress, not only were deficiencies in phosphorus removal noted but also accumulations of nitrogenous fractions exceeding 10 mg/L. While these occurrences are not ideal, they are amenable to optimization. Strategies to enrich PAOs and optimize denitrification processes have proven effective, as demonstrated in the staggered systems. These adaptations are crucial to ensure that all parameters of treated effluents comply with legal and environmental requirements, even under challenging conditions.

In summary, when optimized, AGS systems not only meet but can exceed discharge and reuse standards, providing a sustainable and efficient solution for wastewater treatment. Thus, this study's relevance for effluent treatment practice and the advancement of granular sludge technology in the circular economy and sustainable development context is confirmed.

Moreover, the research findings emphasize the crucial role of bioresources - including EPS, ALE, and TRP - in structuring the AGS systems. Continuous monitoring of these compounds throughout the experiments demonstrated their essential roles during the granulation phase, particularly in aerobic granules' formation and structural stabilization. Additionally, the production of these resources was positively influenced by osmotic stress, showing a positive correlation between the presence of salt, bioresource production, and granule stability. In Chapter 4, instabilities observed in one of the reactors indicated that intermittent stress sources may result in improved biosynthesis of resources, confirmed in Chapter 7 by intermittent salt stress, which presented better overall performance. However, the observed decrease in the production of these bioresources during granule maturation, particularly in systems with higher SRT, underscores the importance of SRT control in optimizing bioresource production within AGS systems. Additionally, it was evident that various factors, such as the F/M ratio, substrate type, and developed microbiota, can significantly influence the production of these resources, highlighting the complexity of microbial interactions and stress response mechanisms.

Microbiological analysis revealed significant changes in microbial diversity, showing specific responses in each reactor and indicating adaptations to environmental factors. The salt presence influenced the abundance of certain families, such as *Rhodobacteraceae* and *Rhodocyclacea*e, suggesting the adaptation of these microorganisms to saline conditions. Important bacterial groups associated with bioresource production, granule formation, and stability, such as *Defluviicoccus*, *Pseudofulvimonas*, *Thauera*, and *Lactococcus*, were enriched in AGS systems, with *Thauera* and *Pseudofulvimonas* showing higher abundance in reactors operated at 5 g/L NaCl. These results highlight the complex interaction between operational factors, environmental conditions, and microbial communities in the formation and stability of aerobic granules in wastewater treatment systems, emphasizing the importance of precise SRT control and biomass selective discharge strategies to optimize granule formation, stability, and overall system performance, especially when subjected to the challenge of co-treatment with leachate.

It is important to highlight that the potential applications of these bioresources are diverse and valuable. For instance, ALE-based materials are noted for their biodegradability and recyclability, offering superior alternatives to conventional fossil-based materials. These applications include waterproof coatings, flame-retardant materials, and supports for the controlled release of nutrients into the soil (Zeng *et al*., 2023). Tryptophan, with its antioxidant properties, is significantly applicable in the food and pharmaceutical industries, serving as a natural preservative and as a supplement in animal feeds (Carvalho *et al*., 2021).

Finally, EPS enhances the efficiency of AGS systems by facilitating microbial aggregation and the removal of contaminants. Furthermore, EPS serve as precursors in the production of bioplastics, contributing to the development of sustainable alternatives to conventional plastics. This multifunctionality strengthens the role of AGS systems as key resource recovery units. Integrated into urban resource factories, these systems can promote innovative technologies for a circular economy (Semaha *et al*., 2023). Additionally, it is worth highlighting that ALE values were significantly higher throughout the investigation than TRP. The literature (Schambeck *et al*., 2020; van Leeuwen *et al*., 2018) has also demonstrated greater potential for ALE recovery, especially due to its higher added value. Therefore, it is evident that bio-ALE is the bioresource of greatest interest, given its higher production levels and greater economic value.

Therefore, considering the wide practical applications of this research, especially regarding the treatment of various saline effluents from sectors such as textiles, tanneries, diverse industries, fisheries, and even leachates, the relevance of this study's contributions to the optimization of these processes becomes evident. Although each type of effluent presents specific characteristics that require individual assessments, the outlined strategies, involving staggered feeding, intermittent salt stress, SRT control and co-treatment of leachate with domestic effluents, emerge as a promising approach (Figure 49). Furthermore, it became evident that these improvements and variations can also optimize the production and recovery of bioresources, specifically ALE, presenting a promising and viable reality to be considered in a WWTP focused on the circular economy. Thus, the study highlights nuances and key aspects that, even considering the particularities of each effluent, can drive significant advancements in this field, contributing to the effectiveness and sustainability of treating various saline and/or domestic effluents.

Figure 47 – Diagram of wastewater treatment by AGS systems with saline pulses during start-up for rapid granulation.

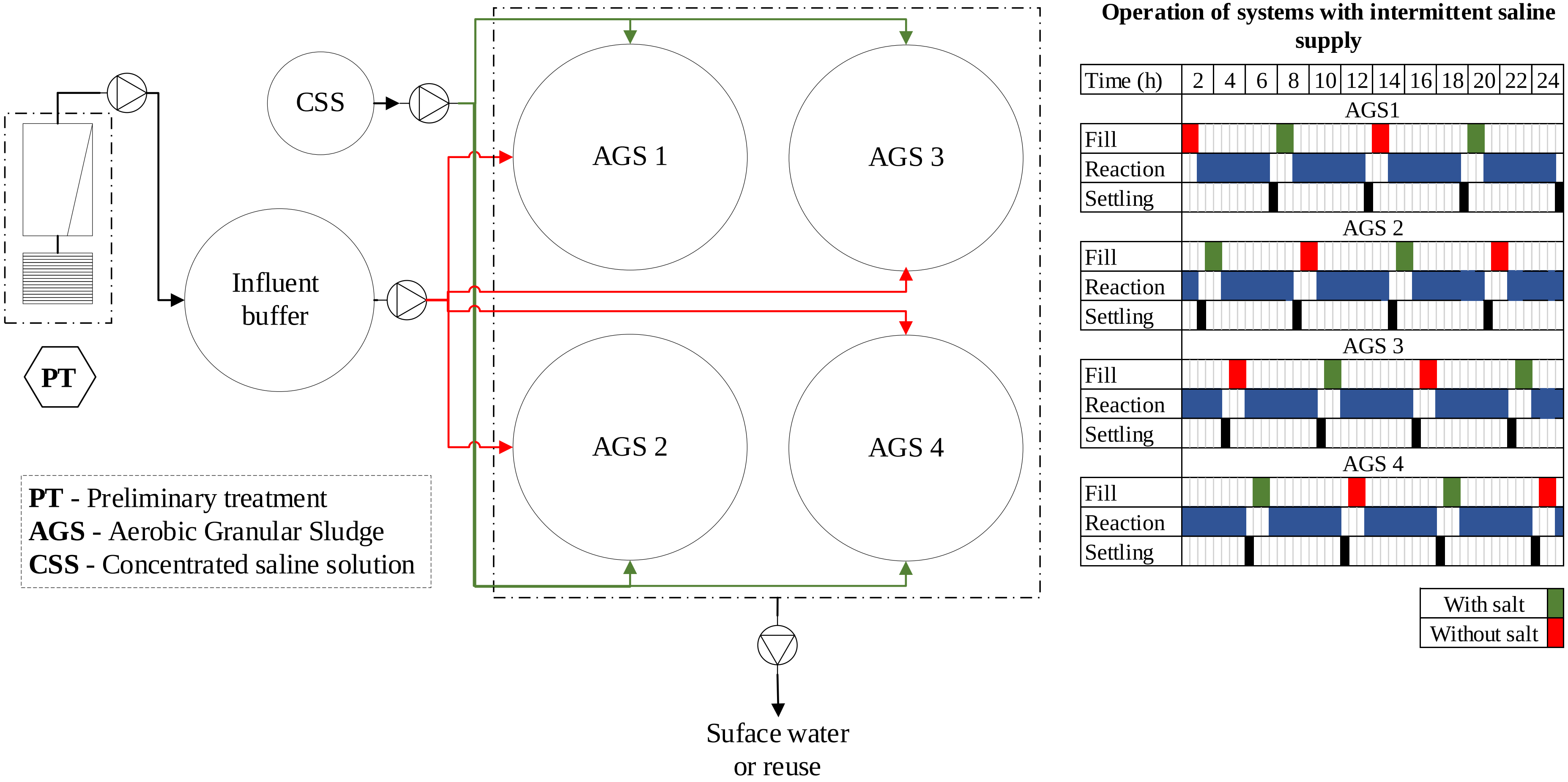

Figure 48 – Diagram of wastewater treatment by AGS systems with secondary accelerated granule production.

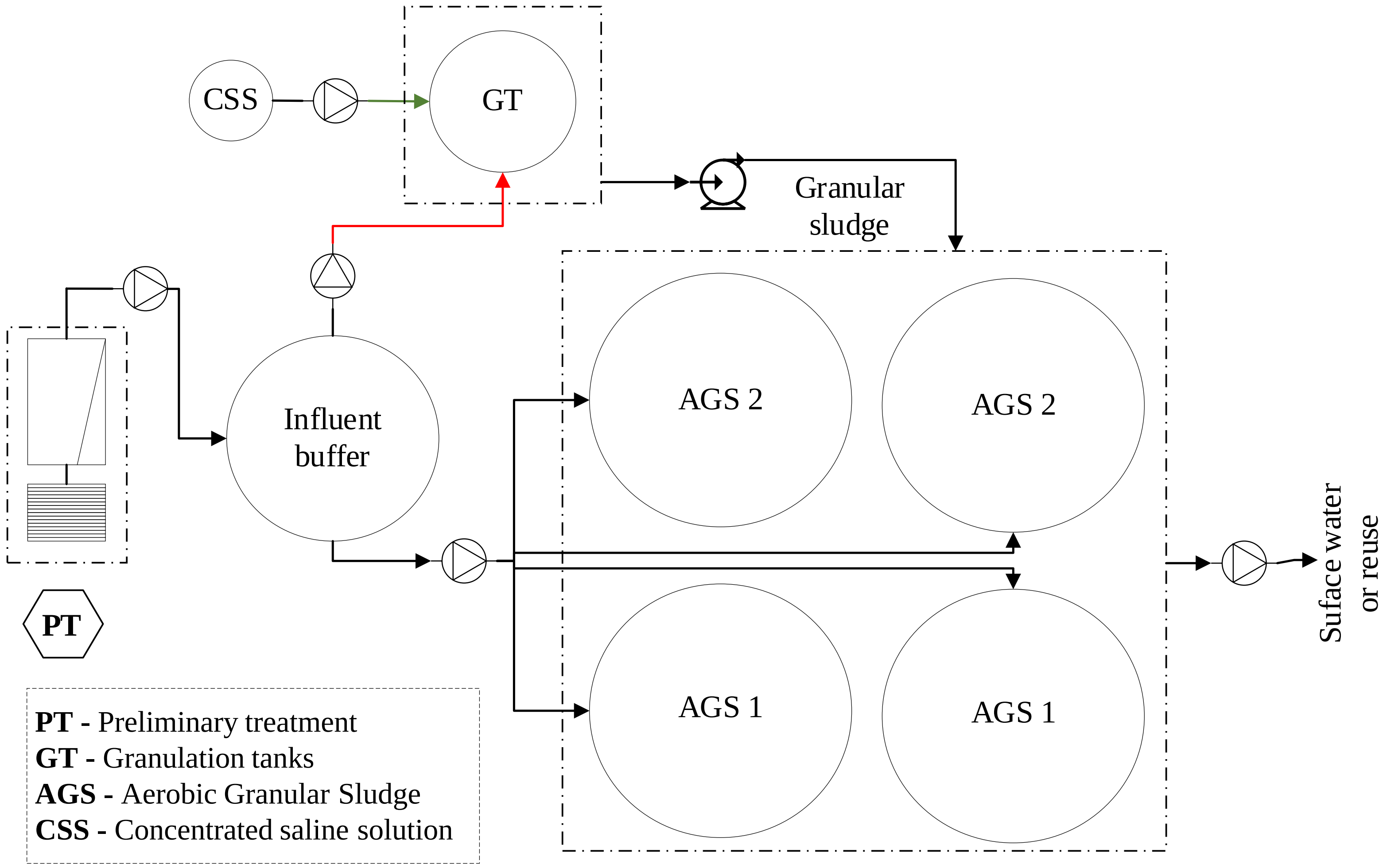

Figure 49 – Integration of effluent treatment and circular economy: a sustainable model for resource recovery.

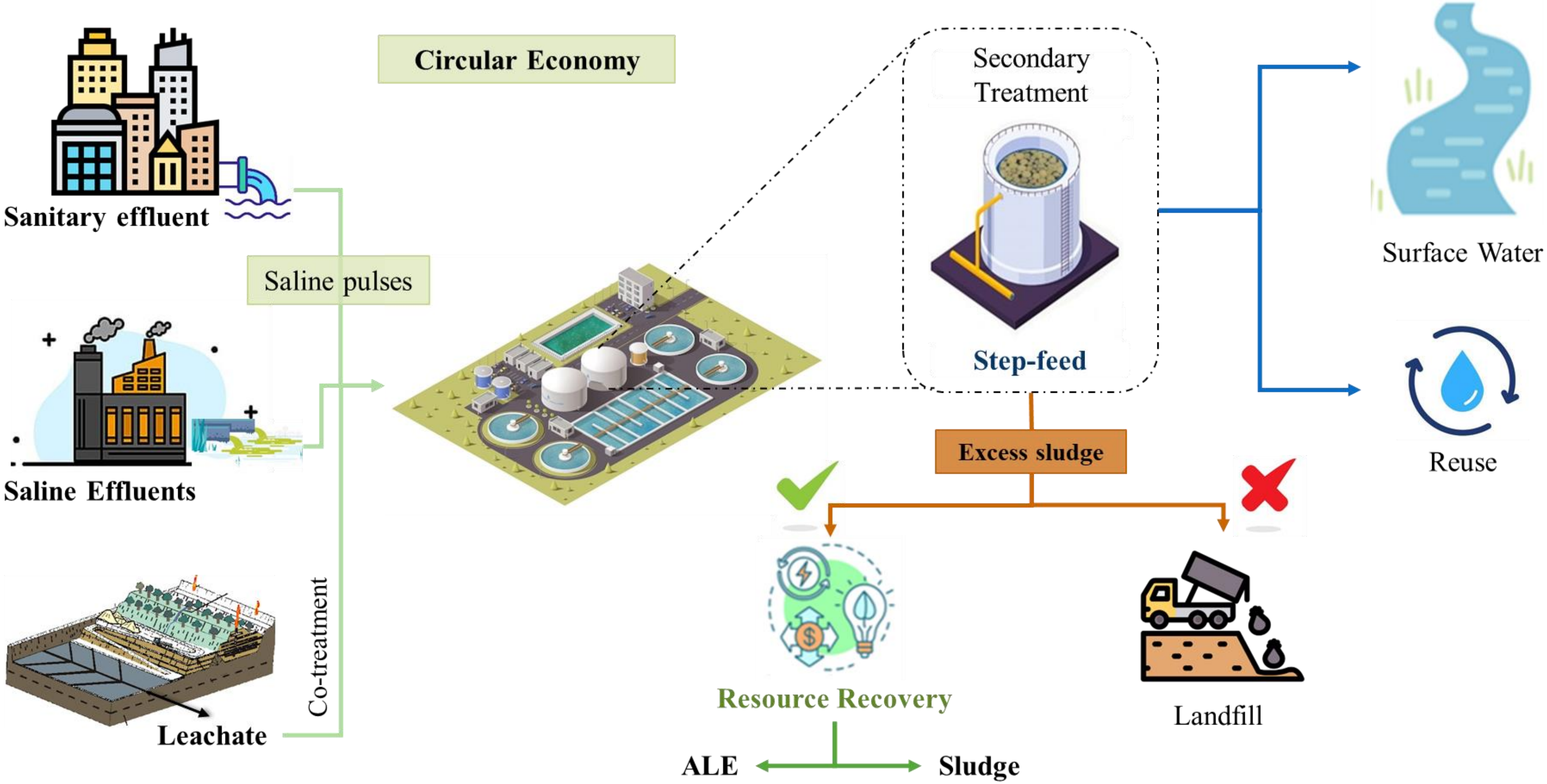

10. GENERAL CONCLUSION

The investigations confirmed that the variability in the feeding substrate, feeding regime, and sources of stress, such as salt addition, had significant impacts on the characteristics and stability of the sludge, corroborating the initial hypothesis. Therefore, seven main conclusions stand out, each addressing a question from the initial hypothesis:

1. Different substrates impacted bioresources formation on the AGS matrix distinctly, with acetate leading in producing ALE and tryptophan. This finding supports the hypothesis that certain substrates promote greater bioresource production;
2. The staggered feeding regime did not directly influence EPS production, but it favored denitrification and provided better resilience under osmotic pressures, indicating an improvement in granule stability;
3. Concentrations up to 7.5 g/L NaCl did not compromise the granules' physical characteristics or stability, indicating that acclimatization to these salt concentrations is feasible without impairing the treatment system's efficiency;
4. Controlled salt addition improves bioresource production by contributing to stability and aerobic granule formation;
5. Microbial adaptations to intermittent saline stresses, as evidenced by the increased presence of genus such as *Thauera* and *Pseudofulvimonas*, showed a positive correlation with enhanced granulation and bioresource production;
6. The presence of leachate up to a co-treatment concentration of 10% was successfully managed, although higher concentrations impacted hydrogel formation;
7. Prolonged SRTs above 20 days were detrimental to bioresource production due to increased endogenous respiration and EPS consumption, highlighting the importance of controlling SRT to optimize bioresource production and nutrient removal efficiency.

11. RECOMMENDATIONS

Incorporating advanced analytical and operational strategies to enhance the outcomes discussed and address potential improvements in AGS systems is crucial. One significant area for future exploration involves using metagenomic studies to gain a more comprehensive understanding of microbial dynamics within AGS systems. Such studies can illuminate the specific microbial interactions at different stages of wastewater treatment, offering insights that could lead to more targeted and effective management strategies, thus improving the overall efficiency of wastewater treatment processes.

Furthermore, resource recovery, particularly of ALE, has demonstrated substantial promise for incorporation into a circular economy model within wastewater treatment plants. To optimize this process, it is advisable to begin with conventional feeding to establish robust granule formation and then transition to staggered feeding to enhance the stability and efficiency of nutrient removal and bioresources production. Implementing intermittent stress sources, such as controlled saline stress, can further accelerate granulation and optimize resource production. For saline stress specifically, maintaining concentrations up to 5 g/L is recommended. For sanitary effluents, it is suggested that the saline stress be restricted to the start-up phase of the system or handled in a separate unit, as detailed in Figure 47 and 48. Investigating the impact of other types of stress on granulation and resource production could also result in beneficial operational insights.

Further research into strategies for maintaining nutrient removal efficiency under increased saline conditions is crucial in treating effluents with high salinity.

Additionally, the control of SRT through intentional sludge discharge is crucial for maintaining optimal system performance and maximizing resource production. An ideal SRT of around 15 days is recommended. Shorter SRTs, particularly those less than or equal to 10 days, may negatively impact the quality of bioresources produced, while longer SRTs, those 20 days or more, might lead to a decrease in the quantity of available bioresources due to increased endogenous respiration and EPS consumption.

Figure 50 proposes an operational schematic for an AGS system, considering these strategies, focusing on rapid granulation and production of bioresources. These strategic adjustments and further research can help refine AGS technology for broader application in complex effluent treatment scenarios.

Figure 50 – Proposal for an AGS system focusing on rapid granulation and bioresource production.

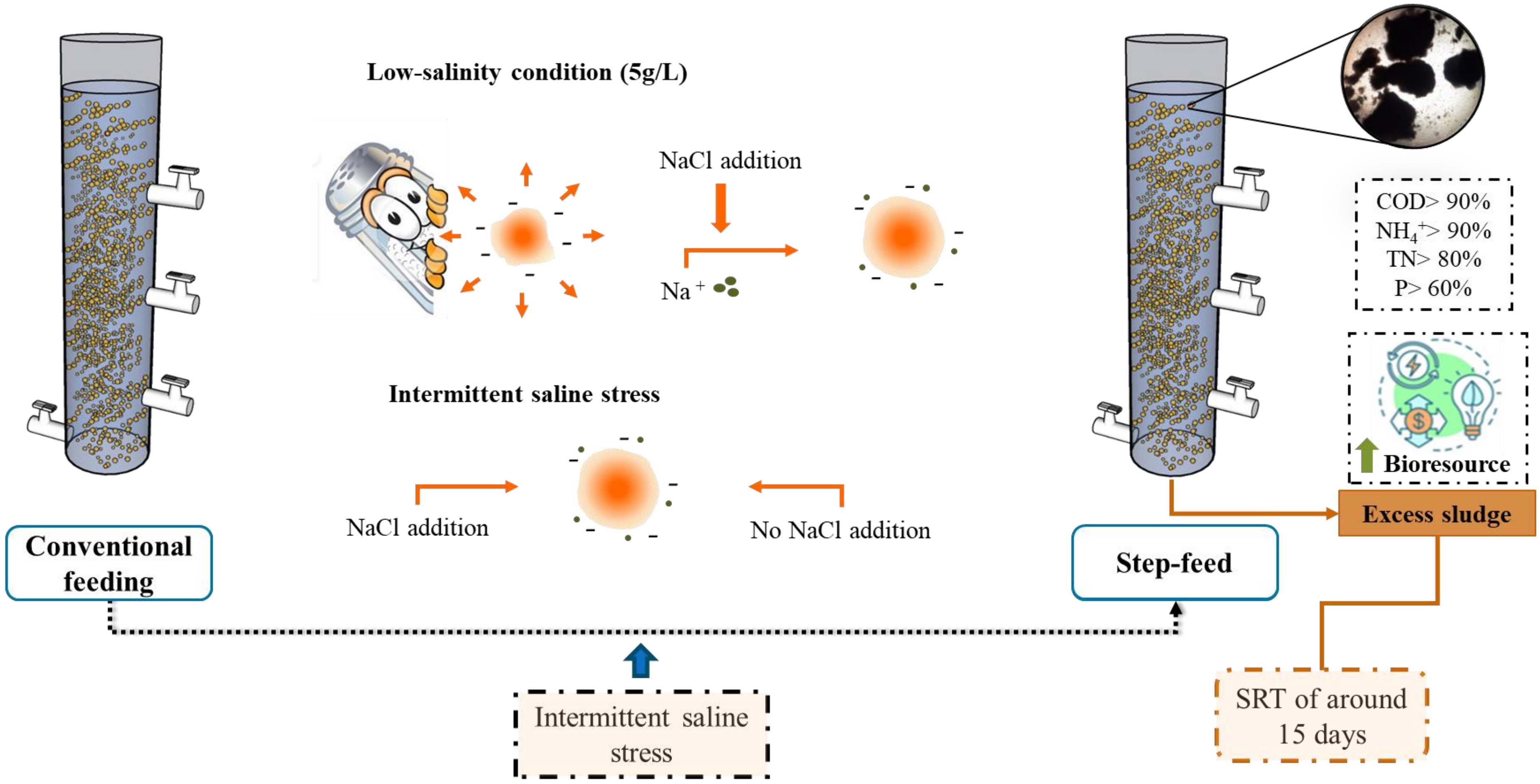

REFERENCES

ADAV, S. S. *et al*. Microbial community of acetate utilizing denitrifiers in aerobic granules. **Applied Microbiology and Biotechnology**, v. 85, p. 753–762, 2010.

AMERICAN PUBLIC HEALTH ASSOCIATION – APHA. **Standard Methods for the Examination of Water and Wastewater**. 22. ed. Washington: American Public Health Association, 2012.

ARGENTA, T. S. *et al*. Parabens in aerobic granular sludge systems: Impacts on granulation and insights into removal mechanisms. **Science of The Total Environment**, v. 753, n. 142105, 2021.

BAHGAT, N. T. *et al*. Integrated resource recovery from aerobic granular sludge plants. **Water Research**, v. 234, n. 119819, 2023.

BHALLA, B.; SAINI, M. S.; JHA, M. K. Effect of age and seasonal variations on leachate characteristics of municipal solid waste landfill. **International Journal of Research in Engineering and Technology**, v. 02, n. 08, p. 223-232, 2013.

BARROS, A. R. M. *et al*. Effects of coal ash supplementation on aerobic granular sludge cultivated in a simultaneous fill/draw sequencing batch reactor. **Eng. Sanit. Ambient**., v. 25, p. 691–700, 2020a.

BARROS, A. R. M. *et al*. Effect of calcium addition on the formation and maintenance of aerobic granular sludge (AGS) in simultaneous fill/draw mode sequencing batch reactors (SBRs). **Journal of Environmental Management**, v. 255, n. 109850, 2020b.

BARROS, A. R. M. *et al*. Effects of the antibiotics trimethoprim (TMP) and sulfamethoxazole (SMX) on granulation, microbiology, and performance of aerobic granular sludge systems. **Chemosphere**, v. 262, n. 127840, 2021a.

BARROS, A. R. M. *et al*. Effect of calcium addition to aerobic granular sludge systems under high (conventional SBR) and low (simultaneous fill/draw SBR) selection pressure. **Environmental Research**, v. 194, 2021b.

BASSIN, J. P. *et al*. M. Effect of Elevated Salt Concentrations on the Aerobic Granular Sludge Process: Linking Microbial Activity with Microbial Community Structure. **Applied and Environmental Microbiology**., v. 77, p. 7942–7953, 2011.

BASSIN, J. P. *et al*. Improved phosphate removal by selective sludge discharge in aerobic granular sludge reactors. **Biotechnology and Bioengineering**., v. 109, n. 8, p. 1919–1928, 2012a.

BASSIN, J. P. *et al*. Effect of different salt adaptation strategies on the microbial diversity, activity, and settling of nitrifying sludge in sequencing batch reactors. **Applied microbiology and biotechnology**, v. 93, p. 1281–1294, 2012b.

BELLA, G. D.; TORREGROSSA, M. Aerobic granular sludge for leachate treatment. **Chemical Engineering Transactions**, v. 38, p. 493–498, 2014.

BELLA, G.; TORREGROSSA, M. Simultaneous nitrogen and organic carbon removal in aerobic granular sludge reactors operated with high dissolved oxygen concentration. **Bioresource Technology**, v. 142, p. 706–713, 2013.

BEUN, J. J. *et al.* Aerobic granulation in a sequencing batch reactor. **Water Research**, v. 33, p. 2283–2290, 1999.

BIN, Z. *et al*. Dynamic and distribution of ammonia-oxidizing bacteria communities during sludge granulation in an anaerobic-aerobic sequencing batch reactor. **Water Research**., v. 45, n. 18, p. 6207–6216, 2011.

BOLEIJ, M. *et al*. Solubilization and characterization of extracellular proteins from anammox granular sludge. **Water Research**, v. 164, n. 114952, 2019.

BORGOS, S. E. F. *et al*. Mapping global effects of the anti-sigma factor MucA in Pseudomonas fluorescens SBW25 through genome-scale metabolic modeling. **BMC Systems Biology**, v. 7, p. 1-15, 2013.

CALLAHAN, B. *et al*. DADA2: high-resolution sample inference from Illumina amplicon data. **Nat. Methods**, v. 13, n. 7, p. 581-583, 2016.

CAMPO, R. *et al*. The role of extracellular polymeric substances on aerobic granulation with stepwise increase of salinity. **Separation and Purification Technology**, v. 195, p. 12–20, 2018.

CARVALHEIRA, M. *et al*. The impact of aeration on the competition between polyphosphate accumulating organisms and glycogen accumulating organisms. **Water Research**, v. 66, p. 296-307, 2014.

CARVALHO, C. A. *et al*. Resource recovery in aerobic granular sludge systems: is it feasible or still a long way to go? **Chemosphere**, v. 274, n. 129881, 2021.

CHEN, F. Y. *et al*. Operational strategies for nitrogen removal in granular sequencing batch reactor. **Journal of Hazardous Materials**., v. 189, n. 1–2, p. 342–348, 2011.

CHEN, F. Y. *et al*. Alternating anoxic/oxic condition combined with step-feeding mode for nitrogen removal in granular sequencing batch reactors (GSBRs). **Separation and Purification Technology**, v. 105, p. 63–68, 2013.

CHEN, H.; HE, L. L.; LIU, A. N. *et al*. Start-up of granule-based denitrifying reactors with multiple magnesium supplementation strategies. **Journal of Environmental Management**, v. 155, p. 204–211, 2015.

CHEN, H. *et al*. Bis-(3'-5')-cyclic dimeric guanosine monophosphate (c-di-GMP) mediated membrane fouling in membrane bioreactor. **Journal of Membrane Science**, v. 646, n. 120224, 2022a.

CHEN, X. *et al*. A comparative study on simultaneous recovery of phosphorus and alginate-like exopolymers from bacterial and algal-bacterial aerobic granular sludges: Effects of organic loading rate. **Bioresource Technology**, v. 357, n. 127343, 2022b.

CHEN, X.; WANG, J.; WANG, Q.; YUAN, T.; LEI, Z.; ZHANG, Z.; SHIMIZU, K.; LEE, D. J. Simultaneous recovery of phosphorus and alginate-like exopolysaccharides from two types of aerobic granular sludge. **Bioresource Technology**, v. 346, n. 126411, 2022c.

CHEN, X. *et al*. A review on recovery of extracellular biopolymers from flocculent and granular activated sludges: cognition, key influencing factors, applications, and challenges. **Bioresource Technology**, v. 363, 2022d.

CHEN, J. *et al*. Microbial synergy achieving simultaneous nitrification-denitrification (SND) in salt-tolerant aerobic granular sludge. **Journal Of Water Process Engineering**, v. 60, n. 105138, 2024.

CHENG, W.; MA, C.; BAO, R. *et al*. Effect of influent ammonia nitrogen concentration on the phosphorus removal process in the aerobic granular sludge reactor. **Journal of Environmental Chemical Engineering**, v. 11, n. 110476, 2023.

CHOU, S. H.; GALPERIN, M. Y. Diversity of the c-di-GMP binding proteins and mechanisms. **Journal of bacteriology**, v. 198, n. 1, p. 32–46, 2016.

CORSINO, S. F. *et al*. Study of aerobic granular sludge stability in a continuous-flow membrane bioreactor. **Bioresource Technology**, v. 200, p. 1055–1059, 2016a.

CORSINO, S. F.; CAPODICI, M.; TORREGROSSA, M. *et al*. Fate of aerobic granular sludge in the long-term: The role of EPSs on the clogging of granular sludge porosity. **Journal of Environmental Management**, v. 183, p. 541–550, 2016b.

CORSINO, S. F.; CAPODICI, M.; TORREGROSSA, M.; VIVIANI, G. Physical properties and Extracellular Polymeric Substances pattern of aerobic granular sludge treating hypersaline wastewater. **Bioresource Technology**, v. 229, p. 152–159, 2017.

CORSINO, S. F. *et al*. Comparison between kinetics of autochthonous marine bacteria in activated sludge and granular sludge systems at different salinity and SRTs. **Water Research**, v. 148, p. 425–437, 2019.

COSTA, N. P. A. V. *et al*. Impact of additive application on the establishment of fast and stable aerobic granulation. **Appl. Microbiol. Biotechnol.**, v. 104, p. 5697–5709, 2020.

CUI, Y. W.; HUANG, J. L.; ALAM, F. Fast granulation of halophilic activated sludge treating low-strength organic saline wastewater via addition of divalent cations. **Chemosphere**, v. 264, n. 128396, 2021.

CUI, Y.; SU, H.; CHEN *et al*. Mechanism of activated sludge floc disintegration induced by excess addition of NaCl. **Clean**, v. 43, p. 1197–1206, 2015.

CYDZIK-KWIATKOWSKA, A. Biopolymers in aerobic granular sludge: their role in wastewater treatment and possibilities of re-use in line with circular economy. **Energies**, v. 14, n. 7219, 2021.

DE KREUK, M. K. *et al*. Simultaneous COD, nitrogen, and phosphate removal by aerobic granular sludge. **Biotechnology and Bioengineering**, v. 90, n. 6, p. 761-769, 2005.

DE KREUK, M. K.; KISHIDA, N.; VAN LOOSDRECHT, M. C. M. Aerobic granular sludge – state of the art. **Water Science and Technology**, v. 55, p. 75–81, 2007.

DECHO, A. W.; GUTIERREZ, T. Microbial extracellular polymeric substances (EPSs) in ocean systems. **Front. Microbiol.**, v. 8, n. 922, 2017.

DERLON, N. *et al*. Formation of aerobic granules for the treatment of real and low-strength municipal wastewater using a sequencing batch reactor operated at constant volume. **Water Research**, v. 105, p. 341-350, 2016.

DI BELLA, G.; TORREGROSSA, M. Aerobic granular sludge for leachate treatment. **Chemical Engineering Transactions**, v. 38, p. 493–498, 2014.

DOUGLAS, G. M. *et al*. PICRUSt2 for prediction of metagenome functions. **Nat. Biotechnol.**, v. 38, n. 6, p. 685-688, 2020.

DUBOIS, M. *et al*. Colorimetric method for determination of sugars and related substances. **Anal. Chem.**, v. 28, p. 350–356, 1956.

DUEHOLM, M. K. D. *et al*. MiDAS 5: Global diversity of bacteria and archaea in anaerobic digesters. **bioRxiv**, 2023.

FELZ, S. *et al*. Extraction of structural extracellular polymeric substances from aerobic granular sludge. **JoVE**, n. 54534, 2016.

FELZ, S. *et al*. Aerobic granular sludge contains hyaluronic acid-like and sulfated glycosaminoglycans-like polymers. **Water Research**, v. 169, n. 115291, 2020.

FELZ, S. *et al*. Chemical characterization methods for the analysis of structural extracellular polymeric substances (SPE). **Water Research**, v. 157, p. 201–208, 2019.

FENG, C. *et al*. Extracellular biopolymers recovered as raw biomaterials from waste granular sludge and potential applications: a critical review. **Sci. Total Environ**., v. 753, n. 142051, 2021.

FENG, S. *et al*. Predation by Bdellovibrio bacteriovorus significantly reduces viability and alters the microbial community composition of activated sludge flocs and granules. **FEMS Microbiol. Ecol.**, v. 93, n. 4, 2017.

FERRAZ, F. M. *et al*. Co-treatment of landfill leachate and domestic wastewater using a submerged aerobic biofilter. **Journal of Environmental Management**, v. 141, p. 9–15, 2014.

FUJII, N. *et al*. Metabolic Potential of the Superphylum *Patescibacteria* Reconstructed from Activated Sludge Samples from a Municipal Wastewater Treatment Plant. **Microbes and Environments**, v. 37, n. a, 2022.

GAO, J. *et al*. The present status of landfill leachate treatment and its development trend from a technological point of view. **Reviews in Environmental Science and Bio/Technology**, v. 14, n. 1, p. 93-122, 2015.

GENG, M. *et al*. Enhanced aerobic sludge granulation in a Sequencing Batch Reactor (SBR) by applying mycelial pellets. **Journal of Cleaner Production**, v. 274, n. 123037, 2020.

GUIMARÃES, L. B. **Caracterização microbiológica do lodo granular na remoção de nutrientes e potencial de recuperação de exopolímeros de efluentes reatores em bateladas sequenciais**. 2017. 261 p. Dissertação (Mestrado em Engenharia Ambiental) - Universidade Federal de Santa Catarina, Florianópolis.

GUO, H. *et al*. Structural extracellular polymeric substances determine the difference in digestibility between waste activated sludge and aerobic granules. **Water Research**, v. 181, n. 115924, 2020.

GRAAFF, D. R. *et al*. Sialic acids in the extracellular polymeric substances of seawater-adapted aerobic granular sludge. **Water Research**, v. 155, p. 343–351, 2019.

HAMZA, R. *et al*. A review of the state of development of aerobic granular sludge technology over the last 20 years: Full-scale applications and resource recovery. **Case Studies in Chemical and Environmental Engineering**, v. 5, n. 100173, 2022.

HAMZA, R. A. *et al*. Impact of food-to-microorganisms ratio on the stability of aerobic granular sludge treating high-strength organic wastewater. **Water Research**, v. 147, p. 287–298, 2018.

HAN, F. *et al*. Enhancing robustness of halophilic aerobic granule sludge by granular activated carbon at decreasing temperature. **Chemosphere**, v. 292, n. 133507, 2022.

HE, Q. *et al*. Robustness of an aerobic granular sludge sequencing batch reactor for low strength and salinity wastewater treatment at ambient to winter temperatures. **Journal of Hazardous Materials**, v. 384, n. 121454, 2020.

HE, Q. *et al*. Simultaneous nitrification, denitrification and phosphorus removal in an aerobic granular sequencing batch reactor with mixed carbon sources: reactor performance, extracellular polymeric substances and microbial successions. **Chemical Engineering Journal**. 331, p. 841–849, 2018.

HENGGE, R. Principles of c-di-GMP signalling in bacteria. **Nat Rev Microbiol**, v. 7, p. 263–273, 2009.

HONG, P. N. *et al*. Optimum selection of extraction methods of extracellular polymeric substances in activated sludge for effective extraction of the target components. **Biochemical Engineering Journal**, v. 127, p. 136–146, 2017.

HOU, Y. *et al*. Structural Characteristics of Aerobic Granular Sludge and Factors That Influence Its Stability: A Mini Review. **Water**, v. 13, n. 19, p. 2726, 2021.

HUANG, J. L. *et al*. Granulation of halophilic sludge inoculated with estuarine sediments for saline wastewater treatment. **Sci. Total Environ**., v. 682, p. 532–540, 2019.

HUBER, W. *et al*. Orchestrating high-throughput genomic analysis with Bioconductor. **Nature Methods**, v. 12, n. 2, p. 115-121, 2015.

HUNIK, J. H.; MEIJER, H. J. G.; TRAMPER, J. Kinetics of Nitrobacter agilis at extreme substrate, product and salt concentrations. **Applied Microbiology and Biotechnology**, v. 40, 1993.

ILLUMINA. **16S Metagenomic Sequencing Library Preparation**. Illumina Guides, 2013. Available in: https://support.illumina.com/content/dam/illumina-support/documents/documentation/chemistry_documentation/16s/16s-metagenomic-library-prep-guide-15044223-b.pdf. Accessed 26 out 23.

JIANG, Y.; SHI, X.; NG, H. Y. Aerobic granular sludge systems for treating hypersaline pharmaceutical wastewater: start-up, long-term performances and metabolic function. **Journal of Hazardous Materials**, v. 412, n. 125229, 2021.

KAUMERA. 2023. **Infinite application possibilities.** Available in: https://kaumera.com/english/kaumera/. Accessed 25 set. 2023.

KAYAALP, N. *et al*. A new approach for chemical oxygen demand (COD) measurement at high salinity and low organic matter samples. **Environmental Science and Pollution Research**, v. 17, n. 9, p. 1547–1552, 2010.

KEGGREST: **Client-side REST access to the Kyoto Encyclopedia of Genes and Genomes (KEGG)**. R package version 1.32.0: Tenenbaum, D; Maintainer, B., 2021.

KEHREIN, P. *et al*. Exploring resource recovery potentials for the aerobic granular sludge process by mass and energy balances-energy, biopolymer and phosphorous recovery from municipal wastewater. **Environmental Science: Water Research and Technology**, v. 6, n. 8, p. 2164–2179, 2020.

KJELDSEN, P. *et al*. Present and Long-Term Composition of MSW Landfill Leachate: A Review. **Critical Reviews in Environmental Science and Technology**, v. 32, n. 4, p. 297-336, 2002.

KONOSUKE, M. S.; MITSUGI, Y. K. **Method of preparing l-tryptophan**. US3929573A. Concessão: 30 dez. 1975.

KULICHEVSKAYA, I. S. *et al*. Schlesneria paludicola gen. nov., sp. nov., the first acidophilic member of the order Planctomycetales, from Sphagnum-dominated boreal wetlands. **International Journal of Systematic and Evolutionary Microbiology**, v. 57, p. 2680–2687, 2007.

LAYER, M. et al. Limited simultaneous nitrification-denitrification (SND) in aerobic granular sludge systems treating municipal wastewater: Mechanisms and practical implications. **Water Research X**, v. 7, p. 100048, 2020.

LASHKARIZADEH, M.; YUAN, Q.; OLESZKIEWICZ, J. A. Influence of carbon source on nutrient removal performance and physical–chemical characteristics of aerobic granular sludge. **Environ. Technol**., v. 36, p. 2161–2167, 2015.

LEAL, D. *et al*. FT-IR spectra of alginic acid block fractions in three species of brown seaweeds. **Carbohydrate Research**, v. 343, n. 2, p. 308–316, 2008.

LEMA, J. M.; MENDEZ, R.; BLAZQUEZ, R. Characteristics of landfill leachates and alternatives for their treatment: A review. **Water, Air, and Soil Pollution**, v. 40, p. 223–250, 1988.

LEMAIRE, R.; MARCELINO, M.; YUAN, Z. Achieving the nitrite pathway using aeration phase length control and step-feed in an SBR removing nutrients from abattoir wastewater. **Biotechnol. Bioeng**., v. 100, n. 6, p. 1228–1236, 2008.

LI, D. C. *et al*. Enhanced granulation process, a more effective way of aerobic granular sludge cultivation in pilot-scale application comparing to normal granulation process: From the perspective of microbial insights. **Sci. Total Environ.**, v. 707, n. 136106, 2020a.

LI, J. *et al*. Controlling factors and involved mechanisms on forming alginate like extracellular polymers in flocculent sludge. **Chemical Engineering Journal**, v. 439, n. 135792, 2022a.

LI, J. *et al*. Enhanced aerobic granulation at low temperature by stepwise increasing of salinity. **Science of The Total Environment**, v. 722, n. 137660, 2020b.

LI, J. *et al*. Accelerating aerobic sludge granulation by adding dry sewage sludge micropowder in sequencing batch reactors. **International Journal of Environmental Research and Public Health**, v. 12, n. 8, p. 1056–10065, 2015.

LI, S. *et al*. Startup and stable operation of advanced continuous flow reactor and the changes of microbial communities in aerobic granular sludge. **Chemosphere**, v. 243, n. 125434, 2020c.

LI, N.; LI, X.; FAN, X.-Y. Biofilm development under different pipe materials and water quality conditions in raw water transportation system: Bacterial communities and nitrogen transformation. **Journal of Cleaner Production**, v. 343, n. 130952, 2022.

LI, X. *et al*. Seawater-based wastewater accelerates development of aerobic granular sludge: A laboratory proof-of-concept. **Water research**, v. 115, p. 210-21, 2017.

LI, X. Y.; YANG, S. F. Influence of loosely bound extracellular polymeric substances (EPS) on the flocculation, settling and dewaterability of activated sludge. **Water Research**, v. 41, p. 1022–1030, 2007.

LI, Z. *et al*. Understanding of the mechanism of extracellular polymeric substances of aerobic granular sludge against tetracycline from the perspective of fluorescence properties. **Science of The Total Environment**, v. 756, n. 144054, 2021a.

LI, Z. *et al*. Understanding the role of cations and hydrogen bonds on the stability of aerobic granules from the perspective of the aggregation and adhesion behavior of extracellular polymeric substances. **Science of The Total Environment**, v. 795, n. 148659, 2021b.

LIN, H. et al. Reviewing bottlenecks in aerobic granular sludge technology: Slow granulation and low granular stability. **Environmental Pollution**, v. 263, p. 114638, 2020.

LIN, Y. *et al*. Characterization of alginate-like exopolysaccharides isolated from aerobic granular sludge in pilot-plant. **Water Research**, v. 44, n. 11, p. 3355–3364, 2010.

LIN, Y. M. *et al*. Bacterial alginate role in aerobic granular bio-particles formation and settleability improvement. **Separation Science and Technology**, v. 43, n. 7, p. 1642–1652, 2008.

LIU, J. *et al*. Rapid aerobic granulation in an SBR treating piggery wastewater by seeding sludge from a municipal WWTP. **Journal of Environmental Sciences**, v. 51, p. 332–341, 2017.

LIU, X. M. et al. Contribution of extracellular polymeric substances (EPS) to the sludge aggregation. **Environmental Science and Technology**, v. 44, n. 11, p. 4355–4360, 2010.

LIU, X.; YANG, H.; YANG, K. Effect of different enrichment methods on the independent biological phosphorus removal performance after nitrogen removal using immobilized fillers. **Biochemical Engineering Journal**, v. 198, n. 109041, 2023.

LIU, Y. Q.; CINQUEPALMI, S. Exploration of mechanisms for calcium phosphate precipitation and accumulation in nitrifying granules by investigating the size effects of granules. **Water Research**, v. 206, n. August, p. 117753, 2021.

LOTTI, T. *et al*. Hydrogels formed by anammox extracellular polymeric substances: structural and mechanical insights. **Scientific Reports**, v. 9, p. 1–9, 2019.

LOWRY, O. H. et al. Protein measurement with the Folin phenol reagent. **The Journal of biological chemistry**, v. 193, n. 1, p. 265–275, 1951.

LONG, B. *et al*. Tolerance to organic loading rate by aerobic granular sludge in a cyclic aerobic granular reactor. **Bioresource Technology**, v. 182, p. 314–322, 2015.

LU, C. S. *et al*. A review of anaerobic granulation under high-salinity conditions: Mechanisms, influencing factors and enhancement strategies. **Journal of Water Process Engineering**, v. 55, n. 104227, 2023.

LUO, J. *et al*. Impact of influent COD/N ratio on disintegration of aerobic granular sludge. **Water Re**search, v. 62, p. 127–135, 2014.

LV, Y. *et al*. Microbial communities of aerobic granules: Granulation mechanisms. **Bioresource Technology**, v. 169, p. 344-351, 2014.

MACÊDO, W. V. *et al*. Establishing simultaneous nitrification and denitrification under continuous aeration for the treatment of multi-electrolytes saline wastewater**. Bioresource Technology**, v. 288, n. 121529, 2019.

MENG, F. *et al*. Application of aerobic granules-continuous flow reactor for saline wastewater treatment: granular stability, lipid production and symbiotic relationship between bacteria and algae. **Bioresource Technology**, v. 295, n. 122291, 2020.

MENG, F. *et al*. Effect of salinity on granulation, performance and lipid accumulation of algal-bacterial granular sludge. **Bioresource Technology Reports**, v. 7, n. 100228, 2019a.

MENG, F. *et al*. Enhanced amount and quality of alginate-like exopolysaccharides in aerobic granular sludge for the treatment of salty wastewater. **BioResources**, v. 14, n. 1, p. 139–165, 2019b.

MIAO, L. *et al*. Recent advances in nitrogen removal from landfill leachate using biological treatments – A review. **Journal of Environmental Management**, v. 235, p. 178-185, 2019.

MORADALI, M. F.; GHODS, S.; REHM, B. H. A. **Alginate biosynthesis and biotechnological production**. In: REHM, B. H. A.; MORADALI, M. F. (Eds.). Alginates and Their Biomedical Applications. Singapura: Springer, 2018. p. 1–25.

MORGENROTH, E. *et al*. Aerobic granular sludge in a sequencing batch reactor. **Water Research**, v. 31, p. 3191–3194, 1997.

MOTTERAN, F.; PEREIRA, E. L.; CAMPOS, C. M. M. The behaviour of an anaerobic baffled reactor (ABR) as the first stage in the biological treatment of hog farming effluents. **Brazilian Journal of Chemical Engineering**, v. 30, n. 2, p. 299-310, 2014.

MOURÃO, J. M. M. *et al*. Post-treatment of swine wastewater using aerobic granular sludge: Granulation, microbiota development, and performance. **Bioresource Technology Reports**, v. 16, n. October, 2021.

MOUSSA, M. S. *et al*. Long term effects of salt on activity, population structure and floc characteristics in enriched bacterial cultures of nitrifiers. **Water Research**, v. 40, p. 1377–1388, 2006.

MUSTAFA, A. *et al*. Perspectives of Using L-Tryptophan for Improving Productivity of Agricultural Crops: A Review. **Pedosphere**, v. 28, n. 1, p. 16–34, 2018.

NANCHARAIAH, Y. V.; REDDY, G. K. K. Aerobic granular sludge technology: Mechanisms of granulation and biotechnological applications. **Bioresource Technology**, v. 247, p. 1128-1143, 2018.

NANCHARAIAH, Y. V.; SARVAJITH, M. Aerobic granular sludge process: a fast growing biological treatment for sustainable wastewater treatment. **Current Opinion in Environmental Science & Health**, v. 12, p. 57–65, dez. 2019.

NIELSEN, P. H. *et al*. A conceptual ecosystem model of microbial communities in enhanced biological phosphorus removal plants. **Water Research**, v. 44, n. 17, p. 5070–5088, set. 2010.

NIU, H. *et al*. Metabolic engineering for improving l-tryptophan production in Escherichia coli. **Journal of Industrial Microbiology and Biotechnology**, v. 46, n. 1, p. 55–65, 2019.

NIU, W. *et al*. Rapid start-up of denitrifying granular sludge by dosing with semi-starvation fluctuation C/N ratio strategy. **Bioresource Technology**, v. 241, p. 945–950, 2017.

PANAGOPOULOS, A. Study and evaluation of the characteristics of saline wastewater (brine) produced by desalination and industrial plants. **Environmental Science and Pollution Research**, v. 29, n. 16, p. 23736–23749, abr. 2022.

PENAGOS, D. G.; VICTORIA, J. R.; MANRIQUE, M. V. Formulation of a protocol to evaluate the aerobic granulation potential (AGP) of an inoculum. **MethodsX**, v. 9, p. 101710, 2022.

PENG, T. *et al*. Effect of different forms and components of EPS on sludge aggregation during granulation process of aerobic granular sludge. **Chemosphere**, v. 303, p. 135116, set. 2022.

PRONK, M. *et al*. The acid soluble extracellular polymeric substance of aerobic granular sludge dominated by *Defluviicoccus sp*. **Water Research**, v. 122, p. 148–158, out. 2017b.

PRONK, M. *et al*. Evaluating the main and side effects of high salinity on aerobic granular sludge. **Applied Microbiology and Biotechnology**, v. 98, n. 3, p. 1339–1348, fev. 2014.

PRONK, M. *et al*. Aerobic granular biomass technology: advancements in design, applications and further developments. **Water Practice and Technology**, v. 12, n. 4, p. 987–996, 1 dez. 2017a.

QIU, B. *et al*. Rapid granulation of aerobic granular sludge and maintaining its stability by combining the effects of multi-ionic matrix and bio-carrier in a continuous-flow membrane bioreactor. **Science of The Total Environment**, v. 813, n. 152644, 2022.

QIULAI, H. *et al*. A comprehensive comparison between non-bulking and bulking aerobic granular sludge in microbial communities. **Bioresource Technology**, v. 294, n. 122151, 2019.

QUARTAROLI, L. *et al*. Effect of the gradual increase of salt on stability and microbial diversity of granular sludge and ammonia removal. **Journal of Environmental Management**, v. 248, n. 109273, 2019.

QUAST, C. *et al*. The SILVA ribosomal RNA gene database project: improved data processing and web-based tools. **Nucleic Acids Research**, v. 41, n. 1, p. 590-596, 2013.

REN, Y. *et al*. Comparing young landfill leachate treatment efficiency and process stability using aerobic granular sludge and suspended growth activated sludge. **Journal of Water Process Engineering**, v. 17, p. 161–167, 2017.

RENOU, S. *et al*. Landfill leachate treatment: Review and opportunity. **Journal of Hazardous Materials**, v. 150, n. 3, p. 468-493, 2008.

ROAGER, H. M.; LICHT, T. R. Microbial tryptophan catabolites in health and disease. **Nature Communications**, v. 9, n. 1, p. 3294, dez. 2018.

ROLLEMBERG, S. L. D. S. *et al*. Aerobic granular sludge: Cultivation parameters and removal mechanisms. **Bioresource Technology**, v. 270, p. 678–688, dez. 2018.

ROLLEMBERG, S. L. D. S. *et al*. Effects of carbon source on the formation, stability, bioactivity and biodiversity of the aerobic granule sludge. **Bioresource Technology**, v. 278, p. 195–204, abr. 2019.

ROLLEMBERG, S. L. DE S. L. DE S. *et al*. Pilot-scale aerobic granular sludge in the treatment of municipal wastewater: Optimizations in the start-up, methodology of sludge discharge, and evaluation of resource recovery. **Bioresource Technology**, v. 311, p. 123467, 2020a.

ROLLEMBERG, S. L. DE S. *et al*. Evaluation of the production of alginate-like exopolysaccharides (ALE) and tryptophan in aerobic granular sludge systems. **Bioprocess and Biosystems Engineering**, v. 44, n. 2, p. 259–270, set. 2020b.

ROLLEMBERG, S. L. D. S. *et al*. Impact of cycle type on aerobic granular sludge formation, stability, removal mechanisms and system performance. **Journal of Environmental Management**, v. 256, p. 109970, 2020c.

ROLLEMBERG, S. L. D. S. *et al*. Evaluation of sludge discharge methodologies in aerobic granular sludge reactors. **Bioresource Technology Reports**, v. 18, p. 101018, jun. 2022.

ROYAL HASKONINGDHV. **Nereda® Aerobic Granular Sludge Technology**. 2023. Available in: https://nereda.royalhaskoningdhv.com/. Accessed 25 set. 2023.

SARMA, S. J.; TAY, J. H.; CHU, A. Finding Knowledge Gaps in Aerobic Granulation Technology. **Trends in Biotechnology**, v. 35, n. 1, p. 66–78, jan. 2017.

SANTOS, A. F. D. *et al*. Carbon source affects the resource recovery in aerobic granular sludge systems treating wastewater. **Bioresource Technology**, v. 357, p. 127355, ago. 2022.

SARVAJITH, M.; NANCHARAIAH, Y. V. Properties of alginate-like exopolymers recovered from flocculent and granular microbial sludges of different biological treatment systems treating real municipal wastewater. **Separation and Purification Technology**, p. 123460, fev. 2023.

SAXENA, V. *et al*. Simultaneous removal of carbon, nitrogen, and phosphorus from landfill leachate using an aerobic granular reactor. **Environmental Technology & Innovation**, v. 28, p. 102657, nov. 2022.

SEMAHA, P. *et al*. Transition of biological wastewater treatment from flocculent activated sludge to granular sludge systems towards circular economy. **Bioresource Technology Reports**, v. 21, p. 101294, fev. 2023.

SETHI, S. *et al*. Celebrating 50 years of microbial granulation technologies: from canonical wastewater management to bio-product recovery. **Science of the Total Environment**, v. 872, n. 162213, 2023.

SCHAMBECK, C. M. *et al*. Biopolymers recovery: dynamics and characterization of alginate-like exopolymers in an aerobic granular sludge system treating municipal wastewater without sludge inoculum. **Journal of Environmental Management**, v. 263, p. 110394, jun. 2020.

SHEN, N.; ZHOU, Y. Enhanced biological phosphorus removal with different carbon sources. **Applied Microbiology and Biotechnology**, v. 100, n. 11, p. 4735–4745, jun. 2016.

SILVA, L. C. F. *et al*. Heterotrophic nitrifying/aerobic denitrifying bacteria: Ammonium removal under different physical-chemical conditions and molecular characterization. **J. Environ. Manage**., v. 248, n. 109294, 2019.

SILVA, V. E. P. S. G. D. *et al*. Evaluation of leachate impact on domestic sewage co-treatment in aerobic granular sludge systems. **Chemical Engineering Journal**, v. 470, p. 144178, ago. 2023a.

SILVA, V. E. P. S. G. D.; DE SOUSA ROLLEMBERG, S. L.; BEZERRA DOS SANTOS, A. Step-feeding in aerobic/anoxic cycles enhanced the performance of aerobic granular sludge (AGS) systems treating effluents with low C:N ratios. **Process Safety and Environmental Protection**, v. 171, p. 1031–1042, mar. 2023b.

SILVA, V. E. P. S. G.; ROLLEMBERG, S. L. DE S.; SANTOS, A. B. DOS. Impact of feeding strategy on the performance and operational stability of aerobic granular sludge treating high-strength ammonium concentrations. **Journal of Water Process Engineering**, v. 44, p. 102378, dez. 2021.

SILVA, V. E. P. S. G. D. *et al*. Landfill leachate biological treatment: perspective for the aerobic granular sludge technology. **Environmental Science and Pollution Research**, v. 29, n. 30, p. 45150–45170, jun. 2022.

SUI, Y. *et al*. Feast/famine ratio regulates the succession of heterotrophic nitrification-aerobic denitrification and autotrophic ammonia oxidizing bacteria in halophilic aerobic granular sludge treating saline wastewater. **Bioresource Technology**, v. 393, n. 129995, 2024.

VAN LEEUWEN, K. *et al*. The Energy & Raw Materials Factory: Role and Potential Contribution to the Circular Economy of the Netherlands. **Environmental Management**, v. 61, n. 5, p. 786–795, maio 2018.

VERAWATY, M. *et al*. Breakage and growth towards a stable aerobic granule size during the treatment of wastewater. **Water Research**, v. 47, n. 14, p. 5338–5349, set. 2013.

WAN, C. *et al*. Disintegration of aerobic granules: Role of second messenger cyclic di-GMP. **Bioresource Technology**, v. 146, p. 330–335, 2013.

WAN, C. *et al*. Partial nitrification of wastewaters with high NaCl concentrations by aerobic granules in continuous-flow reactor. **Bioresource Technology**, v. 152, p. 1–6, jan. 2014.

WAN, C. *et al*. Formation of bacterial aerobic granules: Role of propionate. **Bioresource Technology**, v. 197, p. 489–494, dez. 2015.

WANG, B.-B. *et al*. A new classification paradigm of extracellular polymeric substances (EPS) in activated sludge: Separation and characterization of exopolymers between floc level and microcolony level. **Water Research**, v. 64, p. 53–60, nov. 2014.

WANG, G. *et al*. Effect of food-to-microorganisms ratio on aerobic granular sludge settleability: Microbial community, potential roles and sequential responses of extracellular proteins and polysaccharides. **Journal of Environmental Management**, v. 345, p. 118814, nov. 2023.

WANG, H. *et al*. Enhanced aerobic granular sludge by static magnetic field to treat saline wastewater via simultaneous partial nitrification and denitrification (SPND) process. **Bioresource Technology**, v. 350, p. 126891, abr. 2022.

WANG, L. *et al*. Synergy of N-(3-oxohexanoyl)-L-homoserine lactone and tryptophan-like outer extracellular substances in granular sludge dominated by aerobic ammonia-oxidizing bacteria. **Appl. Microbiol. Biotechnol**., v. 102, p. 10779–10789, 2018.

WANG, Z.; VAN LOOSDRECHT, M. C. M.; SAIKALY, P. E. Gradual adaptation to salt and dissolved oxygen: Strategies to minimize adverse effect of salinity on aerobic granular sludge. **Water Research**, v. 124, p. 702–712, nov. 2017.

WATANABE, T.; SNELL, E. E. Reversibility of the Tryptophanase Reaction: Synthesis of Tryptophan from Indole, Pyruvate, and Ammonia. **Proceedings of the National Academy of Sciences**, v. 69, n. 5, p. 1086–1090, maio 1972.

WEI, Y. *et al*. Organic and nitrogen removal from landfill leachate in aerobic granular sludge sequencing batch reactors. **Waste Management**, v. 32, n. 3, p. 448–455, mar. 2012.

WINKLER, M.-K. H. *et al*. Temperature and salt effects on settling velocity in granular sludge technology. **Water Research**, v. 46, n. 16, p. 5445–5451, out. 2012.

WONG, L. L. *et al*. Isolation of a putative S-layer protein from anammox biofilm extracellular matrix using ionic liquid extraction. **BioRxiv**, n. 705566, 2019.

WONG, L. L. *et al*. Extracellular protein isolation from the matrix of anammox biofilm using ionic liquid extraction. **Applied Microbiology and Biotechnology**, v. 104, p. 3643–3654, 2020.

WRIGHT, E. S. Using DECIPHER v2.0 to analyze big biological sequence data in R. **The R Journal**, v. 8, n. 1, p. 352-395, 2016.

WU, L. *et al*. Effect of wastewater COD/N ratio on aerobic nitrifying sludge granulation and microbial population shift. **Journal of Environmental Sciences**, v. 24, n. 2, p. 234–241, fev. 2012.

WU, H. *et al*. Effect of HRT and BDPs types on nitrogen removal and microbial community of solid carbon source SND process treating low carbon/nitrogen domestic wastewater. **Journal of Water Process Engineering**, v. 40, p. 101854, abr. 2021.

WU, X. *et al*. Tolerance to short-term saline shocks by aerobic granular sludge. **Chemosphere**, v. 243, p. 125370, mar. 2020.

XAVIER, J. A. *et al*. Towards a better understanding concerning carbon to nitrogen ratio and the carbon source in aerobic granular sludge. **Journal of Environmental Chemical Engineering**, v. 11, n. 5, p. 110457, out. 2023.

YAN, L. *et al*. Tetracycline removal in granulation: influence of extracellular polymers substances, structure, and metabolic function of microbial community. **Chemosphere**, v. 288, n. 2, 132510, 2022.

YANG, Y.-C. *et al*. Accelerated aerobic granulation using alternating feed loadings: Alginate-like exopolysaccharides. **Bioresource Technology**, v. 171, p. 360–366, nov. 2014.

YU, Z. *et al*. Enhancement of PPCPs removal by shaped microbial community of aerobic granular sludge under condition of low C/N ratio influent. **J. Hazard Mater**., v. 394, n. 122583, 2020.

ZAHRA, S. A. *et al*. Alginate-like exopolysaccharides in aerobic granular sludge: A review. **Materials Today: Proceedings**, p. S2214785322021496, abr. 2022.

ZENG, R. G. *et al*. A review of alginate-like extracellular polymers from excess sludge: extraction, characterization, and potential application. **Journal of Water Process Engineering**, v. 56, n. 104346, 2023.

ZHANG, L. *et al*. Evolution of microbial community during dry storage and recovery of aerobic granular sludge. **Heliyon**, v. 5, n. 12, p. e03023, dez. 2019.

ZHANG, M. *et al*. A review of microbial nitrogen transformations and microbiome engineering for biological nitrogen removal under salinity stress. **Chemosphere**, v. 341, p. 139949, nov. 2023.

ZHANG, W.; HUANG, F.; HU, W. Performance and mechanism of synchronous nitrate and phosphorus removal in constructed pyrite-based mixotrophic denitrification system from secondary effluent. **Environmental Science and Pollution Research**, v. 27, n. 29, p. 36816–36825, out. 2020.

ZHANG, Z. *et al*. Stability of aerobic granular sludge under condition of low influent C/N ratio: correlation of sludge property and functional microorganism. **Bioresour. Technol**., v. 270, p. 391–399, 2018.

ZHU, L. *et al*. Optimization of selective sludge discharge mode for enhancing the stability of aerobic granular sludge process. **Chemical Engineering Journal**, v. 217, p. 442–446, fev. 2013.